Investigations of spicules and spicule formation in Haplosclerida (Porifera, Demospongiae) using a multidisciplinary approach

Thesis submitted for the degree of PhD at the National University of Ireland, Galway by

Jose Maria Aguilar Camacho M.Sc. B.Sc.

School of Natural Sciences

Deparment of Zoology

January 2019

Table of Contents

Declaration

This thesis has not been submitted, in whole or in part, to this, or any other university for degree. The work described here is my own, with the exception of the following:

-TEM photographs of the embryos from *H. viscosa* and *H. cinerea* (Chapter 4, Figure 6, p.117) were taken by M.V. Marra and M.B. Longakit.

Signed:----------

Jose Maria Aguilar-Camacho

Acknowledgements

I thank my supervisor Grace for the good and bad moments that I experienced during the course of my PhD.

I thank my GRC members Anne Marie Power, Cathal Seoighe and Maura Grealy.

I thank NUIG for providing me with a Hardiman Scholarship for four years and the Thomas Crawford Hayes scheme for funding me twice.

I thank the technical and academic staff at the Zoology Department, Anatomy Department, Mathematics Department, Biochemistry Department and Biomedical Department (NUIG).

I thank Peter Crowley, Liam Morisson, Enda O'Connell, Eadaoin Timmins and Liam Doonan.

I met many people during the course of my PhD some of them were lab mates, friends, colleagues and I learned something from every person.

“People are always blaming their circumstances for what they are. I don't believe in circumstances. The people who get on in this world are the people who get up and look for the circumstances they want, and if they can't find them, make them”

George Bernard Shaw

Abstract

Sponges are simple animals and their body is formed by different cell types and a dense skeleton either of collagen, chitin or spicules made of amorphous silica or calcium carbonate that they secrete. The phylum Porifera is divided into four classes, and Demospongiae is the most diverse. The identification and classification of demosponges is primarily based on spicule morphology and the arrangement of these structures in their skeleton. Species belonging to the order Haplosclerida have a skeleton composed mainly of megasclere spicules in a single size category and microscleres if present include sigmas, toxas or microxeas. The classification of this order is complicated and there is discrepancy between the morphological classification and the molecular phylogeny based on ribosomal, nuclear and mitochondrial topologies. In this thesis, a multidisciplinary approach including chemistry, microscopy and genetics was used to gain insights into the formation of spicules in selected marine haplosclerid species.

The chemical composition of the spicules was analyzed in nine *Haliclona* species employing SEM-EDS, ICP-MS, ICP-OES and FTIR-ATR and no phylogenetic pattern was obtained from these analyses and the amounts of biogenic silica was similar in these species. The spicules of one species (*H. indistincta*) contained the highest amounts of trace elements compared to the remaining eight *Haliclona* species and the cause of this difference could be due to environmental factors. The genes responsible for spicule formation (silicatein and silintaphin) were identified in *de novo* assembled transcriptomes from three *Haliclona* species (representatives of three major molecular clades), and in all the available genomes and transcriptomes from Porifera. The silicatein genes were just found in genomes and transcriptomes from Demospongiae bearing siliceous spicules (excluding Keratosa and Verongimorpha) and a new scheme is proposed in which these genes are divided into six major molecular clades (CHNI, CHNII, CHNIII, C/SQN, SHNI and SHNII), however one silicatein from *H. indistincta* was located between the overall silicatein clade and cathepsin-L clade (outgroup). There is a high duplication of silicatein genes and despite the paralogous copies the evolution of these genes in marine haplosclerids reflects the previous molecular topology. I suggest that the simplicity of skeleton in marine haplosclerids is maybe because the transcriptomes and genomes analyzed in this study have only one silicatein of the SHNI type and the absence of the silintaphin protein and SHNII silicatein variants. The analysis of the expression levels of the silicatein genes from the sponge *H. indistincta* through three different developmental stages was investigated and the cells producing spicules and the axial filament protein were identified using microscopic analyses (TEM and SEM). There was positive correlation between the expression levels of silicatein genes with the formation of spicules. In addition, these genes were differentially expressed in two developmental stages producing spicules (pre-settled stage and adult). One silicatein gene from *H. indistincta* was expressed in *E.coli* cells for the production of a recombinant protein. This latter task was carried out for the production of silica nanocrystals for the biotech sector and as a functional study to understand the diversity of silicatein variants from this species. The protein was successfully produced but unfortunately, the refolding and purification was not possible to accomplish.

Chapter 1

General Introduction

Part of this chapter contributed to the book chapter: **Aguilar-Camacho, J. M.,** McCormack, G. P. (2017). Molecular Responses of Sponges to Climate Change. In: Climate Change, Ocean Acidification and Sponges (pp. 79-104). Springer, Cham.

Sponges

Sponges are sessile filter feeding animals that live in subtidal and intertidal areas, deep sea slopes, coral reefs and freshwater habitats (Bell, 2008). Sponges play an important functional role in bentho-pelagic coupling processes in marine ecosystems (De Goeij et al. 2013). They influence the availability and cycling of dissolved carbon, nitrogen compounds and silica (De Goeij et al. 2008; Maldonado et al. 2011).

The sponge body is simple and made of different cell types (i.e. choanocytes, archaeocytes, sclerocytes) and a dense skeleton either of collagen, spongin, chitin fibres or spicules made of biogenic silica or calcium carbonate (Aguilar-Camacho and McCormack, 2017). Most sponges reproduce sexually although asexual reproduction by fragmentation and budding also has been reported (Maldonado and Uriz, 1999; Riesgo and Maldonado, 2008). They can be hermaphroditic or gonochoristic with external or internal fertilization. The majority of sponges are ovoviviparous and larvae are released into the seawater until they settle down and transform into juveniles (Maldonado, 2006). The Phylum Porifera is divided into five main classes: Demospongiae, Hexactinellida, Calcarea, Homoscleromorpha and Archaeocyata (Gazave et al. 2012; Morrow and Cardenas, 2015). Members of the class Archaeocyata are a group of extinct sponges (Wörheide et al. 2012). In three out of four extant classes, the skeleton is made of biogenic amorphous silica (Hexactinellida, Demospongiae and Homoscleromorpha) (Gazave et al. 2012). This is remarkable because silicon is not the most abundant dissolved element in seawater and is also under-saturated in surface waters but not in the deep sea (Maldonado et al. 2011; Dodd et al. 2017). In addition, silicon is the second most abundant element in the earth's crust, existing naturally as silicon dioxide or silicates (Arakaki et al. 2015). The most recent phylogenomics study suggested that sponges are monophyletic and the sister clade to Eumetazoa (including Ctenophora) (Feuda et al. 2017).

The class with the greatest number of species is Demospongiae and is divided into three subclasses; Verongimorpha for sponges having a fibrous skeleton made of chitin or spongin (order Verongida) or sponges with a dense skeleton made of collagen with/without oxypherraster spicules (orders Chondrilliida and Chondrosiida); Keratosa for sponges with a dense skeleton network made of reticulate or anastomosed spongin fibres (orders Dyctioceratida and Dendroceratida) and Heteroscleromorpha for sponges with a skeleton made of spicules of different shapes and sizes (including megascleres and microscleres) (Morrow and Cardenas, 2015). The identification and classification of demosponges bearing siliceous spicules is based on the morphology and the length of the spicules and the arrangement of these structures in the skeleton and currently sixteen orders (including the order Haplosclerida) are considered valid (Morrow and Cardenas, 2015).

The siliceous spicules of demosponges are comprised mainly of glassy amorphous hydrated silica (SiO_2• nH_2O) similar to opal or silica gel (Sandford, 2003). However, traces of other elements such as: Al, Fe, K, Na and Cl have been detected in the spicules of selected species, based on chemical techniques such as: ICP-OES and EDX-RF (Sandford, 2003; Şen et al. 2016). FTIR-ATR is a spectroscopic technique that has been employed to detect certain functional groups (e.g. amines, hydroxils) in the tissue and spicules of selected sponge species (Gan et al. 2015; Şen et al. 2016). This technique has been utilized to discriminate and investigate phylogenetic relationships of some sponge species (Gan et al. 2015; Şen et al. 2016; Bayari et al. 2018).

Order Haplosclerida

Species belonging to the order Haplosclerida have megasclere spicules in a single size category (i.e. oxeas, styles, strongyles) and microscleres, if present, include sigmas, toxas or

microxeas (Redmond et al. 2011; 2013). The classification of species belonging to this order is complicated due to the reduced diversity of spicules compared to species assigned to other heteroscleromorpha orders such as: Poecilosclerida or Tetractinellida (Redmond et al. 2013; Morrow and Cardenas, 2015). The skeleton in species belonging to this order is formed by primary ascending fibres interconnected with secondary fibres each composed of megasclere spicules (van Soest and Hooper, 2002). The primary and secondary fibres can be uni-, bi- or multispicular and there is spongin cementing the nodes of these joins; or the fibres are completely embedded in spongin sheets (van Soest, 1980; de Weerdt, 1986) (Figure 1). The characteristics of these fibres and the amount of spongin in the skeleton (from adult specimens) were diagnostic features to identify and classify species in specific taxonomic ranks (e.g. family, genus and subgenus) (van Soest, 1980; van Soest and Hooper, 2002) (Figure 1).

Molecular studies using ribosomal and mitochondrial loci divided the sequences from marine haplosclerids into five major molecular clades (Redmond et al. 2011; 2013) (Figure 2). Clade A contained sequences from sponges identified as *Chalinula, Haliclona, Cladocroce, Siphonochalina*, *Callyspongia* and the type species of the genus *Haliclona (H. oculata)*. The skeleton in these species is delicate and usually the oxeas are small and the primary ascending fibres could have spongin cementing the joins with either the primary or secondary fibres or the fibres are embedded in spongin sheets. Clade B contained the species *Haliclona simulans, Amphimedon queenslandica* and other species identified under the genera *Haliclona, Neopetrosia*, *Xestospongia* and *Tabulocalyx* (Redmond et al. 2011; 2013). Clade C contained species identified as *Haliclona* (e.g. *H. indistincta*), *Niphates, Neopetrosia, Amphimedon,* and *Acanthostrongylophora* (Stephens, 2013). Clade D contained the sequences of *Gelliodes calista, Dasychalina* sp and *Dasychalina fragilis* while clade E contained sequences of

species identified under the genera *Janulum* and *Siphonodyction* (Redmond et al. 2013). In addition, there are other small clades containing additional sequences from species identified as *Petrosia*, *Haliclona*, *Neopetrosia* and *Oceanapia* (Raleigh et al. 2007; Redmond et al. 2011; 2013) (Figure 2).

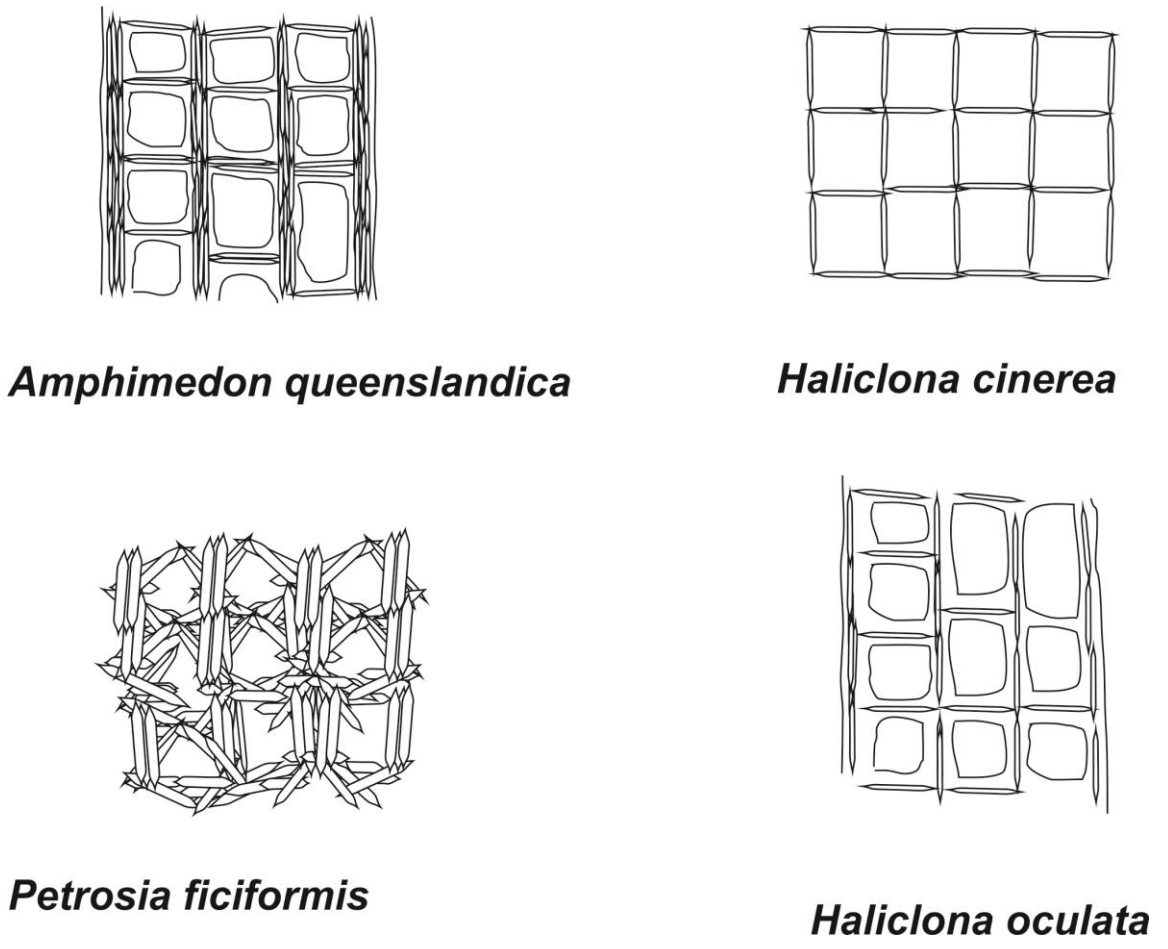

Figure 1. Schematic drawings of skeletal arrangements in some species belonging to the order Haplosclerida adapted from de Weerdt (1986; 2000). The skeleton is always composed of primary ascending fibres interconnected with secondary fibres (composed by megasclere spicule) and the amount of spongin in the fibres is variable.

The molecular phylogeny indicates that species identified under the genus *Haliclona* are polyphyletic and that the diagnostic features (skeleton arrangement and spicule sizes) that are

currently employed as taxonomic features to identify and classify species in this genus do not reflect their evolutionary relationships.

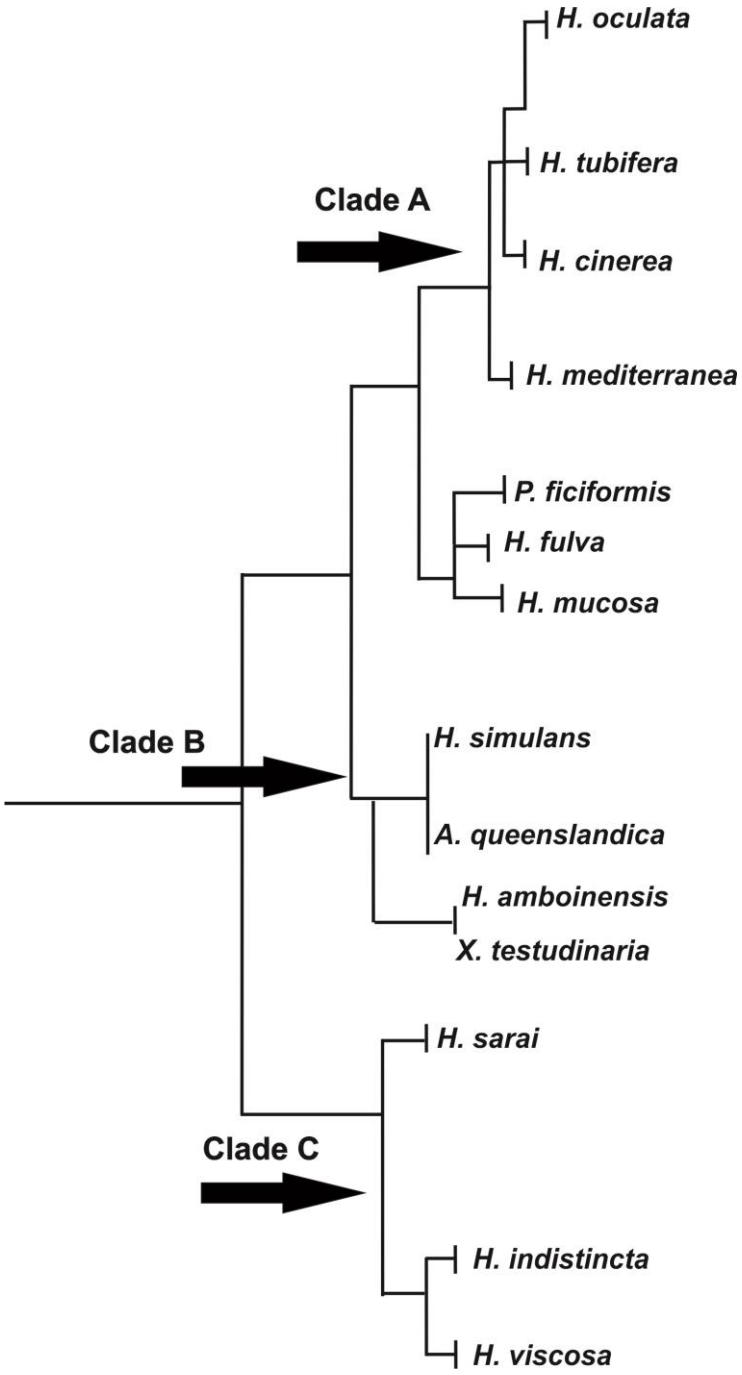

Figure 2. A schematic representation of the maximum-likelihood phylogeny reconstruction from the D1 region of the 28S rRNA gene of selected marine haplosclerid species adapted from Redmond et al. (2011).

For example, the species *H. oculata* has a delicate skeleton formed by primary uni- or bispicular fibres interconnected with secondary unispicular fibres, the oxeas are 80-145 × 4.5-12 µm and based on molecular data is member of clade A (Figures 1, 2 and 3). *H. simulans* has a dense skeleton formed by primary bi- or multispicular fibres interconnected with secondary uni- or bispicular fibres, the oxeas are 130-155 × 8-11 µm and based on molecular data is a member of clade B (Figures 2 and 3).These two species have a similar ladder-like skeleton formed by primary ascending fibres interconnected with secondary fibres (pauci- or unispicular) (Figure 3) and they were classified based on these morphological features in the genus *Haliclona* and within the same group (*oculata* type) by de Weerdt (1986), and later they were allocated in the subgenus *Haliclona* (de Weerdt, 2000). However, the molecular data clearly indicates that these two species are not closely related (Redmond et al. 2011; 2013).

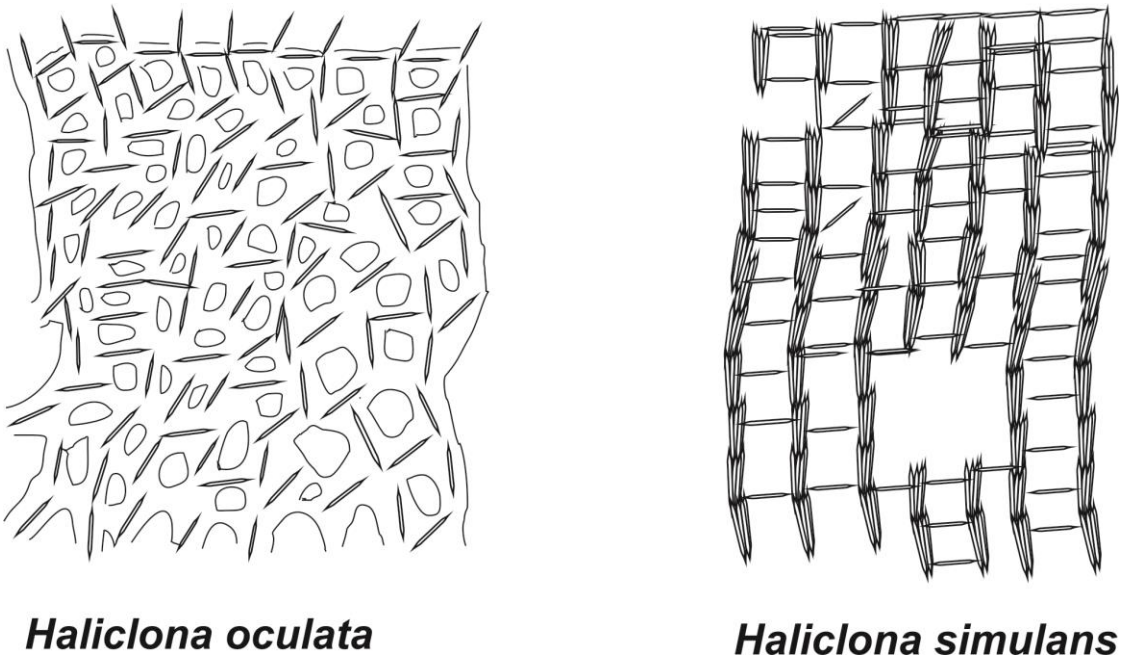

Figure 3. Schematic representation of skeletal arrangements in *H. oculata* and *H. simulans* adapted from de Weerdt (1986).

Hypotheses of the evolutionary relationships of marine haplosclerids with species from other orders from Heteroscleromorpha (bearing siliceous spicules) suggested three possible scenarios in which: a) marine haplosclerids and freshwater sponges are monophyletic within a molecular clade that is a sister to sequences from the remaining heteroscleromorpha based on nuclear genes (Sperling et al. 2010; Hill et al. 2013); b) marine haplosclerids are in a different clade which is a sister to data containing sequences from freshwater sponges and heteroscleromorpha based on mitochondrial loci (Lavrov et al. 2008; Ma and Yang, 2016) and c) marine haplosclerids is a sister clade to data from freshwater sponges and heteroscleromorpha but they are located in one overall clade based on ribosomal topology (Redmond et al. 2013; Morrow and Cardenas, 2015). It is clear however from all of these scenarios that marine haplosclerids are somewhat distinct from the remaining demosponges bearing siliceous spicules based on morphological and molecular data (Redmond et al. 2011). Given that species belonging to this order have megasclere spicules in a single size category compared to the high number of spicule categories found in freshwater sponges and other heteroscleromorpha, and that these structures are used as diagnostic features for species classification and identification, I decided to identify the genes responsible for spicule formation in representatives of three major molecular clades from Haplosclerida, particularly species identified under the genus *Haliclona*. I determined the diversity and evolutionary relationships of these genes in Porifera and corroborate whether or not the evolution of these genes in marine haplosclerids will follow the current molecular topology.

Gene expression and genomics in sponges

Isolating specific genes and investigating how they are expressed (switched on/off, producing high/low amounts of mRNA/protein) across organisms and tissues have been important for

determining the evolutionary origin, function and importance of proteins. Sponges have fewer cell types than other complex animals but members of the phylum Placozoa have been reported with six somatic cell types (Eitel et al. 2011).

Sponge cells will produce different mRNAs at differing amounts (Aguilar-Camacho and McCormack, 2017). The mRNA moves out of the nucleus to the ribosomes in the cytoplasm where the information they contain is translated into proteins (Figure 4). To investigate patterns of expression of particular genes first involves obtaining cDNA of the targeted gene from extracted RNA using a specific commercial kit or via RT-PCR. Western or northern blots are then used to determine to what degree a particular gene is active (e.g. Pfeifer et al. 1993). Another approach involves *in situ* hybridization where probes are applied directly to the tissue of the species to determine where the gene is expressed and at what level of expression (e.g. Adell et al. 2003). More recently quantitative real time PCR is being applied to detect the copy number of specific mRNA's as a way to detect differential levels of expression (e.g. López-Legentil et al. 2008). High numbers of a particular mRNA would indicate that the gene in question is highly expressed and cause high levels of fluorescence, while lower fluorescence would indicate a lower number of copies of mRNA, which in turn indicates a lower level of expression.

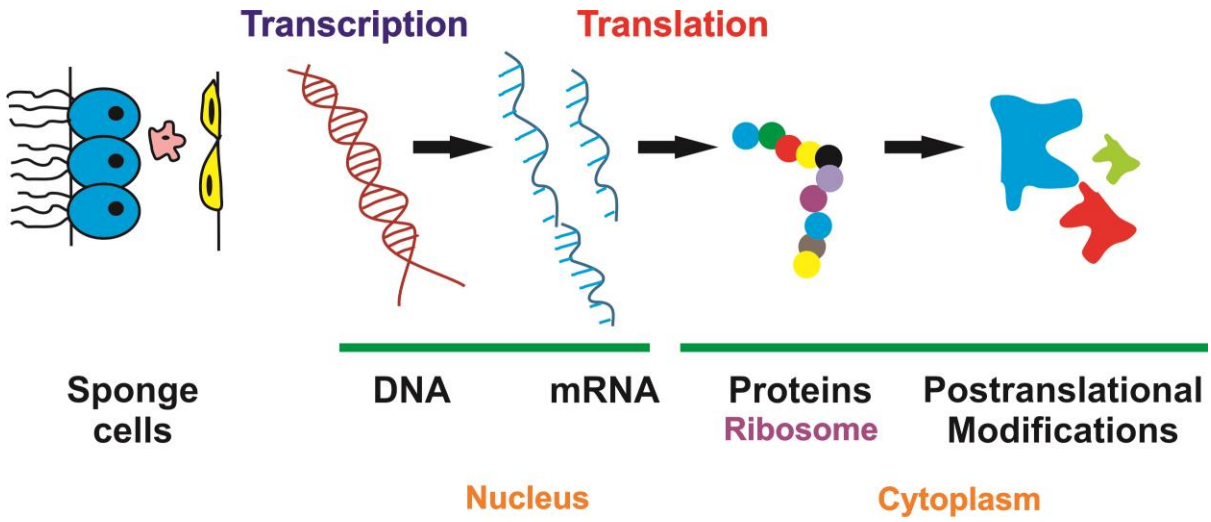

Figure 4. A schematic representation of gene expression in sponges from Aguilar-Camacho and McCormack, 2017.

Sponges are simple animals but their genomic architecture contains many homologs of genes found in other complex metazoans (Riesgo et al. 2014). For instance, the first sponge genome sequenced was that of the demosponge *Amphimedon queenslandica* containing a large number of genes related to cell cycling and growth (ie. p53, cyclin dependent-kinases, Myc), programmed cell death (i.e. Bcl-2, caspases, APAF1, TNRF), cell matrix adhesion (i.e. collagens, integrins, cadherins), developmental signaling and gene regulation pathways (i.e. Sox, Fkh, Wnt, TG-F β), allorecognition innate immunity (Toll Like receptors, MDA-5-like RNA helicases, Aggregation factors) and specialization of cell types (Laminin like domains, GPCRs, Dlgs) (Srivastava et al. 2010). Currently there are fewer than eight genomes available from sponges (Aguilar-Camacho and McCormack, 2017; Renard et al. 2018) (Table 1). In addition, several transcriptomes have been sequenced to identify metazoan genes in sponges and to compare patterns of evolution across phyla (Alié et al. 2015; Aguilar-Camacho and McCormack, 2017), as well as, to provide additional data for phylogenomics studies (Whelan et al. 2015), compare gene expression patterns mainly through different life stages (Conaco et

al. 2012; Pérez-Porro et al. 2013) or the gene changes in response to the increase of temperature (Guzman and Conaco, 2016). Here I set out to generate transcriptomes from representatives of the three major molecular clades of Haplosclerida and I identifed the genes responsible for the spicule formation and investigate their expression levels under different conditions (i.e. life stages, parts of the sponge) (Table 1).

Table 1. A comparative table of the sponge genomes and transcriptomes sequenced including information about the class, number of proteins identified and/or contigs assembled

.

GENOMES			
Species	**Class**	**Contigs (DNA) or Proteins Assembled**	**Reference**
Amphimedon queenslandica	Demospongiae	40, 122 proteins	Fernandez-Valverde et al. 2015*
Xestospongia testudinaria	Demospongiae	22, 327 proteins	Ryu et al. 2016*
Tethya wilhelma	Demospongiae	127,012 contigs	Francis et al. 2017
Oscarella carmella	Homoscleromorpha	67, 767 contigs	Nichols et al. 2012*
Stylissa carteri	Demospongiae	26, 967 proteins	Ryu et al. 2016*
Sycon ciliatum	Calcarea	50, 731 proteins	Fortunato et al. 2014a;b*
Leucoselonia complicata	Calcarea	92, 106 proteins	Fortunato et al. 2014a; b*
TRANSCRIPTOMES			
Species	**Class**	**Contigs (DNA) or Proteins Assembled**	**Reference**
Ephydatia muelleri	Demospongiae	85, 971 contigs 28, 154 proteins	Peña et al. 2016*
Haliclona amboensis	Demospongiae	44, 693 contigs 20, 280 proteins	Guzman and Conaco 2016*
Haliclona tubifera	Demospongiae	50, 067 contigs 18, 000 proteins	Guzman and Conaco 2016*
Oscarella sp	Homoscleromorpha	172, 354 contigs	Ritchter et al. 2011*
Aphrocallistes vastus	Hexactinellid	46, 897 contigs 28, 243 proteins	Riesgo et al. 2014a
Spongilla lacustris	Demospongiae	70; 220 contigs 15, 025 proteins	Riesgo et al. 2014a
Petrosia ficiformis	Demospongiae	49, 507 contigs 20, 152 proteins	Riesgo et al. 2014a
Pseudospongorites suberitoides	Demospongiae	20, 925 contigs 11, 536 proteins	Riesgo et al. 2014a
Ircina fasciculata	Demospongiae	34, 868 contigs 16, 898 proteins	Riesgo et al. 2014a
Chondrilla nucula	Demospongiae	56, 696 contigs 21, 229 proteins	Riesgo et al. 2014a

Sycon coactum	Calcarea	41, 571 contigs 19, 062 proteins	Riesgo et al. 2014a
Corticium candelabrum	Homoscleromorpha	141, 629 contigs 41, 146 proteins	Riesgo et al. 2014a
Cliona varians	Demospongiae	292, 108 contigs	Riesgo et al. 2014b
Mycale phyllophila	Demospongiae	76, 640 contigs 12,142 proteins	Quiu et al. 2015
Crella elegans	Demospongiae	203, 078 contigs	Perez-Porro et al. 2013
Latrunculia apicalis	Demospongiae	76, 210 contigs	Whelan et al. 2015
Kirkpatrickia variolosa	Demospongiae	100, 231 contigs	Whelan et al. 2015
Hyalonema populiferum	Hexactinellid	58, 839 contigs	Whelan et al. 2015
Rosella fibulata	Hexactinellid	40, 103 contigs	Whelan et al. 2015
Sympagella unix	Hexactinellid	85,237 contigs	Whelan et al. 2015
Chondrosia reniformis	Demospongiae	19, 678 contigs	Pozzolini et al. 2016
Ephydatia fluviatilis	Demospongiae	17, 149 proteins	Alié et al. 2015
Xestospongia muta	Demospongiae	35, 219 contigs	Fiore et al. 2015
Cinachyrella sp	Demospongiae	34, 147 contigs	Smith, 2013
Halisarca dujardini	Demospongiae	138, 992 contigs	Borisenko et al. 2016
Vaceletia sp	Demospongiae	Unknown	Germer et al. 2015
Oscarella carmela	Homoscleromorpha	Unknown	Schenkelaars et al. 2015;2016
Oopsacas minuta	Hexactinellid	Unknown	Schenkelaars et al. 2015, 2016
Microciona prolifera	Demospongiae	Unknown	Gaiti et al. 2015

Silicateins and spicule formation in sponges

The process of spicule formation in sponges is really complex and involves multiple chemical reactions (Wang et al. 2012; Arakaki et al. 2015). Sponges contain specific cells named "sclerocytes" which are responsible for spicule secretion (Uriz et al. 2000). The identification of these cells is via electron microscopy in which the spicule sections and the axial filament have been observed inside the cells (Leys, 2003; Uriz et al. 2003). The axial filament is a proteinaceous core formed by an organic lattice that is found inside the spicules (Werner et al. 2017). The form of this filament has been reported to be hexagonal, triangular or rhomboidal depending on the species analyzed (Garrone, 1969; Uriz et al. 2003; Werner et al. 2017). Different proteins have been reported as being responsible for the formation of spicules in representatives from the four sponge classes: silicateins and silintaphins in demosponges, silicateins and glassin in hexactinellids, carbonic anhydrases in calcareous sponges and there

is an unknown protein in homoscleromorpha sponges bearing siliceous spicules (Shimizu et al. 1998; 2015; Veremeichik et al. 2011; Riesgo et al. 2015; Voigt et al. 2017). The silicatein protein was first reported in the axial filament of the megasclere spicules from the demosponge *Tethya aurantium* comprising three isoforms (variants), with 29, 28 and 27 kDA (named alpha, beta and gamma respectively) based on a SDS/PAGE analysis. These proteins were present in relative proportions: (alpha:beta:gamma) 12:6:1 based on densitometric analyses (Shimizu et al. 1998). The silicatein alpha from this species was similar to human cathepsin L, but silicatein had a serine (at position 26) instead of a cysteine and a particular motif following this amino acid (S-YAF) (Cha et al. 1999; Fairhead et al. 2008; Brutchey and Morse, 2008). The axial filament from this species catalyzed the synthesis of silica from tetraethoxysilane (T.E.O.S.) which is a water soluble silica precursor (Cha et al. 1999; Zhou et al. 1999) and two of the amino acids forming the catalytic triad (S and H excluding N) are responsible for the alkoxysilane polycondensation at neutral pH and low temperatures (based on experimental data) (Cha et al. 1999; Brutchey and Morse, 2008). The sequences of the three silicatein variants from *T. aurantium* are not similar, but they do contain the three aminoacids forming the catalytic triad (SHN) and the motif following the serine (S-YAF) (Brutchey and Morse, 2008). Silicatein protein molecules self-assemble via "fractal intermediates" to form stable silicatein filaments (Cha et al. 1999: Murr and Morse, 2005; Wang et al. 2012). Experimental data suggested that silicatein functions both as an enzyme and as a structure-forming template for silica formation (Müller et al. 2005; 2013; Murr and Morse, 2005).

Silicateins have been characterized, by sequencing the genes using either RT-PCR followed by Sanger sequencing or transcriptomics, from some demosponge species bearing spicules belonging to marine haplosclerids, freshwater sponges and other heteroscleromorpha (SHN

type) (Pozzolini et al. 2004; Müller et al. 2013; Riesgo et al. 2015). In addition, silicatein sequences were reported for a demosponge lacking spicules (*Acanthodendrilla* sp) and three hexactinellid species (Müller et al. 2008; Kozhemyako et al. 2010; Veremeichik et al. 2011). The number of silicatein variants described in selected species is very diverse; for example one silicatein was reported for *Petrosia ficiformis* but six for *Ephydatia fluviatilis* (Pozzolini et al. 2004; Mohri et al. 2008). Molecular phylogenetic studies revealed that silicateins evolved from cathepsins-L and they are grouped into three main clades: alpha and gamma, beta, and freshwater sponges (SHN type) (Mohri et al. 2008; Kozhemyako et al. 2010; Riesgo et al. 2015).

In addition, unusual silicateins with a cysteine instead of a serine but the -YAF motif were reported for some demosponge species bearing spicules (CHN type) (i.e. *Latrunculia oparinae*, *Amphimedon queenslandica* and *Petrosia ficiformis*) (Kozhemyako et al. 2010; Gauthier, 2015; Riesgo et al. 2015) and other silicatein variants with either a cysteine or serine in the active site but the histidine replaced by glutamine (C/SQN type). These alternative variants were present only in the genomes and transcriptomes from two marine haplosclerids (Gauthier, 2015; Riesgo et al. 2015). Sequences from such alternative silicatein variants (CHN and C/SQN type) were found to belong to the overall silicatein clade but not in any of the three major clades containing the silicateins of the SHN type (Riesgo et al. 2015). Prior to commencing any functional work on the skeleton of the Irish haplosclerid species included here, it was necessary to first identify the genes/variants that are involved and their evolutionary relationships. I determined the diversity and phylogenetic relationships of all the silicatein variants (SHN, CHN and C/SQN) by identifying these genes in all the available genomes and transcriptomes from Porifera with particular focus on marine haplosclerids.

The “glassin” protein has been reported inside the siliceous skeletal system in the hexactinellid sponge *Euplectella* sp. This protein has a high histidine content and the recombinant form had the capacity to condense silica from silicic acid at neutral pH (Shimizu et al. 2015).

The mechanism of spicule formation has only been characterized in primmorphs from the demosponge *Suberites domuncula* that has tylostyles as megasclere spicules (Müller et al. 2005). In this species, silicateins alpha and beta form pentameric units via fractal intermediates that are stabilized by the silintaphin-1 protein (Müller et al. 2013) and these three proteins are the units forming the axial filament. The silicatein proteins also have an enzymatic activity depositing the biosilica around the proteinaceous core. Another interacting proteins such as silintaphin-2 and Bone Morphogenetic Protein (BMP-1), provide calcium cations for the formation of organic cilinders in the growing spicules. In addition, galectin form together with silicatein molecules the organic sheets that are layered around the growing spicule (Müller et al. 2013) (Figure 5).

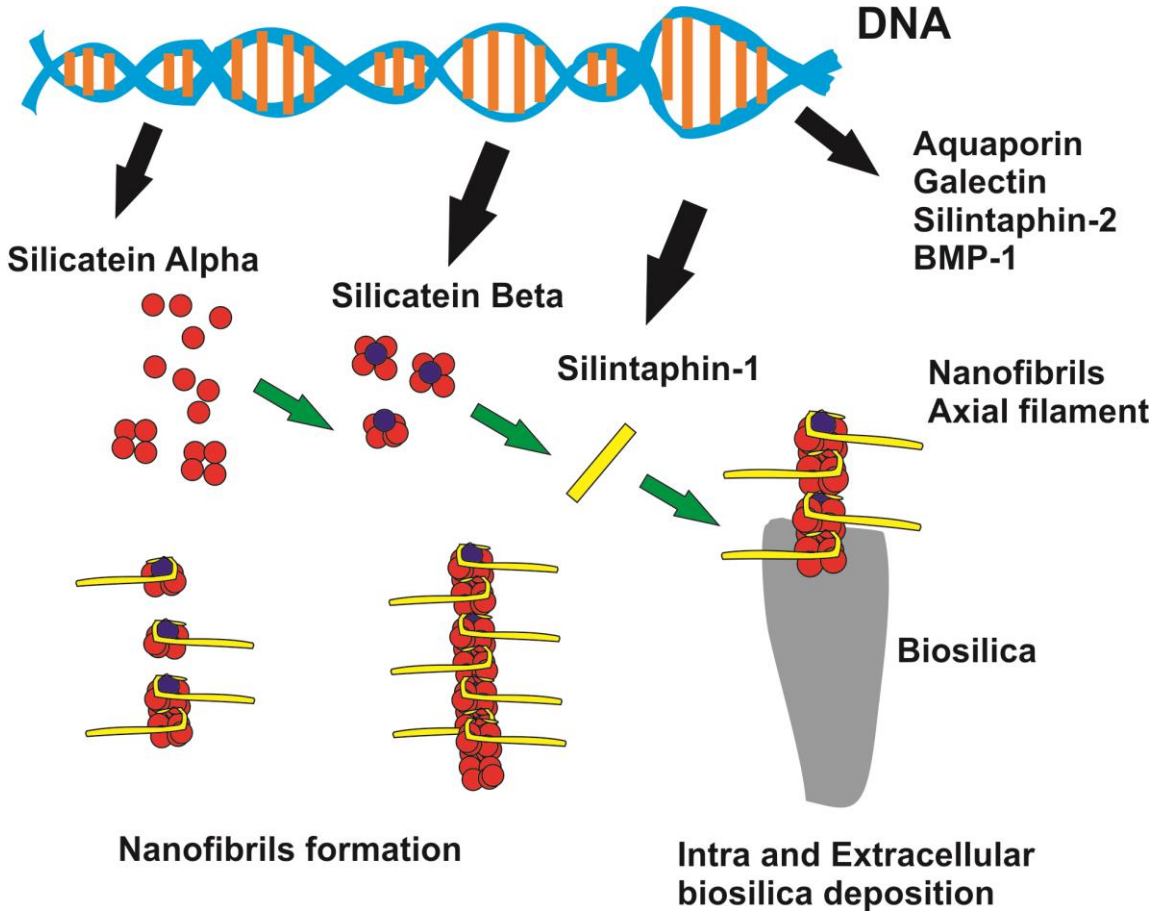

Figure 5. Schematic drawing outlining the genetic hierarchy of gene expression of *S. domuncula* adapted from Müller et al. (2013) during which sequentially silicatein alpha and beta are expressed, followed by the synthesis of silintaphin-1 that together form the initial nanofibrils that allow the synthesis and deposition of biosilica material around them. Additional interacting proteins are expressed after.

The synthesis of biosilica includes the formation of monomeric orthosilicate building blocks from which the water is eliminated after hardening. Initial spicule formation starts intracellularly in special vesicles (named silicasomes) (Schröder et al. 2006). Then the spicules are extruded into the extracellular space where they are completed (Müller et al. 2005). The axial filament (within the axial canal) is employed as a template for the spicule growth in the axial direction and around the axial canal where the silica is deposited (Wang et al. 2014). Two deposition centers exist in the spicules, the first one around the axial filament

in the axial canal and the second one on the surface of the growing spicules (Müller et al. 2013). The spicule is molded by the silicatein proteins (biosilica is pressed and hardened) and additional interacting proteins such as galectin and collagen.

Studies about the expression and localization of silicatein genes are relatively scarce. For instance, different silicatein variants were present in the ectosome and choanosome (containing different spicules) of the demosponge *Geodia cydonium* based on SDS/PAGE (Müller et al. 2007). Six silicatein variants (SHN type) were differentially expressed during the formation of two spicule types (gemmuloscleres and oxeas) from the freshwater sponge *Ephydatia fluviatilis* based on Whole Mount *in situ* Hybridization (Mohri et al. 2008). The expression levels of four silicatein variants (SHN type) were investigated in three different parts (top, middle part and base) of the arborescent freshwater sponge *Lubomirskia baicalensis* based on Northern Blots (Wiens et al. 2006). The four variants were expressed at the top part but not at the base part, while only two variants were expressed at the middle part (Wiens et al. 2006). Gauthier (2015) studied the levels of expression of six silicatein variants of the three types (CHN, SHN and SQN) through different developmental stages in the sponge *A. queenslandica* based on RT-qPCR. At all these phases, the spicules were produced (e.g. embryo, larva and competent larva) and the genes were differentially expressed but they showed the same sequential expression pattern. All these studies showed that silicatein genes were expressed during the formation of spicules and that some variants are much more highly expressed than others. In addition, some silicateins were highly expressed during the formation of one of the spicule types found in a particular species, while others were expressed during the formation of additional spicule types. There are still gaps in the knowledge of the expression levels of each of the silicatein variants in additional species and

there is little information whether or not there is the same sequential pattern through different developmental stages. In this thesis, I investigated the expression levels of all the silicatein variants of one haplosclerid species (which I generated via transcriptomics) through different developmental phases.

Biotechnological applications of the silicatein protein

There is a great biotechnological interest in the catalytic activity of the silicatein protein that can condense silicon alkoxides at low temperature and neutral pH (Cha et al. 2000; Sumerel et al. 2003; Curnow et al. 2006; Shkryl et al. 2017). Silica crystalline nanocrystals that could be employed as drug delivery systems, novel electronic devices or light emitting diodes were obtained using recombinant silicateins with water soluble silica precursors (i.e. T.E.O.S. or T.H.E.O.S.) (Bawazer et al. 2012; Priolo et al. 2014; Peng et al. 2014; Shkryl et al. 2016). The formation of uniform silica films with controlled thickness, roughness and hydrophilicity has been achieved using immobilized silicateins on gold coated surfaces (Belton et al. 2010; Rai and Perry, 2012). Recombinant silicateins have successfully been used to produce layers of titania, silica and zirconia from Ti(BALDH), T.E.O.S. and hexafluorozirconate (Tahir et al. 2004; 2005). Titania coating from Ti(BALDH) on the surface of WS_2 nanotubes was also mediated by the immobilized recombinant silicatein (Tahir et al. 2009). Tissue culture plates modified with silicatein-mediated deposition of silica enhanced the activity of bone mineralizing cells (Schröder et al. 2005). Glu-tag immobilized recombinant silicateins catalyzed the synthesis of biosilica coatings from sodium metasilicate on both synthetic hydroxyapatite nanofibrils and dental hydroxyapatite (Natalio et al. 2010).

Given that the production of recombinant silicateins allows the synthesis of metal oxides from water soluble precursors of some elements (e.g. Titania from Ti(BALDH)), and that

recombinant silicateins were able to condense silica nanocrystals, I was keen to produce a recombinant silicatein from one haplosclerid species mainly for the condensation of silica nanocrystals but also as an approach to investigate the function of non SHN variants present in the genomes and transcriptomes from marine haplosclerids.

Scope of this thesis

The major objective of this thesis is to gain insights into the evolution and development of the skeleton in selected marine haplosclerids using a multidisciplinary approach to understand how the spicules are constructed in selected species.

In **Chapter 2**, I studied the chemical composition of the spicules and tissue from nine marine *Haliclona* species from the Mediterranean and Irish coast employing ICP-MS, ICP-OES, SEM-EDS and FTIR-ATR. The purpose of this study was to verify whether or not the composition of the elements (spicules) of the skeleton in these species could reflect a phylogenetic pattern. However, there were no differences in the major elements of these structures (similar amounts of biogenic silica). However, one species had the highest amounts of other trace elements (*H. indistincta*) compared to the remaining eight *Haliclona* species and the cause of this difference could be an environmental factor.

In **Chapter 3**, I generated transcriptomes from marine haplosclerid species that are dispersed in the three major molecular clades: A) *H. oculata*, B) *H. simulans* and C) *H. indistincta*. These species have the same megasclere spicules (oxeas) but different skeletal arrangements and spicule sizes. The purpose of this study was to identify the main genes producing spicules (silicateins and silintaphin) in these selected species to determine the number of silicatein

variants of the three types (SHN, CHN and C/SQN) in these three species; which led to a study of these genes in all the available genomes and transcriptomes from Porifera. Silicateins were only found in species belonging to the Class Demospongiae (marine haplosclerids, freshwater sponges and other heteroscleromorpha excluding Verongimorpha and Keratosa) and there is a high duplication and diversity of these genes. A molecular phylogenetic analysis of the silicatein genes is presented and a new scheme proposed in which these genes are divided into six major clades. The molecular phylogeny of orthologous silicatein copies from marine haplosclerids reflected the previous ribosomal and mitochondrial topology. In addition, the sequences of marine haplosclerids were located in a different subclade compared to sequences from freshwater sponges and other heteroscleromorpha. The CHNI clade contained sequences of freshwater sponges and haplosclerids and was a sister to the remaning silicatein clades. One silicatein from *H. indistincta* was more closely related to the cathepsins L (outgroup) clade rather than to the overall silicatein clade . These data could suggest that marine haplosclerids were one of the first groups of extant demosponges that acquired silicatein genes. Furthermore, the genomes and transcriptomes from marine haplosclerids analyzed in this study, do not have silicateins of the SHNII type, just one silicatein of the SHNI type, and the silintaphin gene is lacking. This genomic characteristic could be associated with the simplicity of the skeleton in species belonging to this order.

In **Chapter 4**, I investigated the expression levels of the silicatein variants through different developmental stages in the sponge *H. indistincta* to verify whether or not the silicateins of the CHN and C/SQN could be expressed in the phases when the spicules were produced based on RT-qPCR. I identified the cells and the axial filament using microscopic techniques at early developmental stages. This species was selected because the reproductive cycle is

known and the free swimming larvae lack spicules and these structures are formed at later stages. In general, there was a positive correlation between the expression levels of the silicatein genes and the production of the spicules at the pre-settled stage. The silicateins of the CHN and C/SQN were highly expressed at the stages when the spicules were formed and the five genes were differentially expressed at all the developmental phases studied. The production of these structures is intracellular and the axial filament has an hexagonal shape at the middle part of the spicule and a triangular shape at the end of the spicule.

In **Chapter 5,** I overexpressed one silicatein gene (SHN type) from *H. indistincta* in the cytoplasmic region of *E. coli* BL21 (DE3) strain. The aim of this experiment was to refold and purify a recombinant silicatein of the SHN type that can condense silica nanocrystals. I also wanted to develop a standard methodology for this variant that could be applied to the non-SHN variants that were found in the transcriptomes from marine haplosclerids as an additional approach to investigate their function. The silicatein of the SHN type was expressed in the bacterial vector and the recombinant protein was successfully produced. SDS/PAGE revealed that this protein formed inclusion bodies (22 kDA). Two methods to purify and refold this protein were attempted but unfortunately they were not successful. The production of recombinant silicateins is very complicated, while the refolding and purification of these proteins is very difficult because the silicatein tends to precipitate, has limited solubility after refolding and has many cysteines.

References

Adell, T., Nefkens, I., Müller, W. E. (2003). Polarity factor 'Frizzled' in the demosponge *Suberites domuncula*: identification, expression and localization of the receptor in the epithelium/pinacoderm. FEBS letters, 554(3), 363-368.

Aguilar-Camacho, J. M., McCormack, G. P. (2017). Molecular Responses of Sponges to Climate Change. In: Climate Change, Ocean Acidification and Sponges (pp. 79-104). Springer, Cham.

Alié, A., Hayashi, T., Sugimura, I., Manuel, M., Sugano, W., Mano, A., Sato, N., Agata, K., Funayama, N. (2015). The ancestral gene repertoire of animal stem cells. Proceedings of the National Academy of Sciences, 112(51), E7093-E7100.

Arakaki, A., Shimizu, K., Oda, M., Sakamoto, T., Nishimura, T., Kato, T. (2015). Biomineralization-inspired synthesis of functional organic/inorganic hybrid materials: organic molecular control of self-organization of hybrids. Organic and biomolecular chemistry, 13(4), 974-989.

Bawazer, L. A., Izumi, M., Kolodin, D., Neilson, J. R., Schwenzer, B., Morse, D. E. (2012). Evolutionary selection of enzymatically synthesized semiconductors from biomimetic mineralization vesicles. Proceedings of the National Academy of Sciences, 109(26), E1705-E1714.

Bayari, S.H., Şen, E.H., Ide, S., Topaloglu, B. (2018) Structural studies on Demospongiae sponges from Gökçeada Island in the Northern Aegean Sea. Spectrochimica Acta Part A, 192, 368–377.

Bell, J. J. (2008). The functional roles of marine sponges. Estuarine, coastal and shelf science, 79(3), 341-353.

Belton, D. J., Deschaume, O., Patwardhan, S. V., Perry, C. C. (2010). A solution study of silica condensation and speciation with relevance to in vitro investigations of biosilicification. The Journal of Physical Chemistry B, 114(31), 9947-9955.

Brutchey, R. L., Morse, D. E. (2008). Silicatein and the translation of its molecular mechanism of biosilicification into low temperature nanomaterial synthesis. Chemical reviews, 108(11), 4915-4934.

Cha, J. N., Shimizu, K., Zhou, Y., Christiansen, S. C., Chmelka, B. F., Stucky, G. D., Morse, D. E. (1999). Silicatein filaments and subunits from a marine sponge direct the polymerization of silica and silicones in vitro. Proceedings of the National Academy of Sciences, 96(2), 361-365.

Cha, J. N., Stucky, G. D., Morse, D. E., Deming, T. J. (2000). Biomimetic synthesis of ordered silica structures mediated by block copolypeptides. Nature, 403(6767), 289.

Conaco, C., Neveu, P., Zhou, H., Arcila, M. L., Degnan, S. M., Degnan, B. M., Kosik, K. S. (2012). Transcriptome profiling of the demosponge *Amphimedon queenslandica* reveals genome-wide events that accompany major life cycle transitions. BMC genomics, 13(1), 209.

Curnow, P., Kisailus, D., Morse, D. E. (2006). Biocatalytic Synthesis of Poly (L–Lactide) by Native and Recombinant Forms of the Silicatein Enzymes. Angewandte Chemie, 118(4), 629-632.

de Goeij, J. M., van den Berg, H., van Oostveen, M. M., Epping, E. H., Van Duyl, F. C. (2008). Major bulk dissolved organic carbon (DOC) removal by encrusting coral reef cavity sponges. Marine Ecology Progress Series, 357, 139-151.

De Goeij, J. M., Van Oevelen, D., Vermeij, M. J., Osinga, R., Middelburg, J. J., de Goeij, A. F., Admiraal, W. (2013). Surviving in a marine desert: the sponge loop retains resources within coral reefs. Science, 342(6154), 108-110.

de Weerdt, W. H. (1986). A systematic revision of the north-eastern Atlantic shallow-water Haplosclerida (Porifera, Demospongiae): 2. Chalinidae. Beaufortia, (6), 81-165.

de Weerdt, W. H. (2000). A monograph of the shallow-water Chalinidae (Porifera, Haplosclerida) of the Caribbean. Beaufortia, 50(1), 1-67.

Dodd, J. P., Wiedenheft, W., Schwartz, J. M. (2017). Dehydroxylation and diagenetic variations in diatom oxygen isotope values. Geochimica et Cosmochimica Acta, 199, 185-195.

Eitel, M., Guidi, L., Hadrys, H., Balsamo, M., Schierwater, B. (2011). New insights into placozoan sexual reproduction and development. PLoS One, 6(5), e19639.

Fairhead, M., Johnson, K. A., Kowatz, T., McMahon, S. A., Carter, L. G., Oke, M., Liu, H., Naismith, J.H., van der Walle, C. F. (2008). Crystal structure and silica condensing activities of silicatein α–cathepsin L chimeras. Chemical Communications, (15), 1765-1767.

Feuda, R., Dohrmann, M., Pett, W., Philippe, H., Rota-Stabelli, O., Lartillot, N., Wörheide, G. Pisani, D. (2017). Improved Modeling of Compositional Heterogeneity Supports Sponges as Sister to All Other Animals. Current Biology, 27(24), 3864-3870.

Francis, W. R., Eitel, M., Vargas, S., Adamski, M., Haddock, S. H., Krebs, S., Blum, H., Erpenbeck, D., Wörheide, G. (2017). The Genome Of The Contractile Demosponge Tethya wilhelma And The Evolution Of Metazoan Neural Signalling Pathways. bioRxiv, 120998.

Gan, J.H., Xu, C.H., Zhu, H.Z., Mao, F., Yang, F., Zhou, Q., Sun, S.Q. (2015) Analysis and discrimination of ten different sponges by multi-step infrared spectroscopy. Chinese Chemical Letters, 26, 215–220.

Garrone, R. (1969) Collagéne, spongine et squelette mineral chez l'éponge Haliclona rosea (O.S.). Journal of Microscopy 8, 581-598.

Gauthier A (2015). Analysis of silicatein gene expression and spicule formation in the demosponge Amphimedon queenslandica. MS thesis. The University of Queensland, 84 pp.

Gazave, E., Lapébie, P., Ereskovsky, A. V., Vacelet, J., Renard, E., Cárdenas, P., Borchiellini, C. (2012). No longer Demospongiae: Homoscleromorpha formal nomination as a fourth class of Porifera. In: Ancient Animals, New Challenges (pp. 3-10). Springer, Dordrecht.

Guzman, C.,Conaco, C. (2016). Gene expression dynamics accompanying the sponge thermal stress response. PloS one, 11(10), e0165368.

Hill, M.S., Hill, A.L., Lopez, J., Perterson, K.J., Pomponi, S., Diaz, M.C., Thacker, R.W., Adamska, M., Boury-Esnault, N., Cárdenas, P., Chaves-Fonnegra, A., Danka, E., De Laine, B., Formica, D., Hajdu, E., Lobo-Hajdu, G., Klontz, S., Morrow, C.C., Patel, J., Picton, B., Pisani, D., Pohlmann, D., Redmond, N.E., Reed, J., Richie, S., Riesgo, A., Rubin, E., Russell, Z., Rützler, K., Sperling, E.A., di Stefano, M., Tarver, J.D., Collins A.G. (2013) Reconstruction of family level phylogenetic relationships within Demospongiae (Porifera)

using nuclear encoded housekeeping genes. Public Library of Science. PLOS One, 8(1): e50437.

Kozhemyako, V. B., Veremeichik, G. N., Shkryl, Y. N., Kovalchuk, S. N., Krasokhin, V. B., Rasskazov, V. A., Zhuravlev Y.N., Bulgakov V.P., Kulchin, Y. N. (2010). Silicatein genes in spicule-forming and nonspicule-forming Pacific demosponges. Marine biotechnology, 12(4), 403-409.

Lavrov, D. V., Wang, X., Kelly, M. (2008). Reconstructing ordinal relationships in the Demospongiae using mitochondrial genomic data. Molecular phylogenetics and evolution, 49(1), 111-124.

Leys, S. P. (2003). Comparative study of spiculogenesis in demosponge and hexactinellid larvae. Microscopy research and technique, 62(4), 300-311.

López-Legentil, S., Song, B., Mcmurray, S. E., Pawlik, J. R. (2008). Bleaching and stress in coral reef ecosystems: hsp70 expression by the giant barrel sponge *Xestospongia muta*. Molecular Ecology, 17(7), 1840-1849.

Ma, J. Y., Yang, Q. (2016). Early divergence dates of demosponges based on mitogenomics and evaluated fossil calibrations. Palaeoworld, 25(2), 292-302.

Maldonado, M. (2006). The ecology of the sponge larva. Canadian Journal of Zoology, 84(2), 175-194.

Maldonado, M., Uriz, M. J. (1999). Sexual propagation by sponge fragments. Nature, 398(6727), 476.

Maldonado, M., Navarro, L., Grasa, A., Gonzalez, A., Vaquerizo, I. (2011). Silicon uptake by sponges: a twist to understanding nutrient cycling on continental margins. Scientific reports, 1, 30.

Mohri, K., Nakatsukasa, M., Masuda, Y., Agata, K., Funayama, N. (2008). Toward understanding the morphogenesis of siliceous spicules in freshwater sponge: Differential mRNA expression of spicule-type-specific silicatein genes in *Ephydatia fluviatilis*. Developmental Dynamics, 237(10), 3024-3039.

Morrow, C., Cárdenas, P. (2015). Proposal for a revised classification of the Demospongiae (Porifera). Frontiers in Zoology, 12(1), 7.

Müller, W. E., Rothenberger, M., Boreiko, A., Tremel, W., Reiber, A., Schröder, H. C. (2005). Formation of siliceous spicules in the marine demosponge *Suberites domuncula*. Cell and tissue research, 321(2), 285-297.

Müller, W. E., Schloßmacher, U., Eckert, C., Krasko, A., Boreiko, A., Ushijima, H., Wolf, S., Tremel, W., Müller, I., Schröder, H. C. (2007). Analysis of the axial filament in spicules of the demosponge *Geodia cydonium*: different silicatein composition in microscleres (asters) and megascleres (oxeas and triaenes). European journal of cell biology, 86(8), 473-487.

Müller, W. E., Schröder, H. C., Burghard, Z., Pisignano, D., Wang, X. (2013). Silicateins—a novel paradigm in bioinorganic chemistry: enzymatic synthesis of inorganic polymeric silica. Chemistry-A European Journal, 19(19), 5790-5804.

Müller, W. E., Wang, X., Kropf, K., Boreiko, A., Schloßmacher, U., Brandt, D., Schröder, H.C., Wiens, M. (2008). Silicatein expression in the hexactinellid *Crateromorpha meyeri*: the lead marker gene restricted to siliceous sponges. Cell and tissue research, 333(2), 339-351.

Murr, M. M., Morse, D. E. (2005). Fractal intermediates in the self-assembly of silicatein filaments. Proceedings of the National Academy of Sciences of the United States of America, 102(33), 11657-11662.

Natalio, F., Link, T., Müller, W. E., Schröder, H. C., Cui, F. Z., Wang, X., Wiens, M. (2010). Bioengineering of the silica-polymerizing enzyme silicatein-α for a targeted application to hydroxyapatite. Acta biomaterialia, 6(9), 3720-3728.

Peng, F., Su, Y., Zhong, Y., Fan, C., Lee, S. T., He, Y. (2014). Silicon nanomaterials platform for bioimaging, biosensing, and cancer therapy. Accounts of chemical research, 47(2), 612-623.

Pfeifer, K., Frank, W., Schroder, H. C., Gamulin, V., Rinkevich, B., Batel, R., Muller, I. M., Muller, W. E. (1993). Cloning of the polyubiquitin cDNA from the marine sponge *Geodia cydonium* and its preferential expression during reaggregation of cells. Journal of cell science, 106(2), 545-553.

Pérez-Porro, A. R., Navarro-Gómez, D., Uriz, M. J., Giribet, G. (2013). A NGS approach to the encrusting Mediterranean sponge Crella elegans (Porifera, Demospongiae, Poecilosclerida): transcriptome sequencing, characterization and overview of the gene expression along three life cycle stages. Molecular ecology resources, 13(3), 494-509.

Pozzolini, M., Sturla, L., Cerrano, C., Bavestrello, G., Camardella, L., Parodi, A. M., Raheli, F., Benatti, U., Müller W.E.G., Giovine, M. (2004). Molecular cloning of silicatein gene from marine sponge Petrosia ficiformis (Porifera, Demospongiae) and development of primmorphs as a model for biosilicification studies. Marine biotechnology, 6(6), 594-603.

Priolo, F., Gregorkiewicz, T., Galli, M., Krauss, T. F. (2014). Silicon nanostructures for photonics and photovoltaics. Nature nanotechnology, 9(1), 19.

Rai, A., Perry, C. C. (2012). Mussel adhesive protein inspired coatings: a versatile method to fabricate silica films on various surfaces. Journal of Materials Chemistry, 22(11), 4790-4796.

Raleigh, J., Redmond, N. E., Delahan, E., Torpey, S., van Soest, R. W., Kelly, M., McCormack, G. P. (2007). Mitochondrial Cytochrome oxidase 1 phylogeny supports alternative taxonomic scheme for the marine Haplosclerida. Journal of the Marine Biological Association of the United Kingdom, 87(6), 1577-1584.

Redmond NE, Morrow CC, Thacker RW, Diaz MC, Boury-Esnault N, Cárdenas P, Hajdu E, Lôbo-Hajdu G, Picton BE, Pomponi SA, Kayal E, Collins AG (2013). Phylogeny and systematics of Demospongiae in light of new small-subunit ribosomal DNA (18S) sequences. Integrative and comparative biology, 53,388–415.

Redmond NE, Raleigh J, van Soest RW, Kelly M, Travers SA, Bradshaw B, Vartia S, Stephens K, McCormack G.P. (2011). Phylogenetic relationships of the marine Haplosclerida (Phylum Porifera) employing ribosomal (28S rRNA) and mitochondrial (cox1, nad1) gene sequence data. PLoS One, 6(9), e24344.

Renard, E., Leys, S. P., Wörheide, G., Borchiellini, C. (2018). Understanding Animal Evolution: The Added Value of Sponge Transcriptomics and Genomics. BioEssays, 40(9):1700237.

Riesgo, A., Maldonado, M. (2008). Differences in reproductive timing among sponges sharing habitat and thermal regime. Invertebrate Biology, 127(4), 357-367.

Riesgo, A., Farrar, N., Windsor, P. J., Giribet, G., Leys, S. P. (2014). The analysis of eight transcriptomes from all poriferan classes reveals surprising genetic complexity in sponges. Molecular biology and evolution, 31(5), 1102-1120.

Riesgo, A., Maldonado, M., López-Legentil, S., Giribet, G. (2015). A Proposal for the Evolution of Cathepsin and Silicatein in Sponges. Journal of molecular evolution, 80(5-6), 278-291.

Sandford, F. (2003) Physical and chemical analysis of the siliceous skeletons in six sponges of two groups (Demospongiae and Hexactinellida). Microscopy Research and Technique, 62(4), 336–355.

Schröder, H. C., Boreiko, A., Korzhev, M., Tahir, M. N., Tremel, W., Eckert, C., Ushijima, I., Müller, I., Müller, W. E. (2006). Co-expression and Functional Interaction of Silicatein with Galectin matrix-guided formation of siliceous spicules in the marine demosponge *Suberites domuncula*. Journal of Biological Chemistry, 281(17), 12001-12009.

Schröder, H. C., Boreiko, O., Krasko, A., Reiber, A., Schwertner, H., Müller, W. E. (2005). Mineralization of SaOS-2 cells on enzymatically (silicatein) modified bioactive osteoblast-

stimulating surfaces. Journal of Biomedical Materials Research Part B: Applied Biomaterials, 75(2), 387-392.

Şen, E.H., Ide, S., Bayari, S.H., Hill, M. (2016) Micro-and nano-structural characterization of six marine sponges of the class Demospongiae. European Biophysics Journal, 45(8), 831–842.

Shimizu, K., Amano, T., Bari, M. R., Weaver, J. C., Arima, J., Mori, N. (2015). Glassin, a histidine-rich protein from the siliceous skeletal system of the marine sponge Euplectella, directs silica polycondensation. Proceedings of the National Academy of Sciences, 112(37), 11449-11454.

Shimizu, K., Cha, J., Stucky, G. D., Morse, D. E. (1998). Silicatein α: cathepsin L-like protein in sponge biosilica. Proceedings of the National Academy of Sciences, 95(11), 6234-6238.

Shkryl, Y. N., Bulgakov, V. P., Veremeichik, G. N., Kovalchuk, S. N., Kozhemyako, V. B., Kamenev, D. G., Semiletova, I.V., Timofeeva, Y.O., Scchipunov, Y.A., Kulchin, Y. N. (2016). Bioinspired enzymatic synthesis of silica nanocrystals provided by recombinant silicatein from the marine sponge Latrunculia oparinae. Bioprocess and Biosystems Engineering, 39(1), 53-58.

Shkryl, Y. N., Veremeichik, G. N., Kamenev, D. G., Gorpenchenko, T. Y., Yugay, Y. A., Mashtalyar, D. V., Nepomnyaschiy, A.V., Avramenko, T.V., Karabtsov, A.A., Ivanov, V.V., Bulgakov, V. P., Gnedenkov, S.V., Kulchin, Y.N., Zhuravlev, Y.N. (2017). Green synthesis of silver nanoparticles using transgenic Nicotiana tabacum callus culture expressing silicatein gene from marine sponge *Latrunculia oparinae*. Artificial cells, nanomedicine, and biotechnology, 1-13.

Sperling, E. A., Robinson, J. M., Pisani, D., Peterson, K. J. (2010). Where's the glass? Biomarkers, molecular clocks, and microRNAs suggest a 200-Myr missing Precambrian fossil record of siliceous sponge spicules. Geobiology, 8(1), 24-36.

Srivastava, M., Simakov, O., Chapman, J., Fahey, B., Gauthier, M. E., Mitros, T., Richards, G.S., Conaco, C., Dacre, M., Hellsten, U., Larroux, C., Putnam, N.H., Stanke, M., Adamska, M., Darling, A., Degnan, S.M., Oakley, T.H., Plachetzki, D.C., Zhai, Y., Adamski, M., Calcino, A., Cummins S.F., Goodstein, D.M., Harris, C., Jackson, D.J., Leys, S.P., Shu, S., Woodcroft, B.J., Vervoort, M., Kosik, K.S., Manning, G., Degnan, B.M., Rokhsar, D. S. (2010). The *Amphimedon queenslandica* genome and the evolution of animal complexity. Nature, 466(7307), 720-726.

Stephens, K. (2013).Insights into the evolution and development of *Haliclona indistincta* (Porifera, Haplosclerida)(Doctoral dissertation) N.U.I.G. 225 pp.

Sumerel, J. L., Yang, W., Kisailus, D., Weaver, J. C., Choi, J. H., Morse, D. E. (2003). Biocatalytically templated synthesis of titanium dioxide. Chemistry of materials, 15(25), 4804-4809.

Tahir, M. N., Natalio, F., Therese, H. A., Yella, A., Metz, N., Shah, M. R., Mugnainoli, E., Berger, R., Theato, P., Schröder, H. C., Müller, W. E., Tremel, W. (2009). Enzyme-mediated deposition of a TiO_2 coating onto biofunctionalized WS_2 chalcogenide nanotubes. Advanced Functional Materials, 19(2), 285-291.

Tahir, M. N., Théato, P., Müller, W. E., Schröder, H. C., Borejko, A., Faiß, S., Janshoff, A., Huth, J., Tremel, W. (2005). Formation of layered titania and zirconia catalysed by surface-bound silicatein. Chemical Communications, (44), 5533-5535.

Tahir, M. N., Théato, P., Müller, W. E., Schröder, H. C., Janshoff, A., Zhang, J.,Huth, J.,Tremel, W. (2004). Monitoring the formation of biosilica catalysed by histidine-tagged silicatein. Chemical Communications, (24), 2848-2849.

Uriz, M. J., Turon, X., Becerro, M. A. (2000). Silica deposition in Demosponges: spiculogenesis in *Crambe crambe*. Cell and tissue research, 301(2), 299-309.

Uriz, M. J., Turon, X., Becerro, M. A., Agell, G. (2003). Siliceous spicules and skeleton frameworks in sponges: origin, diversity, ultrastructural patterns, and biological functions. Microscopy research and technique, 62(4), 279-299.

Van Soest, R. W. M. (1980). Marine sponges from Curaçao and other Caribbean localities Part II. Haplosclerida. Studies on the Fauna of Curaçao and other Caribbean Islands, 62(1), 1-173.

Van Soest, R. W., Hooper, J. N. (2002). Order Haplosclerida Topsent, 1928. In: Systema Porifera (pp. 831-832). Springer, Boston, MA.

Veremeichik, G. N., Shkryl, Y. N., Bulgakov, V. P., Shedko, S. V., Kozhemyako, V. B., Kovalchuk, S. N., Krasokhin, V. B., Zhuralev, Y.N., Kulchin, Y. N. (2011). Occurrence of a silicatein gene in glass sponges (Hexactinellida: Porifera). Marine biotechnology, 13(4), 810-819.

Voigt, O., Adamska, M., Adamski, M., Kittelmann, A., Wencker, L., Wörheide, G. (2017). Spicule formation in calcareous sponges: Coordinated expression of biomineralization genes and spicule-type specific genes. Scientific Reports, 7:45658.

Wang, X., Schloßmacher, U., Wiens, M., Batel, R., Schröder, H. C., Müller, W. E. (2012). Silicateins, silicatein interactors and cellular interplay in sponge skeletogenesis: formation of glass fiber-like spicules. The FEBS journal, 279(10), 1721-1736.

Wang, X., Schröder, H. C., Müller, W. E. (2014). Enzyme-based biosilica and biocalcite: biomaterials for the future in regenerative medicine. Trends in biotechnology, 32(9), 441-447.

Werner, P., Blumtritt, H., Natalio, F. (2017). Organic crystal lattices in the axial filament of silica spicules of Demospongiae. Journal of structural biology, 198(3), 186-195.

Wiens, M., Belikov, S. I., Kaluzhnaya, O. V., Krasko, A., Schröder, H. C., Perovic-Ottstadt, S., Müller, W. E. (2006). Molecular control of serial module formation along the apical–basal axis in the sponge *Lubomirskia baicalensis*: silicateins, mannose-binding lectin and mago nashi. Development genes and evolution, 216(5), 229.

Whelan, N. V., Kocot, K. M., Moroz, L. L., Halanych, K. M. (2015). Error, signal, and the placement of Ctenophora sister to all other animals. Proceedings of the National Academy of Sciences, 112(18), 5773-5778.

Zhou, Y., Shimizu, K., Cha, J. N., Stucky, G. D., Morse, D. E. (1999). Efficient catalysis of polysiloxane synthesis by silicatein α requires specific hydroxy and imidazole functionalities. Angewandte Chemie International Edition, 38(6), 779-782.

Chapter 2

Insights gained from the chemical composition of spicules from marine sponges (Phylum Porifera, Order Haplosclerida).

Introduction

Sponges (Phylum Porifera) have a skeleton composed of silica or calcium carbonate. The varying shapes and sizes of the skeletal structures, called spicules, and how they are arranged to provide support to the sponge body are used both as diagnostic features for species identification and also for their classification. Members of the class Demospongiae have siliceous spicules and comprise the vast majority of the species (Uriz et al. 2013; Wörheide et al. 2012). Silica materials are of great interest in nanobiotechnology, microelectronics and drug delivery but controllable silicate formation is very difficult (Cha et al. 2000; Fairhead et al. 2008; Wibowo et al. 2017). Understanding the nature and the production of spicules in sponges may provide insight into their correct classification and also contribute to development of applications in the biomaterials sector.

The most diverse class Demospongiae is currently divided in to three subclasses, and while members of Heteroscleromorpha have a wide diversity of spicules (Morrow and Cárdenas, 2015) members of the demosponge order Haplosclerida possess very simple skeletal structures primarily comprised of large spicules (megascleres) pointed at both ends, called oxeas, and smaller spicules (microscleres), if they are present, are sigmas, toxas and microxeas (van Soest, 2017). Due to the simplicity of the skeleton in haplosclerid sponges, and the paucity of morphological traits to compare between species, classification in this group is difficult and has a long and complicated history. The current classification divides the order Haplosclerida into six families and the species-rich genus *Haliclona* into seven subgenera (*Haliclona* Grant 1841, *Flagellia* van Soest 2017, *Gellius* Gray 1867, *Rhizoniera* Griessinger 1971, *Reniera* Schmidt 1862, *Halichoclona* de Laubenfels 1932 and *Soestella* de Weerdt 2002) housing approximately 500 species which are important components of benthic

ecosystems, and are prolific producers of bioactive compounds (Senthilkumar et al. 2013; Zovko et al. 2014). Recent molecular studies revealed polyphyly at all taxonomic ranks in the order based on mitochondrial and ribosomal markers (Redmond et al. 2007; 2011; 2013). This suggests that classification of species assigned to the genus *Haliclona* based on current interpretations of their skeletal architecture may not accurately reflect their evolutionary history. Therefore, it is important to further investigate the skeleton in species of *Haliclona* to help understand which elements of its features maybe shaped by environmental factors and which have a strong genetic basis.

The siliceous spicules in demosponges are produced mainly by silicatein proteins through enzymatic reactions (Pozzolini et al. 2004). The spicules are embedded in collagen sheets or fibres by specific cell types and they form the skeletal architecture of a particular species (Nakayama et al. 2015; van Soest, 2017). The nine species included in this study are well known species, which have been included in a phylogenetic framework based on molecular data and they all have oxeas and no microscleres and so provide a good group of species for investigation. The relative positions of each species within the order Haplosclerida based on molecular data are presented in Figure 1. This Figure also shows their generalized skeletal arrangements. *H. cinerea*, *H. mediterranea* and *H. oculata* have a delicate choanosomal skeleton made of uni- or bispicular primary tracts connected by secondary unispicular tracts and is a member of clade A (Redmond et al. 2011; 2013). *H. simulans* has a dense skeleton made of primary multispicular tracts connected by secondary uni- bi- or multispicular tracts and is a member of Clade B (Redmond et al. 2011*). H. sarai, H. viscosa* and *H. indistincta* have a partially disorganized choanosomal skeleton made of primary multispicular tracts connected by secondary uni- or bispicular tracts and are member of clade C (Longakit,

unpublished data) while *H. fulva* and *H. mucosa* have a choanosomal skeleton made of primary uni- or bispicular tracts interconnected by secondary uni- or bispicular tracts and are currently in an unresolved position in a poorly sampled clade close to Clade A (Redmond et al. 2011). Given that molecular data indicates that the species of *Haliclona* included are placed in very distinct clades of the order Haplosclerida (itself a very large and diverse group of demosponges), I considered that the chemical composition of the spicules and tissue may provide useful phylogenetic information on the evolution of the skeleton in this group.

The chemical composition of demosponge and hexactinellid spicules are reported to be largely comprised of glassy amorphous hydrated silica ($SiO_2 \bullet nH_2O$) (Uriz et al. 2003), but also containing traces of other elements (such as: S, Al, P, K, Na, Ca and others) via SEM-EDS and ICP-MS analyses (Sandford, 2003; Şen et al. 2016). Currently, there is little information whether or not the chemical composition of spicules is the same in closely related species (Sandford, 2003). FTIR-ATR is a spectroscopic technique, that have been utilized to detect certain functional groups and also to distinguish species and investigate phylogenetic relationships in organisms such as fungi, flowering plants and cyanobacteria, based on the spectrum profile from the tissue (or cell) of each species investigated (Naumann, 2009; Kim et al. 2004; Kenne and van der Merwe, 2013). This spectroscopic technique has been applied also to the tissue from sponges to discriminate between species and investigate phylogenetic relationships (Gan et al. 2015; Şen et al. 2016). The aims of this study were to determine the chemical composition of spicules and tissue from nine *Haliclona* species (Atlantic and Mediterranean) using a suite of microscopic, chemical and spectroscopic techniques.

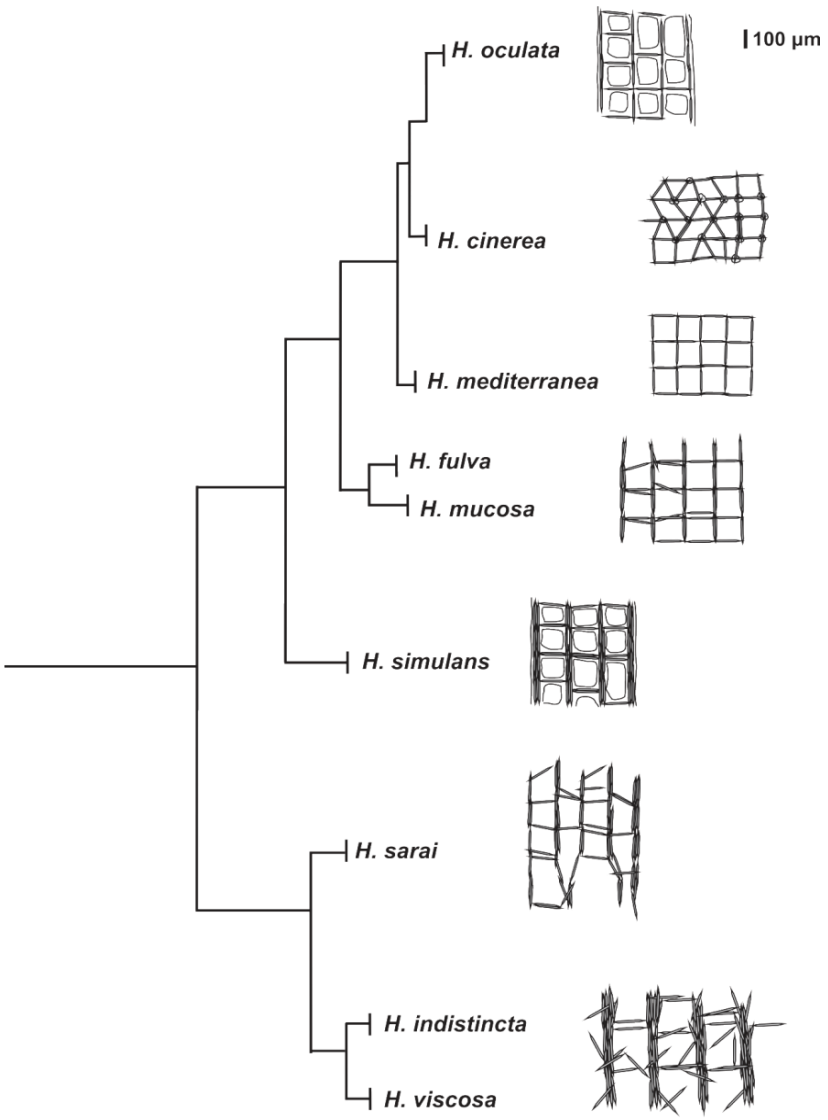

Figure 1. Proposed phylogeny of the *Haliclona* species in this study with my interpretations of their skeletal arrangement (based on de Weerdt, 1986; Redmond et al. 2011; 2013).

Materials and Methods

Sample collection

Sponge samples were collected in four different localities in European waters by hand collection on the shore or by scuba diving: *Haliclona oculata*, Strangford Lough, Northern Ireland (N 54°, 23.355; W 05°, 34.340), *H. simulans*, *H. cinerea*, *H. viscosa*, Gurraig Sound, Galway, Ireland (N 53°, 18.944; W 09°, 40.140), *H. indistincta*, Corranroo, Co. Clare, Ireland

(N 053°09.100, W 009°,00. 550) and *H. sarai*, *H. mucosa*, *H. mediterranea*, *H. fulva*, Villefranche sur Mer, France (N 43° 41' 31.487; E 7° 19' 12.1856) (Table 1) and fixed in reagent ethanol (70%, ACS Reagent, Sigma-Aldrich, Missouri, USA).

Table 1. Comparative table of the *Haliclona* species of this study. Spicule measurements in μm from the original description: a) de Weerdt, 1986. b) Griessinger, 1971.

Species	Code	Collection Date	Locality	Coordinates	Depth	Spicule measurements (Length × Width)
H. oculata	MIIG 1098	01/12/2014	Stranford Lough, UK	N 54°, 23.355; W 05°, 34.340	12 m	90–135 × 4–12.5[a]
H. cinerea	MIIG 1104	02/12/2014	Gurraig Sound, IRE	N 53°, 18.944; W 09°, 40.140	5 m	80–120 × 4–8[a]
H. simulans	MIIG 1014	22/05/2014	Gurraig Sound, IRE	N 53°, 18.944; W 09°, 40.140	6 m	100–175 × 7–13.5[a]
H. viscosa	MIIG 1012	21/05/2014	Gurraig Sound, IRE	N 53°, 18.944; W 09°, 40.140	6 m	110–150 × 3– 7.5[a]
H. indistincta	MIIG 1124	19/01/2015	Corranroo, IRE	N 53°09.100; W 09,°00.550	0.5 m	110–150 × 3 – 7.5[a]
H. mucosa	IRC 425	26/06/2015	Villefranche sur Mer, FRA	N 43° 41.314; E 07°, 19.121	10 m	100–280 × 2.5–8.5[b]
H. sarai	IRC 428	26/06/2015	Villefranche sur Mer, FRA	N 43° 41.314; E 07°, 19.121	10 m	90–195 × 2.5–7.5[b]
H. fulva	IRC 423	26/06/2015	Villefranche sur Mer, FRA	N 43° 41.314; E 07°, 19.121	10 m	130–300 × 3–13.5[b]
H. mediterranea	IRC 427	26/06/2015	Villefranche sur Mer, FRA	N 43° 41.314; E 07°, 19.121	10 m	70–110 ×1.5–4.5[b]

Spicule preparation

In order to remove the organic matter, sponge fragments were placed in 20 ml Pyrex® test tubes with 15 ml of the oxidizing agent nitric acid (65 % HNO_3, trace metal free grade, Fisher Scientific, Loughborough, UK). Spicules were subsequently washed with Milli-Q™ water (18.3 MΩ·cm, Millipore, Bedford, USA) to remove salts and then were transferred to 1.5 ml polypropylene Eppendorf® tubes and centrifuged at 500 rpm for 1 minute (Galaxy 14D VWR™, Pennsylvania, USA).

Attenuated total reflectance Fourier transform infrared spectroscopy (FTIR-ATR)

Attenuated total reflectance and Fourier transform infrared spectroscopy (ATR/FTIR) was used to analyze the spicules and tissue from the nine species. The spicule samples were placed in an Eppendorf Thermomixer® at 99°C until the water evaporated and the spicules were dry. Freeze dried material (tissue) from each species was also analyzed. The absorbance for spicules and tissue samples was obtained using a Schimadzu FTIR-8300 (Schimadzu Corporation, Kyoto, Japan) at 4 cm^{-1} resolution and spectra were collected over the wavenumber range of 600-4000 cm-^{1} (20 scans per sample) (Jonker et al. 2015). The absorbance of silica (Sigma-Aldrich, Missouri, USA) was also measured for comparison. For each sample, a background spectrum of the instrument was recorded over the same wavenumber range as that of the sample. Each background spectrum was then automatically subtracted from each sample spectrum. Dendrograms of the ATR / FTIR spectra were created using MATLAB® 7.7.0.471 (The Mathworks Inc., Natick, MA). The height of the peak from 1000 to 1100 cm^{-1} was selected as a reference, to normalize the height of ten selected peaks of each species, as it was the strongest in the spectra from the tissue samples. Dendrograms were created with the normalized data using average Euclidean distance hierarchical cluster analysis for each data set of the spectra and the Cophenetic Correlation Coefficient was estimated (Kenne and van der Merwe, 2013). The final dendrogram was constructed based on the intensity of the ten peaks of the spectra profile of the freeze dried tissue.

Scanning Electron Microscopy and Energy Dispersive Spectrometry (SEM-EDS)

Spicules were gold coated (Emitech K550, Quorum Technologies Ltd, West Sussex, United Kingdom) and subjected to scanning electron microscopy (SEM) in secondary electron mode using a Hitachi model S-4700 (Hitachinaka, Japan). The analyses were performed at an acceleration voltage of 20 kv, an emission current (Ic) of 10 µA and a working distance of 12 mm (Morrison et al. 2009). Energy dispersive spectrometry (EDS) [INCA®; Oxford Instruments (High Wycombe, Uk)] in point and mapping modes were employed to determine the presence of a range of elements on the spicule surface and interior. Spatial element distribution mapping of the spicules were performed, and the maps generated represented the spatial abundance of an element over a predetermined area where the pixel brightness represents the relative intensity. A color scale from black to white presented below each spicule element distribution map represents low to high element abundances respectively (Morrison et al. 2009).

Inductively Coupled Plasma - Mass Spectrometry (ICP-MS) and Inductively Coupled Plasma – Optical Emission Spectrometry (ICP-OES)

Spicule samples were pulverized and approximately 0.1g (dry weight) of spicules was fused using lithium metaborate/lithium tetraborate (0.9g). The resulting melt was dissolved in dilute aqua regia (HNO_3 : HCL, 3:1). Major (Si, Al, Ca, Mg, Na, K, Fe, Ti, Mn and P), rare earth (Ce, Dy, Er, Eu, Gd, Ho, La, Lu, Nd, Pr, Sm, Tb, Tm, Y and Yb) and trace element (Ba, Cr, Cs, Ga, Hf, Nb, Rb, Sn, Ta, Th, U, V, W, Zr, Co, Cu, Mo, Ni, Pb and Zn) concentrations were determined using an Agilent 725 ICP-OES system and 7700x ICP-MS system (Agilent

Technology, Santa Clara, CA, USA). These analyses were performed by the accredited ALS Minerals Laboratory (Galway, Ireland) (ALS method code: ME-ICP06 and ME-MS81).

Results

The FTIR spectra for the spicules of the nine *Haliclona* species are very similar (Figure 2a). They are characterized by the presence of typical vibrational modes of silica (Si-O-Si): one peak corresponding to a stretching vibration from 1020 to 1040 cm^{-1} and two additional peaks corresponding to medium vibrations from 770 to 790 cm^{-1} and from 910 to 940 cm^{-1} (Hunt, 1970; Gendron-Badou et al. 2003). The spectra also show some peaks corresponding to bending vibrations from 1600 to 1630 cm^{-1} and from 3400 to 3600 cm^{-1} (not shown in the figure) corresponding of -OH and -NH groups engaged in hydrogen bonds (Sandford, 2003; Gendron-Badou et al. 2003; Croce et al. 2004). The FTIR-ATR spectrum of silica (SiO_2) is similar to the spectra of the spicules from the nine *Haliclona* species (Figure 2b).

The SEM-EDS spatial distribution mapping detected only silica from the spicules (Figure 3). Using ICP-OES the highest percentage of biogenic silica in the spicules was found in *H. sarai* (89.4%) while *H. mediterranea* contained the lowest value (75.4%) (Table 2 and Figure 4). ICP-OES and ICP-MS analysis confirmed the presence of additional elements in the spicules and in most cases the amount present in *H. indistincta* was much greater than those present in the other sponge species, often by an order of magnitude or higher (Table 2; Figure 4). As detailed in Table 2 the major elements detected were Al (ranging from 0.03% in *H. simulans* to 1.54% in *H. indistincta*), Na (ranging from 0.014% in *H. cinerea* to 0.363% in *H. indistincta*), Fe (ranging from 0.006% in *H. simulans* to 0.202% in *H. indistincta*), K (ranging from 0.008% in *H. simulans* to 0.498% in *H. indistincta*),Ca (ranging from 0.007% in *H. simulans* to 0.078% in *H. indistincta*), Ti (ranging from <0.005% in *H. simulans* to 0.95% in

H. indistincta) Mg (ranging from <0.006% ion *H. fulva* a 0.066% in *H. indistincta*), and Mn (ranging from <0.007% in *H. simulans* to 0.015% in *H. indistincta*).

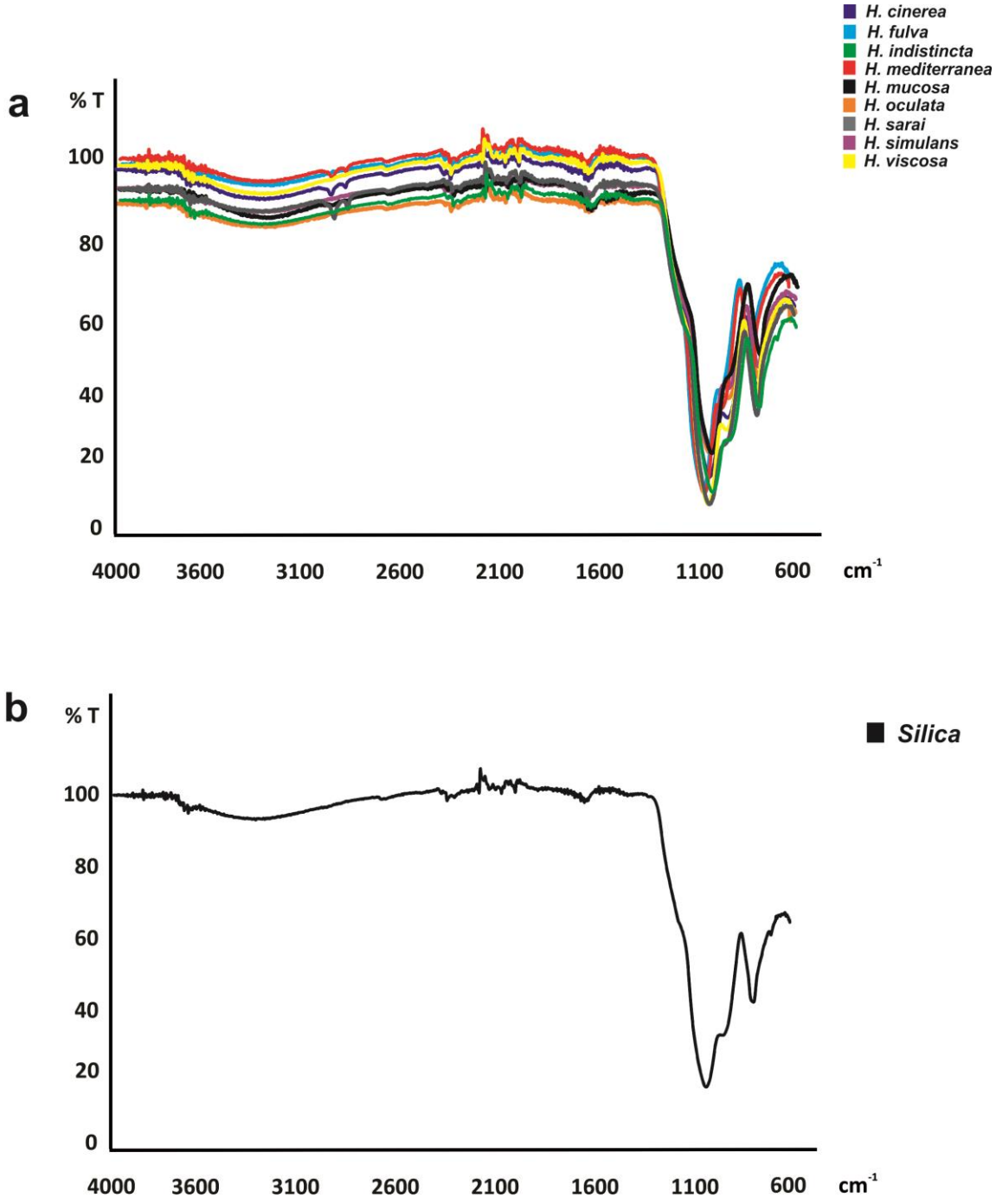

Figure 2. FTIR/ATR spectra profile a) of the spicules from the nine *Haliclona* species and b) spectrum of silica (SiO_2).

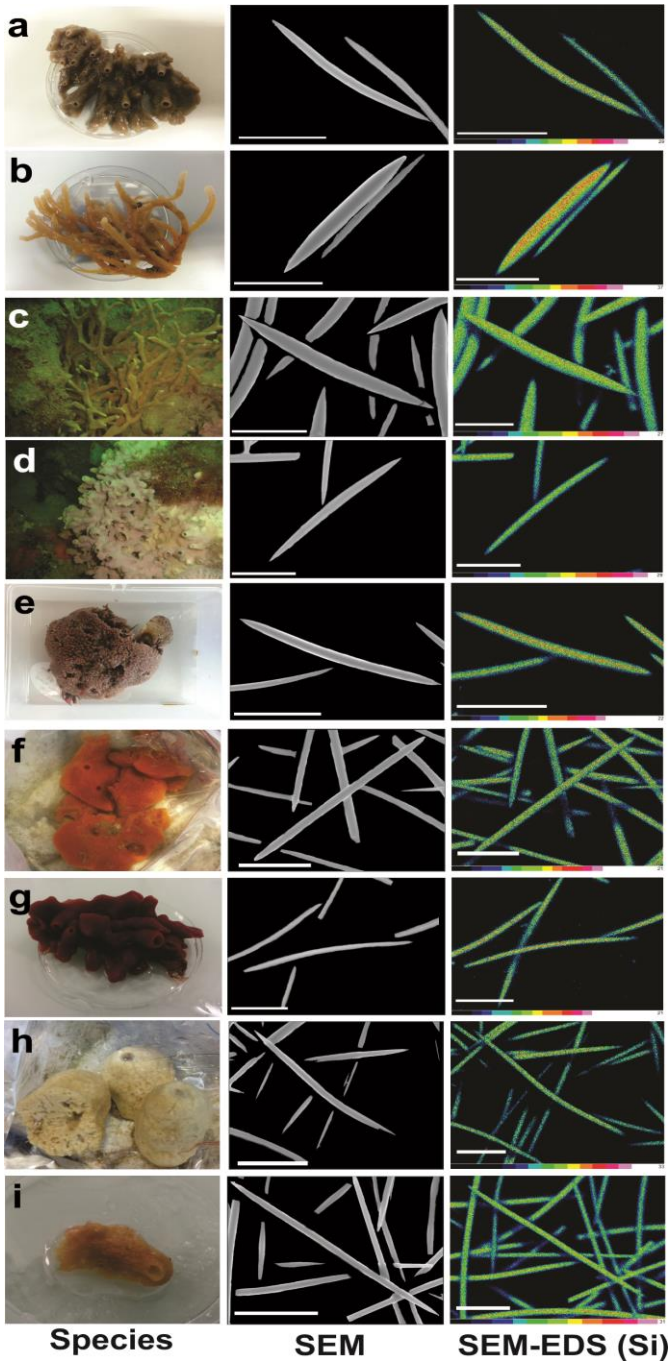

Figure 3. Photographs of the nine *Haliclona* species studied including Scanning Electron Microscope images of the spicules and Spatial Distribution Maps of Silica: a) *Haliclona cinerea*, b) *Haliclona oculata*, c) *Haliclona simulans*, d) *Haliclona viscosa*, e) *Haliclona indistincta*, f) *Haliclona fulva*, g) *Haliclona mediterranea* h) *Haliclona sarai*, i) *Haliclona mucosa*. Scale bars (50 µm).

Table 2. Chemical composition of the major elements from the spicules (% by weight) using the ICP-OES.

Element	*H. viscosa*	*H. cinerea*	*H. fulva*	*H. mediterranea*	*H. oculata*	*H. sarai*	*H. mucosa*	*H. simulans*	*H. indistincta*
SiO_2	78.2	77.7	87.7	75.4	80.5	89.4	88.3	86.8	81.2
Si	36.554	36.320	40.994	35.245	37.629	41.789	41.275	40.574	37.956
Al	0.259	0.211	0.058	0.195	0.344	0.111	0.037	0.037	1.540
Fe	0.062	0.041	0.020	0.048	0.062	0.020	0.013	0.006	0.202
Ca	0.042	0.035	0.021	0.035	0.035	0.021	0.014	0.007	0.078
Mg	0.006	<0.006	<0.006	0.012	0.018	0.006	<0.006	<0.006	0.066
Na	0.081	0.014	0.126	0.089	0.103	0.140	0.178	0.037	0.363
K	0.066	0.066	0.215	0.058	0.116	0.116	0.174	0.008	0.498
Ti	0.017	0.011	0.005	0.017	0.023	0.005	0.005	<0.005	0.095
Mn	0.007	0.007	0.007	0.007	0.007	0.007	<0.007	<0.007	0.015
P	<0.004	0.017	<0.004	0.008	<0.004	0.004	<0.004	0.004	<0.017
Total	78.744	78.108	88.162	75.869	81.212	89.83	88.738	88.917	84.074

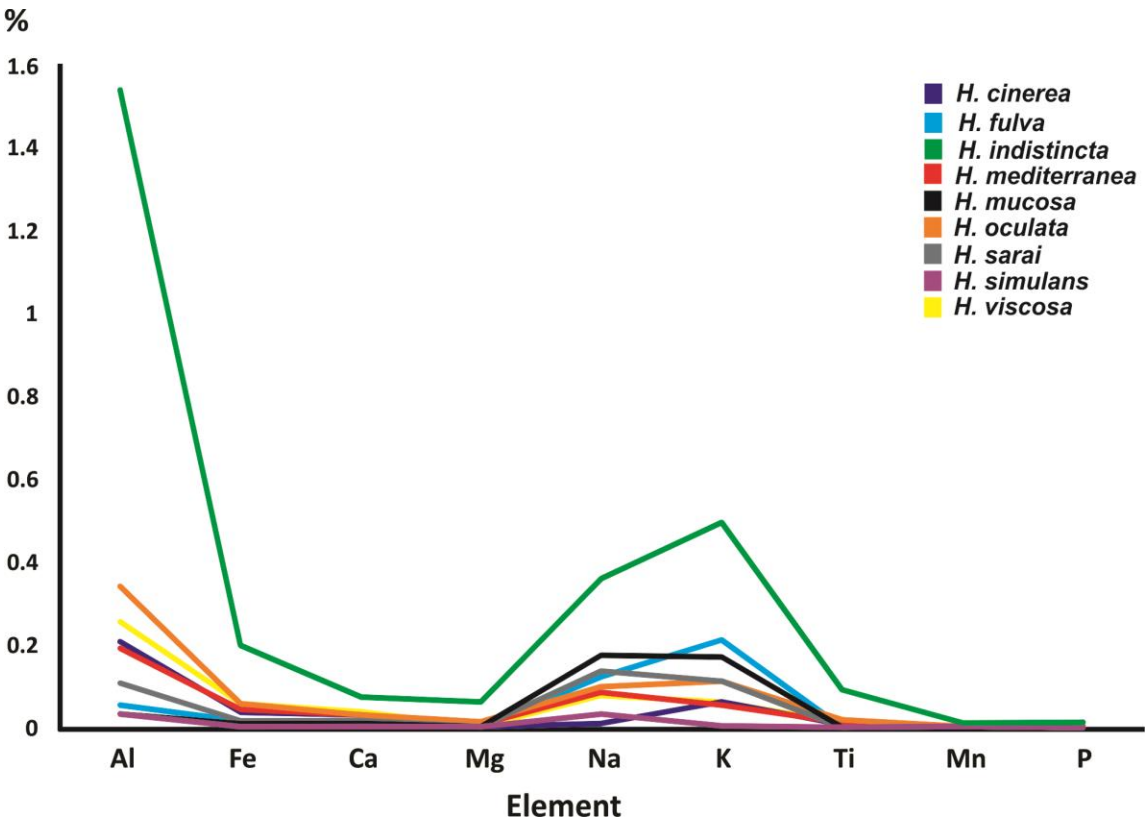

Figure 4. Line graph of the major elements detected in the spicules from the nine *Haliclona* species using ICP-OES.

A total of 36 minor elements (including trace and rare earth) were detected and, as above, there was a large variation in amounts detected across the species. As detailed in Figure 5 and table 3 those with higher concentrations (>10 ppm) included Zn (ranging from <5 ppm in *H. cinerea* to 103 ppm in *H. viscosa*), Ba (ranging from 4.4 ppm in *H. simulans* to 93 ppm in *H. indistincta*), Cu (ranging from 5 ppm in *H. cinerea* to 66 ppm in *H. indistincta*), Zr (ranging from 3 ppm in *H. simulans* to 49 ppm in *H. indistincta*), Ni (ranging from 6 ppm in *H. simulans* to 47 ppm in *H. indistincta*), Cr (ranging from <10 ppm in *H. cinerea* to 40 ppm in *H. indistincta*), Rb (ranging from 1.1 ppm in *H. simulans* to 21.8 ppm in *H. indistincta*) Sr (ranging from 0.8 ppm in *H. simulans* to 15.8 ppm in *H. indistincta*), and Ce (ranging from 0.6 ppm in *H. simulans* to 10.2 ppm in *H. indistincta*) (Figure 5 and Table 3).

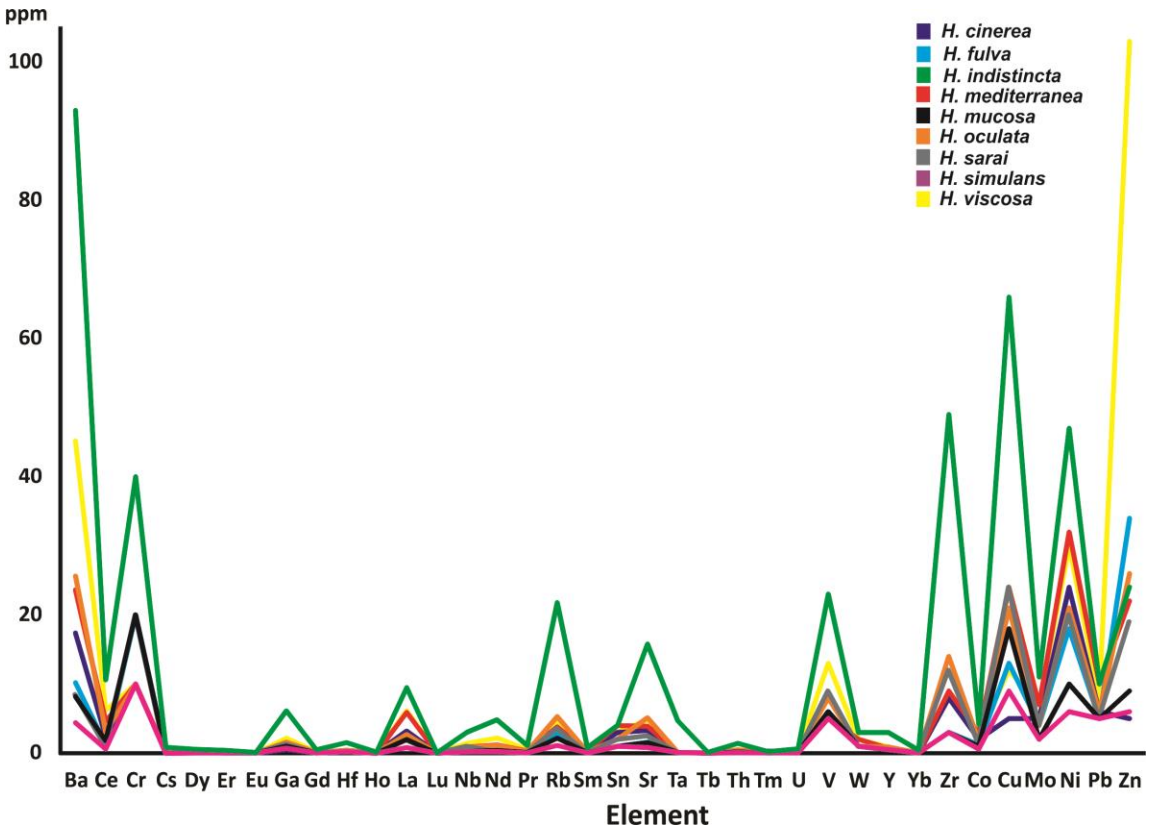

Figure 5. Line graph showing the trace elements detected in the spicules from the nine *Haliclona* species using ICP-MS.

Table 3. Chemical composition of the rare and trace elements from spicules (ppm) using the ICP-MS.

Element	*H. viscosa*	*H . cinerea*	*H. fulva*	*H. mediterranea*	*H. oculata*	*H. sarai*	*H. mucosa*	*H. simulans*	*H. indistincta*
Ba	45.2	17.4	10.2	23.6	25.6	8.5	8.2	4.4	93
Ce	6.2	2.4	1.2	4.6	3	1	1.8	0.6	10.6
Cr	10	<10	20	<10	10	20	20	<10	40
Cs	0.13	0.05	<0.01	0.01	0.19	0.01	0.01	0.01	0.83
Dy	0.15	0.09	<0.05	0.15	0.1	<0.05	0.06	<0.05	0.55
Er	0.11	0.03	<0.03	0.08	0.1	0.03	0.04	<0.03	0.42
Eu	0.04	0.05	<0.03	0.06	0.05	<0.03	<0.03	<0.03	0.12
Ga	2.2	0.5	1	1.4	1.6	1.3	1	0.7	6.1
Gd	0.18	0.07	<0.05	0.12	0.16	<0.05	<0.05	<0.05	0.48
Hf	0.2	0.4	<0.2	0.2	0.4	0.2	<0.2	<0.2	1.5
Ho	0.02	0.02	<0.01	0.04	0.02	0.01	0.01	<0.01	0.13
La	6.1	3.2	2.1	5.9	2.7	1.9	2	0.8	9.5
Lu	0.02	<0.01	<0.01	0.01	<0.01	0.01	0.01	<0.01	0.04
Nb	1.4	0.5	0.2	0.9	0.8	1	0.2	<0.2	3
Nd	2.2	0.9	0.4	1.2	1.1	0.2	0.4	0.2	4.8
Pr	0.52	0.19	0.14	0.34	0.29	0.08	0.12	0.05	1.09
Rb	4.6	3.5	2.8	3.8	5.3	3.6	2.2	1.1	21.8
Sm	0.32	0.12	0.1	0.28	0.16	0.05	0.08	0.04	0.76
Sn	3	3	1	4	2	2	1	1	4
Sr	4.8	3.3	1.6	3.9	5.1	2.5	1.5	0.8	15.8
Ta	<0.1	<0.1	<0.1	<0.1	<0.1	<0.1	<0.1	<0.1	4.7
Tb	0.01	0.03	0.02	0.02	0.04	0.01	0.01	0.01	0.09
Th	0.44	0.26	0.09	0.37	0.48	0.17	0.17	0.06	1.41
Tm	0.11	0.29	0.07	0.12	0.07	0.05	0.05	0.03	0.2
U	0.13	0.14	0.05	0.11	0.22	0.11	0.06	<0.05	0.62
V	13	6	6	<5	8	9	6	<5	23
W	2	1	1	2	1	1	1	<1	3
Y	0.9	0.5	<0.5	0.7	0.9	<0.5	<0.5	<0.5	3
Yb	0.05	0.03	<0.03	0.06	0.04	0.05	0.03	<0.03	0.45
Zr	8	8	3	9	14	12	3	3	49
Co	2.4	2	1.2	2.9	1.8	1.4	1	0.6	4.2
Cu	12	5	13	24	21	24	18	9	66
Mo	7	5	4	7	4	4	2	<2	11
Ni	30	24	18	32	21	20	10	6	47
Pb	8	6	<5	10	6	5	<5	<5	10
Zn	103	<5	34	22	26	19	9	6	24

FTIR spectra of the tissue from the nine *Haliclona* are shown in Figure 6. Apart from the peak associated with Si-O-Si (1030 to 1035 cm^{-1}, Şen et al. 2016), peaks relating to hydroxyls (-OH) or amines (-NHx) (3200 to 3600 cm^{-1}), amides I and II (1600 to 1690 cm^{-1} and 1480-1550 cm^{-1}) and –CH (2800 to 2900 cm-1) were also clearly detected (Gan et al. 2015; Barth, 2007, Sudharsan et al. 2013; Şen et al. 2017; Bayari et al. 2018). The dendrogram constructed (using the height of ten peaks) separated the Mediterranean species from the Atlantic species rather than separating species by phylogenetic relationships. In the Mediterranean group *H. fulva* and *H. mucosa* were distinct from *H. mediterranea* and *H. sarai* (Figure 7).

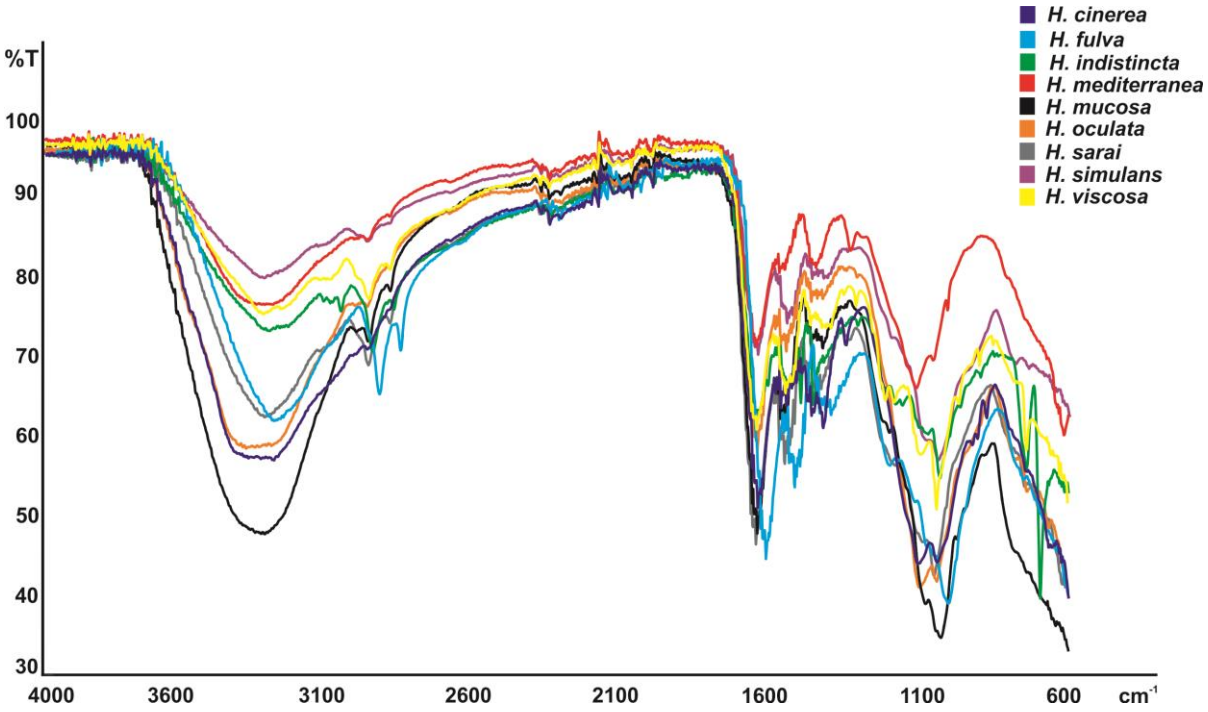

Figure 6. FTIR/ATR spectra of the tissue from all the *Haliclona* species in this study.

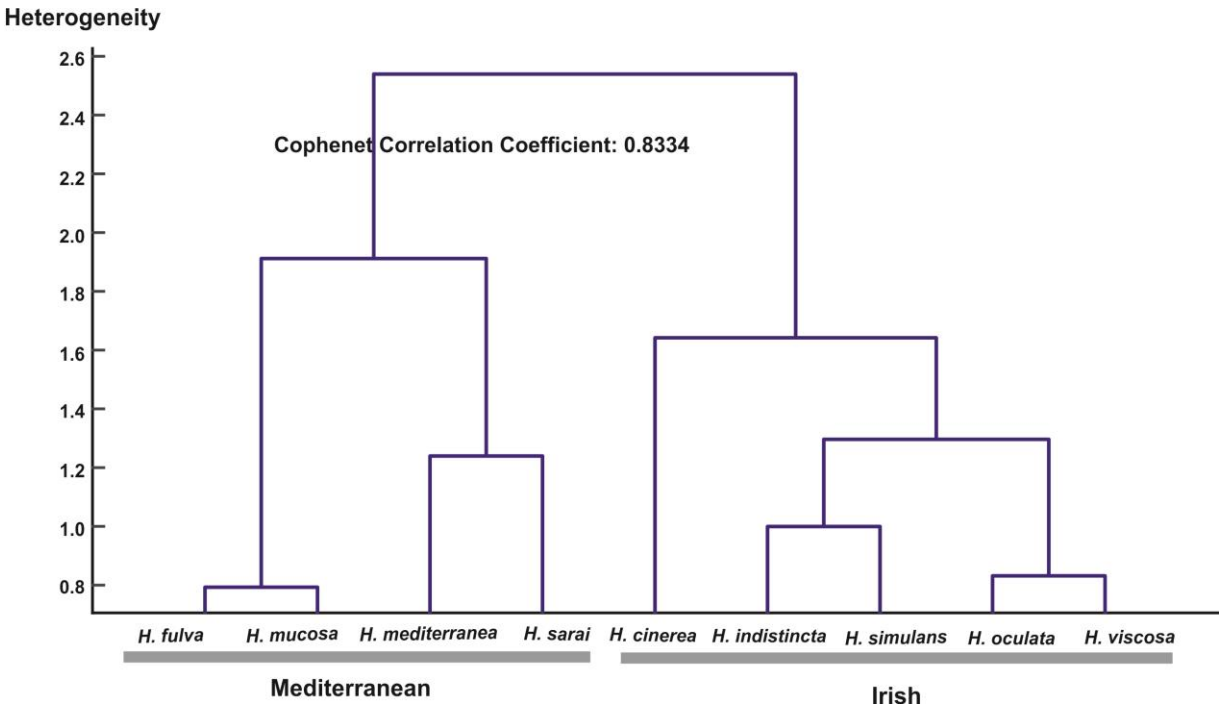

Figure 7. Dendrograms of the FTIR/ATR spectra profile from the tissue of the nine *Haliclona* species (Table 1).

Discussion

Sponges are capable to take up silic acid (as $Si(OH)_4$) from the seawater and transform into microscopic structures (spicules) to construct their skeleton (Reincke and Barthel, 1997 ;Uriz et al. 2003). This is remarkable because silicon is not the most abundant dissolved element in seawater and is also under-saturated in surface areas but not in the deep sea (Zhang et al. 2001). The FTIR spectra of the spicules from the nine *Haliclona* species were not capable to distinguish species and the spectra were similar to the spicules from other demosponges (including haplosclerids) and hexactinellids (Sandford, 2003; Croce et al. 2004; Şen et al. 2016). Unsurprisingly perhaps, the only element detected using SEM-EDS was Silica (Si) and while other elements were detected using ICP-OES the values of biogenic silica (SiO_2) were comparable to those reported previously by Schwab and Shore (1971) and Sandford (2003)

(89.7% and 85.2% respectively) if slightly lower with three of the nine species showing values under 80% (*H. viscosa*, *H. cinerea* and *H. mediterranea*). The estimated weight percentage of biogenic silica was different between the nine species (with *H. sarai* showing the highest percentage of silica) however, no specific pattern linked with phylogenetic position was apparent.

Differences existed between the nine *Haliclona* species in terms of major and trace element concentrations detected in the spicules. However, similarity/dissimilarity in spicule composition did not reflect currently understood phylogenetic relationships and therefore the composition of the spicules is likely primarily driven by environmental factors. For the major elements, the spicules of *H. indistincta* had the highest values of Al, Ca, Fe, Na, Mg, Ti, Mn and K among the nine species analyzed (Table 2). This species was collected immediately below low water level in the sublittoral while all other species included were collected further offshore at depths of 10-20 m. Sandford (2003) studied the chemical composition of the spicules of two demosponges and four hexactinellid species that were collected at different depths and locations. The shallowest was *P. suberitoides* at 0.3-1 m (Florida, USA) while the others (i.e. *Suberites* sp, *Aphrocallistes* sp) were collected between 35 and 42 m in Scotland and Vancouver. The highest value for Ca corresponded to the shallowest sponge *P. suberitoides* while the highest value of K was present in the spicules of the hexactinellid *Aphrocallistes* sp (Sandford, 2003) and these values were higher than those from the nine *Haliclona* species in this study.

While values of Fe and Al in *H. indistincta* (Corranroo, Ireland) were higher than the highest values of any of the six species recorded by Sandford (2003), the concentration of the remaining major elements (Na, Ti, Mg and Mn), detected in the spicules in the current study

were similar to those observed by Sandford (2003). Overall no pattern relating element concentration and depth (intertidal vs subtidal) could be found across both studies suggesting that water depth was not likely to be responsible for the difference in concentration of the major elements between *H. indistincta* and the subtidal species.

The variations in elemental concentrations in the spicules observed in this study and previous studies are likely related to concentrations in the surrounding environment (sediments and seawater). The presence of many major elements in the spicules of the nine *Haliclona* species indicates clearly that sponges also incorporate elements other than Si that are available in seawater. Aluminium is a major component of the continental crust and its presence in the seawater is mainly attributed to inputs of atmospheric dust (Vink and Measures, 2001). Sources of Fe in seawater are largely associated with riverine discharges (resulting in increases to coastal waters), hydrothermal activity (leading to local increases in the vicinity of vents), atmospheric dust (leading to enrichment in near surface waters), and maximum concentrations are found at the surface (Moore et al. 2001).

H. indistincta spicules also contained the highest concentrations of Ni, Cu, Ba, Zr, Cr, Sr, Rb and Ce while the spicules of *H. viscosa* had the highest concentration of Zn (Table 3). Some of the same trace elements were present in even higher amounts in the intertidal sponge *Acarnus erithacus*, from the Californian coast, USA (Schwab and Shore, 1971) and similarly in higher concentrations in *Aphrocallistes* and *Rhabdocalyptus* (Sandford, 2003) and other shallow water demosponge species from the Antartic and Mediterranean (Truzzi et al. 2008; Annibaldi et al. 2011; Illuminati et al. 2016). Furthermore, the concentration of seven metals (As, Cd, Co, Cu, Fe, Mn and Ni) in the tissue of the sponge *H. tenuiramosa* were higher in specimens collected nearer shore than those found off-shore in the Gulf of Mannar (Rao et al.

2009). This indicated that the concentration of these metals was higher near shore as a result of closer proximity to land-based anthropogenic sources and inputs (Rao et al. 2009). Similarly in the present study, *H. indistincta* was collected from the shallowest site and the spicules contained the highest concentration of some minor and major elements among the nine species studied. However, no pattern related to depth, geographical location or phylogeny clearly explains the concentration of trace elements in sponge spicules across studies.

Many of the trace elements detected in the spicules are generally found in low concentrations in seawater (Bruland and Lohan, 2006; Millero, 2013). Sponges are considered good biomonitors of metal contamination in the marine environment because of their sessility, widespread geographic abundance, long life, ease of sampling and ability to concentrate metals in their tissue from the surrounding sedimentary, particulate and dissolved phase (Hansen et al. 1995; Cebrian et al. 2007; Pan et al. 2011; Mayzel et al. 2014; Illuminati et al. 2016). In the present study, the primary focus was on sponge spicules as it was not anticipated that a pattern involving elevated concentrations of elements in *H. indistincta* in comparison to the other species tested would be revealed. Therefore, sediment and seawater samples were not collected for the determination of elements from the sites where the sponges were collected. As a result it was not possible to conclude that the concentration of the elements detected in the spicules were correlated with those from the surrounding environment or suggest *H. indistincta* as a potential biomonitor of pollution/metal availability in the marine environment (Cebrian et al. 2007; Rao et al. 2007; Pan et al. 2011; Srikanth and Rao, 2014). However, all the trace elements detected in the spicules may have both natural and anthropogenic source (Pan et al. 2011) and the highest values were present in *H. indistincta*

which could indicate that the site from where this sponge was collected (Corranroo) may potentially have greater element concentrations in the ambient environment. It is clear that the chemical composition of spicules is influenced not by common ancestry but rather by the interactions between sponges and their environment.

FTIR spectra of the tissue were previously found to be useful in discriminating demosponge species belonging to the orders Axinellida, Suberitiida, Dyctioceratida and Poecilosclerida (Gan et al. 2015). Furthermore, dendrograms of FTIR spectra from other organisms such as fungi, flowering plants and cyanobacteria showed congruence between the phylogeny of these groups with their FTIR spectra (Naumann, 2009; Kim et al. 2004; Kenne and van der Merwe, 2013). Despite some differences in the spectrum profile from the tissue across the nine *Haliclona* species that may be helpful in differentiating species, no phylogenetic pattern emerged here for marine haplosclerids, based on the dendrogram constructed (Figure 7). This result was similar to the dendrogram constructed by Şen et al. (2016), in which six sponge species belonging to Haplosclerida and Heteroscleromorpha grouped in clusters with no phylogenetic relationships. Here, an environmental pattern is apparent, with Mediterranean species grouping in one cluster and the Irish species in another.

References

Annibaldi, A., Truzzi, C., Illuminati, S., Bassotti, E., Finale, C., Scarponi, G. (2011) First systematic voltammetric measurements of Cd, Pb, and Cu in hydrofluoric acid-dissolved siliceous spicules of marine sponges: Application to Antarctic specimens. Analytical Letters 44(17), 2792–2807.

Barth, A. (2007) Infrared spectroscopy of proteins. Biochimica et Biophysica Acta 1767, 1073–1101.

Bayari, S.H., Şen, E.H., Ide, S., Topaloglu, B. (2018) Structural studies on Demospongiae sponges from Gökçeada Island in the Northern Aegean Sea. Spectrochimica Acta Part A, 192, 368–377.

Bruland, K.W. (1980) Oceanographic distributions of cadmium, zinc, nickel, and copper in the North Pacific. Earth and Planetary Science Letters, 47(2), 176–198.

Bruland, K.W., Lohan, M.C. (2006) Controls of trace metals in seawater. The oceans and marine geochemistry, 6, 23–47.

Cebrian, E., Uriz, M.J., Turon, X. (2007) Sponges as biomonitors of heavy metals in spatial and temporal surveys in northwestern Mediterranean: multispecies comparison. Environmental Toxicology Chemistry, 26(11), 2430–2439.

Cha, J.N., Stucky, G.D., Morse, D.E., Deming, T.J. (2000) Biomimetic synthesis of ordered silica structures mediated by block copolypeptides. Nature, 403(6767), 289–292.

Croce, G., Frache, A., Milanesio, M., Marchese, L., Causa, M., Viterbo, D., Barbaglia, A., Bolis, V., Bavestrello, G., Cerrano, C., Benatti, U., Giovine, M., Amenitsh, H. (2004) Structural characterization of siliceous spicules from marine sponges. Biophysical Journal, 86(1), 526–534.

Fairhead, M., Johnson, K.A., Kowatz, T., McMahon, S.A., Carter, L.G., Oke, M., Liu, H., Naismith, J.H., van der Walle, C.F. (2008) Crystal structure and silica condensing activities of silicatein α–cathepsin L chimeras. Chemical Communications, 15, 1765–1767.

Gan, J.H., Xu, C.H., Zhu, H.Z., Mao, F., Yang, F., Zhou, Q., Sun, S.Q. (2015) Analysis and discrimination of ten different sponges by multi-step infrared spectroscopy. Chinese Chemical Letters, 26, 215–220.

Gendron-Badou, A., Coradin, T., Maquet, J., Fröhlich, F., Livage, J. (2003) Spectroscopic characterization of biogenic silica. Journal of Non–Crystal Solids, 316(2),331–331–3Hansen, I.V., Weeks, J.M., Depledge, M.H. (1995) Accumulation of copper, zinc, cadmium and chromium by the marine sponge *Halichondria panicea* Pallas and the implications for biomonitoring. Marine Pollution Bulletin, 31(1–3), 133–138.

Hunt, G.R- (1970) Visible and near-infrared spectra of minerals and rocks: I silicate minerals. Modern Geology, 1, 283–300.

Illuminati, S., Annibaldi, A., Truzzi, C., Scarponi, G. (2016). Heavy metal distribution in organic and siliceous marine sponge tissues measured by square wave anodic stripping voltammetry. Marine Pollution Bulletin, 111(1–2), 476–482.

Jonker, J.L., Morrison, L., Lynch, E.P., Grunwald, I., von Byern, J., Power, A.M. (2015) The chemistry of stalked barnacle adhesive (*Lepas anatifera*), Interface Focus, 5(1), 20140062.

Kenne, G., van der Merwe, D. (2013) Classification of Toxic Cyanobacterial Blooms by Fourier-Transform Infrared Technology (FTIR). Advances in Microbiology, 3, 1–8.

Kim, S.W., Ban, S.H., Chung, H., Cho, S., Chung, H.J., Choi, P.S., Yoo, O.J., Liu, J.R. (2004) Taxonomic discrimination of flowering plants by multivariate analysis of Fourier transform infrared spectroscopy data. Plant Cell Reports, 23, 246–250.

Millero, F.J. (2013) Chemical oceanography. CRC press.

Mayzel, B., Aizenberg, J., Ilan, M. (2014) The elemental composition of Demospongiae from the Red Sea, Gulf of Aqaba. PloS One, 9(4)e95775.

Moore, J.K., Doney, S.C., Glover, D.M., Fung, I.Y. (2001) Iron cycling and nutrient-limitation patterns in surface waters of the World Ocean. Deep Sea Research Part II Tropical Studies of Oceanography, 49(1), 463–507.

Morrison, L., Feely, M., Stengel, D.B., Blamey, N., Dockery, P., Sherlock, A., Timmins, E. (2009) Seaweed attachment to bedrock: biophysical evidence for a new geophycology paradigm. Geobiology, 7, 477–487.

Morrow, C., Cárdenas, P. (2015) Proposal for a revised classification of the Demospongiae (Porifera). Frontiers in Zoology, 12,7.

Naumann, A. (2009) A novel procedure for strain classification of fungal mycelium by cluster and artificial neural network analysis of Fourier transform infrared (FTIR) spectra. Analyst, 134, 1215–1223.

Pan, K., Lee, O.O., Qian, P.Y., Wang, W.X. (2011) Sponges and sediments as monitoring tools of metal contamination in the eastern coast of the Red Sea, Saudi Arabia. Marine Pollution Bulletin, 62(5), 1140–1146.

Pozzolini, M., Sturla, L., Cerrano, C., Bavestrello, G., Camardella, L., Parodi, A. M., Raheli, F., Benatti, U., Müller W.E.G., Giovine, M. (2004). Molecular cloning of silicatein gene from marine sponge Petrosia ficiformis (Porifera, Demospongiae) and development of primmorphs as a model for biosilicification studies. Marine biotechnology, 6(6), 594-603.

Rao, J.V., Kavitha, P., Srikanth, K., Usman, P.K., Rao, T.G. (2007) Environmental contamination using accumulation of metals in marine sponge, *Sigmadocia fibulata* inhabiting the coastal waters of Gulf of Mannar, India. Toxicology and Environmental Chemistry, 89(3), 487–498.

Rao, J.V., Srikanth, K., Pallela, R., Rao, T.G. (2009) The use of marine sponge, Haliclona tenuiramosa as bioindicator to monitor heavy metal pollution in the coasts of Gulf of Mannar, India. Environmental Monitoring and Assessment, 156(1–4), 451.

Redmond, N.E., Morrow, C.C., Thacker, R.W., Diaz, M.C., Boury-Esnault, N., Cárdenas, P., Hajdu, E., Lôbo-Hajdu, G., Picton, B.E., Pomponi, S.A., Kayal, E., Collins, A.G. (2013) Phylogeny and systematics of Demospongiae in light of new small-subunit ribosomal DNA (18S) sequences. Integrative Comparative Biology, 53, 388–415.

Redmond, N.E., Raleigh, J., van Soest, R.W., Kelly, M., Travers, S.A., Bradshaw, B., Vartia, S., Stephens, K., McCormack, G.P. (2011) Phylogenetic relationships of the marine Haplosclerida (Phylum Porifera) employing ribosomal (28S rRNA) and mitochondrial (cox1, nad1) gene sequence data. PLoS One, 6(9)e24344.

Redmond, N.E., Van Soest, R.W.M., Kelly, M., Raleigh, J., Travers, S.A.A., McCormack, G.P. (2007) Reassessment of the classification of the Order Haplosclerida (Class Demospongiae, Phylum Porifera) using 18S rRNA gene sequence data. Molecular Phylogenetics and Evolution, 43(1), 344–352.

Reincke, T., Barthel, D. (1997). Silica uptake kinetics of Halichondria panicea in Kiel Bight. Marine Biology, 129(4), 591–593.

Sandford, F. (2003) Physical and chemical analysis of the siliceous skeletons in six sponges of two groups (Demospongiae and Hexactinellida). Microscopy Research and Technique, 62(4), 336–355.

Schwab, DW., Shore, R.E. (1971) Fine structure and composition of a siliceous sponge spicule. Biological Bulletin, 140(1), 125–136.

Şen, E.H., Ide, S., Bayari, S.H., Hill, M. (2016) Micro-and nano-structural characterization of six marine sponges of the class Demospongiae. European Biophysics Journal, 45(8), 831–842.

Senthilkumar, K., Venkatesan, J., Manivasagan, P., Kim, S.K. (2013) Antiangiogenic effects of marine sponge derived compounds on cancer. Environmental Toxicology and Pharmacy, 36, 1097–1108.

Srikanth, K., Rao, J.V. (2014) Spatial and seasonal variation of potential toxic elements in *Adocia pigmentifera*, seawater and sediment from Rameswaram, southeast coast of India. Environmental Earth Sciences, 72(8), 2905–2916.

Truzzi, C., Annibaldi, A., Illuminati, S., Bassotti, E., Scarponi, G. (2008) Square-wave anodic-stripping voltammetric determination of Cd, Pb, and Cu in a hydrofluoric acid solution of siliceous spicules of marine sponges (from the Ligurian Sea, Italy, and the Ross Sea, Antarctica). Analytical and Bioanalytical Chemistry, 392(1–2), 247–262.

Van Soest, R.W. (2017). *Flagellia*, a new subgenus of *Haliclona* (Porifera, Haplosclerida). European Journal Taxonomy, 351.

Sudharsan, S., Seedevi, P., Saravanan, R., Ramasamy, P., Kumar, S.V., Vairamani, S., Srinivasan, A., Shanmugam, A. (2013) Isolation, characterization and molecular weight

determination of collagen from marine sponge *Spirastrella inconstans* (Dendy). African Journal of Biotechnology, 12, 504–511.

Uriz, M.J., Turon, X., Becerro, M.A., Agell, G. (2003) Siliceous spicules and skeleton frameworks in sponges: origin, diversity, ultrastructural patterns, and biological functions. Microscopy Research and Technique, 62(4), 279–299.

Vink, S., Measures, C.I. (2001) The role of dust deposition in determining surface water distributions of Al and Fe in the South West Atlantic. Deep Sea Research Part II Tropical Studies of Oceanography, 48(13), 2787–2809.

Wibowo, D., Yang, G.Z., Middelberg, A.P., Zhao, C.X. (2017) Non chromatographic bioprocess engineering of a recombinant mineralizing protein for the synthesis of silica nanocapsules. Biotechnology and Bioengineering, 114(2), 335–343.

Wörheide, G., Dohrmann, M., Erpenbeck, D., Larroux, C., Maldonado, M., Voigt, O., Borchiellini, C., Lavrov, D.V. (2012). Deep Phylogeny and Evolution of Sponges (Phylum Porifera). Advances in Marine Biology, 61, 1–178.

Zhang, Y., Amakawa, H., Nozaki, Y. (2001) Oceanic profiles of dissolved silver: precise measurements in the basins of western North Pacific, Sea of Okhotsk, and the Japan Sea. Marine Chemistry, 75(1–2),151–163.

Zovko, A., Viktorsson, K., Haag, P., Kovalerchick, D., Farnegardh, K., Alimonti, A., Ilan, M., Carmeli, S., Lewensohn, R. (2014) Marine Sponge Cribrochalina vasculum Compounds Activate Intrinsic Apoptotic Signaling and Inhibit Growth Factor Signaling Cascades in Non-Small Cell Lung Carcinoma. Molecular Cancer Therapeutics, 13, 2941–29.

Chapter 3

Evolution of the main skeleton-forming genes in sponges (phylum Porifera) with special focus on the marine Haplosclerida (class Demospongiae).

This work has been accepter for publication: **Aguilar-Camacho, JM;** Doonan, L., McCormack G.P. Evolution of the main skeleton-forming genes in sponges (phylum Porifera) with special focus on the marine Haplosclerida (class Demospongiae). *Molecular Phylogenetics and Evolution*

Introduction

Sponges are simple fiter-feeding animals with a body containing relatively few cell types supported by a skeleton of collagen and spongin fibres, and, if present, calcareous or siliceous spicules. Based on molecular phylogenetic studies, the phylum Porifera is divided into four main classes: Hexactinellida, Demospongiae, Homoscleromorpha and Calcarea, (Morrow and Cardenas, 2015). For the first three classes the spicules are siliceous while for Calcarea they are calcium-based (Sperling et al. 2010). In the class Homoscleromorpha, species belonging to the family Oscarellidae Lendenfeld, 1887) lack spicules (Gazave et al. 2010) as do the demosponge members of the subclasses Keratosa and Verongimorpha (excluding members of the family Chondrillidae) lack spicules (Erpenbeck et al. 2012).

The current classification of Demospongiae, the class with greatest number of species, is based on spicule shape and size when present, and the arrangement of the skeleton (Hooper and van Soest, 2002; Morrow and Cardenas, 2015). Members of the order Haplosclerida have a simple skeleton mostly made only of oxeas, and microscleres if present are limited to sigmas, toxas and microxeas (van Soest, 2017). Freshwater sponges also only have oxeas as megascleres but they possess a high diversity of microscleres and gemmuloscleres (Morrow and Cardenas, 2015). In contrast, species belonging to the remaining demosponge orders have a wide diversity of megascleres and microscleres (Morrow and Cardenas, 2015; Botting et al. 2015). Molecular studies, based on mitochondrial and some nuclear genes, divide the class Demospongiae into four main clades: G1: Keratosa; G2: Verongimorpha; G3: Haploscleromorpha (marine haplosclerids) and G4: Heteroscleromorpha (Lavrov et al. 2008; Sperling et al. 2010; Hill et al. 2013; Ma and Yang, 2016). Conversely, some studies using ribosomal data (18S rRNA and 28S rRNA) prefer to include Haploscleromorpha within

Heteroscleromorpha (Thacker et al. 2013; Morrow et al. 2013; Morrow and Cardenas, 2015) until more data is available, although there are large insertions in the SSU of some marine haplosclerid species (Redmond et al. 2007; 2011; 2013). Relationships within the Haploscleromorpha are also largely unresolved due to large discrepancies between molecular data and the existing classification based on morphology (e.g. McCormack et al. 2002; Redmond et al. 2011). Three strongly supported clades are present in trees drawn from ribosomal and mtDNA data (Redmond et al. 2011). Clade A contains many *Haliclona* species (including the type species *H. oculata*) + *Callyspongia* species. Clade B is poorly sampled but contains *Amphimedon queenslandica* and the Irish species *H. simulans*. Clade C is also poorly sampled and contains additional *Haliclona* species (including *H. indistincta*) + *Niphates* species + *Amphimedon* species amongst others (Redmond et al. 2011; Stephens, 2013). Some species are morphologically similar, being placed within the same subgenus grouping via morphology (De Weerdt, 2002) e.g. *H. oculata* and *H. simulans* but belonging to two different clades via molecular data (Redmond et al. 2011). Therefore a major question remains regarding the relative importance of environmental versus genetic factors in shaping the skeleton in marine haplosclerids and other sponges. Here I set out to investigate the evolutionary patterns of the genes responsible for skeleton formation to investigate if they will provide any further insight into the evolution of morphologies in sponges and particularly the Haplosclerida.

The primary genes responsible for spicule formation in Demospongiae are silicateins, DNA sequences of which have been generated from a number of species to date (Cha et al. 1999; Pozzolini et al. 2004; Kaluzhnaya et al. 2007; 2011, Veremeichik et al. 2011). Silicateins are unique to sponges, are monophyletic and were shown to have evolved from cathepsins L, a

family of proteases with varied functions in collagen degradation and ecdysis amongst others, though their role in sponges is still poorly known (Riesgo et al. 2015 and references therein). Fractal monomers of silicatein proteins form an axial filament, which is a proteinaceous core found inside the spicule (Shimizu et al. 1998; Murr and Morse, 2005; Wang et al. 2014) while silicatein also acts as an enzyme that condenses silica to form the spicule around the protein core (Wang et al. 2014). Silicatein proteins have two main components: an inhibitor, and a peptidase containing the active site (Brutchey and Morse, 2008). The aminoacid composition of silicatein is similar to that of cathepsins L but instead of a cysteine (C), the silicateins have a serine (S) that in conjunction with a histidine (H) and asparagine (N) forms the active site (SHN) responsible for silica condensation (Cha et al. 1999; Zhou et al. 1999; Fairhead et al. 2008; Schröder et al. 2012). A particular motif following the serine in the silicateins (-YAF) is also different from the cathepsins L (-WAF).

Silicateins are currently grouped into three different clades, i.e. beta silicateins, alpha and gamma silicateins and silicateins from freshwater sponges (Kaluzhnaya et al. 2007; Mohri et al. 2008; Veremeichik et al. 2011). The number of silicatein variants that are found in the axial filament can vary across species (e.g. alpha, beta and gamma silicatein variants are all present in *Tethya californiana*, but in *Suberites domuncula* just alpha and beta variants are present) (Cha et al. 1999; Brutchey and Morse, 2008). Another protein named silintaphin, has been reported in the axial filament interacting with the silicatein-alpha in biosilica synthesis from *Suberites domuncula* (Schlossmacher et al. 2011).

Kozhemyako et al. (2010) sequenced a putative silicatein from Latrunculia oparinae that had a cysteine instead of a serine at the active site (characteristic of cathepsins-L), but contained the YAF motif instead of WAF (characteristic of silicateins). Riesgo et al. (2015) found another

two of these unusual silicateins in the transcriptome of the haplosclerid Petrosia ficiformis and one silicatein variant also having a glutamine (Q) instead of a histidine (H) in the active site (CQN). Gauthier (2015) found one SHN, one SQN and four CHN variants in the genome of yet another haplosclerid, A. queenslandica. The phylogenetic position of all these sequences was determined to be within the overall silicatein clade but distinct from the three SHN silicatein variants of other demosponges, (Kozhemyako et al. 2010; Gauthier, 2015; Riesgo et al. 2015). Currently, it is unknown if the silicateins with CHN and C/SQN aminoacid configurations function in spicule formation because the active site does not have all three amino acids thought to be necessary for silica condensation (SHN) (Shimizu et al. 1998; Zhou et al. 1999; Fairhead et al. 2008). It is also unknown how common these silicatein variants are in marine haplosclerid and other demosponge species. As a precursor to functional studies we sought to explore the types and phylogenetic relationships of the silicatein genes present in three Irish *Haliclona* species, which were chosen to represent three major haplosclerid clades (Redmond et al. 2011). With the affordable development of genomics technologies, several sponge genomes and transcriptomes from the four classes are now available for comparison (reviewed in Aguilar-Camacho and McCormack, 2017) and here we identify and investigate the evolution of all the silicatein variants and silintaphins in Porifera with particular focus on the evolution of these genes in marine haplosclerids.

Materials and Methods

Generation of transcriptome data

RNA was extracted from specimens that are representatives of the three main molecular clades from the order Haplosclerida: A) *H. oculata* (two specimens), B) *H. simulans* (two

specimens) and C) *H. indistincta* (three specimens). Small pieces were dissected under a microscope to remove associated material. The pieces were flash – frozen with LN_2 and stored at -80° C. RNA was extracted from the frozen specimens following the TriReagent protocol (Riesgo et al. 2014) and its quality and quantity was checked using a 2100 Bioanalyzer RNA Eukaryotic Chip before being sent to an external Illumina platform to construct libraries (MACROGEN, INC) using the TruSeq Stranded mRNA Kit sample Prep Kit V2. The HiSeq2000 platform (Illumina, USA) was used for pair end sequencing and three small libraries of *H. indistincta* (10 Mb), two of *H. oculata* (120 Mb) and two of *H. simulans* (120 Mb) were constructed and sequenced.

The quality of the reads was checked using the FASTQC software (Gordon and Hannon, 2010). FAST –X Clipper software was employed to trim sequence reads with low quality score (below 30) leaving only sequences >70 bp. For each of the paired sequences *de novo* assemblies were carried out using the Trinity software to construct the contigs for each species (Haas et al. 2013). This software assembles transcript sequences from Illumina RNA-Seq data without having any reference genome. Contig assemblies were carried out using an ICHEC account (Irish Center of High End Computing) and the NUIG Bioinformatics server (School of Mathematics, Statistics and Applied Mathematics).

Gene identification

A reference fasta file (proteins) with all the silicateins and cathepsins-L from the genome of the sponge *A. queenslandica* was constructed (Srivastava et al. 2010, Fernandez-Valverde et al. 2015). The three assembled transcriptomes generated were blasted (blastx) manually against this database. Resulting hits were translated using the best Open Reading Frame and

complete silicatein and cathepsins L sequences were used for further phylogenetic analysis. The same process was carried out for the available assembled genomes and transcriptomes from the COMPAGEN dataset (Hemmrich and Bosch, 2001): *Oscarella carmella* (Nichols et al. 2012), *Xestospongia testudinaria* (Ryu et al. 2016), *Stylissa carteri* (Ryu et al. 2016), *Sycon cilliatum* (Fortunato et al. 2014), *Leucoselonia complicata* (Fortunato et al. 2014), *Ephydatia muelleri* (Peña et al. 2016), *Haliclona tubifera* and *Haliclona amboinensis* (Guzman and Conaco, 2016); the genome of *Tethya wilhelma* (Francis et al. 2017), as well as, the assembled transcriptomes from *Aphrocallistes vastus, P. ficiformis, Ircinia fasciculata, Chondrilla caribbea* and *Corticium candelabrum, Pseudospongorites suberitoides, Spongilla lacustris* (Riesgo et al. 2014 Harvard Dataverse Network, doi:10.7910/DVN/24737); *Latrunculia apicalis, Kirkpatrickia variolosa, Hyalonema populiferum, Rosella fibulata* and *Sympagella nux* (Whelan et al. 2015, doi:10.6084/m9.figshare.1334306), *Halisarca dujardini* (Borisenko et al. 2016 http://www.ebi.ac.uk/ena/data/view/HADA01000001-HADA01138992), *Ephydatia fluviatilis* (Alie et al. 2015), *Mycale phyllophyla* (Quiu et al. 2015), *Cymbastela concentrica, Tedania anhelens* and *Scopalina* sp (Diez-Vives et al. 2017 http://datadryad.org/resource/doi:10.5061/dryad.7717q) and the unpublished assembled transcriptome of *Cinanchyrella* sp (Joe Lopez). DNA sequences of complete silicateins from Genbank were also downloaded and included for phylogenetic analysis (Appendix 1). In addition, the silintaphin gene from *S. domuncula* was blasted (blastx) manually against the transcriptomes and genomes used in this study, and the glassin gene from *Euplectella* sp was blasted (blastx) against the four hexactinellid transcriptomes.

Phylogenetic analysis of silicatein genes

Amino acid sequences were aligned with the SEAVIEW software (Gouy et al. 2010). The initial alignment contained 421 amino acid sequences (149 silicateins and 272 cathepsins L). Due to the very high number of cathepsins L in the alignment, from initial trees and the existing knowledge of the origin of silicateins (Shimizu et al. 1998; Riesgo et al. 2015), I selected a monophyletic group of six cathepsins L sequences from haplosclerids as outgroup sequences to the silicatein clade. A conservative alignment strategy was employed where all the positions that were spuriously aligned were excluded. I analyzed three nested datasets to explore the impact of taxon removal/addition to relationships within the phylogeny; the first contained all the sequences (155) with fewest characters (179) due to alignment difficulties and short sequences. The second dataset excluded the significantly shorter sequences (22) and therefore additional characters (313) from 133 sequences were obtained. Based on phylogenetic trees reconstructed from the second dataset, sequences were pruned that generated very long branches. In addition a new outgroup sequence was selected that was closer to the main ingroup and thus the cathepsins L sequences were also removed (17) (Appendix 2). The resulting alignment contained 320 characters from 116 sequences and the alignments are available on request. ProtTest 2.4 Software (Abascal et al. 2005) was employed to find the best evolutionary model for each dataset and WAG was the best fitting evolutionary substitution model for all the three datasets analyzed. Five random starting trees using SPR and NNI moves were executed in PhyML 3.0 (Guindon et al. 2010) for each dataset and the tree with the best likelihood value was selected (4 rate classes). Bootstrap analysis using 1000 replicates was also performed. Bayesian Inference was estimated using Mr Bayes 3.2.1 (Ronquist and Huelsenbeck, 2003), two runs of over 3000000 were carried

out with sampling every 100 generations for the three datasets. The appropriate burnin value was determined by examining the standard deviation of split frequencies (<0.01). A 50% majority rule consensus tree was constructed from all generations sampled after the burnin. The branch supports (>70%) from Mr. Bayes are shown as posterior probabilities (PP) and those from ML are in bootstrap proportions (BP) in the trees and text. To explore possible motifs of importance in silicateins, motifs were detected using the MEME software in the overall alignment and in each alignment of the major clades obtained from the molecular phylogenetic analysis (Bailey et al., 2006).

Results

Transcriptome data from Irish species

Summary statistics of the raw reads and the assembled transcriptomes from the three *Haliclona* species are presented in Table 1 and 2. A total of 48,520 contigs (N50=1596) were assembled for *H. indistincta*, 76, 641 contigs (N50=1286) for *H. simulans* and 94, 360 contigs (N50=1357) for *H. oculata*. The distribution of contig size was similar for the three transcriptomes assembled (Table 3).

Table 1. Summary statistics for the mRNA reads before and after trimming.

Sample	Raw Reads	Trimmed reads	Mean Length of Trimmed Read (Bases)
H. indistincta	30, 942, 438	30,232,951	99.86
H. simulans	208,025,126	207,187,310	100.60
H. oculata	258,734,148	257,993,683	100.56

Table 2. Summary statistics for the assembled reads.

Sample	Total bp Assembled into Contigs	Number of Contigs	Number of real genes excluding isoforms (Trinity software)	Mean contig length (bp)	Contig N50
H. indistincta	43,939,936	48,520	34,263	905.60	1596
H. simulans	57,594,190	76, 641	58,735	751.48	1286
H.oculata	69,624,569	94,360	75,234	737.86	1357

Table 3. Species contigs statistics by size.

	Haliclona indistincta		*Haliclona simulans*		*Haliclona oculata*	
Contig length	Number of contigs	%	Number of contigs	%	Number of contigs	%
<300	13742	28.32	25880	33.77	35170	37.27
300-500	10987	22.65	19418	25.34	24728	26.21
500-1000	10030	20.67	15277	19.93	16011	16.97
1000-2000	8239	16.98	9983	13.03	10708	11.35
2000-3000	3056	6.3	3488	4.55	4013	4.25
3000-4000	1267	2.61	1357	1.77	1847	1.96
4000-5000	608	1.25	629	0.82	898	0.95
5000-6000	266	0.55	276	0.36	464	0.49
>6000	325	0.67	333	0.43	521	0.55
Total	48520	100	76641	100	94360	100

Four silicatein variants were present in *H. oculata* (type species of the genus and representative here of clade A). These included one of the SHN type (SHN beta) and three different variants with the CHN motif at the active site. The same silicatein variants were

recovered from *H. simulans* (representative here of clade B) while five silicateins were present in *H. indistincta* (representative of clade C). Variants from this latter species included one of the SHN-beta type, but just two CHN types, one of which was much closer to cathepsins-L sequences than other silicateins. In addition, one silicatein of the CQN type and one of the SQN type were also recovered. No silintaphin homologs were found in the three transcriptomes from the Irish species (Table 4).

Presence/absence of silicateins, silintaphins and glassin in other available data

Silicatein sequences were not present in any of the transcriptomes or genomes of hexactinellid, calcareous or homoscleromorph sponges. Furthermore, silicateins were not found in three transcriptomes from Demospongiae: *I. fasciculata, C. nucula,* and *H. dujardini* (the first species belongs to the subclass Keratosa and the remaining two to Verongimorpha). Silicateins of the SHN type were found in all the remaining genomes and transcriptomes including haplosclerid sponges. However, few clear patterns emerged for the distribution of silicatein variants across taxonomic ranks and no silicatein variant was present in all sponges investigated.

All haplosclerids contained one sequence variant of the SHN type while the number present in freshwater sponges and heteroscleromorphas ranged from two in *L. apicalis* to nine in *E. muelleri*. Silicatein variants containing CHN at the active site were found in all haplosclerid species examined and in some but not all of the genomes and transcriptomes from freshwater sponges and heteroscleromorpha (i.e. *E. muelleri and E. fluviatilis, and S. carteri, T. wilhelma, M. phyllophyla, C. concentrica, T. anhelens* and *Cynanchyrella sp*). In total, three different silicateins of this type were found in three haplosclerid species (*H. oculata, H.*

simulans and *A. queenslandica*) while all other sponges showed the presence of only one or two CHN variants. One silicatein variant with the C/SQN in the active site was found exclusively in five haplosclerid genomes and transcriptomes (*H. indistincta, H. amboinensis, P. ficiformis, A. queenslandica* and *X. testudinaria*) while *H. indistincta* possessed two of these variants. The distribution of the diverse silicatein types across the phylum is summarized in Table 4.

Silintaphins were not found in the transcriptomes and genomes from marine haplosclerids but one homolog of this gene was present in the genomes and transcriptomes from all heteroscleromorpha and freshwater sponges. In addition, glassin was found in three out of the four hexactinellid transcriptomes (not found in *H. populiferum*) (Amino acid sequences of silintaphin + glassin from all available transcriptomes and genomes are provided here in Appendices 3 and 4).

Table 4. Number of the complete silicateins of the three types found in poriferan genomes and transcriptomes. *The silicatein of this species was incomplete and not included in this analysis. +Incomplete silicateins were not included in this analysis.

Genomes and Transcriptomes	SHN	CHN	C/SQN
HAPLOSCLERIDA			
Haliclona oculata	1	3	0
Haliclona simulans	1	3	0
Haliclona indistincta	1	2	2
Amphimedon queenslandica	1	3	1
Xestospongia testudinaria	1	2	1
Haliclona tubifera	1	2	0
Haliclona amboinensis	1	1	1
Petrosia ficiformis	1	2	1
HETEROSCLEROMORPHA			
Ephydatia muelleri	9	2	0
Ephydatia fluviatilis	7	2	0
Spongilla lacustris	6	0	0
Stylissa carteri+	2	1	0
Tehthya wilhelma	5	1	0
Latrunculia apicalis	2	0	0
Kirkpatrickia variolosa	3	0	0
*Pdeusopsongorites suberitoides**	1	0	0
Mycale phyllophyla	4	2	0
Cymbastela concentrica	5	1	0
Tedania anhelens	5	2	0
Scopalina sp	3	0	0
Cinanchyrella sp	5	2	0
Ircinia fasciculata	0	0	0
Chondrilla caribbea	0	0	0
Halisarca dujardini	0	0	0
HOMOSCLEROMORPHA			
Oscarella carmella	0	0	0
Corticium candelabrum	0	0	0
HEXACTINELLIDA			
Aphrocallistes vastus	0	0	0
Hyalonema populiferum	0	0	0
Rosella fibulata	0	0	0
Sympagella nux	0	0	0
CALCAREA			
Sycon cilliatum	0	0	0
Leucoselonia complicata	0	0	0

Phylogenetic relationships of silicateins

The majority of silicatein sequences were monophyletic (Figure 1a and b). Trees drawn from the first and second datasets suggest that one "silicatein" from *H. indistincta* (*Haliclona_indistincta*5) was more closely related to the cathepsins L sequences rather than to the remaining silicatein sequences (Figure 1a, b; Appendix 5 and 6). Six well-supported clades (SHNI, SHNII, CHNI, CHNII, CHNIII and C/SQN) were recovered in all trees and while removal of sequences did not alter significantly relationships (between clades), bootstrap support was low via ML for some internal branches (Figure 1, Appendix 5 and 6). One clade of sequences with a CHN motif (CHNI) was a sister clade to all remaining silicateins while sequences of the SHN type evolved twice. Support of the monophyly of most clades is strong from ML and BI analyses (Figure 1, Appendix 5 and 6).

The clade CHNI contained sequences from marine haplosclerids and freshwater sponges but none from the other heteroscleromorpha examined (Appendix 7 and 8). Figure 2 indicates that only two groups of haplosclerids contained silicateins of this type, i.e. haplosclerid clades A and B (with *H. indistincta* and other haplosclerids missing the CHNI variant). The CHNII clade contained sequences from the full range of haplosclerid species from which data was available. Relationships between the haplosclerid sequences were what might be expected from other molecular data (i.e. clade A and B representatives as sister groups, and *H. indistincta* (clade C) sister taxon to clade of A+B).

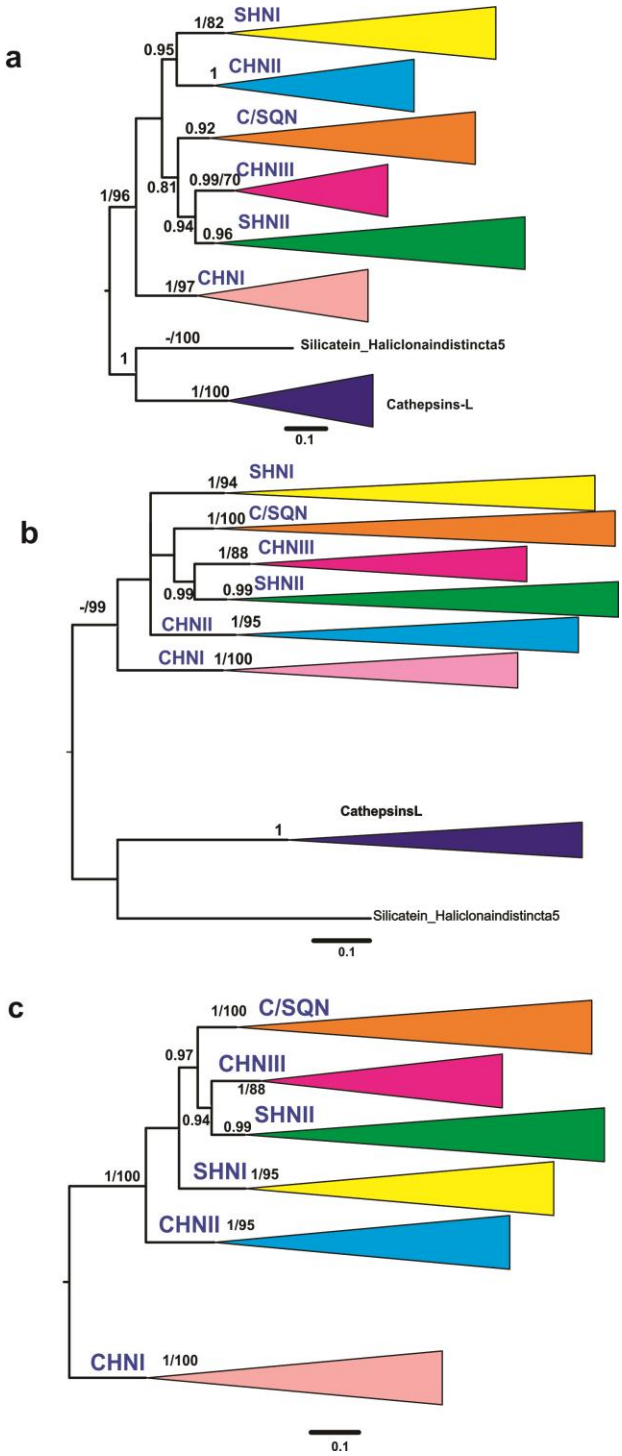

Figure 1. Molecular phylogenetic trees reconstructed using silicatein data, a= all data, b=minus short sequences, c= minus cathepsins L (outgroup) sequences and those that generated very long branches. In the first and second datasets, cathepsins L were used as outgroup to root the tree while in the third tree the CHNI clade was used as outgroup. For better clarity of the general relationships intraclade branches were collapsed and individual clades labelled (CHNI, CHNII, CHIII, SHNI, SHNII, C/SQN). The best Log likelihood (ML) for the first tree was: -19268.0428.; for the second tree: -36357.3599 and for the third tree: -34405.3319. The trees presented are those from Mr. Bayes which were congruent with those from PhyML. Support on the branches represents Bayesian posterior probability/maximum likelihood bootstrap proportion.

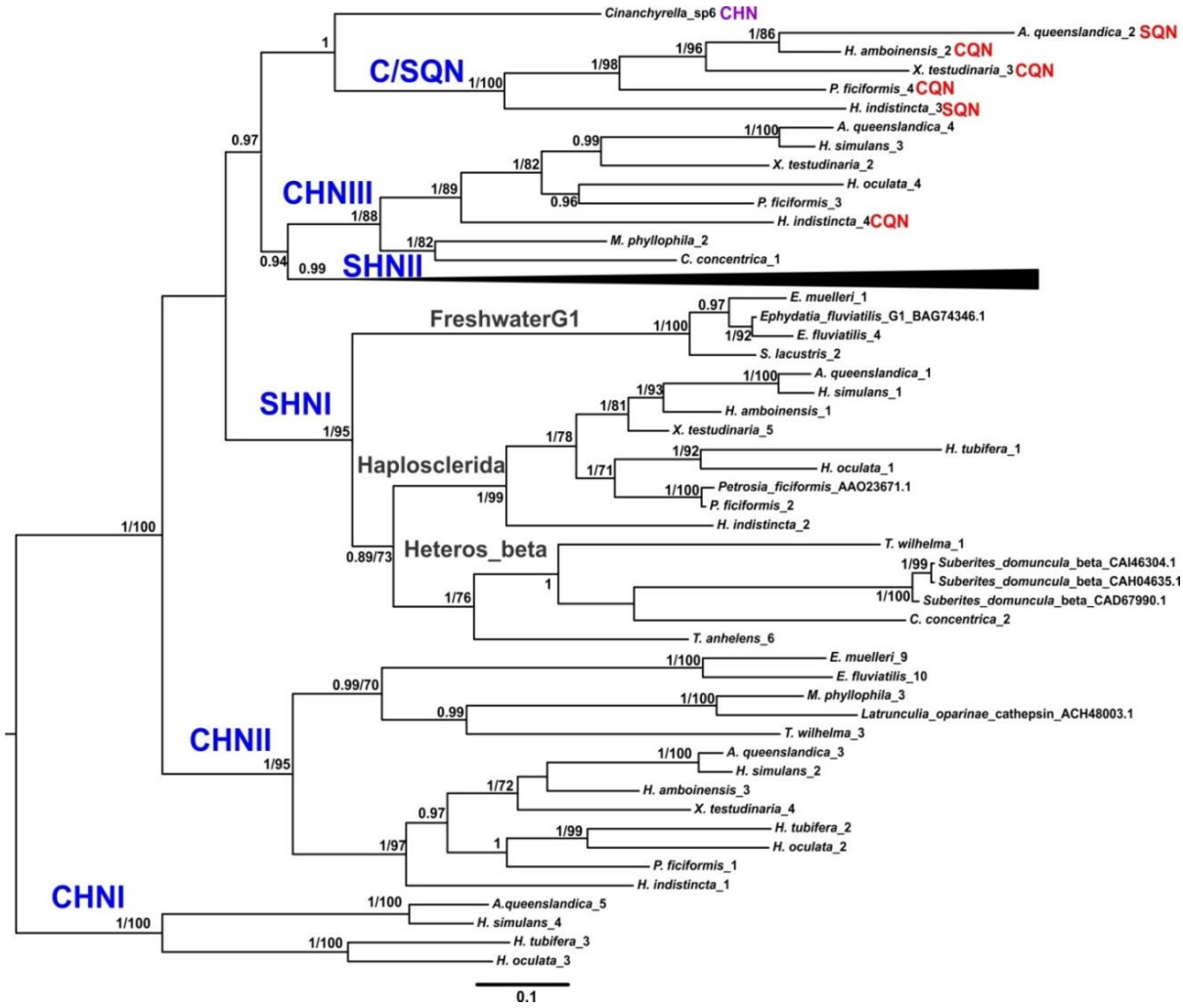

Figure 2. Molecular phylogenetic tree from the final dataset showing the relationships between sequences belonging to the CHN, C/SQN and SHNI clades (part1). Sequences for SHNII were collapsed for clarity. The tree presented is reconstructed using Mr. Bayes which was congruent with those from PhyML. Support on the branches represents Bayesian posterior probability/maximum likelihood bootstrap proportions.

The two sequences from fresh water sponges (*Ephydatia*) formed a sister clade to three representatives from the remaining heteroscleromorpha, i.e. *T. wilhelma*3, *Mycale phyllophyla3* and *Latrunculia_oparinae*. The haplosclerida were also well represented in the CHNIII clade (present in six out of eight species included). No freshwater sponges were found that contained this variant and only two other demosponges were found to contain it, i.e. *Mycale* and *Cymbastela* (Figure 2). The sequence of *Haliclona indistincta*4, which fell

into this clade, contained a Q (Glutamine) instead of a Histidine (H) (CQN type) at the active site.

The C/SQN clade only contained sequences from marine haplosclerids but this variant was not universally present in haplosclerids. The sequences from *A. queenslandica*2 and *H. indistincta*3 had an SQN configuration, while the sequences from *H. amboinesis*2, *X.testudinaria*3 and *P. ficiformis*3 had a CQN configuration at the active site.

The SHNI clade, which can be defined as a silicatein beta clade due to the presence of the *Suberites* beta sequence contained sequences from freshwater sponges that formed a sister clade to a larger clade containing the Haplosclerida and the remaining Heteroscleromorpha. As with the CHN clades, relationships amongst the marine haplosclerid sequences followed an expected phylogenetic pattern, i.e. reflecting ribosomal and mitochondrial data (Figure 2). The SHNII clade contained sequences that were characteristic of silicatein alpha and gamma, from heteroscleromorpha and from freshwater sponges but did not contain any sequences from haplosclerids (Figure 3). Those from freshwater sponges were monophyletic and divided into six subclades. However multiple duplications of this gene is evident with various copies of the gene forming small clades, e.g. sequences from Poecilosclerida were polyphyletic across four subclades, while the relationships between other sequences are unresolved, e.g. *Cinanchyrella*sp3, *Cinanchyrella*sp6, *Cinanchyrella*sp7, *Cymbastelaconcentrica*5. Three silicateins from the transcriptome from *Scopalina* sp. formed a monophyletic subclade. Sequences from *Tedaniaanhelens*2 and the hexactinellid *Aulosaccus* sp. contained a CHN configuration at the active site but were found to be members of the SHNII clade rather than to one of the CHN clades. The three amino acids forming the catalytic triad in silicateins (SHN, CHN and C/SQN) did not define the location of the sequences into the six major

molecular clades. I tried to identify whether or not there are some conserved amino acid motifs in the silicatein sequences included in the overall alignment and in the sequences of each alignment (from the six molecular clades), but no clear motifs were detected (Appendices 9 to 16).

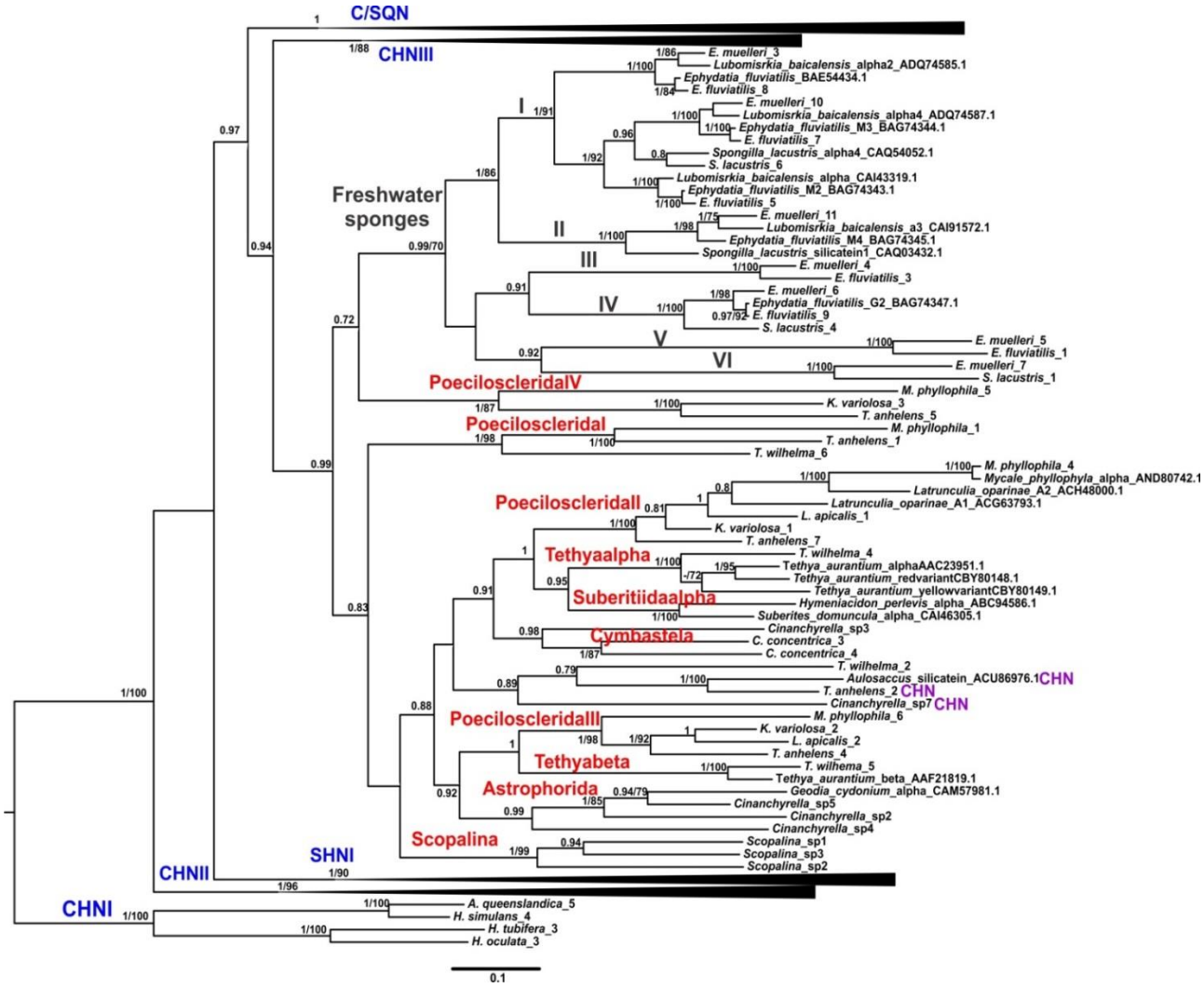

Figure 3. Molecular phylogenetic tree from the final dataset showing the relationships between sequences of the SHNII clade, other clades are collapsed for clarity (part2). The tree presented is reconstructed using Mr. Bayes which was congruent with those from PhyML. Support on the branches represents Bayesian posterior probability/maximum likelihood bootstrap proportions.

Discussion

This chapter demonstrates a higher diversity of silicatein genes of the three types (CHN, SHN, C/SQN) in the transcriptomes and genomes of selected species belonging to the class Demospongiae than was previously recognized. These results indicate a frequent duplication of the silicatein genes, which makes inferring their evolutionary relationships complex. I find the previous classification of silicatein genes into three main groups: beta, alpha/gamma and freshwater sponges (Mohri et al., 2008; Kozhemyako et al., 2010) to be too simple and instead show that the silicatein variants are located into six major clades. Furthermore, the pattern of the phylogenetic trees generated indicates that CHN silicateins were the first to appear and are the more prevalent silicatein types in haplosclerid sponges.

The silicateins of the SHN type are reported to form the proteinaceous core found inside the spicules and also responsible for silica condensation (Shimizu et al., 1998; Cha et al., 1999; Fairhead et al., 2008; Wang et al., 2014). However, I show that silicateins of the CHN type are common, have also diversified in demosponges bearing silica spicules and therefore are likely to have a role in skeleton construction. Although, this fact needs further corroboration, a number of studies indicate a role for these silicatein types in spicule formation. For instance, silicatein transcripts of the CHN type were identified in the sclerocytes of juvenile *A. queenslandica* using whole mount *in situ* hybridization (Gauthier, 2015). Likewise, a recombinant silicatein of the CHN type from *L. oparinae* (named as a cathepsins by the authors, but member of clade CHNII) was able to precipitate hexahedral or octagonal silica nanoparticles in a medium with THEOS (Kamenev et al., 2015) and this variant was reported by Shkryl et al. (2016) as the second-most highly expressed gene among five silicateins using RT-qPCR. In addition, silicateins of the CHN type were the most highly expressed genes in

H. indistincta adult specimens, and in the larval stage that produces spicules (Chapter 4). Therefore it is highly likely that silicatein variants with CHN at the active site can also condense silica and play a primary role in spicule formation in haplosclerid sponges.

Some molecular studies place marine haplosclerids as a sister clade to the heteroscleromorpha (Lavrov et al., 2008; Sperling et al., 2010; Redmond et al., 2013; Hill et al., 2013; Thacker et al., 2013). Given the arrangement of the silicatein variants on the phylogenies here it appears that CHN variants are the ancestral silicatein types and are commonly used silicateins in haplosclerids. Furthermore, *H. indistincta* contains perhaps an early silicatein form or a cathepsin/silicatein intermediate (*H. indistincta* belongs to clade C, a sister clade to the rest of the haplosclerids (Redmond et al., 2013)). When viewed together this data may suggest that the haplosclerid lineage was one of the first to acquire silicatein genes to form spicules when compared to heteroscleromorpha and that some species of the clade C have retained older versions of silicatein copies.

The megascleres in haplosclerid species are confined to simple needle-like monaxons similar to those found in some crown-group demosponge families, e.g. Hazelidae Walcott, 1920 (Li et al. 1998; Botting, 2003; Botting et al. 2013; 2017, Yang et al. 2017). I suggest that the simplicity of spicule morphology in marine haplosclerids could be due to the presence of only a single SHNI variant (SHNII alpha and gamma variants are missing and may have evolved later). In addition, the silintaphin gene is also absent in this group. It may be feasible that spicule variation in demosponges is linked to the number of silicatein variants present in their respective genomes, particularly SHNII copies. For instance, different SHNII variants were reported to be differentially expressed in distinct spicule types in the sponge *Ephydatia fluviatilis* (Mohri et al. 2008) and silicatein alpha (missing in Haplosclerida) has been reported

to have a role in the external shaping of spicules in *Suberites domuncula* (Müller et al. 2005). This data, especially when viewed in addition to the presence of multiple CHN copies in haplosclerids but not in other heterocleromorpha, might also indicate that the process of spicule formation in marine haplosclerids is different from freshwater sponges and other heteroscleromorpha even if they have silicatein genes. In turn this evidence provides support for a distinct Haplosclerомorpha (Redmond et al. 2013) rather than haplosclerids being part of the Heteroscleromorpha.

With regard to the Haplosclerida, the gene trees here reconstructed from orthologous of silicatein variants offer further support to existing molecular phylogenies of relationships within the haplosclerida. While *H. simulans* sequences are consistently separated from those from *H. oculata* (both previously placed within the same subgenus) indicating a good deal of time since the species/clade separated, regrettably no taxon-specific variants of CHN or SHN were found nor indeed particular motifs in the silicatein variants, that would clearly explain taxonomic differences. It is likely that differences in expression of the variants, and/or epigenetic effects are responsible for the differences in skeletal architecture. Furthermore, much more work needs to be carried out now on functional and structural aspects of the silicatein variants, including different forms of CHN as well as C/SQN to further understand skeleton-formation in Haplosclerida, which in turn will assist in understanding more about the evolution of these enigmatic sponges.

No silicateins were found in the transcriptomes of the demosponges: *I. fasciculata, H. dujardini and C. nucula*. The first species belongs to the subclass Keratosa in which the skeleton is formed of anastomosed spongin fibres lacking spicules (Erpenbeck et al. 2012). The remaining two species belong to the subclass Verongimorpha: *H. dujardini* lacks spicules

and the body is formed of fibrillar collagen while the body of *C. nucula* is formed of nodular collagen and silica microscleres named oxyphaerrasters (Redmond et al. 2013). There are two different evolutionary schemes for sponges belonging to Keratosa and Verongimorpha, based on different loci: either they formed a monophyletic clade which is a sister to the remaining demosponges bearing silica spicules (Lavrov et al. 2008; Redmond et al. 2013) or they are paraphyletic in which Verongimorpha is a sister clade to Keratosa + demosponges bearing silica spicules (Sperling et al. 2010; Hill et al. 2013; Thacker et al. 2013). If they are monophyletic and the last common ancestor of Demospongiae had spicules (produced by silicatein genes), as it has been hypothesized based on fossil data (Botting, 2003; Ehrlich et al. 2013; Botting et al. 2017; Botting and Muir, 2018), spicule proteins (presumed silicateins) were lost in the lineage leading to these two groups. On the other hand, the paraphyletic scheme proposed would mean that the genes were lost twice but retained in Chondrillidae (Yang et al. 2017; Botting et al. 2017). A third scenario is possible, i.e. that the last common ancestor of Demospongiae had no spicules (or silicatein genes) and silicatein genes were acquired exclusively in demosponges that contain spicules formed by these proteins. The silintaphin gene was acquired exclusively in freshwater sponges and heteroscleromorpa (Figure 4). In contrast, the skeleton of horny sponges developed spongin, collagen or chitin fibres and an as yet unknown protein is responsible for spicule formation in species belonging to the family Chondrillidae (subclass Verongimorpha). Although, this hypothesis needs further corroboration, there is evidence (biomarkers and molecular clock analysis) that suggest demosponges existed through the terminal of the Neoproterozoic era (Love et al. 2009; Sperling et al. 2010; Erwin et al. 2011; Antcliffe 2013; Gold et al. 2016) prior to the earliest biomineralizing fossil sponge record (Sperling et al. 2010; Chang et al. 2017). Furthermore, a sponge fossil, *Eocyathispongia qiania*, dated from 600 Ma prior to the

Cambrian era resembles some extant sponges lacking spicules (Yin et al. 2015; Botting and Muir, 2018).

The picture becomes more complicated however, given that Kozhemyako et al. (2010) and Riesgo et al. (2015) reported the presence of silicateins in the keratose and spicule-free species *Acanthodendrilla* sp and *Spongia lamella* respectively. The silicatein sequences of both species are incomplete (that from *S. lamellae* comprising of just a few amino acids) and were not included in this analysis. However, a phylogenetic tree reconstructed via neighbor-joining which included the short sequences from *Acanthodendrilla* sp showed them grouped in the SHNII clade. Given that the subclass Keratosa is very distinct and likely distantly related from the main heteroscleromorpha, and given that silicateins from freshwater sponges are distinct from remaining heteroscleromorpha, I might expect that silicateins from keratose species would be distinct from other demosponge sequences. Finding this short sequence inside the SHNII clade raises questions as to whether the silicateins reported from *Acanthodendrilla* sp originate from another sponge species co-located with the specimen at the moment of collection or laboratory contamination. Given that the sequences are so short however and not having any further information on the specimen I cannot be sure. Therefore, confirming the presence/absence of silicateins in more spicule-less species would be very informative.

Silicateins were not found in the five transcriptomes from hexactinellids and two genomes from calcareous sponges which is not surprising given that calcareous sponges have spicules made of calcium carbonate and various carbonic anhydrases are the main proteins responsible for this process, while glassin is the main protein for the siliceous skeletal system in the hexactinellid *Euplectella* sp. (Voigt et al. 2014; 2017; Shimizu et al. 2015). Silicateins were

previously reported however, in three hexactinellid species using molecular cloning approaches (Müller et al. 2008; Veremeichik et al. 2011). The sequence of *Crateromorpha meyeri* was incomplete and not included in this analysis while the sequences of *Aulosaccus* sp. (CHN) and *Euplectella aspergillum* were included (members of clade SHNII). I cannot fully explain the presence of these short sequences, as different laboratories generated them. I could assume that hexactinellid sequences should be distantly related to demosponge silicateins given the evolutionary distances and the divergence already noted amongst silicateins in the phylogenetic trees seen here. In that case these short sequences might also represent contamination, a notorious issue for sponges. However, the sequences are incomplete and their positions may potentially be artifacts of the analyses or probably these silicateins are rare cathepsins-L accumulating multiple mutations with similar amino acid composition to silicateins. If the silicateins are present in the genomes of hexactinellids but not expressed (and so absent from the transcriptomes I examined) then it is highly unlikely that they are responsible for skeleton formation in these sponges and therefore why they would exist remains a good question. It is more likely that they are artifacts of some sort of contamination but without further work I won't know for sure. No silicateins were found in the two transcriptomes from homoscleromorpha (*Oscarella carmela* and *Corticium candelabrum*) and currently, the protein responsible for spicule formation in members of this group that do have siliceous spicules is unknown (Maldonado and Riesgo, 2007; Riesgo et al. 2015). From this data it seems likely that in the four sponge classes, different proteins have evolved for spicule formation, which might indicate that these molecular mechanisms were acquired independently and perhaps the last common ancestor of Porifera had no spicules (Figure 4).

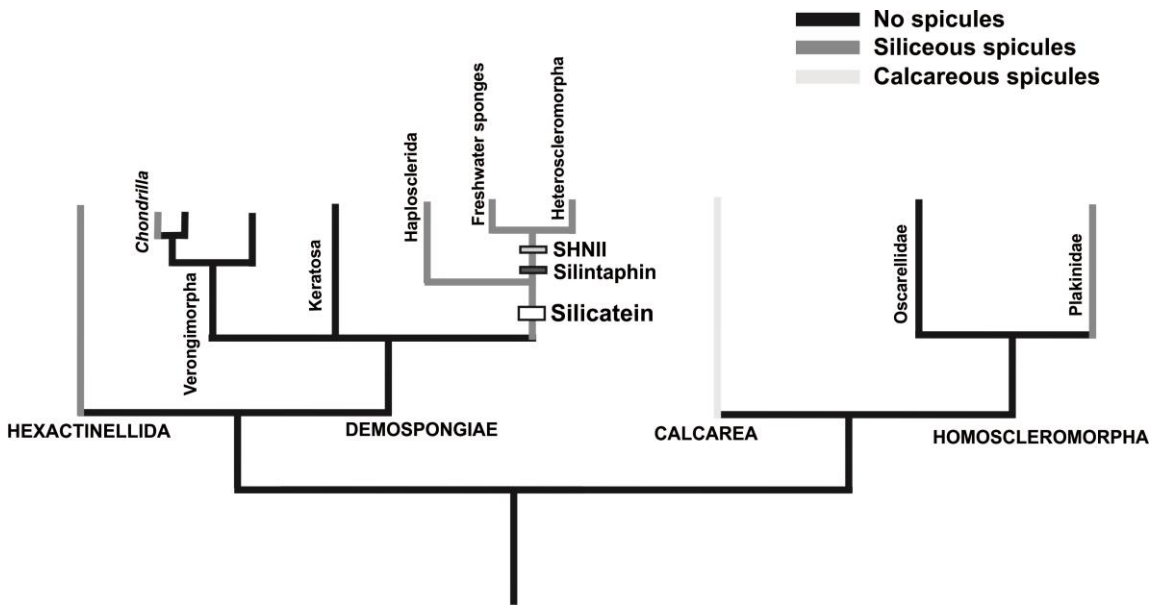

Figure 4. A proposed cladogram following Feuda et al. (2017) showing the findings regarding the acquisition of silicatein and silintaphin genes and the presence/absence of siliceous spicules in the four sponge classes. While silicateins first appear in Haplosclerida and some Heteroscleromorpha-proper, those of the SHNII type and silintaphins are absent in Haplosclerida. Silicateins are not responsible for spicule formation in the demosponge *Chondrilla* (Verongimorpha) or in Hexactinellid, Homoscleromorpha or Calcareous sponges with spicules. This cladogram also suggests that the last common ancestor or Porifera had no spicules.

References

Abascal, F., Zardoya, R., Posada, D. (2005). ProtTest: selection of best-fit models of protein evolution. Bioinformatics, 21(9), 2104–2105.

Aguilar-Camacho, J. M. McCormack, G. P. (2017). Molecular Responses of Sponges to Climate Change. In: Climate Change, Ocean Acidification and Sponges(pp. 79–104). Springer, Cham.

Alié, A., Hayashi, T., Sugimura, I., Manuel, M., Sugano, W., Mano, A., Sato, N., Agata, K., Funayama, N. (2015). The ancestral gene repertoire of animal stem cells. Proceedings of the National Academy of Sciences, 112(51), E7093–E7100.

Antcliffe, J. B. (2013). Questioning the evidence of organic compounds called sponge biomarkers. Palaeontology, 56(5), 917–925.

Bailey, T. L., Williams, N., Misleh, C., Li, W. W. (2006). MEME: discovering and analyzing DNA and protein sequence motifs. Nucleic acids research, 34(suppl_2) W369–W373.

Borisenko, I., Adamski, M., Ereskovsky, A., Adamska, M. (2016). Surprisingly rich repertoire of Wnt genes in the demosponge *Halisarca dujardini*. BMC evolutionary biology, 16(1), 123.

Botting, J. P. (2003). *Cyathophycus* and the origin of demosponges. Lethaia, 36(4), 335–343.

Botting, J. P., Cárdenas, P., Peel, J. S. (2015). A crown-group demosponge from the early Cambrian Sirius Passet Biota, North Greenland. Palaeontology, 58(1), 35–43.

Botting, J. P., Muir, L. A. (2013). Spicule structure and affinities of the Late Ordovician hexactinellid-like sponge *Cyathophycus loydelli* from the Llanfawr Mudstones Lagerstätte, Wales. Lethaia, 46(4), 454–469.

Botting, J. P., Muir, L. A. (2018). Early sponge evolution: A review and phylogenetic framework. Palaeoworld, 27(1), 1–29.

Botting, J. P., Muir, L. A., Lin, J. P. (2013). Relationships of the Cambrian protomonaxonida (Porifera). Palaeontologia Electronica, 16(2), 1–23.

Botting, J. P., Zhang, Y., Muir, L. A. (2017). Discovery of missing link between demosponges and hexactinellids confirms palaeontological model of sponge evolution. Scientific reports, 7(1), 5286.

Brutchey, R. L., Morse, D. E. (2008). Silicatein and the translation of its molecular mechanism of biosilicification into low temperature nanomaterial synthesis. Chemical reviews, 108(11), 4915–4934.

Cao, X., Fu, W., Yu, X., Zhang, W. (2007). Dynamics of spicule production in the marine sponge Hymeniacidon perlevis during in vitro cell culture and seasonal development in the field. Cell and tissue research, 329(3), 595–608.

Cárdenas, P., Pérez, T., Boury-Esnault, N. (2012). Sponge Systematics Facing New Challenges. Advances in marine biology, 61 (1), 1–79.

Cha, J. N., Shimizu, K., Zhou, Y., Christiansen, S. C., Chmelka, B. F., Stucky, G. D., Morse, D. E. (1999). Silicatein filaments and subunits from a marine sponge direct the polymerization of silica and silicones in vitro. Proceedings of the National Academy of Sciences, 96(2), 361–365.

Chang, S., Feng, Q., Clausen, S., Zhang, L. (2017). Sponge spicules from the lower Cambrian in the Yanjiahe Formation, South China: The earliest biomineralizing sponge record. Palaeogeography, Palaeoclimatology, Palaeoecology, 474, 36–44.

De Weerdt, W. H. 2002. Family Chalinidae Gray, 1867. In: Systema Porifera (pp. 852–873). Springer, Boston, MA.

Díez-Vives, C., Moitinho-Silva, L., Nielsen, S., Reynolds, D., Thomas, T. (2017). Expression of eukaryotic-like protein in the microbiome of sponges. Molecular ecology, 26(5), 1432–1451.

Ehrlich, H., Rigby, J. K., Botting, J. P., Tsurkan, M. V., Werner, C., Schwille, P., Petrášek, Z., Pisera, A., Simon, P., Sivkov, N.V., Vyalikh, D.V., Molodtsov, S. L., Kurek, D., Kammer, M., Hunoldt, S., Born, R., Stawski, D., Steinhof, A., Bazhenov V.V., Geisler, T. (2013). Discovery of 505-million-year old chitin in the basal demosponge *Vauxia gracilenta*. Scientific reports, 3:3497.

Erpenbeck, D., Sutcliffe, P., Cook, S. D. C., Dietzel, A., Maldonado, M., van Soest, R. W., Hooper J.N.A., Wörheide, G. (2012). Horny sponges and their affairs: On the phylogenetic relationships of keratose sponges. Molecular Phylogenetics and Evolution, 63(3), 809–816.

Erwin, D. H., Laflamme, M., Tweedt, S. M., Sperling, E. A., Pisani, D., Peterson, K. J. (2011). The Cambrian conundrum: early divergence and later ecological success in the early history of animals. Science,334(6059), 1091–1097.

Fairhead, M., Johnson, K. A., Kowatz, T., McMahon, S. A., Carter, L. G., Oke, M., Liu, H., Naismith, J.H., van der Walle, C. F. (2008). Crystal structure and silica condensing activities of silicatein α–cathepsin L chimeras. Chemical Communications, (15), 1765–1767.

Fernandez-Valverde, S. L., Calcino, A. D., Degnan, B. M. (2015). Deep developmental transcriptome sequencing uncovers numerous new genes and enhances gene annotation in the sponge *Amphimedon queenslandica*. BMC genomics, 16(1), 387.

Francis, W. R., Eitel, M., Vargas, S., Adamski, M., Haddock, S. H., Krebs, S., Blum, H., Erpenbeck, D., Wörheide, G. (2017). The Genome Of The Contractile Demosponge Tethya wilhelma And The Evolution Of Metazoan Neural Signalling Pathways. bioRxiv, 120998.

Funayama, N., Nakatsukasa, M., Kuraku, S., Takechi, K., Dohi, M., Iwabe, N., Miyata, T., Agata, K. (2005). Isolation of Ef silicatein and Ef lectin as Molecular Markers Sclerocytes and Cells Involved in Innate Immunity in the Freshwater Sponge *Ephydatia fluviatilis*. Zoological science, 22(10), 1113–1122.

Gauthier A (2015). Analysis of silicatein gene expression and spicule formation in the demosponge *Amphimedon queenslandica*. MS thesis. The University of Queensland, 84 pp.

Gazave, E., Lapébie, P., Ereskovsky, A. V., Vacelet, J., Renard, E., Cárdenas, P., Borchiellini, C. (2012). No longer Demospongiae: Homoscleromorpha formal nomination as a fourth class of Porifera. Hydrobiologia, 687(1), 3–10.

Gold, D. A., Grabenstatter, J., de Mendoza, A., Riesgo, A., Ruiz-Trillo, I., Summons, R. E. (2016). Sterol and genomic analyses validate the sponge biomarker hypothesis. Proceedings of the National Academy of Sciences, 113(10), 2684–2689.

Gordon, A., Hannon, G. J. (2010). Fastx-toolkit. FASTQ/A short-reads preprocessing tools (unpublished*) http://hannonlab. cshl. edu/fastx_toolkit*, *5*.

Gouy, M., Guindon, S., Gascuel, O. (2010). SeaView version 4: a multiplatform graphical user interface for sequence alignment and phylogenetic tree building. Molecular biology and evolution, 27(2), 221–224.

Guindon, S., Dufayard, J. F., Lefort, V., Anisimova, M., Hordijk, W., Gascuel, O. (2010). New algorithms and methods to estimate maximum-likelihood phylogenies: assessing the performance of PhyML 3.0. Systematic biology, 59(3), 307–321.

Guzman, C., Conaco, C. (2016). Comparative transcriptome analysis reveals insights into the streamlined genomes of haplosclerid demosponges. Scientific reports, 6: 18774.

Haas, B. J., Papanicolaou, A., Yassour, M., Grabherr, M., Blood, P. D., Bowden, J.,MacManes, M. D. (2013). De novo transcript sequence reconstruction from RNA-seq using the Trinity platform for reference generation and analysis. Nature protocols, 8(8), 1494–1512.

Hill, M.S., Hill, A.L., Lopez, J., Perterson, K.J., Pomponi, S., Diaz, M.C., Thacker, R.W., Adamska, M., Boury-Esnault, N., Cárdenas, P., Chaves-Fonnegra, A., Danka, E., De Laine, B., Formica, D., Hajdu, E., Lobo-Hajdu, G., Klontz, S., Morrow, C.C., Patel, J., Picton, B., Pisani, D., Pohlmann, D., Redmond, N.E., Reed, J., Richie, S., Riesgo, A., Rubin, E., Russell, Z., Rützler, K., Sperling, E.A., di Stefano, M., Tarver, J.D., Collins A.G. (2013) Reconstruction of family level phylogenetic relationships within Demospongiae (Porifera) using nuclear encoded housekeeping genes. Public Library of Science. PLOS One, 8(1): e50437.

Hooper, J. N., Van Soest, R. W. M. (2002). Systema Porifera. A guide to the classification of sponges. Springer, Boston, MA.

Kaluzhnaya, O. V., Belikov, S. I., Schröder, H. C., Wiens, M., Giovine, M., Krasko, A., Müller I.B., Müller, W. E. (2005). Dynamics of skeleton formation in the Lake Baikal sponge *Lubomirskia baicalensis*. Part II. Molecular biological studies. Naturwissenschaften, 92(3), 134–138.

Kaluzhnaya, O. V., Belikova, A. S., Podolskaya, E. P., Krasko, A. G., Müller, W. E. G., Belikov, S. I. (2007). Identification of silicateins in freshwater sponge *Lubomirskia baicalensis*. Molecular Biology, 41(4), 554-561.

Kalyuzhnaya, O. V., Krasko, A. G., Grebenyuk, V. A., Itskovich, V. B., Semiturkina, N. A., Solovarov, I. S., Müller, W. E. G., Belikov, S. I. (2011). Freshwater sponge silicateins: comparison of gene sequences and exon-intron structure. Molecular Biology, 45(4), 567.

Kamenev, D. G., Shkryl, Y. N., Veremeichik, G. N., Golotin, V. A., Naryshkina, N. N., Timofeeva, Y. O., Kovalchuk, S.N., Semiletova, I.V., Bulgakov, V. P. (2015). Silicon Crystals Formation Using Silicatein-Like Cathepsin of Marine Sponge *Latrunculia oparinae*. Journal of nanoscience and nanotechnology, 15(12), 10046–10049.

Kozhemyako, V. B., Veremeichik, G. N., Shkryl, Y. N., Kovalchuk, S. N., Krasokhin, V. B., Rasskazov, V. A., Zhuravlev Y.N., Bulgakov V.P., Kulchin, Y. N. (2010). Silicatein genes in spicule-forming and nonspicule-forming Pacific demosponges. Marine biotechnology, 12(4), 403–409.

Krasko, A., Lorenz, B., Batel, R., Schröder, H. C., Müller, I. M., Müller, W. E. (2000). Expression of silicatein and collagen genes in the marine sponge *Suberites domuncula* is controlled by silicate and myotrophin. The FEBS Journal, 267(15), 4878–4887.

Lavrov, D. V., Wang, X., Kelly, M. (2008). Reconstructing ordinal relationships in the Demospongiae using mitochondrial genomic data. Molecular phylogenetics and evolution, 49(1), 111–124.

Leys, S. P., Hill, A. (2012). The Physiology and Molecular Biology of Sponge Tissues. Advances in marine biology, 62, 1.

Li, C.W., Chen, J.Y. and Hua, T.E. (1998). Precambrian sponges with cellular structures. Science, 279(5352), 879–882.

Love, G. D., Grosjean, E., Stalvies, C., Fike, D. A., Grotzinger, J. P., Bradley, A. S., Kelly, A.E., Bhatia, M., Meredith, W., Snape, C.E., Bowring, S. A., Condon, D.J., Summons, R.E. (2009). Fossil steroids record the appearance of Demospongiae during the Cryogenian period. Nature, 457(7230), 718–721.

Ma, J. Y., Yang, Q. (2016). Early divergence dates of demosponges based on mitogenomics and evaluated fossil calibrations. Palaeoworld, 25(2), 292–302.

Maldonado, M., Riesgo, A. (2007). Intra-epithelial spicules in a homosclerophorid sponge. Cell and Tissue Research, 328(3), 639–650.

Mohri, K., Nakatsukasa, M., Masuda, Y., Agata, K., Funayama, N. (2008). Toward understanding the morphogenesis of siliceous spicules in freshwater sponge: Differential mRNA expression of spicule-type-specific silicatein genes in *Ephydatia fluviatilis*. Developmental Dynamics, 237(10), 3024–3039.

Morrow, C. C., Picton, B. E., Erpenbeck, D., Boury-Esnault, N., Maggs, C. A., Allcock, A. L. (2012). Congruence between nuclear and mitochondrial genes in Demospongiae: A new hypothesis for relationships within the G4 clade (Porifera: Demospongiae). Molecular Phylogenetics and Evolution, 62(1), 174-–190.

Morrow, C., Cárdenas, P. (2015). Proposal for a revised classification of the Demospongiae (Porifera). Frontiers in Zoology, 12(1), 7.

Müller, W. E. G., Schröder, H. C., Wrede, P., Kaluzhnaya, O. V., Belikov, S. I. (2006). Speciation of sponges in Baikal-Tuva region: an outline. Journal of Zoological Systematics and Evolutionary Research, 44(2), 105–117.

Müller, W. E., Boreiko, A., Wang, X., Belikov, S. I., Wiens, M., Grebenjuk, V. A., Schloßmacher, U., Schröder, H. C. (2007). Silicateins, the major biosilica forming enzymes present in demosponges: protein analysis and phylogenetic relationship. Gene, 395(1), 62–71.

Müller, W. E., Rothenberger, M., Boreiko, A., Tremel, W., Reiber, A., Schröder, H. C. (2005). Formation of siliceous spicules in the marine demosponge *Suberites domuncula*. Cell and tissue research, 321(2), 285–297.

Müller, W. E., Schloßmacher, U., Eckert, C., Krasko, A., Boreiko, A., Ushijima, H., Wolf, S.E., Tremel, W., Müller, I.M., Schröder, H. C. (2007b). Analysis of the axial filament in spicules of the demosponge *Geodia cydonium*: different silicatein composition in microscleres (asters) and megascleres (oxeas and triaenes). European journal of cell biology, 86(8), 473–487.

Müller, W. E., Wang, X., Kropf, K., Boreiko, A., Schloßmacher, U., Brandt, D., Schröder, H.C., Wiens, M. (2008). Silicatein expression in the hexactinellid *Crateromorpha meyeri*: the lead marker gene restricted to siliceous sponges. Cell and tissue research, 333(2), 339–351.

Murr, M. M., Morse, D. E. (2005). Fractal intermediates in the self-assembly of silicatein filaments. Proceedings of the National Academy of Sciences of the United States of America, 102(33), 11657–11662.

Nakayama S, Arima K, Kawai K, Mohri K, Inui C, Sugano W, Koba H, Tamada K, Nakata YJ, Kishimoto K, Arai–Shindo M, Kojima C, Matsumoto T, Fujimori T, Agata K, Funayama N (2015) Dynamic transport and cementation of skeletal elements build up the pole–and–beam structured skeleton of sponges. Curr Biol 25(19) 2549–2554.

Nichols, S. A., Dirks, W., Pearse, J. S., King, N. (2006). Early evolution of animal cell signaling and adhesion genes. Proceedings of the National Academy of Sciences, 103(33), 12451-–12456.

Peña, J. F., Alié, A., Richter, D. J., Wang, L., Funayama, N., Nichols, S. A. (2016). Conserved expression of vertebrate microvillar gene homologs in choanocytes of freshwater sponges. EvoDevo, 7(1), 13.

Pozdnyakov, I. R., Sokolova, A. M., Ereskovsky, A. V., Karpov, S. A. (2018). Kinetid structure in sponge choanocytes of Spongillida in the light of evolutionary relationships within Demospongiae. Zoological Journal of the Linnean Society.

Pozzolini, M., Sturla, L., Cerrano, C., Bavestrello, G., Camardella, L., Parodi, A. M., Raheli, F., Benatti, U., Müller W.E.G., Giovine, M. (2004). Molecular cloning of silicatein gene from marine sponge Petrosia ficiformis (Porifera, Demospongiae) and development of primmorphs as a model for biosilicification studies. Marine biotechnology, 6(6), 594–603.

Qiu, F., Ding, S., Ou, H., Wang, D., Chen, J., Miyamoto, M. M. (2015). Transcriptome Changes during the Life Cycle of the Red Sponge, *Mycale phyllophila* (Porifera, Demospongiae, Poecilosclerida). Genes, 6(4), 1023–1052.

Redmond NE, Morrow CC, Thacker RW, Diaz MC, Boury-Esnault N, Cárdenas P, Hajdu E, Lôbo-Hajdu G, Picton BE, Pomponi SA, Kayal E, Collins AG (2013). Phylogeny and systematics of Demospongiae in light of new small-subunit ribosomal DNA (18S) sequences. Integrative and comparative biology, 53:388–415.

Redmond NE, Raleigh J, van Soest RW, Kelly M, Travers SA, Bradshaw B, Vartia S, Stephens K, McCormack GP (2011). Phylogenetic relationships of the marine Haplosclerida (Phylum Porifera) employing ribosomal (28S rRNA) and mitochondrial (cox1, nad1) gene sequence data. PLoS One, 6(9), e24344.

Riesgo, A., Farrar, N., Windsor, P. J., Giribet, G., Leys, S. P. (2014). The analysis of eight transcriptomes from all poriferan classes reveals surprising genetic complexity in sponges. Molecular biology and evolution, msu057.

Riesgo, A., Maldonado, M., López-Legentil, S., Giribet, G. (2015). A Proposal for the Evolution of Cathepsin and Silicatein in Sponges. Journal of molecular evolution, 80(5–6), 278–291.

Ronquist, F., Huelsenbeck, J. P. (2003). MrBayes 3: Bayesian phylogenetic inference under mixed models. Bioinformatics, 19(12), 1572–1574.

Ryu, T., Seridi, L., Moitinho-Silva, L., Oates, M., Liew, Y. J., Mavromatis, C., Wang, X., Haywood, A., Lafi, F.F., Kupresanin, M., Sougrat, R., Alzahrani, M.A., Giles, E., Ghosheh, Y., Shunter, C., Baumgarten, S., Berumen, M.L., Gao, X., Aranda, M., Foret, S., Gough, J., Voolstra, C.R., Henstchel, U., Ravasi, T. (2016). Hologenome analysis of two marine sponges with different microbiomes. BMC genomics, 17(1), 158.

Schloßmacher U, Wiens M, Schröder HC, Wang X, Jochum KP, Müller WE. (2011). Silintaphin1–interaction with silicatein during structure-guiding biosilica formation. The FEBS journal. 278(7):1145–1155.

Schröder, H. C., Perovic-Ottstadt, S., Grebenjuk, V. A., Engel, S., Müller, I. M., Müller, W. E. (2005). Biosilica formation in spicules of the sponge Suberites domuncula: synchronous expression of a gene cluster. Genomics, 85(6), 666–678.

Shimizu, K., Amano, T., Bari, M. R., Weaver, J. C., Arima, J., Mori, N. (2015). Glassin, a histidine-rich protein from the siliceous skeletal system of the marine sponge *Euplectella*, directs silica polycondensation. Proceedings of the National Academy of Sciences, 112(37), 11449–11454.

Shimizu, K., Cha, J., Stucky, G. D., Morse, D. E. (1998). Silicatein α: cathepsin L-like protein in sponge biosilica. Proceedings of the National Academy of Sciences, 95(11), 6234–6238.

Shkryl, Y. N., Bulgakov, V. P., Veremeichik, G. N., Kovalchuk, S. N., Kozhemyako, V. B., Kamenev, D. G., Semiletova, I.V., Timofeeva, Y.O., Scchipunov, Y.A., Kulchin, Y. N. (2016). Bioinspired enzymatic synthesis of silica nanocrystals provided by recombinant silicatein from the marine sponge Latrunculia oparinae. Bioprocess and Biosystems Engineering, 39(1), 53–58.

Sperling, E. A., Robinson, J. M., Pisani, D., Peterson, K. J. (2010). Where's the glass? Biomarkers, molecular clocks, and microRNAs suggest a 200–Myr missing Precambrian fossil record of siliceous sponge spicules. Geobiology, 8(1), 24–36.

Srivastava, M., Simakov, O., Chapman, J., Fahey, B., Gauthier, M. E., Mitros, T., Richards, G.S., Conaco, C., Dacre, M., Hellsten, U., Larroux, C., Putnam, N.H., Stanke, M., Adamska, M., Darling, A., Degnan, S.M., Oakley, T.H., Plachetzki, D.C., Zhai, Y., Adamski, M., Calcino, A., Cummins S.F., Goodstein, D.M., Harris, C., Jackson, D.J., Leys, S.P., Shu, S., Woodcroft, B.J., Vervoort, M., Kosik, K.S., Manning, G., Degnan, B.M., Rokhsar, D. S.

(2010). The *Amphimedon queenslandica* genome and the evolution of animal complexity. Nature, 466(7307), 720–726.

Stephens, K. (2013).Insights into the evolution and development of Haliclona indistincta (Porifera, Haplosclerida)(Doctoral dissertation) N.U.I.G. 225 pp.

Stothard, P. (2000) The Sequence Manipulation Suite: JavaScript programs for analyzing and formatting protein and DNA sequences. Biotechniques 28, 1102–1104.

Thacker, R. W., Hill, A. L., Hill, M. S., Redmond, N. E., Collins, A. G., Morrow, C. C., Spicer, L., Carmack, C., Zappe, M.E., Pohlmann, D., Hall, C., Diaz, M.C., Bangalore, P.V. (2013). Nearly complete 28S rRNA gene sequences confirm new hypotheses of sponge evolution. Integrative and Comparative Biology, 53(3), 373-387.

Veremeichik, G. N., Shkryl, Y. N., Bulgakov, V. P., Shedko, S. V., Kozhemyako, V. B., Kovalchuk, S. N., Krasokhin, V. B., Zhuralev, Y.N., Kulchin, Y. N. (2011). Occurrence of a silicatein gene in glass sponges (Hexactinellida: Porifera). Marine biotechnology, 13(4), 810–819.

Voigt, O., Adamska, M., Adamski, M., Kittelmann, A., Wencker, L., Wörheide, G. (2017). Spicule formation in calcareous sponges: Coordinated expression of biomineralization genes and spicule-type specific genes. Scientific Reports, 7:45658.

Voigt, O., Adamski, M., Sluzek, K., Adamska, M. (2014). Calcareous sponge genomes reveal complex evolution of α-carbonic anhydrases and two key biomineralization enzymes. BMC evolutionary biology, 14: 230.

Wang X, Schröder HC, Müller WE (2014). Enzyme-based biosilica and biocalcite: biomaterials for the future in regenerative medicine, Trends in biotechnology,32(9), 441–447.

Whelan, N. V., Kocot, K. M., Moroz, L. L., Halanych, K. M. (2015). Error, signal, and the placement of Ctenophora sister to all other animals. Proceedings of the National Academy of Sciences, 112(18), 5773-5778.

Wörheide, G., Dohrmann, M., Erpenbeck, D., Larroux, C., Maldonado, M., Voigt, O., Borchiellini, C.,Lavrov, D. V. (2012). Deep Phylogeny and Evolution of Sponges (Phylum Porifera). Advances in marine biology,61, 1.

Yang, X. L., Zhao, Y. L., Babcock, L. E., Peng, J. (2017). Siliceous spicules in a vauxiid sponge (Demospongia) from the Kaili Biota (Cambrian Stage 5), Guizhou, South China. Scientific Reports, 7, 42945.

Yin, Z., Zhu, M., Davidson, E. H., Bottjer, D. J., Zhao, F., Tafforeau, P. (2015). Sponge grade body fossil with cellular resolution dating 60 Myr before the Cambrian. Proceedings of the National Academy of Sciences, 112(12), E1453-E1460.

Zhou, Y., Shimizu, K., Cha, J. N., Stucky, G. D., Morse, D. E. (1999). Efficient catalysis of polysiloxane synthesis by silicatein α requires specific hydroxy and imidazole functionalities. Angewandte Chemie International Edition, 38(6), 779–782.

Chapter 4

Analysis of the expression levels of the silicateins through different developmental stages in the sponge *Haliclona indistincta* (Porifera, Demospongiae, Haplosclerida)

Introduction

Sponges are simple animals that are capable of secreting inorganic structures such as microscopic elements called spicules (Uriz et al. 2003; Werner et al. 2017). These structures are made of biogenic silica in sponges belonging to the classes Demospongiae, Hexactinellida and Homoscleromorpha (Wörheide et al. 2012). The spicules are produced at least initially by particular sponge cells named sclerocytes (Uriz et al. 2003; Schröder et al. 2012). The identification of these cells is based on the presence of spicule sections containing a proteinaceous core (axial filament) inside the sclerocytes observed via electron microscopic analysis (Simpson, 1978; Leys, 2003; Uriz et al. 2000). Some species have spicules >500 µm long, which might indicate that many cells are responsible for the production of a single spicule or that the secretion could be extracellular rather than intracellular (Uriz et al. 2003; Müller et al. 2007; Schröder et al. 2012). In addition, the axial filament (lacking any surrounding silica layer) was observed within the mesohyl in some demosponge species such as *Crambe crambe* (Uriz et al. 2000).

The main protein responsible for spicule formation in species belonging to the class Demospongiae is silicatein (Cha et al. 1999; Shimizu et al. 1998; Müller et al. 2005). This protein forms fractal monomers to construct the axial filament that is found inside the spicules and also has a role in the external shaping of these structures and in silica deposition (Cha et al. 1999; Weaver and Morse, 2003; Brutchey and Morse, 2008; Schoeppler et al. 2017). Silicateins having three particular amino acids in the active site (SHN type) have been sequenced from several demosponge species (Chapter, 3; Shkryl et al. 2016). A species may have different silicatein variants of this type forming part of the axial filament of their spicules (e.g. alpha, beta and gamma in the styles of *Tethya auramtium*), or different silicatein

variants are expressed during the formation of specific spicule types (e.g. silicateins beta were expressed during gemmulosclere formation while silicateins alpha were expressed during the megasclere formation in the freshwater sponge *Ephydatia fluviatilis*) (Shimizu et al. 1998; Mohri et al. 2008).

In the genome of the haplosclerid *Amphimedon queenslandica,* Gauthier (2015) found six silicatein genes (one of the SHN type, one of the SQN type and four of the CHN type) and the majority of these variants do not have the two amino acids in the active site (S and H belonging to the SHN type), that have been reported as being necessary for silica deposition (Zhou et al. 1999; see Chapter 3). However, expression levels of all these silicateins were investigated in different developmental stages of *A. queenslandica* based on RT-qPCR (Gauthier, 2015) all containing spicules (i.e. embryos, larvae and competent larvae) which showed that silicatein of the SHN type was the most highly expressed gene followed by two silicateins of the CHN type and one silicatein of the SQN at all these developmental stages. While this sequential expression pattern was the same; there was a higher expression of all genes at two phases: the embryo stage and during larval metamorphosis. In general, no significant association was detected between the expression levels of silicatein genes and the numbers of spicules present during these life stages, i.e. embryos have fewer spicules than free swimming larvae but the genes were expressed similarly at these two stages (Gauthier, 2015). However, this latter work suggests possible involvement of CHN + SQN variants in spicule production and thus an ability to condense silica.

Given that the above is the only investigation on the expression levels of very different silicatein variants through different developmental stages in a particular species, and there is clear evidence that silicateins of the CHN type could have a role in spicule formation in *A.*

queenslandica, additional information from the expression levels of these variants in other closely or distantly related species would be useful to confirm this information. Here, I will set out to investigate the expression levels in one haplosclerid species that acquires spicules later in development than *A. queenslandica* in which silicatein variants of the three types (SHN, CHN, C/SQN) are present in its respective transcriptome.

Haliclona indistincta is viviparous and the larvae are found within the mesohyl of mature specimens in late July to early August (Stephens et al. 2013a). This species belongs to the order Haplosclerida and based on molecular data (mitochondrial and ribosomal) is member of clade C which is a sister group to the remaining haplosclerid species members of different clades (e.g. *Haliclona oculata* and *Haliclona cinerea* are members of clade A and *A. queenslandica* and *Haliclona simulans* are members of clade B) (Stephens, 2013 and unpublished data). The free swimming larvae lack spicules in comparison to some other haplosclerid species reported with spicules at this stage (e.g. *A. queenslandica, H. cinerea, H. simulans*) (Leys, 2003; Stephens et al. 2013a) and the *H. indistincta* transcriptome contains a similar but still different complement of silicatein variants to those found in *A. queenslandica*, i.e. five silicatein variants: two of the CHN type, one of the CQN type, one of the SQN type and one of the SHN type (Chapter 3). Four of these silicatein variants grouped in four out of six of the major molecular clades from the silicateins phylogeny (CHNII, CHNIII, SHNI, C/SQN) while one silicatein (CHN type) is located between the overall silicatein clade and cathepsin-L clade (Chapter 3). Here I decided to investigate the expression levels of the five silicatein variants in *H. indistincta* a) to determine which of the variants are expressed in this species, which in turn may provide further evidence about whether or not the CHN and C/SQN variants have a role in spicule construction; b) to investigate expression levels of the

five silicatein genes at distinct developmental stages and corroborate whether the expression is the same at each of these phases. In addition, certain aspects of spicule formation were studied through the identification of the cells producing spicules (sclerocytes) and the axial filament, using microscopic techniques (TEM and SEM).

Materials and Methods

Collection of larvae

Several adult sponges with larvae in the mesohyl were collected in Corranroo (Co Clare, N 53°09.100; W 09, °00.550) in July 2017. The sponges were transferred to the laboratory in buckets with aeration and then they were placed in a big tray with seawater and aeration. The specimens were dissected under the microscope and the released free swimming larvae collected using a micropipette. The free swimming larvae were placed in five petri dishes with approximately 100 larvae in each one. Ten larvae were fixed immediately in primary fixatives for SEM and TEM analyses (see below) and a total of 50 larvae were also immediately transferred into an eppendorf tube containing seawater for the RT-qPCR experiment (see below). The remaining free swimming larvae transformed into rounded larvae after approximately 24 hours, into presettled larvae after a subsequent 6 to 8 hours , followed by settled individuals after another 6 hours and finally after an additional 4 hours into juveniles (Stephens et al. 2013a). At each of these stages, ten specimens were fixed for SEM and TEM analyses. A total of 50 combined pre-settled and settled specimens were collected from the petri dish using a scalpel and transferred into an eppendorf tube containing seawater for further RT-qPCR experiment.

RT-qPCR

Expression of the silicatein genes of *H. indistincta* during three life stages was measured: 1) free swimming larvae (no spicules), 2) pre-settled and settled juvenile sponges (some spicules) and 3) adult specimens (spicules). In brief, the tube containing the free swimming larvae was centrifuged at 5000×g for 10 s and the seawater was taken out using a micropipette. 500 µl of nuclease free water was added to the tube and then centrifuged at 5000×g for 10 s and the water was taken out. One ml of Trizol was added to the tube, the tissue was homogenized using a syringe and the RNA extracted following the Trizol protocol (Riesgo et al. 2014) adjusted to the RNAeasy Mini Kit (Qiagen). The same methodology was employed for the pre-settled and settled specimens that were combined and placed into an eppendorf tube. A total of three biological replicates for these two developmental stages (free swimming larvae and presettled/settled individuals) were investigated. In addition, three adult sponges were collected and a small piece from the apical part cut for each specimen, and transferred into different eppendorf tubes for further RNA extraction (as above). The RNA extracted was resuspended in 50 µl of DEPC water (Sigma Aldrich). RNA quality and quatity (RIN value >7.0) was checked using a Bioanalyzer 2100 (Agilent Technologies) (Appendix 17). Five silicatein gene sequences of four variants (CHN × 2, SHN, CQN and SQN) were identified from the transcriptome of *H. indistincta* and specific primers designed using the NCBI Blast primer blast tool: http://www.ncbi.nlm.nih.gov/tools/primer-blast/, and synthetized (Table 1). Reverse transcription (RT) was carried out using a 20µL reaction using the RT-PCR kit (Promega) with 1 µg of RNA per sample and 50 pmol Oligo dT. The Real Time PCR (qPCR) for each sample included 5 µl of Power SYBR Green Master Mix (Applied Biosystems), 1 µl of Nuclease Free Water, 2 µl of cDNA (1:20) and 1 µl of the

forward and reverse primer of each gene and three replicates for the three life stages were examined. The samples were subjected to 40 cycles of amplification in an ABI Step One Plus Real-Time PCR System (Applied Biosystems). Data were analyzed using the ΔΔCt method and the relative levels of expression were calculated by the $2^{-\Delta\Delta Ct}$ method (Rao et al. 2013; Livak and Schmittgen, 2001) which is expressed as RQ (relative quantity). All relative levels of gene expression were normalized to the housekeeping gene HGPRT (Hypoxanthine-guanine phosphoribosyltransferase) and the control selected was the free swimming larval stage. At this phase the spicules are lacking and changes in expression levels of silicateins can be investigated. The reference gene (HGPRT) was selected because its expression was the most stable throughout development, in comparison to other three housekeeping genes that were investigated (Appendices 18, 19, 20 and 21).

Table 1. Primer sequences employed for the Real Time PCR Analysis. Brackets include the length of the primer/ Melting temperature / %GC content.

Gene	5'-Forward Primer-3' (length/Tm/%GC)	5'-Reverse Primer-3' (length/Tm/%GC)
Silicatein CHNI	ACGCCTGATGAGCTTGAAGA (20 bp / 59.39 °C/ 50%)	CCTTGGTCTTTGACGGGTGT (20 bp/ 60.18 °C/ 55%)
Silicatein CHNII	TTGAGTGGCCAAAGGGACTG (20 bp/ 60.18°C/ 55%)	TTGCCAGAGCATGTTGTCCT (20 bp/ 59.89°C/ 50%)
Silicatein CQN	TCGAGCTCTTGAGTTTGGGT (20 bp/ 58.95 °C/ 50%)	TTGGTTGGAGCAACGTCAGA (20 bp/ 59.82°C/ 50%)
Silicatein SQN	ACCTGAGATGGTCGATTGGC (20 bp /59.82°C/ 55%)	CTGTGCACTAAGCTCGACCA (20 bp/ 60.04°C /55%)
Silicatein SHN	CAAATCACACCGAACGCCTC (20 bp /59.83 °C /55%)	ATGAACATCCGCAACGCAAC (20 bp / 60.11 °C /50 %)
HGPRT	CCATGATCTGAGTGGGCCTC (20 bp/ 59.89°C/ 60%)	CTTGCATTCGGAAAGATCGCT (21 BP/ 59.33°C/ 47.62%)

Statistical analyses

Data were logtransformed and differences in the relative levels of expression between the five silicatein genes, the three developmental stages and the interaction of these two variables, were investigated using a a two way analysis of variance (ANOVA). Multiple comparisons of the interactions of these two variables were determined using Tukey's post hoc tests and statistical significance in all cases was defined at $p < 0.05$. These analyses were performed with the Graphpad Prism software.

TEM and SEM

Specimens of free swimming larvae, rounded larvae, presettled larvae, settled and juveniles were fixed in a primary fixative solution composed of 2.5% glutaraldehyde, 10% paraformaldehyde in a buffer solution of 0.2 mol. L^{-1} sodium cacodylate/ HCl buffer (pH 7.2) (1,400 mOsm) for 24 h. Specimens were then post-fixed in 1% osmium tetroxide in 0.2 mol. L^{-1} (p H7.2) (with a 1:1 volume ratio; 420 mOsm) for approximately 2 h. Fixed specimens were dehydrated in a graded ethanol series. Samples for TEM analysis were embedded in agar low viscosity resin (R1078 resin kit, Agar Scientific, Essex, United Kingdom). Ultra and semi-thin sections were obtained with a Reichert-Jung Z00M Stereo-Star Ultra-cut ultra-microtome (Wetzlar, Germany). The sections were mounted on copper (200 µm) mesh grids. Hitachi H7000 TEM (Tokyo, Japan), operating at 75 kV, was used to conduct the observations of the grids (Stephens et al. 2013b). For SEM analysis, samples were finally dehydrated in hexamethyldisilazane (HMDS) for 24 hours and after air-dried in a desiccator. Samples were gold sputter coated using an EMSCOPE SC500 (Quorum Technologies) and imaged in secondary electron mode on the S2600N scanning electron microscope (Hitachi,

Japan). The analyses were performed at an acceleration voltage of 20 kV, an emission current (Ic) of 10 µA and a working distance of 13.2 mm. TEM photographs (taken by MV Marra and MB Longakit) were available from individuals of two additional *Haliclona* species that contained embryos (*H. cinerea* and *H. viscosa*) for comparison.

Results

Gene expression levels: Relative patterns of gene expression of silicatein genes showed that the five silicatein variants were expressed at low levels at the free swimming stage (lacking spicules). At the presettled and settled stages (having some spicules) there was an increase in the expression of all five genes compared to the expression levels of the free swimming stage. The silicatein of the SQN was the most highly expressed gene at these stages followed by the silicatein of the CHNII and SHN. In comparison, the silicatein of the CHNI type was highly expressed at the adult stage and its expression levels were much higher than the other variants. The second and third most expressed genes at this stage were SQN and CQN. In addition, there were lower expression levels of SHN and slightly lower expression levels of CHNII types in the adult specimen compared to the expression at the presettled and settled stages (Figure 1).

Statistics: There were significant differences in the relative expression levels between life stages, silicatein variants and the interaction of these two variables (Table 2). The tukey post hoc tests analysis for multiple comparisons revealed that there were significant differences in 25 out of 105 interactions (Table 3; Appendix 22).

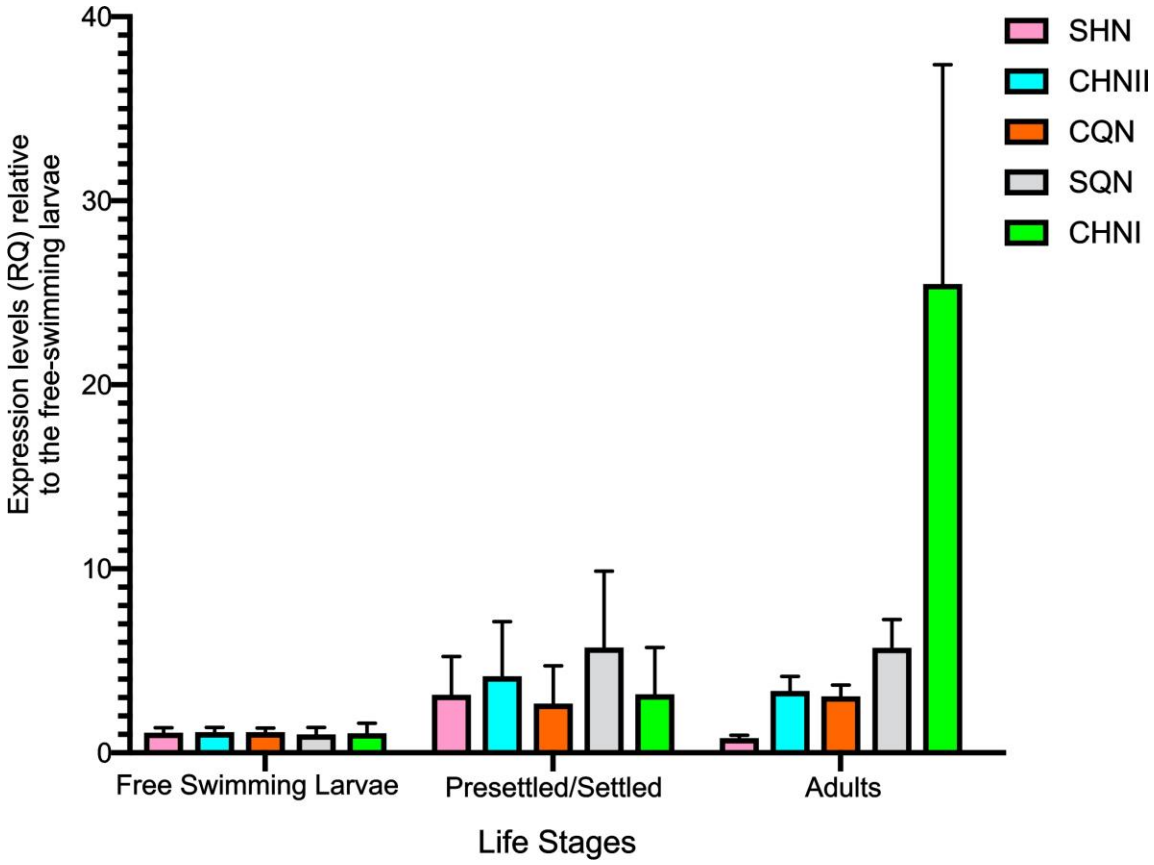

Figure 1. RT-qPCR analysis of the silicatein genes during different developmental stages of *Haliclona indistincta*. Gene expression levels are plotted relative to free swimming larvae (lacking spicules) and normalized to the housekeeping gene (HGPRT) expression levels at each stage. Y-axis denotes relative levels of expression (RQ) to the free swimming larvae. Bars represent mean +/- SE of n = 3 replicates.

Table 2. Two-way ANOVA to compare differences in the relative expression levels between silicatein variants, life stages and the interaction of these two variables in *H. indistincta*.

ANOVA table	SS	DF	MS	F (DFn, DFd)	P value
Interaction	13.71	8	1.714	F (8, 30) = 6.678	P<0.0001
Silicatein variants	7.455	4	1.864	F (4, 30) = 7.260	P=0.0003
Life Stages	17.6	2	8.8	F (2, 30) = 34.28	P<0.0001
Residual	7.701	30	0.2567		

Table 3. Tukey's multicomparison tests in which there were significant differences between the relative expression levels of the five silicatein genes and the three life stages; $p < 0.05$. * = 0.0332; **= 0.0021; ***= 0.0002; **** = <0.0001.

Tukey's multiple comparisons test	Mean Diff.	95.00% CI of diff.	Significant?	Summary	P Value
Presettled/Settled:SQN vs. Larvae:SHNI	1.746	0.2215 to 3.270	Yes	*	0.0137
Adults:SQN vs. Larvae:SHNI	1.742	0.2175 to 3.266	Yes	*	0.014
Adults:CHNI vs. Larvae:SHNI	3.233	1.709 to 4.758	Yes	****	<0.0001
Presettled/Settled:SQN vs. Larvae:CHNII	1.746	0.2215 to 3.270	Yes	*	0.0137
Adults:SQN vs. Larvae:CHNII	1.742	0.2175 to 3.266	Yes	*	0.014
Adults:CHNI vs. Larvae:CHNII	3.233	1.709 to 4.758	Yes	****	<0.0001
Presettled/Settled:SQN vs. Larvae:CQN	1.746	0.2215 to 3.270	Yes	*	0.0137
Adults:SQN vs. Larvae:CQN	1.742	0.2175 to 3.266	Yes	*	0.014
Adults:CHNI vs. Larvae:CQN	3.233	1.709 to 4.758	Yes	****	<0.0001
Presettled/Settled:SQN vs. Larvae:SQN	1.746	0.2215 to 3.270	Yes	*	0.0137
Adults:SQN vs. Larvae:SQN	1.742	0.2175 to 3.266	Yes	*	0.014
Adults:CHNI vs. Larvae:SQN	3.233	1.709 to 4.758	Yes	****	<0.0001
Presettled/Settled:SQN vs. Larvae:CHNI	1.746	0.2215 to 3.270	Yes	*	0.0137
Adults:SQN vs. Larvae:CHNI	1.742	0.2175 to 3.266	Yes	*	0.014
Adults:CHNI vs. Larvae:CHNI	3.233	1.709 to 4.758	Yes	****	<0.0001
Adults:CHNI vs. Presettled/Settled:SHNI	2.103	0.5789 to 3.628	Yes	**	0.0014
Adults:SHNI vs. Presettled/Settled:CHNII	-1.742	-3.267 to -0.2177	Yes	*	0.014
Adults:CHNI vs. Presettled/Settled:CHNII	1.835	0.3103 to 3.359	Yes	**	0.0079
Adults:CHNI vs. Presettled/Settled:CQN	2.294	0.7700 to 3.819	Yes	***	0.0004
Adults:SHNI vs. Presettled/Settled:SQN	-2.09	-3.614 to -0.5652	Yes	**	0.0016
Adults:CHNI vs. Presettled/Settled:CHNI	2.116	0.5921 to 3.641	Yes	**	0.0013
Adults:SQN vs. Adults:SHNI	2.086	0.5613 to 3.610	Yes	**	0.0016
Adults:CHNI vs. Adults:SHNI	3.577	2.052 to 5.101	Yes	****	<0.0001
Adults:CHNI vs. Adults:CQN	2.141	0.6170 to 3.666	Yes	**	0.0011

Microscopy: The larval morphology at the free swimming stage is that of a non-tufted parenchymulla (Figures 2a, 3a). The larvae are fully ciliated and the internal part contains cells that were identified previously as archaeocytes, amoebocytes and cells with inclusions, while the outer surface contained ciliated cells (see Stephens et al. 2013b, Figures 3b, 3c and 3d). At a later stage, the larvae transform into a compact rounded shape and the cilia on the outer surface are not as abundant as in the free swimming stage (Figures 2b, 3e and 3f) and in

these two phases the spicules are not visible. The larvae then become more circular rotating on their axis and the spicules (fusiform oxeas) develop and protrude mainly from the posterior pole, which is the side where it settles (pre-settled stage) (Figures 2c, 4a, 4b). The settled individuals have a flat posterior pole that is attached to the substratum, and the spicules are clearly visible on the surface, while the anterior pole is rounded (Figures 2d, 4c and 4d). The juveniles have a flattened body and spicules are more abundant making them very visible (Figures 2e, 4e and 4f).

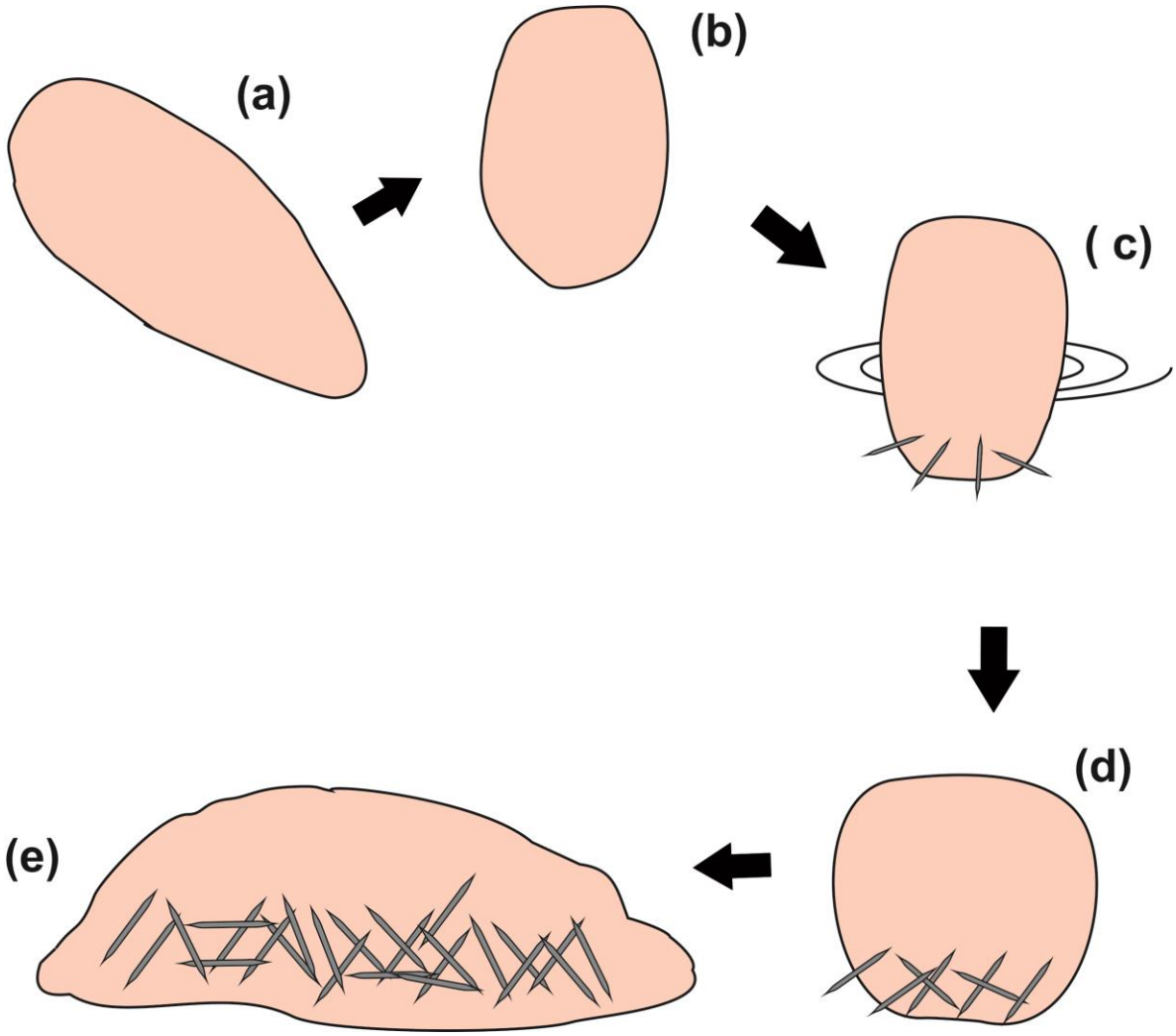

Figure 2. Schematic representation of the developmental stages of *H. indistincta*; a) free swimming larva, b) rounded larva, c) pre-settled sponge spinning around (spicules are forming), d) settled individual, e) juvenile (see Stephens et al. 2013a).

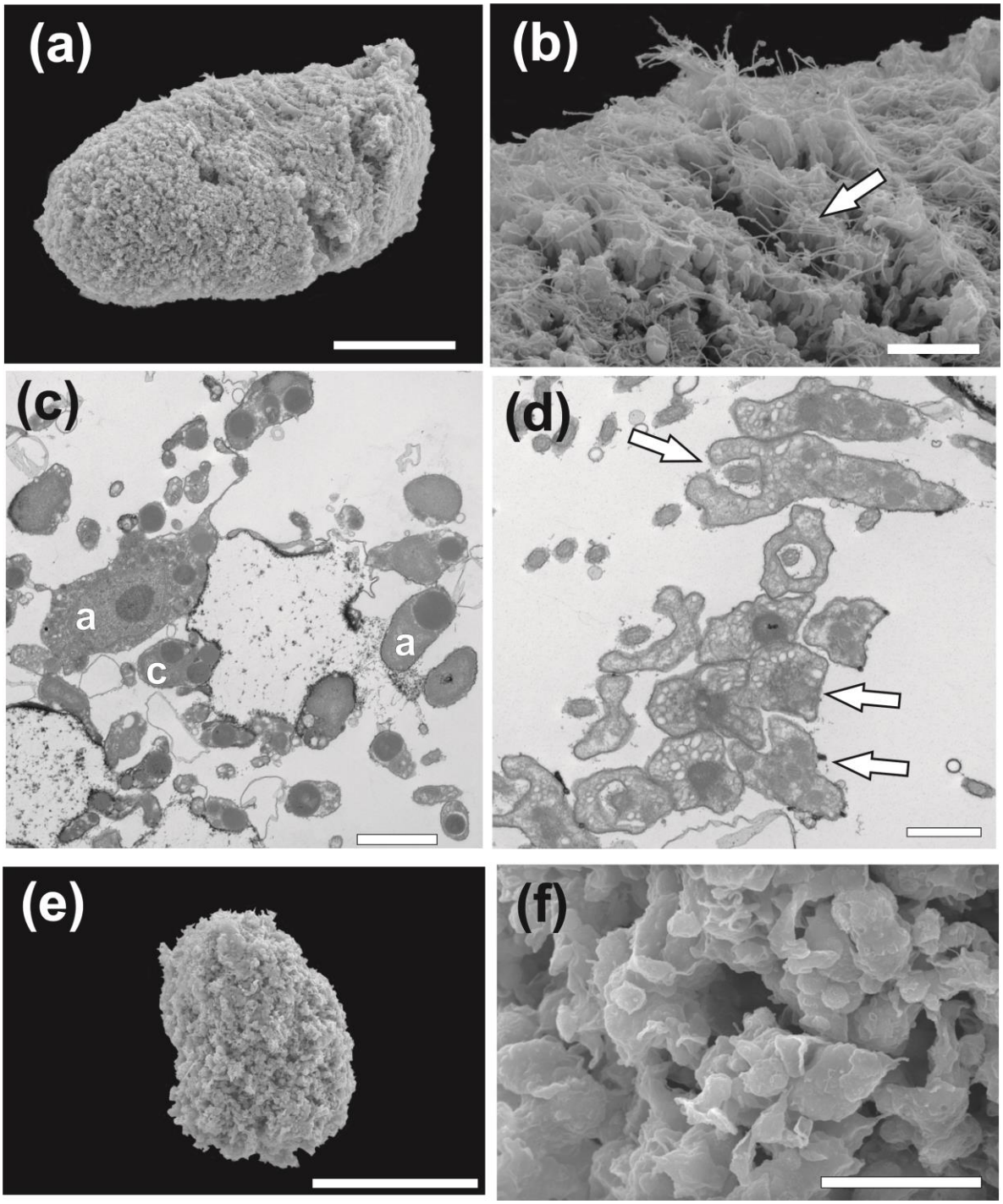

Figure 3. SEM and TEM photographs of initial developmental stages of *H. indistincta*. a) SEM photograph of one free swimming larva; b) Closer view of the surface of the larva covered with cilia; c) TEM photograph of the cells found at the free swimming larval stage; d) TEM photograph of the ciliated cells; (e) SEM photograph of the rounded larva stage; f) Closer view of the surface of the rounded larva, at this stage the cilia have disappeared. Scale bars: a) 150 µm; b) 20 µm; c) 2 µm; d) 500 nm; e) 200 µm; f) 2 µm. a= archeaocytes, c= cells with inclusions; white arrows= cilia (SEM) and ciliated cells (TEM).

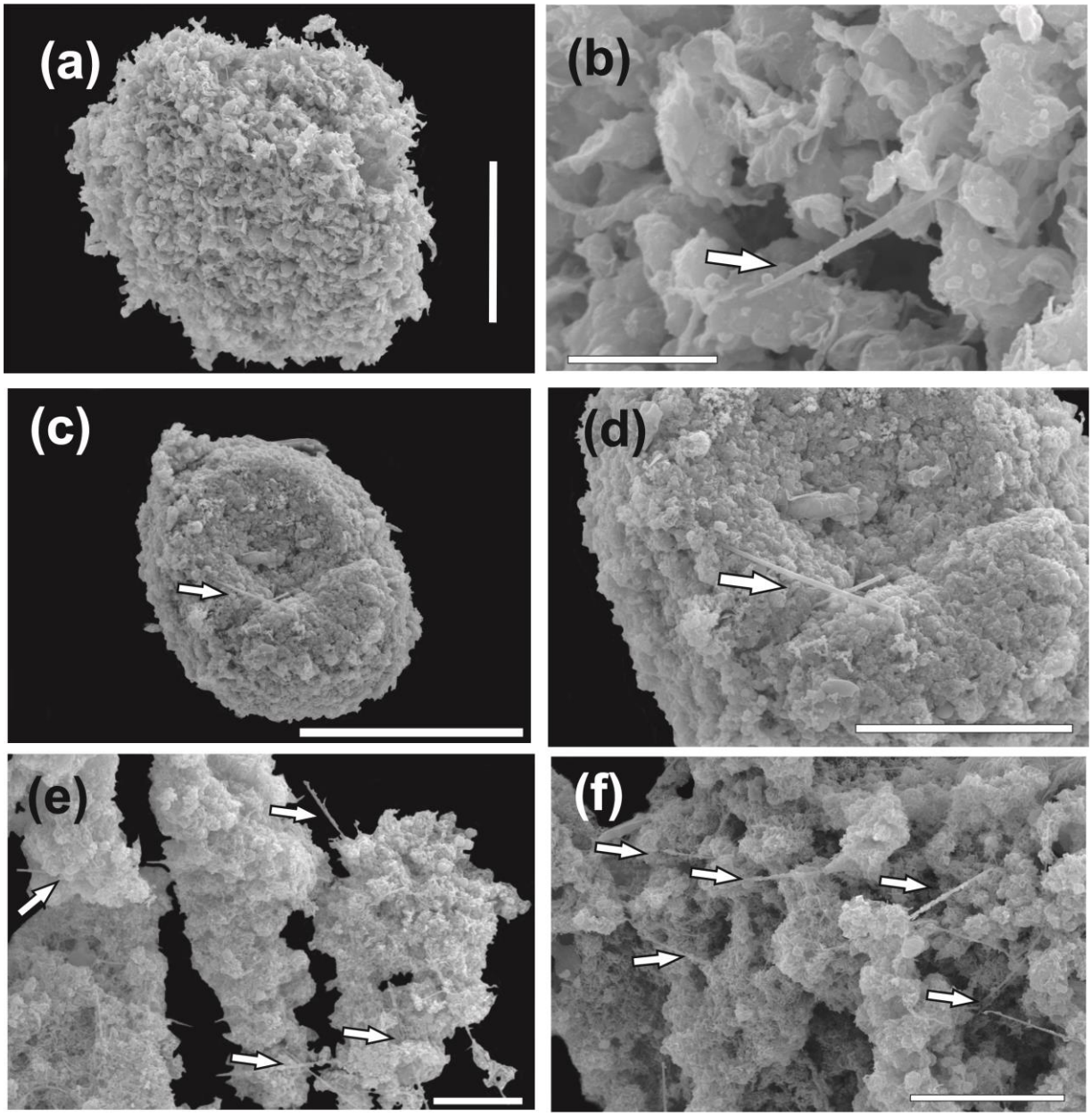

Figure 4. SEM photographs of the developmental stages of *H. indistincta*. a) SEM photograph of the pre-settled stage; b) Closer view of the surface where spicules are visible; c) SEM photograph of the settled individual. d) Closer view of the posterior pole where spicules are visible; e) SEM photographs of a juvenile; f) Closer view of the surface when some spicules are protruding.. Scale bars: a) 100 µm; b) 10 µm; c) 100 µm; d) 50 µm; e) 20 µm; f) 50 µm. white arrows = spicules.

TEM images confirm that the spicules are formed intracellularly at least at the early stages because spicule sections were found inside the nucleolated sclerocytes (Figure 5a). There were abundant rounded vesicles, which were in proximity to the spicule in formation (Figures 5b, 5c, and 5d). The axial filament has two morphologies that are related to the location of the spicule section: triangular at the end (the surrounding spicule has a triangular shape) (Figure 5e) and hexagonal at the middle part (the surrounding spicule has a circular shape) (Figure 5f).

The embryos from *H. indistincta* were not examined but the free swimming larvae lack spicules. TEM sections of the embryos of *H. viscosa* (a sister species of *H. indistincta* based on molecular data) indicated a lack of spicules (Figures 6a, 6b and 6c). In contrast, transmission electron micrographs of tissue sections- containing embryos from *H. cinerea* (a distantly related species) clearly showed spicules (Figures 6d, 6e and 6f).

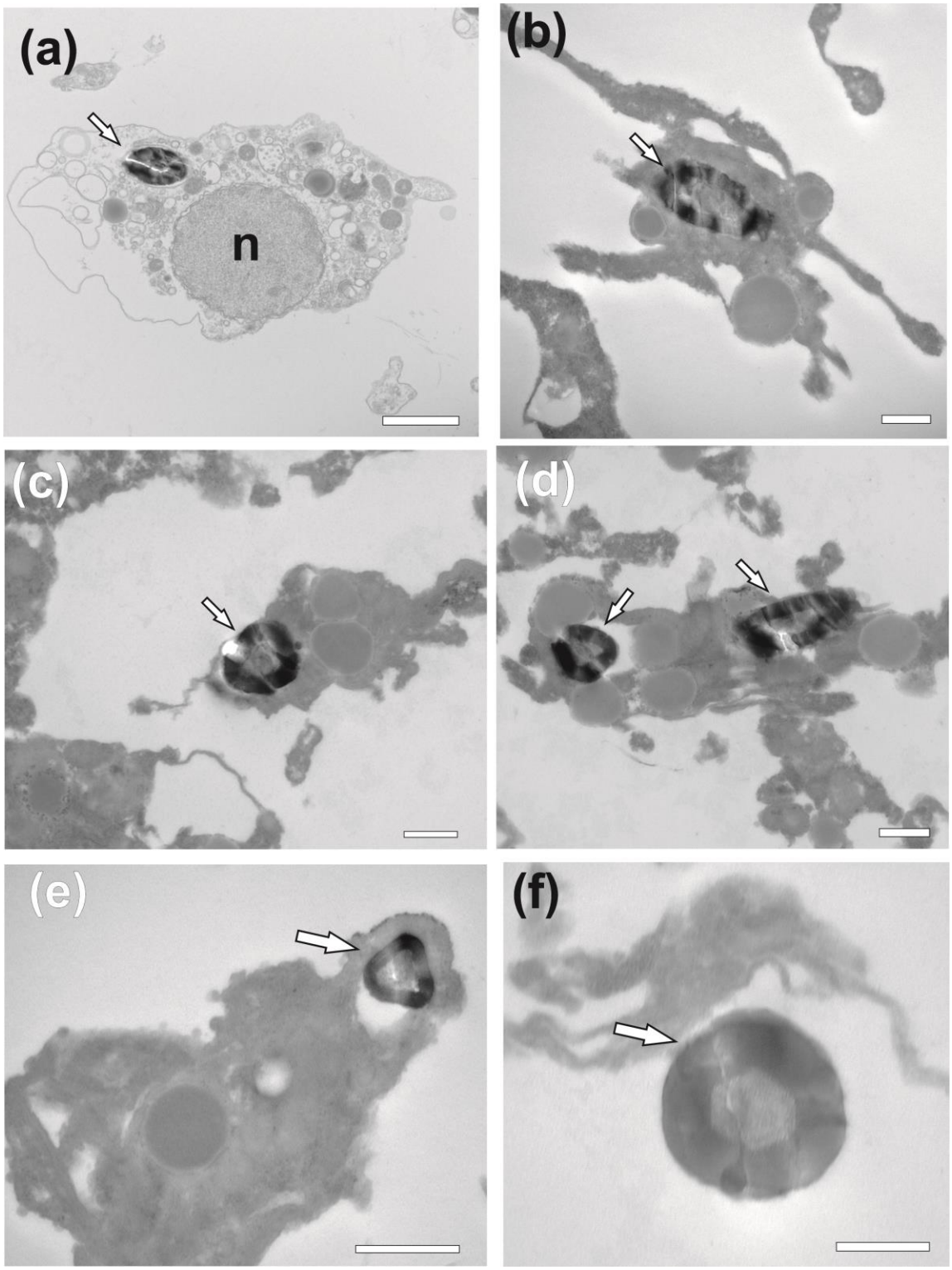

Figure 5. TEM photographs of the spicule formation at the presettled-stage. a) sclerocyte I; b)sclerocyte II;c) sclerocyte III; d) sclerocyte IV; e) sclerocyte showing the upper part of the spicule with a triangular axial filament; f) middle part of the spicule with an hexagonal axial filament.Scale bars: a); c); f) 500 nm; ; b); d) 1 µm; e) 1.25 µm. n = nucleus, white arrow= spicules.

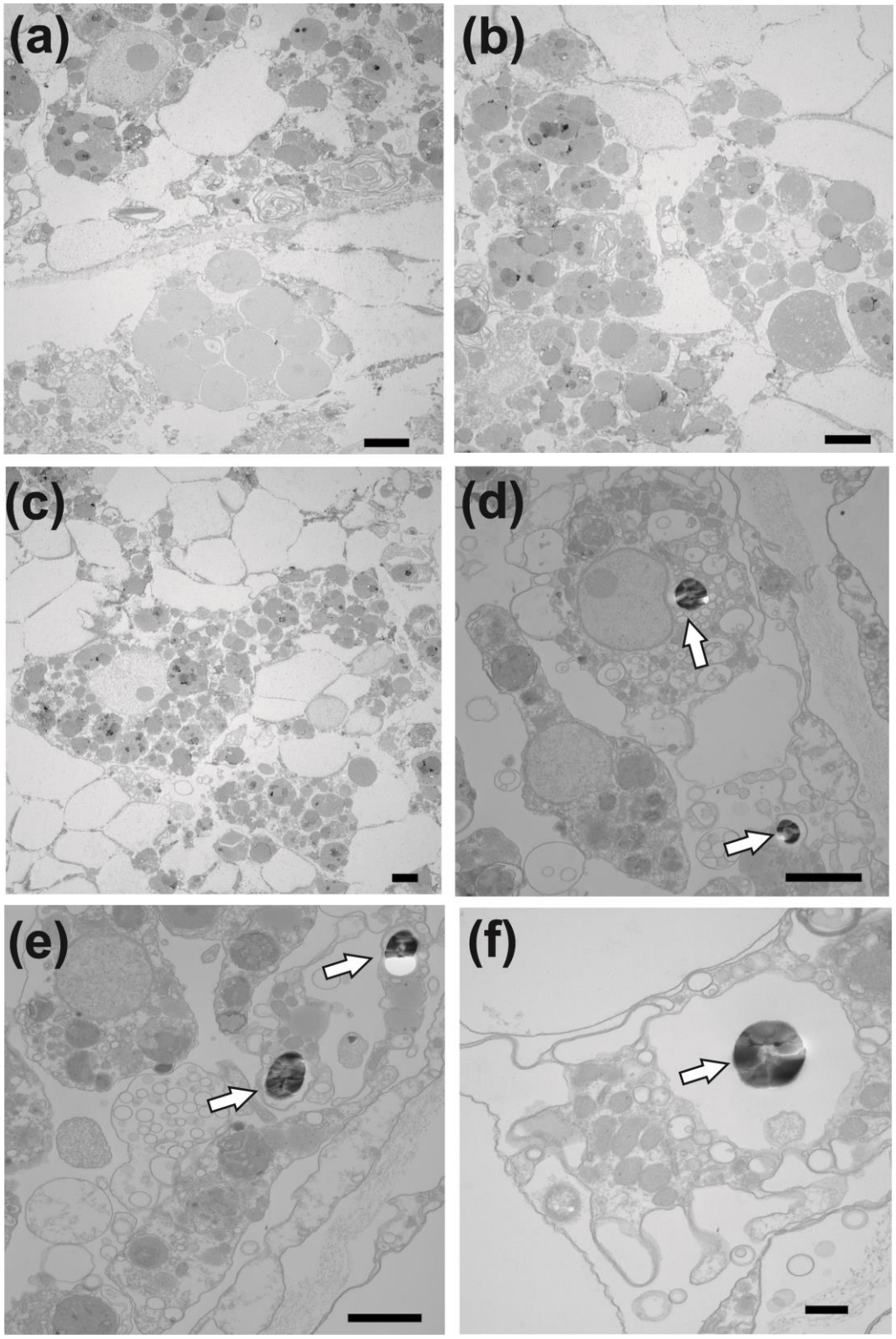

Figure 6. TEM photographs of the embryos from *Haliclona viscosa* (clade C) and *Haliclona cinerea* (clade A). The first species lacks spicules at this stage (a, b and c) while the second has spicules (d, e and f). Scale bars: a) – e): 2 µm; f) 500 nm. White arrows = spicules. The photographs were taken by M.V. Marra and M.B. Longakit.

Discussion

This chapter demonstrates that the five silicatein variants were differentially expressed at three distinct life stages in the sponge *H. indistincta* unlike the pattern described for *A. queenslandica* where the sequential expression pattern did not change across early life history stages. The free swimming larvae of *H. indistincta* lack spicules and the genes were expressed at lower levels at this stage when compared to the other stages where the spicules were present. TEM images from this stage do not show any sclerocytes instead other cells that have been identified previously as archeaocytes, ciliated cells or cells with inclusions are evident (see Stephens et al. 2013b). It is possible that sclerocytes (lacking spicules) were expressing the mRNA of the silicatein genes at this stage and that these RNA molecules did not experience yet the transformation into a functional protein. It is also possible that some of the archeaocytes found at this stage had started the differentiation process into early sclerocytes but their morphology had not yet altered significantly.

This work clearly shows an increase in the expression levels of silicatein genes from the free swimming larvae (lacking spicules) to the pre-settled/settled individuals (having spicules). This is to be entirely expected, and previous studies also reported a positive correlation between the expression levels of the silicatein genes and the formation of siliceous spicules in demosponges (Krasko et al. 2000; Cao et al. 2007; Müller et al. 2013; Nakayama et al. 2015).

Although silicateins of the SHN type have been reported as the gene responsible for spicule formation in demosponges, silicatein of the CHN and C/SQN types were highly expressed at the stages when *H. indistincta* was producing spicules, in fact they were much more highly expressed than SHN. Gauthier (2015) found that two CHN and one SQN variants were the

second, third and fourth most expressed genes at different developmental phases producing spicules in *A. queenslandica,* while two variants of the CHN type were localized in the sclerocytes based on whole mount *in situ* hybridization. In addition, Shkryl et al. (2016) found that a silicatein of the CHN type was the second most highly expressed gene in adult specimens from *Latrunculia oparinae* among five silicatein genes (four with a SHN configuration) using RT-qPCR. Furthermore, a recombinant enzyme of this variant was also able to condense silica nanocrystals in a medium with T.H.E.O.S. (Kamenev et al. 2015). All of these data suggest strongly that the silicateins of the CHN and C/SQN types have a role in spicule construction and therefore that the two amino acids that are part of the catalytic triad (S-H) are probably not necessary for silica condensation contrary to what previous studies have reported (Cha et al. 1999, Zhou et al. 1999; Fairhead et al. 2008). However, additional studies on expression levels and localization of these variants in other related species will validate this statement.

In this work I have also clearly shown that expression levels of each of the five silicatein variants were different at the two developmental stages (presettled/settled and adult) in which the specimens were producing spicules. For example, the SQN was the most highly expressed gene at the presettled and settled stages followed by the silicatein of the CHNII while the CHNI variant was the most highly expressed gene followed by the SQN type in adult specimens. It is possible that the different expression levels of the silicatein genes between these two stages producing spicules could have an effect on the size and number of spicules (adult specimens have longer and more spicules than those found in larvae) (Bergquist and Green, 1977; Maldonado and Bergquist, 2002; Maldonado, 2006). For example, Mohri et al. (2008) investigated the expression levels of four silicatein variants (alpha type) during the

formation of megasclere spicules in the freshwater sponge *E. fluviatilis* based on Whole Mount *in situ* Hybridization (W.I.S.H.) and they demonstrated that there is a temporal expression pattern in which two of these variants were highly expressed during the initial megasclere formation while other two variants were more highly expressed when megascleres were longer than 150 µm. It is likely that some silicatein variants are expressed during the initial stages of megascleres formation in *H. indistincta* while other variants are highly expressed when megascleres reach their maximum length and perhaps these variants are more highly expressed in adults than at early stages.

The production of the oxeas in the larvae of *H. indistincta* occurs intracellularly, a pattern also found in the larvae from *A. queenslandica* (named as *Reniera*) (Leys, 2003) and in adult specimens from the freshwater sponges *E. fluviatilis* (Nakayama et al. 2015), *S. lacustris* (Simpson and and Vaccaro, 1974) and in adults from *Mycale* (Custodio et al. 2002). In contrast, spicule secretion in other demosponges occurs extracellularly such as *C. crambe* (Uriz et al. 2000) and *Microciona prolifera* (Simpson, 1978) while in primmorphs from the demosponge *S. domuncula,* the secretion of tylostyles started intracellularly and then the immature spicule was reportedly released into the mesohyl in a final step headed to the mature spicule (Müller et al. 2005; 2013). The axial filament of *H. indistincta* has two distinct shapes: hexagonal at the middle part of the spicule and triangular at the end (tip) of the spicule. A hexagonal shape was reported for the oxeas of two haplosclerid species e.g.: *A. queenslandica* (named as *Reniera*) (Leys, 2003) and *H. rosea* (Garrone, 1969). This shape was also reported for the spicules (oxeas) from the freshwater sponge *S. lacustris* (Simpson and Vaccaro, 1974) and the megascleres and microscleres from the sponge *Steletta grubi* (Simpson et al. 1985). In contrast, the triangular axial filament shape was reported for the

styles from *C. crambe* (Uriz et al. 2000), the tylostyles from *S. domuncula* (Müller et al. 2005) and the oxeas from *Geodia cydonium* (Müller et al. 2007). Recently, Werner et al. (2017) found that the axial filament inside the tylostyles from *S. domuncula* was triangular in proximity to the head (tylostyle) and hexagonal at the middle part of the spicule and this pattern was also found in the axial filament of the species analyzed here. The sclerocytes identified in this study were nucleolated with abundant rounded vesicles. These vesicles, located in proximity to the spicule in formation, were described for other demosponge species producing spicules such as: *S. lacustris* (Simpson and and Vaccaro, 1974), *C. crambe* (Uriz et al. 2000) and the primmorphs from *S. domuncula* (Müller et al. 2005; Schröder et al. 2007; Mugnaioli et al. 2009). Schröder et al. (2007) found that the cellular vesicles (named silicasomes) from *S. domuncula* contained silica, and may have a role in the deposition of this element in the spicules in formation (based on X-Ray analysis).

The free swimming larvae of *H. indistincta* lack spicules and these structures are also missing in the embryos of a close sister species (*H. viscosa*) (Figure 7). These two species are assigned to clade C (based on molecular data) and the absence of spicules at early stages might indicate a synapmorphy for this group of sponges. For instance, spicules at the free swimming stages were reported in species belonging to clade A such as: *H. tubifera* (Woollacott, 1993), *H. cinerea* (Meewis, 1941), *C. limbata* (Meewis, 1939) and *H. xena* (Wapstra and van Soest, 1987); and to clade B such as: *A. queenslandica* (named as *Reniera*) (Leys, 2003), *H. caerulea* (Maldonado et al. 1997) and *H. simulans* (Lévi, 1956) (Figure 7). In Chapter 3, I suggested that perhaps the last common ancestor of demosponges lack spicules and it is possible that this ancestral feature is conserved at early developmental stages (e.g.

embryos and free swimming larvae) in some marine haplosclerid species, particularly those members of clade C (which is a sister clade to the remaining haplosclerids).

In addition, the morphology and ciliation pattern of *H. indistincta* larvae are different to other haplosclerid species and these morphological features correlate with the molecular phylogeny of this group and might indicate further phylogenetic signal (Figure 7). Ontogenetic characters have previously been suggested as synapomorphic features that might help to solve phylogenetic relationships in sponges (Lévi, 1957; Boury-Esnault, 2006) and these features were dismissed by van Soest (1980) and de Weerdt (1986) for the classification of the order Haplosclerida.

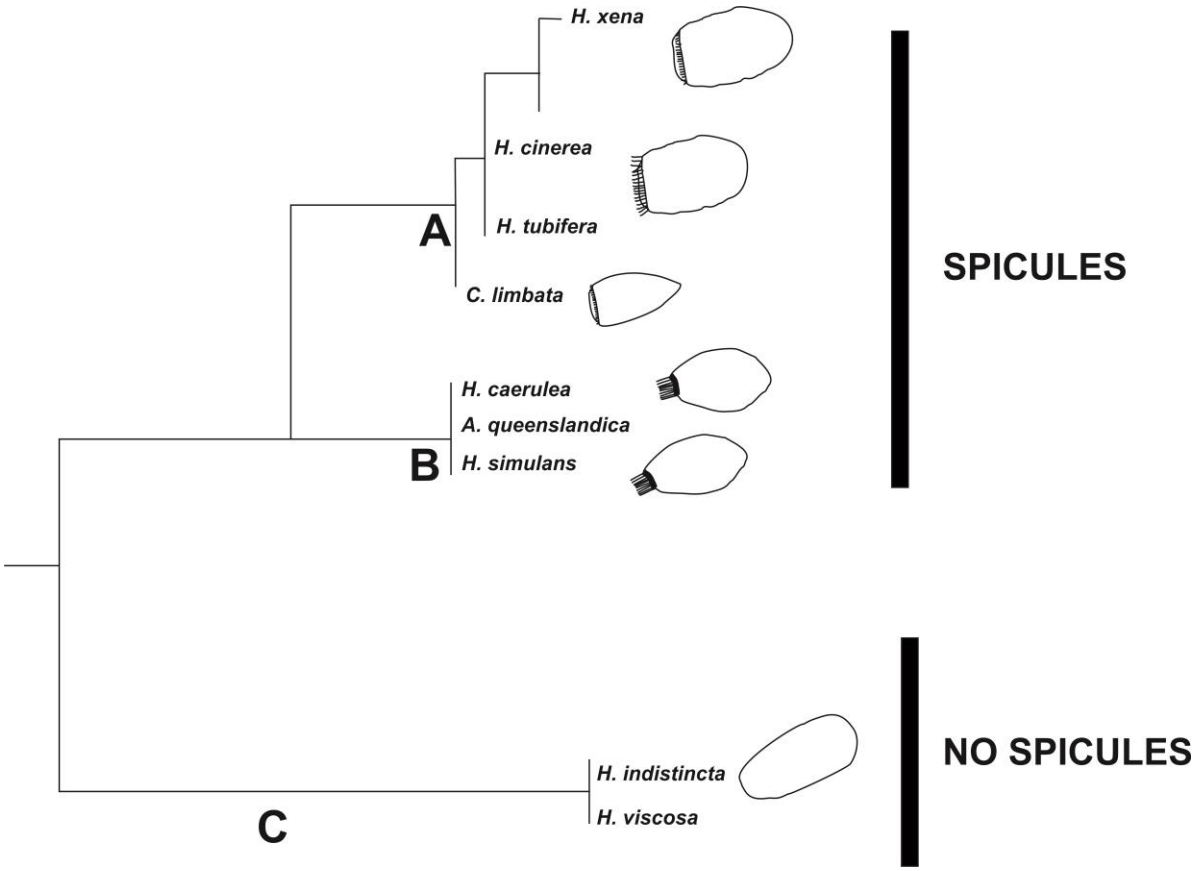

Figure 7. A schematic drawing of the free swimming larval type from marine haplosclerids (based on the literature) and the presence or absence of spicules at this stage. The molecular systematics position of each species is based on mitochondrial and ribosomal data (see Redmond et al. 2011; 2013, Stephens, 2013). The free swimming larva of *H. viscosa* is similar to *H. indistincta* (unpublished data)

In summary, the secretion of the oxeas at early stages in *H. indistincta* occurred intracellularly and the silicatein genes were expressed at lower amounts in the free swimming larvae (lacking spicules). The expression of the silicatein variants increased at later stages when the spicules were present and these genes were differentially expressed in the two stages producing spicules (presettled stage and adults).

References

Bergquist , P. R., Green, C. R. (1977). An ultrastructural study of settlement and metamorphosis in sponge larvae. Cahiers De Biologie Marine 18: 289–302.

Boury-Esnault, N. (2006). Systematics and evolution of Demospongiae. Canadian Journal of Zoology, 84(2), 205-224.

Brutchey, R. L., Morse, D. E. (2008). Silicatein and the translation of its molecular mechanism of biosilicification into low temperature nanomaterial synthesis. Chemical reviews, 108(11), 4915–4934.

Cao, X., Fu, W., Yu, X., Zhang, W. (2007). Dynamics of spicule production in the marine sponge *Hymeniacidon perlevis* during in vitro cell culture and seasonal development in the field. Cell and tissue research, 329(3), 595–608.

Cha, J. N., Shimizu, K., Zhou, Y., Christiansen, S. C., Chmelka, B. F., Stucky, G. D., Morse, D. E. (1999). Silicatein filaments and subunits from a marine sponge direct the polymerization of silica and silicones in vitro. Proceedings of the National Academy of Sciences, 96(2), 361–365.

Custódio, M. R., Hajdu, E., Muricy, G. (2002). In vivo study of microsclere formation in sponges of the genus *Mycale* (Demospongiae, Poecilosclerida). Zoomorphology, 121(4), 203–211.

de Weerdt, W. H. (1986). A systematic revision of the north-eastern Atlantic shallow-water Haplosclerida (Porifera, Demospongiae): 2. Chalinidae. Beaufortia, (6), 81-165.

Fairhead, M., Johnson, K. A., Kowatz, T., McMahon, S. A., Carter, L. G., Oke, M., Liu, H., Naismith, J.H., van der Walle, C. F. (2008). Crystal structure and silica condensing activities of silicatein α–cathepsin L chimeras. Chemical Communications, (15), 1765-1767.

Garrone, R. (1969). Collagéne, spongine et squelette mineral chez l'éponge Haliclona rosea (O.S.). Journal of Microscopy 8,581–598.

Gauthier A (2015). Analysis of silicatein gene expression and spicule formation in the demosponge *Amphimedon queenslandica*. MS thesis. The University of Queensland, 84 pp.

Kamenev, D. G., Shkryl, Y. N., Veremeichik, G. N., Golotin, V. A., Naryshkina, N. N., Timofeeva, Y. O., Kovalchuk, S.N., Semiletova, I.V., Bulgakov, V. P. (2015). Silicon Crystals Formation Using Silicatein-Like Cathepsin of Marine Sponge *Latrunculia oparinae*. Journal of nanoscience and nanotechnology, 15(12), 10046–10049.

Krasko, A., Lorenz, B., Batel, R., Schröder, H. C., Müller, I. M., Müller, W. E. (2000). Expression of silicatein and collagen genes in the marine sponge *Suberites domuncula* is controlled by silicate and myotrophin. The FEBS Journal, 267(15), 4878–4887.

Lévi, C. (1956). Étude des Halisarca de Roscoff. Embryologie et systematique des Demosponges. Archs Zool. Exp. Gen. 93: 1–184.

Lévi, C. (1957). Ontogeny and systematics in sponges. Systematic Zoology, 6(4), 174-183.

Leys, S. P. (2003). Comparative study of spiculogenesis in demosponge and hexactinellid larvae. Microscopy research and technique, 62(4), 300–311.

Livak, K. J., Schmittgen, T. D. (2001). Analysis of relative gene expression data using real-time quantitative PCR and the 2− ΔΔCT method. Methods, 25(4), 402-–408.

Maldonado, M. (2006). The ecology of the sponge larva. Canadian Journal of Zoology, 84(2), 175–194.

Maldonado, M., Bergquist, P. (2002). Phylum Porifera. In: Atlas of Marine Invertebrae Larvae, pp 21–50. Academic Press, San Diego.

Maldonado, M., George, S. B., Young, C. M., Vaquerizo, I. (1997). Depth regulation in parenchymella larvae of a demosponge: relative roles of skeletogenesis, biochemical changes and behavior. Marine Ecology Progress Series, 115–124.

Meewis, H. (1939). Contribution à l'étude de l'embryogénèse des Chalinidae: *Haliclona limbata* (Mont.). Annales de la Société royale zoologique de Belgique, 70, 201–243.

Meewis, H. (1941) Contribution a létude de l’embryogénese des éponges siliceuses. Annales de la Société royale zoologique de Belgique. 72,126–149.

Mohri, K., Nakatsukasa, M., Masuda, Y., Agata, K., Funayama, N. (2008). Toward understanding the morphogenesis of siliceous spicules in freshwater sponge: Differential mRNA expression of spicule-type-specific silicatein genes in *Ephydatia fluviatilis*. Developmental Dynamics, 237(10), 3024-3039.

Mugnaioli, E., Natalio, F., Schloßmacher, U., Wang, X., Müller, W. E., Kolb, U. (2009). Crystalline nanorods as possible templates for the synthesis of amorphous biosilica during spicule formation in Demospongiae. ChemBioChem, 10(4), 683-689.

Müller, W. E., Rothenberger, M., Boreiko, A., Tremel, W., Reiber, A., Schröder, H. C. (2005). Formation of siliceous spicules in the marine demosponge Suberites domuncula. Cell and tissue research, 321(2), 285–297.

Müller, W. E., Schloßmacher, U., Eckert, C., Krasko, A., Boreiko, A., Ushijima, H., Wolf, S., Tremel, W., Müller, I., Schröder, H. C. (2007). Analysis of the axial filament in spicules of the demosponge *Geodia cydonium*: different silicatein composition in microscleres (asters) and megascleres (oxeas and triaenes). European journal of cell biology, 86(8), 473–487.

Müller, W. E., Schröder, H. C., Burghard, Z., Pisignano, D., Wang, X. (2013). Silicateins—a novel paradigm in bioinorganic chemistry: enzymatic synthesis of inorganic polymeric silica. Chemistry-A European Journal, 19(19), 5790–5804.

Nakayama, S., Arima, K., Kawai, K., Mohri, K., Inui, C., Sugano, W., Koba, H., Tamada, K., Nakata, Y.J., Kishimoto, K., Arai–Shindo, M., Kojima, C., Matsumoto, T., Fujimori, T., Agata, K., Funayama, N. (2015). Dynamic transport and cementation of skeletal elements build up the pole–and–beam structured skeleton of sponges. Current Biology 25(19) 2549–2554.

Redmond, N. E., Morrow, C. C., Thacker, R. W., Diaz, M. C., Boury-Esnault, N., Cárdenas, P., Hajdu, E., Lobo-Hajdu, G., Picton, B.E., Pomponi, S., Kayal, E., Collins A.G. (2013). Phylogeny and systematics of Demospongiae in light of new small-subunit ribosomal DNA (18S) sequences. Integrative and comparative biology, 53(3), 388–415.

Rao, X., Huang, X., Zhou, Z., Lin, X. (2013). An improvement of the 2ˆ (–delta delta CT) method for quantitative real-time polymerase chain reaction data analysis. Biostatistics, bioinformatics and biomathematics, 3(3), 71.

Redmond, N. E., Raleigh, J., van Soest, R. W., Kelly, M., Travers, S. A., Bradshaw, B., Vartia, S., Stephens, K., McCormack, G. P. (2011). Phylogenetic relationships of the marine Haplosclerida (Phylum Porifera) employing ribosomal (28S rRNA) and mitochondrial (cox1, nad1) gene sequence data. PLoS One, 6(9), e24344.

Riesgo, A., Farrar, N., Windsor, P. J., Giribet, G., Leys, S. P. (2014). The analysis of eight transcriptomes from all poriferan classes reveals surprising genetic complexity in sponges. Molecular biology and evolution, 31(5), 1102-1120.

Schoeppler, V., Reich, E., Vacelet, J., Rosenthal, M., Pacureanu, A., Rack, A., Zaslansky, P., Zolotoyabko E., Zlotnikov, I. (2017). Shaping highly regular glass architectures: A lesson from nature. Science Advances, 3(10), eaao2047

Schröder, H. C., Natalio, F., Shukoor, I., Tremel, W., Schloßmacher, U., Wang, X., Müller, W. E. (2007). Apposition of silica lamellae during growth of spicules in the demosponge *Suberites domuncula*: biological/biochemical studies and chemical/biomimetical confirmation. Journal of structural biology, 159(3), 325–334.

Schröder, H. C., Wang, X., Manfrin, A., Yu, S. H., Grebenjuk, V. A., Korzhev, M., Wiens, M., Schlossmacher, U., Müller, W. E. (2012). Acquisition of structure-guiding and structure-forming properties during maturation from the pro-silicatein to the silicatein form. Journal of Biological Chemistry, 287(26), 22196–22205.

Shimizu, K., Cha, J., Stucky, G. D., Morse, D. E. (1998). Silicatein α: cathepsin L-like protein in sponge biosilica. Proceedings of the National Academy of Sciences, 95(11), 6234-6238.

Shkryl, Y. N., Bulgakov, V. P., Veremeichik, G. N., Kovalchuk, S. N., Kozhemyako, V. B., Kamenev, D. G., Semiletova, I.V., Timofeeva, Y.O., Scchipunov, Y.A., Kulchin, Y. N. (2016). Bioinspired enzymatic synthesis of silica nanocrystals provided by recombinant silicatein from the marine sponge *Latrunculia oparinae*. Bioprocess and Biosystems Engineering, 39(1), 53–58.

Simpson, T. L., Langenbruch, P. F., Scalera-Liaci, L. (1985). Silica spicules and axial filaments of the marine sponge *Stelletta grubii* (Porifera, Demospongiae). Zoomorphology, 105(6), 375–382.

Simpson, T. L., Vaccaro, C. A. (1974). An ultrastructural study of silica deposition in the freshwater sponge *Spongilla lacustris*. Journal of ultrastructure research, 47(3), 296–309.

Simpson, T. L. (1978). The biology of the marine sponge *Microciona prolifera* (Ellis and Solander). III. Spicule secretion and the effect of temperature on spicule size. Journal of Experimental Marine Biology and Ecology, 35(1), 31–42.

Stephens, K. (2013).Insights into the evolution and development of Haliclona indistincta (Porifera, Haplosclerida)(Doctoral dissertation) N.U.I.G. 225 pp.

Stephens, K. M., Ereskovsky, A., Lalor, P., McCormack, G. P. (2013b). Ultrastructure of the ciliated cells of the free-swimming larva, and sessile stages, of the marine sponge *Haliclona indistincta* (Demospongiae: haplosclerida). Journal of morphology, 274(11), 1263–1276.

Stephens, K. M., Galvin, J., Lawless, A., McCormack, G. P. (2013a). Reproductive cycle and larval characteristics of the sponge *Haliclona indistincta* (Porifera: Demospongiae). Journal of the Marine Biological Association of the United Kingdom, 93(4), 899–907.

Uriz, M. J., Turon, X., Becerro, M. A. (2000). Silica deposition in Demosponges: spiculogenesis in *Crambe crambe*. Cell and tissue research, 301(2), 299–309.

Uriz, M. J., Turon, X., Becerro, M. A., Agell, G. (2003). Siliceous spicules and skeleton frameworks in sponges: origin, diversity, ultrastructural patterns, and biological functions. Microscopy research and technique, 62(4), 279–299.

Van Soest, R. W. M. (1980). Marine sponges from Curaçao and other Caribbean localities Part II. Haplosclerida. Studies on the Fauna of Curaçao and other Caribbean Islands, 62(1), 1-173.

Wapstra, M., Van Soest, R. W. M. (1987). Sexual reproduction, larval morphology and behaviour in demosponges from the southwest of the Netherlands. In: Taxonomy of Porifera (pp. 281–307). Springer, Berlin, Heidelberg.

Weaver, J. C., Morse, D. E. (2003). Molecular biology of demosponge axial filaments and their roles in biosilicification. Microscopy research and technique, 62(4), 356–367.

Werner, P., Blumtritt, H., Natalio, F. (2017). Organic crystal lattices in the axial filament of silica spicules of Demospongiae. Journal of structural biology, 198(3), 186–195.

Woollacott, R. M. (1993). Structure and swimming behavior of the larva of *Haliclona tubifera* (Porifera: Demospongiae). Journal of Morphology, 218(3), 301–321.

Wörheide, G., Dohrmann, M., Erpenbeck, D., Larroux, C., Maldonado, M., Voigt, O., Borchiellini, C., Lavrov, D. V. (2012). Deep phylogeny and evolution of sponges (Phylum Porifera). Advances in marine biology, 61(1),1–78.

Zhou, Y., Shimizu, K., Cha, J. N., Stucky, G. D., Morse, D. E. (1999). Efficient catalysis of polysiloxane synthesis by silicatein α requires specific hydroxy and imidazole functionalities. Angewandte Chemie International Edition, 38(6), 779-782.

Chapter 5

Cytoplasmic expression of one silicatein gene (SHN type) from *H. indistincta* in *E. coli* BL-21 (DE3) cells

Introduction

Currently, a high number of proteins (including medicines and enzymes) are produced at a large scale through recombinant DNA technology (Rajakaruna and Taylor-Robinson, 2016). Human insulins, Human growth hormones or follicle stimulating hormones are examples of recombinant hormones with a high commercial and pharmacological value (Furuki et al. 2017). The production of recombinant proteins is attractive to the biotechnological industry because it reduces the cost of downstream processing (Wei et al. 1991; Baneyx, 1999; Mergulhao et al. 2005). It is possible now to express recombinant proteins in different vectors such as: bacteria strains, yeasts, mammalian cells, insects or plant cells (Gupta and Shukla, 2016). However, certain proteins sometimes are poorly expressed or improperly folded and they constitute a challenge for any further application (Mergulhao et al. 2005).

The catalytic activity of the silicatein protein, that can condense silicon alkoxides under mild conditions, is of great interest to the biotech sector (Cha et al. 1999; Brutchey and Morse, 2008). The manufacture of siloxane-based materials (e.g. semiconductors, optical fibres and ceramics) requires high temperatures, high pressures or the use of corrosive chemicals (Morse, 1999). The production of recombinant silicateins is an alternative option for the fabrication of these materials with multiple applications (Arakaki et al. 2015).

The silicatein protein was also able to condense amorphous titanium dioxide and spinel gallium dioxide from water soluble precursors from these elements at low temperature (Curnow et al. 2003; Kisailus et al. 2005). In addition, the enzymatic synthesis of the Poly(L-Lactide) polymer from PLA using a recombinant silicatein at low temperature was accomplished (Curnow et al. 2005). Recombinant silicateins with His-Tag could bind to gold

surface, WS_2 nanotubes or hydroxypatite nanofibrils with Ni-NTA and retained the catalytic activity to coat and produce layers of zirconia, titania or silica from water soluble precursors from these elements (Tahir et al. 2004; 2005; 2009; Natalio et al. 2010). Silica nanocrystals that could be employed as medical devices, semiconductors or light emitting diodes were condensed by recombinant silicateins in a buffer medium with T.H.E.O.S. (Kamenev et al. 2015; Shkryl et al. 2016).

In all these experiments, the recombinant silicateins were expressed in *E. coli* cells (different strains) either in the periplasmic or cytoplasmic region (Sumerel et al. 2003; Wolf et al. 2010; Shkryl et al. 2016). The silicatein, expressed in these prokaryotic vectors, is just the peptidase region containing the active site responsible for silica condensation (Zhou et al. 1999; Sumerel et al. 2003; Shkryl et al. 2016). The similarity of the silicatein alpha from *T. aurantium* with human cathepsins-L suggests that the cysteines forming disulfide bonds in the cathepsin L should be the same as those found in silicateins, but this hypothesis has never been corroborated (Shimizu et al. 1998; Fairhead et al. 2008). Currently, there is no crystal structure from any silicatein protein (Fairhead et al. 2008) and only a few crystal structures related to sponges are available: mutant human silicatein/cathepsin (Fairhead et al. 2008), geodin from *Geodia cydonium* (Vergara et al. 2013) and a tetrameric galectin from *Cynachirella* sp (Freymann et al. 2012).

The refolding and purification of recombinant silicateins is complicated because the expressed protein forms inclusion bodies, contains many cysteines, tends to precipitate and has limited solubility after refolding (Brutchey and Morse, 2008; Schröder et al. 2012; Kamenev et al. 2015; Dakhili et al. 2017). The production of recombinant silicateins has only been accomplished for the silicatein alpha from *T. aurantium* (Zhou et al. 1999) and from

Suberites domuncula (Müller et al. 2013) and two silicateins (SHN and CHN types) from *Latrunculia oparinae* (Kamenev et al. 2015; Shkryl et al. 2016) and in these experiments, different methodologies were employed to refold and purify these recombinant proteins. The sequences of the majority of these silicateins are members of clade SHNII and they have the two amino acids in the active site (S and H) that have been reported as responsible for silica condensation (Zhou et al. 1999; see Chapter 3). However, a recombinant silicatein of the CHN type from *L. oparinae* was able to condense silica nanocrystals (Kamenev et al. 2015) and the sequence of this silicatein is a member of clade CHNII (Chapter 3). Recombinant silicateins from marine haplosclerids have not yet been produced, and sequences of the silicateins of this order are located in different molecular clades (e.g. SHNI, CHNI, CHNII, CHNIII and C/SQN).

Silicateins of the CHN and C/SQN type were highly expressed at the stages when *H. indistincta* was producing spicules and it is possible that these proteins have a role in spicule formation in this species (Chapter 4). Here I decided to carry out an experiment for the production of a recombinant silicatein from this haplosclerid species. The ultimate goal of this research is to produce silica nanocrystals that could have an important role in the biotech sector, and also as a standard methodology that could be applied for functional studies in non SHN silicatein variants (CHN and C/SQN types) to investigate function and confirm their ability to condense silica. These variants do not have the two amino acids that have been reported as necessary for silica condensation (S and H) but they are abundant in the genomes and transcriptomes from marine haplosclerids.

Materials and Methods

Plasmid construction, transformation and protein expression

One construct of the silicatein of the SHN type (just the active site) from the sponge *Haliclona indistincta* was synthetized (GENSCRIPT) and inserted into the pET-25b (+) plasmid vector (NdelI-HindIII) . The codon optimization was carried out before the insertion; the isoelectric point and molecular weight of the protein were calculated using the protein expasy website https://web.expasy.org/compute_pi/ (Figure 1).

The *E. coli* BL-21 (DE3) strain was transformed with the plasmid vector containing the silicatein construct by heat shock. Transformed cells were grown overnight onto LB agar plate with Ampicillin (50 mg/mL). The next day, colonies with inserts were grown in 500 ml LB culture (supplemented with 75mg/ml of Carbenicillin and 2mM of $MgSO_4$) at 37°C with shaking (485×g) until OD_{600} = >0.7 was reached. Expression of the recombinant protein was induced with 1mM IPTG and its production was carried out at 37°C with shaking (485×g) for 4 h (Crowley et al. 2011). This interval (4 h) was selected because it was optimal for producing the recombinant protein after the induction (Appendix 23). Aliquots of 50 mL were harvested by centrifugation for 4 min (22770×g) at 4°C. The supernatant for each aliquot was discarded and the cell pellets resuspended in 50mM Tris-HCl, 100mM NaCl, 5 mM EDTA pH 7.5 (5 mL) and stored in the freezer (-20°C). Two aliquots were thawed and disrupted by sonication (3 sec on and 3 sec off × 10, amplitude 5). After sonication, the cell lysate was treated with 1 mg/ml DNase (500 µL) and incubated on ice for 10 min. The solution was centrifuged for 25 min (17894×g) at 4°C. The supernatant was discarded and the cell pellet kept.

Figure 1. The nucleotide and amino acid sequences of the peptidase region of the silicatein of the SHN type from *H. indistincta*. Orange letters in the protein sequence indicate the amino acids forming the catalytic triad (SHN) and the particular motif following the Serine (-YAF).

Refolding and purification of the recombinant silicatein

Because this silicatein protein has eight cysteines and it is likely that it will form inclusion bodies; two different approaches were employed to refold and purify the recombinant silicatein (having a positive charge) employing Ion Exchange Chromatography (CM resin) with the AKTA Purifier FPLC (modified from Burgess (2009) and Shkryl et al. (2016)).

1. – Refolding of protein and purification via HPLC (Figure 2).

The cell pellet was resuspended by vortexing in 50 mM of Tris-HCl, 100 mM NaCl and 5 mM EDTA pH 7.5 (25 mL) and incubated 30 min on ice. The cell suspension was disrupted by sonication (3 sec on and 3 sec off × 10, amplitude 5) using the Sonicator Soniprep 150 plus. After sonication, the cell lysate was centrifuged for 25 min (17894×g) at 4°C. A fraction of the supernatant (soluble) and pellet (insoluble) was collected for further SDS-PAGE analysis and then the supernatant was discarded. A second wash was done as described above and the supernatant was also discarded. To solubilize the protein, the pellet was resuspended by vortexing in 50 mM Tris-HCl, 100 mM NaCl, 5 mM EDTA, 8 M urea, 5 mM DTT, pH 7.5 (1 mL) and incubated one hour on ice. The solution was centrifuged for 15 min (17894×g) at 4°C and the supernatant was stored in the fridge (4°C). A fraction of the supernatant and pellet were collected for further SDS-PAGE analysis. The following day the 1 mL supernatant (dissolved urea inclusion bodies) was added dropwise (10 µL every 4 min) into 50 mL of refolding buffer (50 mM Tris-HCl, 100 mM NaCl, 500mM Arg, 50 mM Glu, 5 mM Glutathione reduced, 0.5 mM Glutathione oxidized, pH 7.0) with gently stirring at 4°C and incubated overnight (4°C). The solution was centrifuged for 15 min (17894×g) at 4°C. After the centrifugation, the solution was filtered (0.2 µm) and a fraction of the filtrate was collected for further SDS-PAGE analysis. The 50 mL solution was centrifuged for 30 min (7320×g) at 25°C (seven times) in a concentrator (AMICON, 3 kDa cut-off) until the volume reached 2 ml. A fraction of this volume was collected for further SDS-PAGE analysis.

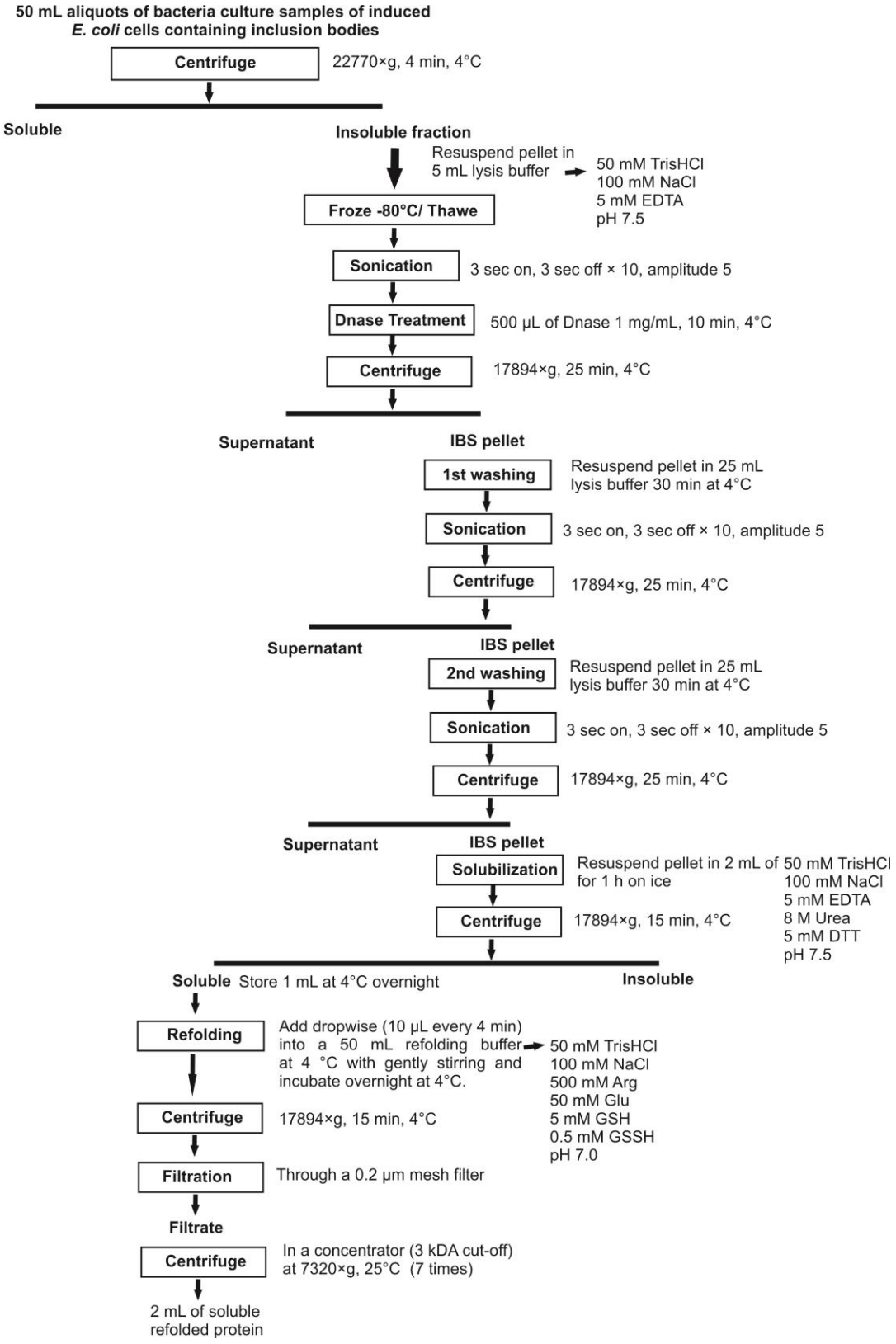

Figure 2. Refolding protocol of the recombinant silicatein from *H .indistincta*.

2. – Protein purification followed by refolding (Figure 3).

The cell pellet for each fraction was resuspended by vortexing in 50 mM Tris-HCl, 100 mM NaCl and 5 mM EDTA pH 7.5 (25 mL) and incubated 30 min on ice. The cell suspension was disrupted by sonication (as above). After sonication, the cell lysate was centrifuged for 25 min (17894×g) at 4°C and the supernatant discarded. A second wash was done as described above and the supernatant was discarded. To solubilize the protein, the pellet was resuspended by vortexing in 20 mM KPi, 100 mM NaCl, 8 M urea, 5 mM DTT, pH 6.0 (1 mL) and incubated one hour on ice. The solution was centrifuged for 15 min (17894×g) at 4°C and the supernatant was stored in the fridge (4°C). Ion Exchange Chromatography (using CM resin) was employed to separate the target protein from the dissolved urea inclusion bodies (2 mL) using the AKTA Purifier FPLC. Two buffer solutions at different salinity concentrations were utilized: A) 20 mM KPi, 100 mM NaCl, 8 M Urea, pH 6.0; B) 20 mM KPi, 1 M NaCl, 8 M Urea, pH 6.0. The dissolved urea inclusion bodies (containing the silicatein protein) were injected through the column (CM resin) with the low salinity solution and then this solution was replaced with the high salinity solution. During this process, the chromatograph recorded the UV and conductivity and fractions of 5 ml were collected at standard time intervals. Fractions showing high UV peaks in the chromatograph were collected for further SDS-PAGE analysis.

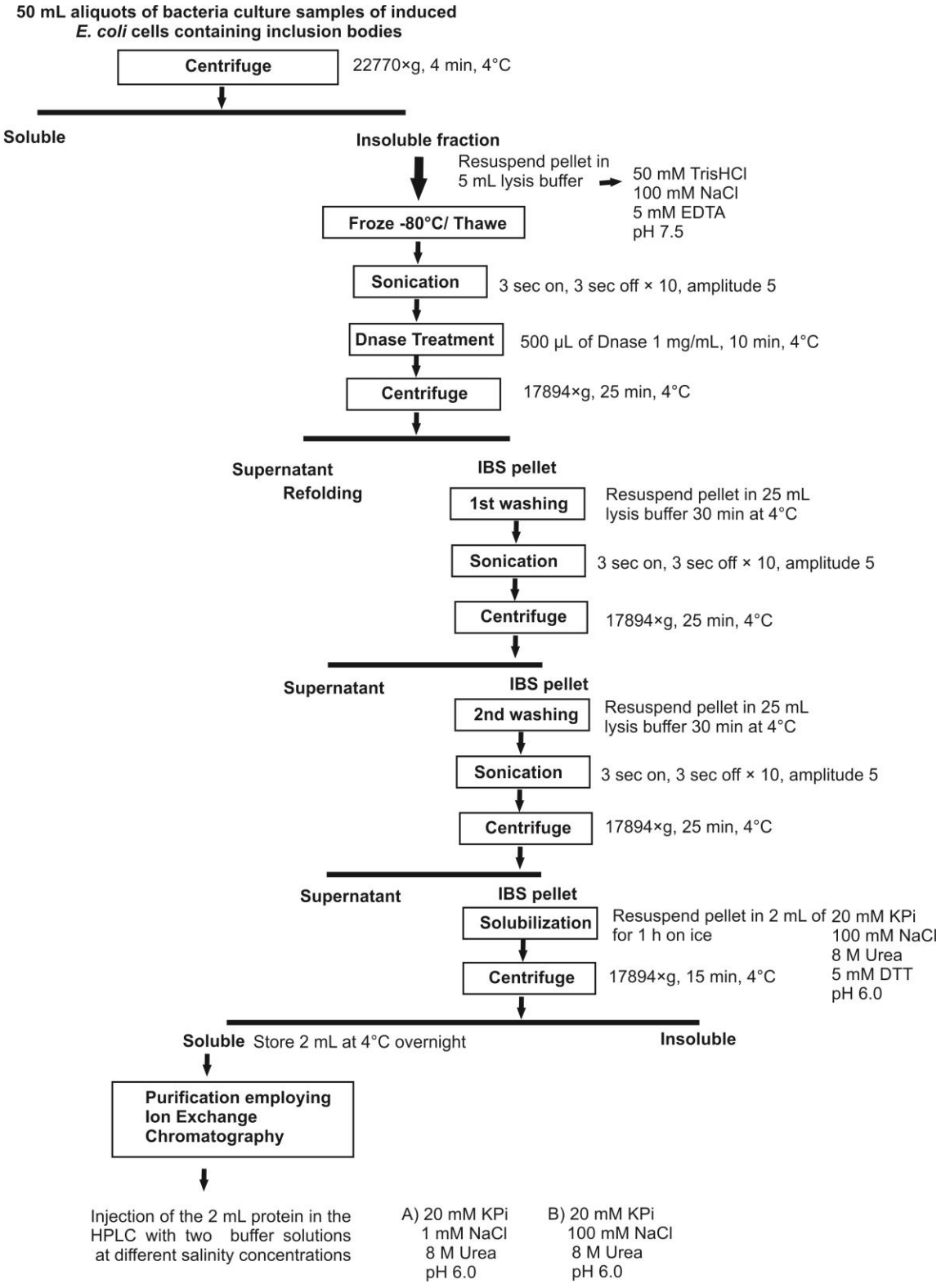

Figure 3. Purification protocol of the recombinant silicatein from *H .indistincta*.

Results

The silicatein gene was successfully expressed in the *E. coli* B-21 cells. SDS-PAGE analysis of the silicatein showed that the expressed silicatein protein was found in the insoluble part of the two washes which confirmed the presence of inclusion bodies. (Figure 4, Lanes 1 and 3). This protein was found in both soluble and insoluble fractions after solubilization with urea (Figure 4, Lanes 5 and 6). After the refolding step the protein was soluble and it was found in the filtered refolding buffer and in the concentrator (Figure 4, Lanes 7 and 8). The silicatein showed a protein band corresponding to 22 kDa (Figure 4). However, the yield of the refolded protein was very low and insufficient for the purification step.

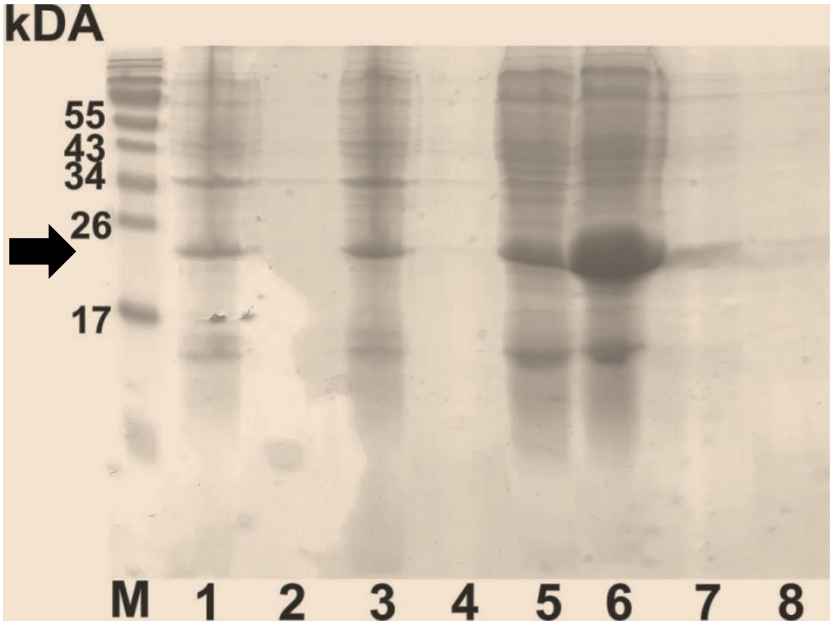

Figure 4. SDS-PAGE analysis of the soluble and insoluble protein fractions expressed in *E. coli* after washes, solubilization and refolding**.** Lanes; M: molecular marker, 1: silicatein insoluble fraction (1st wash), 2: silicatein soluble fraction (1st wash), 3: silicatein insoluble fraction (2nd wash), 4: silicatein soluble fraction (2nd wash), 5: silicatein insoluble fraction after the solubilization with 8 M urea, 6: silicatein soluble fraction after the solubilization with 8 M urea, 7.- silicatein soluble fraction from the concentrator (2 ml), 8: silicatein soluble fraction from the 50 mL refolding buffer (filtered through a 0.2 µm mesh). Black arrow indicates the protein band corresponding to the silicatein in all the lanes (22 kDA).

In the second approach attempted (purification followed by refolding) the dissolved urea inclusion bodies were first injected through the column with the low salinity solution and then this solution was changed with a high salinity solution (containing the CM resin) and the resulting chromatograph showed two UV peaks. The first peak in Figure 5 below corresponded to fractions: 3, 4, 5 and 6 in the low salinity solution while the second peak corresponded to fractions 15 and 16 in the high salinity solution (Figure 5) indicating that the protein (which is positively charged) did not bind into the CM resin (negatively charged) and just passed through it with the two buffer solutions (Figure 5). SDS-PAGE showed a protein band of 22 kDa corresponding to the fractions in the low salinity solution and not present in the fractions in the high salinity solution (Figure 6). The silicatein did not bind (purify) to the column and the refolding step was not possible to carry out.

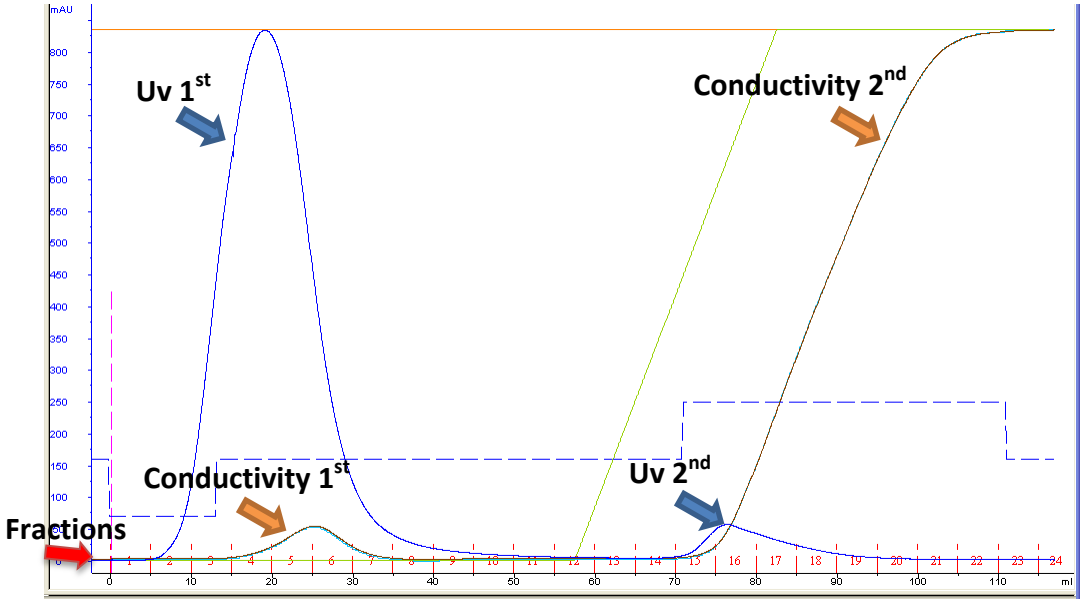

Figure 5. Ion Exchange chromatograph of the experiment carried out with the dissolved urea inclusion bodies containing the silicatein. The blue line corresponds to the absorbance of the protein (UV) and the brown line corresponds to the conductivity of the buffer solutions (salinity). The protein was inserted first in a solution with low salinity (20 mM KPi, 1 mM NaCl, 8 M Urea, pH 6.0) to the CM resin (negatively charged) and then the solution was changed to a higher salinity (20 mM KPi, 100 mM NaCl, 8 M Urea, pH 6.0). The protein did not bind to the resin because when the salinity concentration increased, the chromatogram did not show a high UV peak as at the beginning of the experiment (low salinity). The fractions of this experiment were enumerated and collected. The two peaks (UV) indicated the presence of the protein during the experiment: 1st peak (3, 4, 5, and 6) and 2nd peak (15, 16).

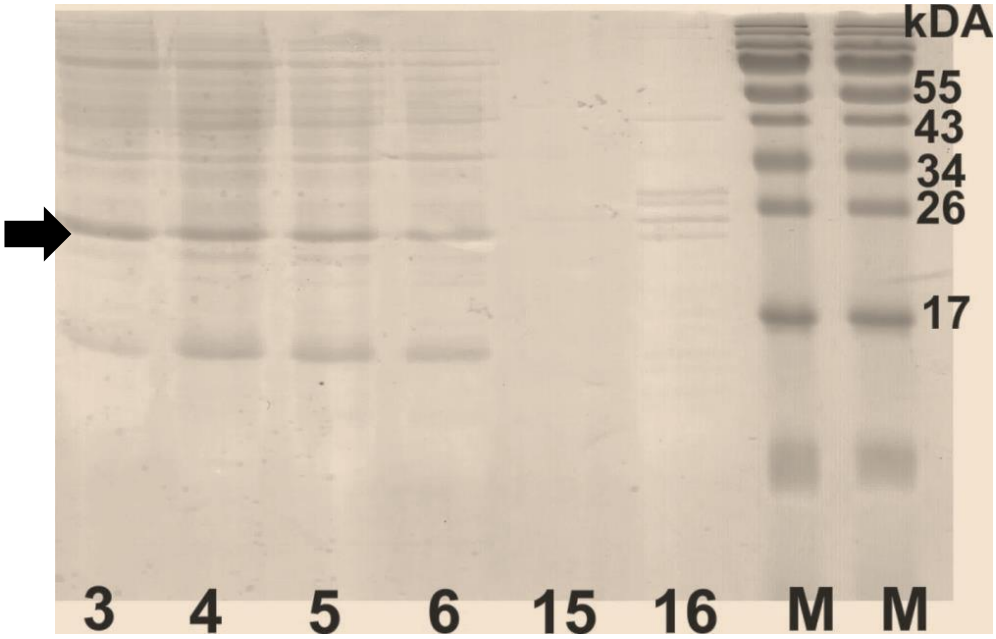

Figure 6. SDS-PAGE analysis of the fractions that had UV peaks from the experiment using Ion Exchange Chromatography. The numbers represent the fractions collected during the experiment (e.g. 3, 4, 5, 6, 15 and 16) M: molecular marker. Black arrow indicates the protein bands of the fractions.

Discussion

In this study I was able to express the peptidase region of the silicatein of the SHN type from *H. indistincta* in the cytoplasmic region of *E. coli* (BL-21 strain). The silicatein from this species formed inclusion bodies as all the recombinant silicateins reported in previous studies (Sumerel et al. 2003; Sclossmacher et al. 2011; Shkryl et al. 2016). Because this protein has a positive charge, the purification step was carried out employing Ion Exchange Chromatography with a negative resin (CM resin) either from the refolded soluble protein or from the dissolved urea inclusion bodies. Unfortunately, the two approaches were not successful and therefore I could not continue the experiment of combining the purified recombinant silicatein with water soluble silica precursors (T.E.O.S and T.H.E.O.S.) to produce silica nanocrystals. A different approach in which a fused protein was added to the

silicatein protein was employed to express and purify recombinant silicateins from other species; the expression of the silicatein alpha from *S. domuncula* included a chaperone fusion tag and the protein was purified using a Ni-NTA column (Schröder et al. 2012). The same silicatein alpha from *S. domuncula* was fused to a GST binding protein and purified using a GHS-coated plate by Ki et al. (2013). The silicatein alpha from *T. aurantium* was fused to the maltose binding protein and purified using an amylose resin by Cha et al. (1999) while this silicatein from *T. aurantium* was fused with the omp A sequence and expressed in the periplasmic region and peptide affinity screenings was employed for purification by Curnow et al. (2005). In these experiments the purified recombinant silicateins retained their catalytic activity and they were able to condense silica from T.E.O.S. indicating that they were refolded.

The recombinant silicateins from *S. domuncula* and *L. oparinae* were purified using Immobilized Metal Ion Affinity Chromatography. This methodology adds a 6× Histidine-Tag either to the N- or C- terminus of the protein that can bind to a Ni+ 2 column (Schlossmacher et al. 2011; Kamenev et al. 2015; Shkryl et al. 2016). In the case of silicateins, the purification step using this technique could be carried out with the dissolved urea inclusion bodies or with the soluble refolded protein (Sclossmacher et al. 2011; Shkryl et al. 2016); when the histidine tag was not added to the silicatein sequence, a hexaglutamate tag could be added instead and this can bind into a MonoQ resin using Ion Exchange Chromatography (Natalio et al. 2010) or a hexacysteine tag and this can bind into a maleimide chip substratum (Wiens et al. 2012). When the dissolved urea inclusion bodies were purified, then the silicatein protein was refolded by dialysis at low concentrations against refolding solutions containing GSH/GSSH and L-Arginine (Wiens et al. 2012; Shkryl et al. 2016). This refolding method was employed

to create disulfide bonds of the cysteines that are found in the silicateins. After this process the refolded silicateins showed their catalytic activity because they condensed silica from T.E.O.S or T.H.E.O.S. (Wiens et al. 2012; Shkryl et al. 2016). In the first attempt to refold and purify the silicatein from *H. indistincta* the dissolved urea inclusion bodies were added drop wise to a refolding buffer containing GSH, GSSH and L-Arginine but unfortunately the soluble yield was very low that I could not continue to the purification step using Ion Exchange Chromatography.

One of the main problems in my experiment was the low yield that I got in the expression of the silicatein from *H. indistincta*. An alternative approach to have a high yield and get a refolded soluble protein is to carry out periplasmic expression (Humphreys et al. 2000). Proteins designed for this expression contain an N-terminal signal peptide that is cleaved by secretion machinery in the plasma membrane and the protein is released usually in an active form (Mergulhao et al. 2005). For instance, the recombinant silicatein of *T. aurantium* was expressed in the periplasmic region by adding the ompA sequence to the N-terminus of the silicatein gene. This protein was either purified or encapsulated in the periplasm by the bacteria and retained its catalytic activity (Zhou et al. 1999; Curnow et al. 2005). Further experiments should be undertaken combining periplasmic expression, histidine tag purification or expression with a fused protein, to get a soluble refolded and purified silicatein for multiple purposes. The production of recombinant silicateins is time demanding and unfortunately, I had no more available time to continue this experiment with an alternative approach as those reported previously in the literature.

Another alternative option, for the production of recombinant proteins, is to utilize yeast cells as vectors (e.g. *Pichia pastoris* and *Saccharomyces cerevisiae*) (Ghaemmaghami et al. 2013).

Yeast cells can perform many post-translational modifications to the expressed recombinant proteins (Macauley-Patrick et al. 2005). These include: processing of signal sequences, disulfide bridge formation, folding and glycosylation (Fletcher et al. 2016). There are many human recombinant proteins expressed in yeast cells that the post-translational modifications are identical to the natural proteins (Redden et al. 2015; Cregg et al. 2018;). Indeed, cathepsin V and pro-cathepsin L from humans have been successfully expressed, refolded and purified in these vectors, and their crystal structure have been achieved (Coulombe et al. 1996; Somoza et al. 2000). However, the expressed proteins in yeast cells, could experience hyperglycosylation or a high number of recombination events (Cereghino and Cregg, 2000). Further experiments should be undertaken using yeast cells as an attempt for the production and refolding of recombinant silicateins.

The recombinant silicatein produced according to the literature have many cysteines and there is no evidence whether they are connected by the proper disulfide bonds. The modification of the cysteine thiols affects protein function and stability and currently several approaches have been applied to understand the chemistry of these disulfide bonds in proteins having cysteines (Borges and Sherma, 2014). Although there are several studies about recombinant silicateins showing their catalytic activity, there is no information that the cysteines from these silicateins are bound with the proper disulfide bonds. In addition, there is no crystal structure available of any silicatein protein (Fairhead et al. 2008). It is possible that these recombinant silicateins were not properly refolded and although they showed catalytic activity; the efficiency is low compared to isolated silicateins from the axial filament of *T. aurantium* (Cha et al. 1999).

The production of recombinant silicateins is complicated and although there are some studies that have successfully expressed, refolded and purified these proteins, there is not a standard protocol to carry out this experiment. More work is required to express all the diversity of silicatein variants that are found in several demosponge species that are located in different molecular clades (see chapter 3) and different experimental approaches are necessary to express, refold and purify these proteins.

References

Arakaki, A., Shimizu, K., Oda, M., Sakamoto, T., Nishimura, T., Kato, T. (2015). Biomineralization-inspired synthesis of functional organic/inorganic hybrid materials: organic molecular control of self-organization of hybrids. Organic and biomolecular chemistry, 13(4), 974-989.

Baneyx, F. (1999). Recombinant protein expression in Escherichia coli. Current opinion in biotechnology, 10(5), 411–421.

Burgess, R R. (2009). Refolding solubilized inclusion body proteins. Methods in enzymology, 463, 259-282.

Borges, C. R., Sherma, N. D. (2014). Techniques for the analysis of cysteine sulfhydryls and oxidative protein folding. Antioxidants and redox signaling, 21(3), 511-531.

Brutchey, R. L., Morse, D. E. (2008). Silicatein and the translation of its molecular mechanism of biosilicification into low temperature nanomaterial synthesis. Chemical reviews, 108(11), 4915-4934.

Cereghino, J. L., Cregg, J. M. (2000). Heterologous protein expression in the methylotrophic yeast Pichia pastoris. FEMS microbiology reviews, 24(1), 45-66.

Cha, J. N., Shimizu, K., Zhou, Y., Christiansen, S. C., Chmelka, B. F., Stucky, G. D., Morse, D. E. (1999). Silicatein filaments and subunits from a marine sponge direct the polymerization of silica and silicones in vitro. Proceedings of the National Academy of Sciences, 96(2), 361-365.

Coulombe, R., Grochulski, P., Sivaraman, J., Menard, R., Mort, J. S., Cygler, M. (1996). Structure of human procathepsin L reveals the molecular basis of inhibition by the prosegment. The EMBO journal, 15(20), 5492-5503.

Cregg, J. M., Tolstorukov, I., Kusari, A., Sunga, A. J., Madden, K., Chappell, T. (2018). Expression of Recombinant Genes in the Yeast Pichia pastoris. Current Protocols Essential Laboratory Techniques, 17(1), e25.

Crowley, P. B., Chow, E., Papkovskaia, T. (2011). Protein interactions in the *Escherichia coli* cytosol: an impediment to in cell NMR spectroscopy. ChemBioChem, 12(7), 1043-1048.

Curnow, P., Bessette, P. H., Kisailus, D., Murr, M. M., Daugherty, P. S., Morse, D. E. (2005). Enzymatic synthesis of layered titanium phosphates at low temperature and neutral pH by cell-surface display of silicatein-α. Journal of the American Chemical Society, 127(45), 15749–15755.

Curnow, P., Kisailus, D., Morse, D. E. (2006). Biocatalytic Synthesis of Poly (L-Lactide) by Native and Recombinant Forms of the Silicatein Enzymes. Angewandte Chemie, 118(4), 629-632.

Dakhili, S. Y. T., Caslin, S. A., Faponle, A. S., Quayle, P., de Visser, S. P., Wong, L. S. (2017). Recombinant silicateins as model biocatalysts in organosiloxane chemistry. Proceedings of the National Academy of Sciences, 114(27), E5285-E5291.

Fairhead, M., Johnson, K. A., Kowatz, T., McMahon, S. A., Carter, L. G., Oke, M., Liu, H., Naismith, J.H., van der Walle, C. F. (2008). Crystal structure and silica condensing activities of silicatein α–cathepsin L chimeras. Chemical Communications, (15), 1765-1767

Fletcher, E., Krivoruchko, A., Nielsen, J. (2016). Industrial systems biology and its impact on synthetic biology of yeast cell factories. Biotechnology and bioengineering, 113(6), 1164-1170.

Freymann, D. M., Nakamura, Y., Focia, P. J., Sakai, R., Swanson, G. T. (2012). Structure of a tetrameric galectin from *Cinachyrella sp.(*ball sponge). Acta Crystallographica Section D: Biological Crystallography, 68(9), 1163-1174.

Furuki, K., Toyooka, T., Yamaguchi, H. (2017). A novel rapid analysis using mass spectrometry to evaluate downstream refolding of recombinant human insulin-like growth factor-1 (mecasermin). Rapid Communications in Mass Spectrometry, 31(15), 1267-1278.

Ghaemmaghami, S., Huh, W. K., Bower, K., Howson, R. W., Belle, A., Dephoure, N., O'Shea, E., Weissman, J. S. (2003). Global analysis of protein expression in yeast. Nature, 425(6959), 737.

Gupta, S. K., Shukla, P. (2016). Advanced technologies for improved expression of recombinant proteins in bacteria: perspectives and applications. Critical reviews in biotechnology, 36(6), 1089-1098.

Humphreys, D. P., Sehdev, M., Chapman, A. P., Ganesh, R., Smith, B. J., King, L. M., Glover, D.J., Reeks, D.G., Stephens, P. E. (2000). High-level periplasmic expression in *Escherichia coli* using a eukaryotic signal peptide: importance of codon usage at the 5′ end of the coding sequence. Protein expression and purification, 20(2), 252-264.

Kamenev, D. G., Shkryl, Y. N., Veremeichik, G. N., Golotin, V. A., Naryshkina, N. N., Timofeeva, Y. O., Kovalchuk, S.N., Semiletova, I.V., Bulgakov, V. P. (2015). Silicon Crystals Formation Using Silicatein-Like Cathepsin of Marine Sponge *Latrunculia oparinae*. Journal of nanoscience and nanotechnology, 15(12), 10046–10049.

Ki, M. R., Yeo, K. B., Pack, S. P. (2013). Surface immobilization of protein via biosilification catalyzed by silicatein fused to glutathione S-transferase (GST). Bioprocess and biosystems engineering, 36(5), 643-648.

Kisailus, D., Choi, J. H., Weaver, J. C., Yang, W., Morse, D. E. (2005). Enzymatic synthesis and nanostructural control of gallium oxide at low temperature. Advanced Materials, 17(3), 314-318.

Macauley-Patrick, S., Fazenda, M. L., McNeil, B., Harvey, L. M. (2005). Heterologous protein production using the Pichia pastoris expression system. Yeast, 22(4), 249-270.

Mergulhao, F. J. M., Summers, D. K., Monteiro, G. A. (2005). Recombinant protein secretion in *Escherichia coli*. Biotechnology advances, 23(3), 177-202.

Morse, D. E. (1999). Silicon biotechnology: harnessing biological silica production to construct new materials. Trends in Biotechnology, 17(6), 230-232.

Natalio, F., Link, T., Müller, W. E., Schröder, H. C., Cui, F. Z., Wang, X., Wiens, M. (2010). Bioengineering of the silica-polymerizing enzyme silicatein-α for a targeted application to hydroxyapatite. Acta biomaterialia, 6(9), 3720-3728.

Rajakaruna, S. S., Taylor-Robinson, A. W. (2016). Application of Recombinant DNA Technology (Genetically Modified Organisms) to the Advancement of Agriculture, Medicine, Bioremediation and Biotechnology Industries. Journal of Applid Biotechnology and Bioengineering, 1(3), 00013.

Redden, H., Morse, N., Alper, H. S. (2015). The synthetic biology toolbox for tuning gene expression in yeast. FEMS Yeast Res, 15(1), 1-10.

Schloßmacher U, Wiens M, Schröder HC, Wang X, Jochum KP, Müller WE. (2011). Silintaphin1–interaction with silicatein during structure-guiding biosilica formation. The FEBS journal. 278(7):1145–1155.

Schröder, H. C., Wang, X., Manfrin, A., Yu, S. H., Grebenjuk, V. A., Korzhev, M., Wiens, M., Schlossmacher, U., Müller, W. E. (2012). Acquisition of structure-guiding and structure-forming properties during maturation from the pro-silicatein to the silicatein form. Journal of Biological Chemistry, 287(26), 22196-22205.

Shimizu, K., Cha, J., Stucky, G. D., Morse, D. E. (1998). Silicatein α: cathepsin L-like protein in sponge biosilica. Proceedings of the National Academy of Sciences, 95(11), 6234–6238.

Shkryl, Y. N., Bulgakov, V. P., Veremeichik, G. N., Kovalchuk, S. N., Kozhemyako, V. B., Kamenev, D. G., Semiletova, I.V., Timofeeva, Y.O., Scchipunov, Y.A., Kulchin, Y. N. (2016). Bioinspired enzymatic synthesis of silica nanocrystals provided by recombinant

silicatein from the marine sponge Latrunculia oparinae. Bioprocess and Biosystems Engineering, 39(1), 53–58.

Somoza, J. R., Zhan, H., Bowman, K. K., Yu, L., Mortara, K. D., Palmer, J. T., Clark, J.M., McGrath, M. E. (2000). Crystal structure of human cathepsin V. Biochemistry, 39(41), 12543-12551.

Sumerel, J. L., Yang, W., Kisailus, D., Weaver, J. C., Choi, J. H., Morse, D. E. (2003). Biocatalytically templated synthesis of titanium dioxide. Chemistry of materials, 15(25), 4804–4809.

Tahir, M. N., Natalio, F., Therese, H. A., Yella, A., Metz, N., Shah, M. R., Mugnainoli, E., Berger, R., Theato, P., Schröder, H. C., Müller, W. E., Tremel, W. (2009). Enzyme-mediated deposition of a TiO_2 coating onto biofunctionalized WS_2 chalcogenide nanotubes. Advanced Functional Materials, 19(2), 285-291.

Tahir, M. N., Théato, P., Müller, W. E., Schröder, H. C., Borejko, A., Faiß, S., Janshoff, A., Huth, J., Tremel, W. (2005). Formation of layered titania and zirconia catalysed by surface-bound silicatein. Chemical Communications, (44), 5533-5535.

Tahir, M. N., Théato, P., Müller, W. E., Schröder, H. C., Janshoff, A., Zhang, J.,Huth, J.,Tremel, W. (2004). Monitoring the formation of biosilica catalysed by histidine-tagged silicatein. Chemical Communications, (24), 2848-2849.

Vergara, A., Grassi, M., Sica, F., Pizzo, E., D'Alessio, G., Mazzarella, L., Merlino, A. (2013). A novel interdomain interface in crystallins: structural characterization of the βγ- crystallin

from Geodia cydonium at 0.99 Å resolution. Acta Crystallographica Section D, 69(6), 960-967.

Wei, L., Alhenc-Gelas, F., Soubrier, F., Michaud, A., Corvol, P., Clauser, E. (1991). Expression and characterization of recombinant human angiotensin I-converting enzyme. Evidence for a C-terminal transmembrane anchor and for a proteolytic processing of the secreted recombinant and plasma enzymes. Journal of Biological Chemistry, 266(9), 5540–5546.

Wiens, M., Link, T., Elkhooly, T. A., Isbert, S., Müller, W. E. (2012). Formation of a micropatterned titania photocatalyst by microcontact printed silicatein on gold surfaces. Chemical Communications, 48(92), 11331-11333.

Wolf, S. E., Schlossmacher, U., Pietuch, A., Mathiasch, B., Schröder, H. C., Müller, W. E., Tremel, W. (2010). Formation of silicones mediated by the sponge enzyme silicatein-α. Dalton transactions, 39(39), 9245-9249.

Zhou, Y., Shimizu, K., Cha, J. N., Stucky, G. D., Morse, D. E. (1999). Efficient catalysis of polysiloxane synthesis by silicatein α requires specific hydroxy and imidazole functionalities. Angewandte Chemie International Edition, 38(6), 779-782.

Chapter 6

General Discussion

Discussion

The main objective of this thesis was to study certain elements of skeleton construction (spicules and genes producing spicules) in selected marine haplosclerid species that might help explain the discrepancy between their morphological classification and patterns of relatedness determined via molecular systematics (based on mitochondrial and ribosomal data) (McCormack et al. 2002; Redmond et al. 2011; 2013). In addition, I wanted to corroborate whether or not some of these elements are distinct from the remaining demosponges bearing spicules (freshwater sponges and other heteroscleromorpha), given that molecular studies located the sequences of marine haplosclerids in a different clade to those from heteroscleromorpha and freshwater sponges (Sperling et al. 2010; Hill et al. 2013; Redmond et al. 2013; Thacker et al. 2013).

The chemical composition of the spicules was similar in the species analyzed here and the values of SiO_2 were also similar to those reported from other heteroscleromorpha and hexactinellid species that have different spicule categories and proteins responsible for spicule formation (Sandford, 2003; Pozzolini et al. 2004; Shimizu et al. 2015). The variation in the amounts of biogenic silica across different species in all these studies is less than 10% (Chapter 2, Sandford 2003) and there is no clear explanation for the similarity/dissimilarity of these values in sponge spicules. The methodology employed in this thesis to discriminate marine haplosclerid species by the chemical composition of spicules was inconclusive and no results were obtained that could reflect any phylogenetic pattern; instead the highest concentrations of trace metals found in one species (*H. indistincta*) could be associated with the high concentrations of these elements in the surrounding environment (sediments and seawater) where this species inhabits (Chapter 2).

The main genes responsible for spicule formation (silicateins and silintaphins) were identified in all the available transcriptomes and genomes from Porifera. They were only present in demosponges bearing siliceous spicules (marine haplosclerids, freshwater sponges and other heteroscleromorpha) excluding *Chondrilla caribbea* that is classified in the subclass Verongimorpha and possesses spicules (Redmond et al. 2013). The identification of other silicatein variants (CHN and C/SQN types), with different amino acids in the active site than those reported previously, makes the genetic basis of spicule formation more complex than was expected (Chapter 3). These unusual silicateins do not have the two amino acids in the active site that have been reported as being responsible for the catalysis of silica (SH) (Cha et al. 1999; Zhou et al. 1999). However, there is clear evidence (gene expression and recombinant enzymes) that these genes have a role in spicule formation (Kamenev et al. 2015; Shkryl et al. 2016; Chapter 4) and more functional studies in additional species are necessary to understand the exact role of these proteins.

Silicatein sequences from marine haplosclerids were located in a different molecular clade than those from other heteroscleromorpha (not including freshwater sponges), but some of them grouped with sequences from freshwater sponges. However, one silicatein from *H. indistincta* (CHN type) was located between the overall silicatein clade and cathepsins-L clade (chapter 3). All the transcriptomes and genomes from marine haplosclerids analyzed here contained almost the same number of silicatein genes: one of the SHNI type, up to three of the CHN type and one of the C/SQN type and they lack silicatein variants of the SHNII type and the silintaphin protein, that were present in the genomes and transcriptomes from freshwater sponges and other heteroscleromorpha. Silicatein variants of the SHNII type have been reported as being responsible for the shaping of megasclere spicules in one

heteroscleromorpha species (*Suberites domuncula*) and different variants of this type were expressed during the formation of megascleres and microscleres in selected species of freshwater sponges and other heteroscleromorpha (Müller et al. 2005; 2007; Mohri et al. 2008). The absence of these silicatein variants (SHNII type) and the silintaphin protein in the genomes and transcriptomes from marine haplosclerids is probably the reason that species of this order have megasclere spicules in a single size category.

Despite the number of paralogous copies, the evolution of the silicatein genes in marine haplosclerids reflects the previous molecular topology from ribosomal, nuclear and mitochondrial data (Redmond et al. 2011; 2013; Thacker et al. 2013; Hill et al. 2013) and the sequences from representatives of the three major clades were distributed accordingly to this topology: clade A (*H. oculata* and *H. tubifera*) and clade B (*A. queenslandica* and *H. simulans*) sister to clade C (*H. indistincta*).

The megasclere spicules of species identified under the genera *Haliclona, Callyspongia* and *Chalinula* have the smallest size, compared to species identified in other genera (e.g.: *Petrosia, Xestospongia* or *Oceanapia*) according to van Soest (1980) and de Weerdt (1986), and the majority of these species are members of clade A based on molecular data (Redmond et al. 2011). In this thesis, transcriptomes of two species from clade A were analyzed (*H. oculata* and *H. tubifera*) and one silicatein type (C/SQN) was not present. It is possible that the absence of this gene in the transcriptomes of these two species could have an effect on the spicule length (small size).

The differences in spicule dimensions across different species could also be associated with variations on the self-assembly of a silicatein protein of a particular species and to date the

posttranslational modification of this protein has only been determined for one variant from the sponge *Petrosia ficiformis* (Armirotti et al. 2009). It is also possible that the control of the expression levels of silicatein genes could have an effect on the spicule dimensions. In chapter 4, I determined that the expression levels of different silicatein genes from *H. indistincta* were distinct between two developmental stages producing spicules: adult specimens and in the pre-settled stage, and although the spicules were not measured they usually are longer in adults than at early developmental stages (Maldonado, 2006). It is likely that the expression levels of different genes are responsible for the dissimilarities in the spicule size at these two life stages and it is also possible that there are different expression levels of silicateins across different lineages within Haplosclerida that could also have an effect on the spicule dimensions across different species.

Further experiments should be undertaken to verify whether or not an increase of silica in the surrounding water where a species inhabits could modify (increase) the length and width of the spicules in one particular species. For instance, Maldonado et al. (1999) demonstrated that an increase of silica was responsible for the formation of thick spicules and hyper silicified microscleres at early stages in the sponge *Crambe crambe*, but the expression levels of the silicatein genes were not determined. Likewise, the haplosclerid *Gelliodes wilsoni* is widely distributed along the Eastern Pacific and the spicules were longer in specimens living near shore (Hawaii) than those specimens living around an isolated island (Palmyra Atoll), but the expression levels of different silicatein genes were not investigated (Carballo et al. 2013). It is likely, that the spicules will be longer in one haplosclerid species living in a coastal locality near river discharges than another haplosclerid belonging to the same or to a closely related

species living around an isolated island (no river discharges), and this variation could be associated with different levels of silicatein genes.

There are different skeletal arrangements in adult specimens that have been employed as diagnostic features for the classification of the order Haplosclerida (van Soest, 1980; Desqueyroux-Faundez, 1999; van Soest and Hopper, 2002). In some haplosclerids the skeleton is delicately formed by primary unispicular fibres connected by secondary unispicular fibres (species members of clade A and identified as *Chalinula* and *Haliclona*) while other species have a dense skeleton formed by primary multispicular ascending fibres interconnected with secondary bi- or multispicular fibres (species members of clades B and C and identified as *Amphimedon*, *Niphates* and some *Haliclona* species). In addition, in some species the spicule fibres (primary or secondary) are embedded by spongin or collagen sheets (members of clades A, B and C and identified as *Callyspongia*, *Niphates*, *Amphimedon*, *Gelliodes*) and in other species the skeleton is rigid (species assigned to clade B and to a small clade close to A but not within and identified as *Petrosia*, *Oceanapia* and *Neopetrosia*) (van Soest, 1980; Desqueyroux-Faundez, 1999; van Soest and Hooper, 2002; Raleigh et al. 2007; Redmond et al. 2011; 2013). In addition, some species may have different levels of spongin embedded in their primary or secondary fibres, for example *H. cinerea* was described with spongin just at the nodes of the primary and secondary fibres while the fibres in *H. simulans* are completely embedded with spongin and in other *Haliclona* species the spongin is lacking (de Weerdt, 1986). The differences of skeletal arrangements across species are not explained by the presence or absence of the silicatein variants in their respective genomes or transcriptomes. Therefore, it is likely that there are some additional proteins (e.g. transcription

factors, collagen genes) and cells responsible for the diversification of skeletal arrangements across different lineages within Haplosclerida.

In addition, skeleton construction could be associated with a response to an external stimulus in the environment. It is likely that sponges that are branching, tubular or arborescent need a firm skeleton to support their body to produce more spicules (van Soest, 1980). In the case of haplosclerids, some species (across different lineages and identified under the genera *Haliclona, Callyspongia* and *Xestospongia*) with these body forms have a dense skeleton formed by primary ascending multispicular fibres that could be embedded with spongin sheets (de Voogd and van Soest, 2002). It is also possible that sponges need to construct a firm skeleton to live in places with high movement of water (affected by strong waves and currents) as well as places affected by seasonal storms, hurricanes or typhoons such as the Caribbean and Indo-Pacific regions (members of clades B and C identified as *Petrosia, Neopetrosia*, *Callyspongia* and *Xestospongia*) (de Voogd and van Soest, 2002; Wulff, 2012). However, there are some cases in which one species inhabiting different environmental conditions (e.g. high movement of water in the intertidal area vs low movement of water in the subtidal area), displays distinct external morphologies but the internal skeleton arrangement is the same. *H. cinerea* is encrusting in the intertidal area and branching in the subtidal zone but specimens in these two contrasting habitats have a delicate skeleton, while *H. simulans* is encrusting in the intertidal and tubular in the subtidal area and specimes in these two habitats have a firm skeleton (de Weerdt, 1986). In this latter case, the conditions of the habitat type do not influence skeletal architecture in these two species and it is the size and shape of the external morphology that appears more important then to deal with varying environment rather than the firmness of the skeleton

To date, the process of skeleton construction in sponges has only been investigated from hatching of the gemmules in the freshwater sponge *E. fluviatilis* (Nakayama et al. 2015). The skeleton construction followed several steps in which one megasclere spicule was secreted by sclerocytes during which one silicatein gene was highly expressed; then transport cells moved the spicule (during which one transcription factor was highly expressed) which pierced through the outer epithelia, was raised up at one end while the other end of the spicule was cemented in a basal collagenous layer by specific cell types. The newly produced spicules were fixed either to a different substratum or to the head of one cemented spicule and the skeleton arrangement included primary uni- or bispicular ascending fibres. The spicules that did not pierce through the outer epithelia formed the secondary fibres with both ends of one spicule fixed to the heads of two held-up cemented spicules (Nakayama et al. 2015). These authors suggested that the arrangement of the skeleton in this freshwater sponge is correlated with a species-specific mechanism that this species evolved to construct its skeleton and different cells and proteins are responsible for this arrangement (Nakayama et al. 2015). The methodology (using microscopy and molecular approaches) employed in this latter study could be applied in selected species belonging to Haplosclerida to identify the proteins and cells responsible for skeletal arrangement.

The megasclere spicules in demosponges have an axial filament composed of the silicatein protein responsible for silica deposition (Shimizu et al. 1998). In contrast, “glassin” was reported as the protein responsible for the formation of the skeletal system and silica formation in *Euplectella,* class Hexactinellida (Shimizu et al. 2015). Currently, the protein responsible forming the axial filament of the siliceous spicules of sponges belonging to the class Homoscleromorpha is unknown (Maldonado and Riesgo, 2007). In this scenario,

different proteins in the three sponge classes have evolved independently to construct an axial filament that can precipitate silica to form the siliceous spicules. However, some sponges belonging to the class Demospongiae, have microsclere siliceous spicules (<100 µm) that do not have an internal axial filament (Uriz et al. 2003). It is likely that there is an independent mechanism and protein(s) (not silicatein) responsible for the formation of these microsclere structures. The formation of the silica wall in diatoms is produced by different silaffins isoforms (Poulsen et al. 2003). The "silaffins" are small peptides (15 and 18 aminoacid residues) containing up to four lysine residues that can precipitate silica (Kröger et al. 2001; Kamalov et al. 2018). The absence of an axial filament in the cell wall of diatoms and in the microsclere spicules in some demosponge species suggest that the formation of a proteinaceous core as a template, is not necessary for the formation of siliceous structures in these organisms.

Review of methodologies used to study the expression, localization and characterization of silicateins

During the course of my PhD, I attempted to isolate the axial filament (silicatein protein) from the sponge *H. indistincta,* through the degradation of the siliceous spicules employing Hydrofluoric acid (HF) as described in Shimizu et al. (1998). The purpose of this technique was to identify the number of silicatein variants that are present in the axial filament (using SDS-PAGE) and also to employ the isolated protein as a template for the condensation of silica from the reaction with T.E.O.S. (Shimizu et al. 1998). However, I was not able to isolate the protein and it seems that the axial filament was destroyed when I carried out this technique. The isolation of the axial filament employing HF acid was successfully done for

the demosponges *T. aurantium, Petrosia ficiformis* and *Lubomirskia baicalensis* (Shimizu et al. 1998; Pozzolini et al. 2004; Kaluzhnaya et al. 2007).

Shimizu et al. (1998) identified three silicateins (alpha, beta and gamma) in the demosponge *T. aurantium* from the isolated axial filament. However, I found six silicateins in the genome of *Tethya wilhelma* (Chapter 3) a related species of *T. aurantium.* It is likely that these two species should have the same number of silicateins because they are closely related and have the same spicule categories. It is possible that some silicatein variants were lost using the HF technique in *T. aurantium* and a further sequencing of the transcriptome or genome from this species will corroborate whether or not there are more than three silicateins.

There are several silicatein variants in the transcriptomes of marine haplosclerids and I was interested to determine the localization of each of these variants in the tissue (protein level) of a particular species using an immunohistochemistry assay (IHC). This technique was employed to localize the silicatein alpha protein in the tissue of *S. domuncula* based on an antigen reaction with a monoclonal antibody from this protein (Müller et al. 2005). In this latter study, the authors showed that the localization of this protein was expressed inside the cells, inside the spicules (axial filament) and within the mesohyl. The amino acid sequence of this silicatein variant is very similar to the silicatein beta from the same species (Chapter 3) and it is likely that the antibody of the silicatein alpha could react against other variants (e.g. silicatein beta) from the same species (cross-reaction). Currently, there is one commercial silicatein alpha from *S. domuncula* that can localize the silicatein protein in the tissue of any demosponges producing these genes. For instance, Belikov et al. (2005) localized the silicatein alpha protein in the tissue of the freshwater sponge *L. baicalensis* employing an IHC assay with an antibody reaction from the silicatein alpha of *S. domuncula*. Therefore, the IHC

technique is not specific and not suitable to localize the expression of one particular silicatein protein in the tissue of a particular species that has multiple variants. The IHC technique might localize the silicatein protein in the tissue of a particular species but it will not determine which of the variants is expressed, and this was the main reason that I did not carry out this methodolody.

In addition, I wanted to identify the expression patterns of each of the silicatein variants in *H. indistincta* (mRNA level) using Whole Mount *in situ* Hybridization (W.I.S.H.). This technique has been successfully employed to localize the expression levels of each of the silicatein variants that were present in the freshwater sponge *E. fluviatilis* (Mohri et al. 2008). The authors demonstrated that four variants were expressed during the formation of megasclere spicules and two additional variants during the formation of gemmulosclere spicules. While this technique is specific for the exact variant under study, this technique is time demanding and requires a lot of expertise and unfortunately I had no more available time to carry out this methodology with the species I was working. In contrast, the mRNA expression levels of different silicatein genes can be detected using RT-qPCR at different developmental stages or parts of the sponge as I determined in chapter 4.

Conclusions and future directions

Spicule formation and skeleton construction have been investigated in few sponge species. This lack of study is due to the difficulty of the topic and different techniques that are necessary to carry out this investigation. Currently, the exact roles of the different silicatein variants are unknown, as are the process of shaping of the spicules and the mechanisms of skeleton construction in marine haplosclerids and other demosponges. In this thesis, I tried to

investigate certain elements of the skeleton (chemical composition of spicules, evolution of the silicatein genes and expression levels) in selected marine haplosclerids that could have a phylogenetic signal. Here I demonstrated for the first time that there is a high diversity of silicatein genes in demosponges bearing siliceous spicules and that the transcriptomes and genomes of marine haplosclerids contain a high diversity of silicateins of the CHN and C/SQN types and they lack silicatein of the SHN II type and the silintaphin gene. I showed that silicatein genes were differentially expressed at distinct developmental stages producing spicules in *H. indistincta*. In addition, marine haplosclerids have different silicatein genes that are probably differentially expressed at different developmental stages and across species, but the majority of these species produce megasclere spicules in a single size category. The data presented in this thesis suggests that the genes responsible for spicule formation in species belonging to Haplosclerida are somewhat different from the remaining species belonging to heteroscleromorpha. This thesis supports the previous molecular topology based on mitochondrial and ribosomal data, that Haplosclerомorpha should be considered as an independent subclass of Demospongiae and not included as an order within Heteroscleromorpha (Lavrov et al. 2008; Redmond et al. 2013; Morrow and Cardenas, 2015).

Future work is required in other aspects of skeleton construction, such as the identification of gene regulatory process (promoters), collagen and spongin genes, transcription factors and the cells responsible for skeleton construction in selected species. Further experiments are required to investigate the impact on the skeleton in a particular species when a silicatein gene is knocked-down. In addition, the influence of the increase of silica on the skeletal architecture in selected species should be investigated and additional work is required to

produce recombinant silicateins for further biotechnological applications, biochemical assays and X-ray crystallography.

References

Armirotti, A., Damonte, G., Pozzolini, M., Mussino, F., Cerrano, C., Salis, A., Benatti, U., Giovine, M. (2009). Primary structure and post-translational modifications of silicatein beta from the marine sponge *Petrosia ficiformis* (Poiret, 1789). Journal of proteome research, 8(8), 3995-4004.

Belikov, S. I., Kaluzhnaya, O. V., Schöder, H. C., Krasko, A., Müller, I. M., Müller, W. E. (2005). Expression of silicatein in spicules from the Baikalian sponge Lubomirskia baicalensis. Cell biology international, 29(11), 943-951.

Carballo, J. L., Aguilar-Camacho, J. M., Knapp, I. S., Bell, J. J. (2013). Wide distributional range of marine sponges along the Pacific Ocean. Marine Biology Research, 9(8), 768-775.

De Voogd, N. J., van Soest, R. W. M. (2002). Indonesian sponges of the genus Petrosia vosmaer (Demospongiae: Haplosclerida). Zoologische Mededelingen, 76, 193-209.

de Weerdt, W. H. (1986). A systematic revision of the north-eastern Atlantic shallow-water Haplosclerida (Porifera, Demospongiae): 2. Chalinidae. Beaufortia, (6), 81-165.

de Weerdt, W. H. (2002). Family Chalinidae Gray, 1867. In: Systema Porifera (pp. 852-873). Springer, Boston, MA.

Desqueyroux-Faúndez, R. (1999). Convenient genera or phylogenetic genera? Evidence from Callyspongiidae and Niphatidae (Haplosclerida). Memoirs Queensland Museum, 44, 131–146.

Desqueyroux-Faúndez, R., Valentine, C. (2002). Family Petrosiidae Van Soest, 1980. In Systema Porifera (pp. 906-917). Springer, Boston, MA.

Hill, M.S., Hill, A.L., Lopez, J., Perterson, K.J., Pomponi, S., Diaz, M.C., Thacker, R.W., Adamska, M., Boury-Esnault, N., Cárdenas, P., Chaves-Fonnegra, A., Danka, E., De Laine, B., Formica, D., Hajdu, E., Lobo-Hajdu, G., Klontz, S., Morrow, C.C., Patel, J., Picton, B., Pisani, D., Pohlmann, D., Redmond, N.E., Reed, J., Richie, S., Riesgo, A., Rubin, E., Russell, Z., Rützler, K., Sperling, E.A., di Stefano, M., Tarver, J.D., Collins A.G. (2013) Reconstruction of family level phylogenetic relationships within Demospongiae (Porifera) using nuclear encoded housekeeping genes. PLOS One, 8(1), e50437.

Fairhead, M., Johnson, K. A., Kowatz, T., McMahon, S. A., Carter, L. G., Oke, M., Liu, H., Naismith, J.H., van der Walle, C. F. (2008). Crystal structure and silica condensing activities of silicatein α–cathepsin L chimeras. Chemical Communications, (15), 1765-1767.

Gauthier A (2015). Analysis of silicatein gene expression and spicule formation in the demosponge Amphimedon queenslandica. MS thesis. The University of Queensland, 84 pp.

Hooper, J. N., Van Soest, R. W. (2006). A new species of *Amphimedon* (Porifera, Demospongiae, Haplosclerida, Niphatidae) from the Capricorn-Bunker Group of Islands, Great Barrier Reef, Australia: target species for the ‘sponge genome project’. Zootaxa, 1314, 31-39.

Kamalov, M., Hajradini, A., Rentenberger, C., Becker, C. F. (2018). N-terminal residues of silaffin peptides impact morphology of biomimetic silica particles. Materials Letters, 212, 114-117.

Kamenev, D. G., Shkryl, Y. N., Veremeichik, G. N., Golotin, V. A., Naryshkina, N. N., Timofeeva, Y. O., Kovalchuk, S.N., Semiletova, I.V., Bulgakov, V. P. (2015). Silicon Crystals Formation Using Silicatein-Like Cathepsin of Marine Sponge Latrunculia oparinae. Journal of nanoscience and nanotechnology, 15(12), 10046-10049.

Kaluzhnaya, O. V., Belikova, A. S., Podolskaya, E. P., Krasko, A. G., Müller, W. E. G., Belikov, S. I. (2007). Identification of silicateins in freshwater sponge *Lubomirskia baicalensis*. Molecular Biology, 41(4), 554-561.

Kröger, N., Deutzmann, R., Sumper, M. (2001). Silica-Precipitating Peptides from Diatoms The Chemical Structure Of Silaffin-1A from Cylindrotheca Fusiformis. Journal of Biological Chemistry, 276(28), 26066-26070.

McCormack, G. P., Erpenbeck, D., Van Soest, R. W. M. (2002). Major discrepancy between phylogenetic hypotheses based on molecular and morphological criteria within the Order Haplosclerida (Phylum Porifera: Class Demospongiae). Journal of Zoological Systematics and Evolutionary Research, 40(4), 237–240.

Maldonado, M. (2006). The ecology of the sponge larva. Canadian Journal of Zoology, 84(2), 175–194.

Maldonado, M., Carmona, M. C., Uriz, M. J., Cruzado, A. (1999). Decline in Mesozoic reef-building sponges explained by silicon limitation. Nature, 401(6755), 785.

Maldonado, M., Riesgo, A. (2007). Intra-epithelial spicules in a homosclerophorid sponge. Cell and Tissue Research, 328(3), 639–650.

Mohri, K., Nakatsukasa, M., Masuda, Y., Agata, K., Funayama, N. (2008). Toward understanding the morphogenesis of siliceous spicules in freshwater sponge: Differential mRNA expression of spicule-type-specific silicatein genes in Ephydatia fluviatilis. Developmental Dynamics, 237(10), 3024-3039.

Müller, W. E., Rothenberger, M., Boreiko, A., Tremel, W., Reiber, A., Schröder, H. C. (2005). Formation of siliceous spicules in the marine demosponge *Suberites domuncula*. Cell and tissue research, 321(2), 285-297.

Nakayama S, Arima K, Kawai K, Mohri K, Inui C, Sugano W, Koba H, Tamada K, Nakata YJ, Kishimoto K, Arai–Shindo M, Kojima C, Matsumoto T, Fujimori T, Agata K, Funayama N (2015) Dynamic transport and cementation of skeletal elements build up the pole–and–beam structured skeleton of sponges. Current Biology 25(19) 2549-2554.

Poulsen, N., Sumper, M., Kröger, N. (2003). Biosilica formation in diatoms: characterization of native silaffin-2 and its role in silica morphogenesis. Proceedings of the National Academy of Sciences, 100(21), 12075-12080.

Pozzolini, M., Sturla, L., Cerrano, C., Bavestrello, G., Camardella, L., Parodi, A. M., Raheli, F., Benatti, U., Müller W.E.G., Giovine, M. (2004). Molecular cloning of silicatein gene from marine sponge *Petrosia ficiformis* (Porifera, Demospongiae) and development of primmorphs as a model for biosilicification studies. Marine biotechnology, 6(6), 594-603.

Raleigh, J., Redmond, N. E., Delahan, E., Torpey, S., van Soest, R. W., Kelly, M., McCormack, G. P. (2007). Mitochondrial Cytochrome oxidase 1 phylogeny supports alternative taxonomic scheme for the marine Haplosclerida. Journal of the Marine Biological Association of the United Kingdom, 87(6), 1577-1584.

Redmond NE, Morrow CC, Thacker RW, Diaz MC, Boury-Esnault N, Cárdenas P, Hajdu E, Lôbo-Hajdu G, Picton BE, Pomponi SA, Kayal E, Collins AG (2013). Phylogeny and systematics of Demospongiae in light of new small-subunit ribosomal DNA (18S) sequences. Integrative and comparative biology, 53,388–415.

Redmond NE, Raleigh J, van Soest RW, Kelly M, Travers SA, Bradshaw B, Vartia S, Stephens K, McCormack G.P. (2011). Phylogenetic relationships of the marine Haplosclerida (Phylum Porifera) employing ribosomal (28S rRNA) and mitochondrial (cox1, nad1) gene sequence data. PLoS One, 6(9), e24344.

Redmond, N. E., Van Soest, R. W. M., Kelly, M., Raleigh, J., Travers, S. A. A., McCormack, G. P. (2007). Reassessment of the classification of the Order Haplosclerida (Class Demospongiae, Phylum Porifera) using 18S rRNA gene sequence data. Molecular Phylogenetics and Evolution,43, 344-352.

Sandford, F. (2003) Physical and chemical analysis of the siliceous skeletons in six sponges of two groups (Demospongiae and Hexactinellida). Microscopy Research and Technique, 62(4), 336–355.

Shimizu, K., Amano, T., Bari, M. R., Weaver, J. C., Arima, J., Mori, N. (2015). Glassin, a histidine-rich protein from the siliceous skeletal system of the marine sponge Euplectella,

directs silica polycondensation. Proceedings of the National Academy of Sciences, 112(37), 11449-11454.

Shimizu, K., Cha, J., Stucky, G. D., Morse, D. E. (1998). Silicatein α: cathepsin L-like protein in sponge biosilica. Proceedings of the National Academy of Sciences, 95(11), 6234-6238.

Shkryl, Y. N., Bulgakov, V. P., Veremeichik, G. N., Kovalchuk, S. N., Kozhemyako, V. B., Kamenev, D. G., Semiletova, I.V., Timofeeva, Y.O., Scchipunov, Y.A., Kulchin, Y. N. (2016). Bioinspired enzymatic synthesis of silica nanocrystals provided by recombinant silicatein from the marine sponge *Latrunculia oparinae*. Bioprocess and Biosystems Engineering, 39(1), 53-58.

Sperling, E. A., Robinson, J. M., Pisani, D., Peterson, K. J. (2010). Where's the glass? Biomarkers, molecular clocks, and microRNAs suggest a 200-Myr missing Precambrian fossil record of siliceous sponge spicules. Geobiology, 8(1), 24-36.

Thacker, R. W., Hill, A. L., Hill, M. S., Redmond, N. E., Collins, A. G., Morrow, C. C., Spicer, L., Carmack, C., Zappe, M.E., Pohlmann, D., Hall, C., Diaz, M.C., Bangalore, P.V. (2013). Nearly complete 28S rRNA gene sequences confirm new hypotheses of sponge evolution. Integrative and Comparative Biology, 53(3), 373-387.

Uriz, M. J., Turon, X., Becerro, M. A., Agell, G. (2003). Siliceous spicules and skeleton frameworks in sponges: origin, diversity, ultrastructural patterns, and biological functions. Microscopy research and technique, 62(4), 279-299.

Van Soest, R. W. M. (1980). Marine sponges from Curaçao and other Caribbean localities Part II. Haplosclerida. Studies on the Fauna of Curaçao and other Caribbean Islands, 62(1), 1–173.

Van Soest, R. W., Hooper, J. N. (2002). Order Haplosclerida Topsent, 1928. In: Systema Porifera (pp. 831-832). Springer, Boston, MA.

Wulff, J. (2012). Ecological interactions and the distribution, abundance, and diversity of sponges. Advances in Marine Biology, 61, 273–344.

Zhou, Y., Shimizu, K., Cha, J. N., Stucky, G. D., Morse, D. E. (1999). Efficient catalysis of polysiloxane synthesis by silicatein α requires specific hydroxy and imidazole functionalities. Angewandte Chemie International Edition, 38(6), 779-782.

Appendices

Appendix 1. List of the complete silicateins downloaded from Genbank employed in this study.

Sequence name	Accesion number	Authority
Petrosia_ficiformis	AAO23671.1	Pozzolini et al. 2004
Ephydatia_fluviatilis	BAE54434.1	Funayama et al. 2005
Halichondria_okadai_partial	BAB86343.1	
Euplectella_aspergillum_partial	CBY80150.1	
Luborsmikia_baicalensis_partial	CAH10753.1	Kaluzhnaya et al. 2005
Ephydatia_fluviatilis_partial	CAJ44453.1	Müller et al. 2006
Latrunculia_oparinae_partial(B)	ACH48002.1	Veremeichik et al. 2011
LatrunculiaoparinaeA3_partial	ACH48001.1	Veremeichik et al. 2011
Latrunculia_oparinae_partial(A1A)	ACH47999.1	Veremeichik et al. 2011
Hymeniacidon_perlevis1_partial	ABM47424.1	
Mycale_phyllophyla_alpha	AND80742.1	
Tethya_aurantium_alpha	AAC23951.1	Shimizu et al. 1998
Tethya_aurantium_beta	AAF21819.1	
Latrunculia_oparinae_A2	ACH48000.1	Veremeichik et al. 2011
Latrunculia_oparinae_A1	ACG63793.1	Veremeichik et al. 2011
Suberites_domuncula_protein	CAC03737.1	Krasko et al. 2000
Tethya_aurantium_yellow_variant	CBY80149.1	
Tethya_aurantium_red_variant	CBY80148.1	
Lubomirskia_baikalensis_alpha4	ADQ74587.1	Kaluzhnaya et al. 2011
Lubomirskia_baicalensis_alpha3	ADQ74586.1	Kaluzhnaya et al. 2011
Lubomirskia_baicalensis_alpha2	ADQ74585.1	Kaluzhnaya et al. 2011
Spongilla_lacustris_alpha4	CAQ54052.1	
Spongilla_lacustris_alpha3(silicatein1)	**CAQ03432.1**	
Ephydatia_muelleri_alpha3	CAQ54047.1	
Ephydatia_muelleri_alpha2	CAQ54046.1	
Ephydatia_spn2_alpha4_partial	CAQ54050.1	
Ephydatia_spn2_alpha2_partial	CAQ54049.1	
Ephydatia_spn1_alpha4_partial	CAQ54045.1	
Geodia_cydoniuma_alpha	CAM57981.1	Müller et al. 2007b
Baikalospongia_intermedia_alpha1_partial	CAQ54043.1	
Hymeniacidon_perlevis_alpha	ABC94586.1	Cao et al. 2007
*Lubomirskia_baicalensis_alpha_*	CAI46306.1	Müller et al. 2007[a]
Suberites_domuncula_alpha	CAI46305.1	Müller et al. 2007[a]
Suberites_domuncula_beta	CAI46304.1	Müller et al. 2007[a]
Lubomirskia_baicalensis_a4	CAI91573.1	Müller et al. 2006[a]
Lubomirskia_baicalensis_a3	CAI91572.1	Müller et al. 2006[a]
Lubomirskia_baicalensisa3_(a2)	CAI91571.1	Müllet et al. 2006[a]
Lubomirskia_baicalensis_alpha	CAI43319.1	Müllet et al. 2006
Suberites_domuncula_beta	CAD67990.1	
Suberites_domuncula_beta	CAH04635.1	Schröder et al. 2005
Latrunculia_oparinae_cathepsin	ACH48003.1	Veremeichik et al. 2011
Ephydatia_fluviatilis_M3	BAG74344.1	Mohri et al. 2008
Ephydatia_fluviatilis_M2	BAG74343.1	Mohri et al. 2008
Ephydatia_fluviatilis_M4	BAG74345.1	Mohri et al. 2008
Ephydatia_fluvitilis_G1	BAG74346.1	Mohri et al. 2008
Ephydatia_fluviatilis_G2	BAG74347.1	Mohri et al. 2008
Aulosaccus_silicatein_like	ACU86976.1	Veremeichik et al. 2011b

Appendix 2. List of the sequences deleted in the alignment to generate a) the tree minus short sequences and b) the tree minus cathepsins and sequences with long branches.

a	b
S. carteri_3	*E. muelleri_8*
T. anhelens_3	*E. fluviatilis_2*
S. carteri_2	*CathepsinL_Amphimedon1*
E. muelleri_2	*CathepsinL_Haliclonaamboinensis4*
Lubomisrkia_baicalensis_partial_CAH10753.1	*CathepsinL_Haliclonaamboinensis5*
Baikalospongia_intermedia_alpha1_partial_CAQ54043.1	*CathepsinL_Haliclonasimulans9*
S. lacustris_5	*CathepsinL_Amphimedon3*
Ephydatia_fluviatilis_partial_CAJ44453.1	*CathepsinL_Amphimedon2*
Ephydatia.sp_alpha4_partial_CAQ54045.1	*H.indistincta_5*
Ephydatia_nsp2_alpha2_partial_CAQ54059.1	*Lubomisrkia_baicalensis_a3_CAI91571.1*
S. lacustris_3	*Ephydatia_muelleri_alpha2_CAQ54046.1*
E. fluviatilis_6	*Lubomisrkia_baicalensis_a4_CAI91573.1*
S. carteri_1	*Lubomisrkia_baicalensis_alpha_CAI46306.1*
Latrunculia_oparinae_partialA1A_ACH47999.1	*Ephydatia_muelleri_alpha3_CAQ54047.1*
Hymeniacidon_perlevis1_partial_ABM47424.1	*Lubomisrkia_baicalensis_alpha3_ADQ74586.1*
Cinanchyrella_sp1	*Latrunculia_oparinae_A1_ACG63793.1*
Latrunculia_oparinae_partialB_ACH48002.1	*C. concéntrica_5*
Halichondria_okadai_partial_BAB86343.1	*E. muelleri_8*
Euplectella_aspergilum_partial_CBY80150.1	
C. concentrica_6	
Latrunculia_oparinae_partial_A3_ACH48001.1	

Appendix 3. Silintaphin proteins found in the demosponge transcriptomes

Pseudospongorites suberitoides

>MSDSELACVYSALILHDAEINITAEKINTLISAAAVTVEPIWPNLFARALEGKDIGALISNVGSGA
AAAAAAPSAGGAATEAGDKEEKKEEKKKEVKQKPKKQPKAAPDYRTSKAGWVQKQGLLFKK
WQRQYMSLDEEDSVLRWWKTENRTSSDGALFMKYCADVSEPKAEATTTWPDDTADRCFVICSP
YRAYFLVAESPEEKNDWKEKLLAAKEKYNTEGRKLITTALISVEGIKASIDSGAADLEKTTKKEGI
VEEKKTEKTEETAPAEGETAPTETEGAAAAVTVEVEVEAQPEEPPKEETPAEEPPKEETPAEEPPK
EETPAEEPPKDETPAAEGGEETKAED

Mycale phyllophyla

>MSEEAAAPKAVEETPTEDTAKTEETKTEETPQKAEDTPAADEGASAEKPADDKPSEEDKSAEDK
PADDKPTEDKPAEDKPEAEATEGEQDKNATAEVEVAVAEGGEAAAGEGDKAEKKSKKKEKPPK
AEKKEKPARVEKPPPDYRTVHSGYVQKKGGLLKRWGRSFLSLDEESSVLRVWKNEDRKSSESIL
MHMNTCVGVSEGSDDTAWPADTAGRCFVLHGQKDIQLIAETEDQRKEWMEKLQEAKDKHNPD
GVRKEPTEGFLKKIKKSVKRPQRPSETKKEEGAEAAEGETKPAEEGGEAKAEEGDKPKEEGEAA
AAAATTETKTEGEVTVEVQVEKDEASKDEAPKEDTPKEEPAPKSEDESPKPADESEATESPEPVA
AADPPKPDEPEPEQKPDESSKQAEPEPAQEPESPKPAEDKPSEQEASSEETKEPEPEESTTEEPSTSE
AATEEPSKTEDEPAAAENED

Ephydatia fluviatilis

>MSQETPEQPTMEASEVKTEETKMEPKPEEPKKEEPTAEVTKTDEPPKPEEPKPEEGAPKAAEGA
TATGEGTKPTRKNTKKAKEPKPQPPPVDYHTIMSGYVEKKGKVFGFSRYWMALDEDGKIVHWY
KTEERGSLDCSAHMDQCNAVSEASDQYHTKWPEQTADRAFVIDTRSRVFYVVAETAEKRG

Spongilla lacustris

>MEAKPEEPKVEEPKAEAPKVEEPPKTEESKPQEVTPAEPQVTEDAAATGLETKQKRKSVKKQKE
PKPPVEYHNIMSGYVEKKGKVFGFGRYWMALDENGMVVRWYKTEERGSIDCTAHMDQCNAV
AEPSDQYTVRWPEGTSDRAFVIDTRDRRFYVVAESAEKRSEWIQKLKEAKEKFTPKEEPKPEPAA
ATPGTAEGTPAATTEGGVASGTTEGGVASGTTEGGVASDTTEGAGKNTLSEEPSAGNTQPATEPA
PEMKNEGESEVAKTE

Tethya wilhelma

>MSEEVQPTDGQPPTDATTEETPKEELVATETPASTETKPDDEPAVTEVTEVTEVTEVTEVTEVTE
QPAAEGQSDEKPKEEEAPKKKKKEEKPKEEKKKKEKPKKAAKPAKPPPDYKTVKASYVQKQGL
FFKSFKRYYMTLDEEGRTLRWYKTEERKSSEGALYMKFCAEVTAPIDKYPARWPEGTQERALVV
CSSNRAYYVVCETVEERDDWIAKLTEAKQKYSDESLEVKGTALFSVGSIKRALKKSERDTNKTLE
EEGVTEKKEEVSKTEETTTEEAAATPAAEQPKTEEEPKAEGGAVTVEVEVSEQPKEEEPKAEEPP
AEEPKTEEPPAEEPKTEEPPAEETPAAEEPTTEDPP

Tedania anhelens

>MKYCTEVTEPIASATTTWPDNTADRCFVVCSASTKYFLVAETVEEKNEWLAKLKECREKFGPT
PEEAAAQPTGFVGKLKASIKKKPREPKAEDEAAAEPKAEGGEAKAEGGEEPKAEGEATVEVQVE

VEVDKKDEEEAAPKDEGASGEEPAAAEAEAAAEDKKEEEEKKEEEEKTEPKEEPAAAAEGGEAK
ED

Cymbastela concentrica

>MAEPAEPQVEPQTQEEPPKTEDQPTEQKQQEQEEPKTEEPKAEGGEEPKKEEAEAPKEEPVKAK
PVDYHTVKAGWVQRRGWLLKRWNKMWMSLDDDGAVLKWFKKENHGGADGAVNLRDVTGIT
DPNPDLPANWPADTDNRSFIVTSVKRNYFIVAETADEKNDWVEKLKEAKEKADKLKAEEEEEAR
RQAEEKARQKAEEEARQKAEAEAKAKAEAEAKAEAEAKAKAEAEEKAKAEAEEKAKAEGEGE
AQADTKAEPEEKPEEAVEGEPKKEEEAPKEPEPQAEPEXXXX

Scopalina sp

>MKQGYLLKKWSRVYMCLDEGGKVLRFYKAEDRKSCDSQLYMNYCVEVLCRSPDYTANWPPN
TEEKRCVTLISPSRAFYLIAESEEDQKEWMEKLSVAKDKNKGEGIKLISTKYVSVEAIKAAFRSGA
ASFEEGTEKTLEEHGTSTKKIESSVDKAVEEVKTDADKVLAKEGTSTDQISHDLDRAGKEIDSDIK
KVEEEVKEDVKAVEKEVEKDVKAVEKEVEKEEEKVTSEVD

Stylissa carteri

>MQKLNAAKDEFNKEGRKVISTALISIEAATTMLQATADQTEAETNKTLGEQGTTTTQIEKDLNK
AADDTQKEVDKELKKDESAVVK

Ephydatia muelleri

>MSQEASEQPTVEAPEVKTEPNAEEPKKEESIAEGPKDEPPKTEEPKPEEPKPTEEAPKPTEVTAEA
PKPTEETPEAPKAAEGAAATGEGSKPTRKNTKKAKEPKPQPPPVDYHSVMSGYVEKKGKLFGFS
RYWMSLDEDGKVARWYKTEERGSVDCSAHMDQCNAVSEPSDQYHVRWPEQTADRAFVIDTRS
RVFYVVAETAEKRGEWIQKLREAKEKYTPKEEPKPEPAAPAPTTTEGTPAATTEGTPAATTEGTP
AAATTEGAAASGTTEEASGTTEAVGTDTMAEKPQEPAAEASQPAAESAPETTKSE*

Latrunculia apicalis

>MTLDEEGSVLRWWKNEDRKSNDSGVYMKFCLSVSEPLADATTTWPADTDPDRCFVVRTTKRN
FFLVAENAEEKSDWIEKIKEAKEKFGPEVEETKPSQGLLGRLKASIKKPKKEEEKGEEKAEEKTEE
QGEDGEAAAAEPKTEAEVTVEVQVEGGETEAAAKTEDKPEESGEAAAAPTEDKKEDDAPAEDK
QEEATPKKETAAESVPAEDNVEEPAAAEGGGETKDE

Kirkpatricia variolosa

>MSLEEEGKVLRWWKTEERKSLDTGVFMQFCLGVTDPVAEATTTWPDDTPDRCFVVRGTKRDF
FLVAPSIEEKKDWMEKLKEARDKYGPEDTTKQPGFLGKLKASMKKPAKAKEPEKTEEATGGEA
AAAEGGEPKAEAEGEVTVEIQVEVSEQAEAKTEEAPQEATPTDAPAEENKEEKKEEEPAADKEEP
ANKEEPAAAESGEAKDE

Appendix 4. Glassin proteins found in the hexactinellid transcriptomes

Rosella_fibulata

>MPSSSTAPSSPKLPPHPKPGPKHESLDLENDSSDEDEQIELTANPDSWTGNANVVYFDFVAGFAR
PSSNDFRFNSVITELCKQFPGLIGSGLYLGGKDLGARLAVEAFEEIRASSNLTELNLKGFLFSLFSPE
DAGRSELIEDITLILNNEQFKQQLGRERDAIWYPYVFNSLRNDQFSYERILKFAEKNSGKYTSIITG
RDISVGDLKRLTN

Sympagella_nux

>MGGKNLGARLAAEAFEEIRDSNFTDLNLKGFVFSLFSEEGSRKSEFVEDVTLVLNNEAFKKQLG
REESDIWYPYLFDSLVNDQFSYEKILKFVEMNSAEFNTIVSGRDITVDDLKQLSK

Aphrocallistes vastus

>MQNSEEIPIQCVASKLCKMHPTLFAHNLYFGGKNFGSNIAASLVENMQYSNFNDMNVKGLVLS
LFVPEDVEKSEFTEDVEFILNEPRFQKELGLPSEVWYPDFPESSSQTQFSYELLLKFVQKNVKESST
IVYGRDISLNDLKSLID

Appendix 5. Molecular phylogenetic tree from the complete dataset showing the relationships of the six major clades (part 1; The SHNII clade is collapsed for clarity). The tree drawn is from Mr. Bayes which was congruent with the tree generated from PhyML. The trees presented are those reconstructed using Mr. Bayes which were congruent with those from PhyML Support on the branches represents Bayesian posterior probability/maximum likelihood bootstrap proportions.

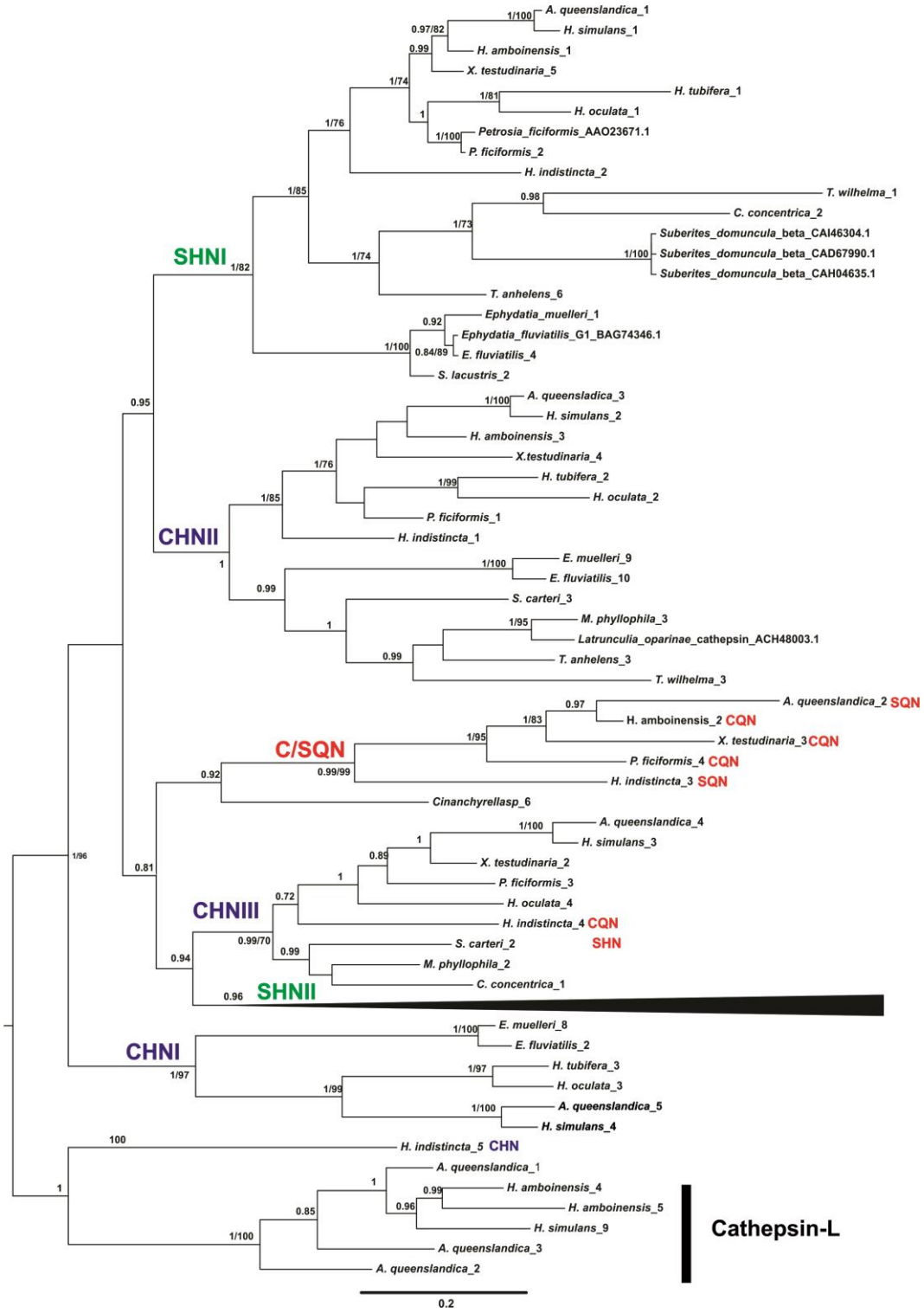

Appendix 6. Molecular phylogenetic tree from the complete dataset showing the relationships of the six major clades (part 2; all clades aprat from SHNII chave collapsed for clarity). The tree drawn is from Mr. Bayes which was congruent with the tree generated from PhyML. The trees presented are those reconstructed using Mr. Bayes which were congruent with those from PhyML Support on the branches represents Bayesian posterior probability/maximum likelihood bootstrap proportions.

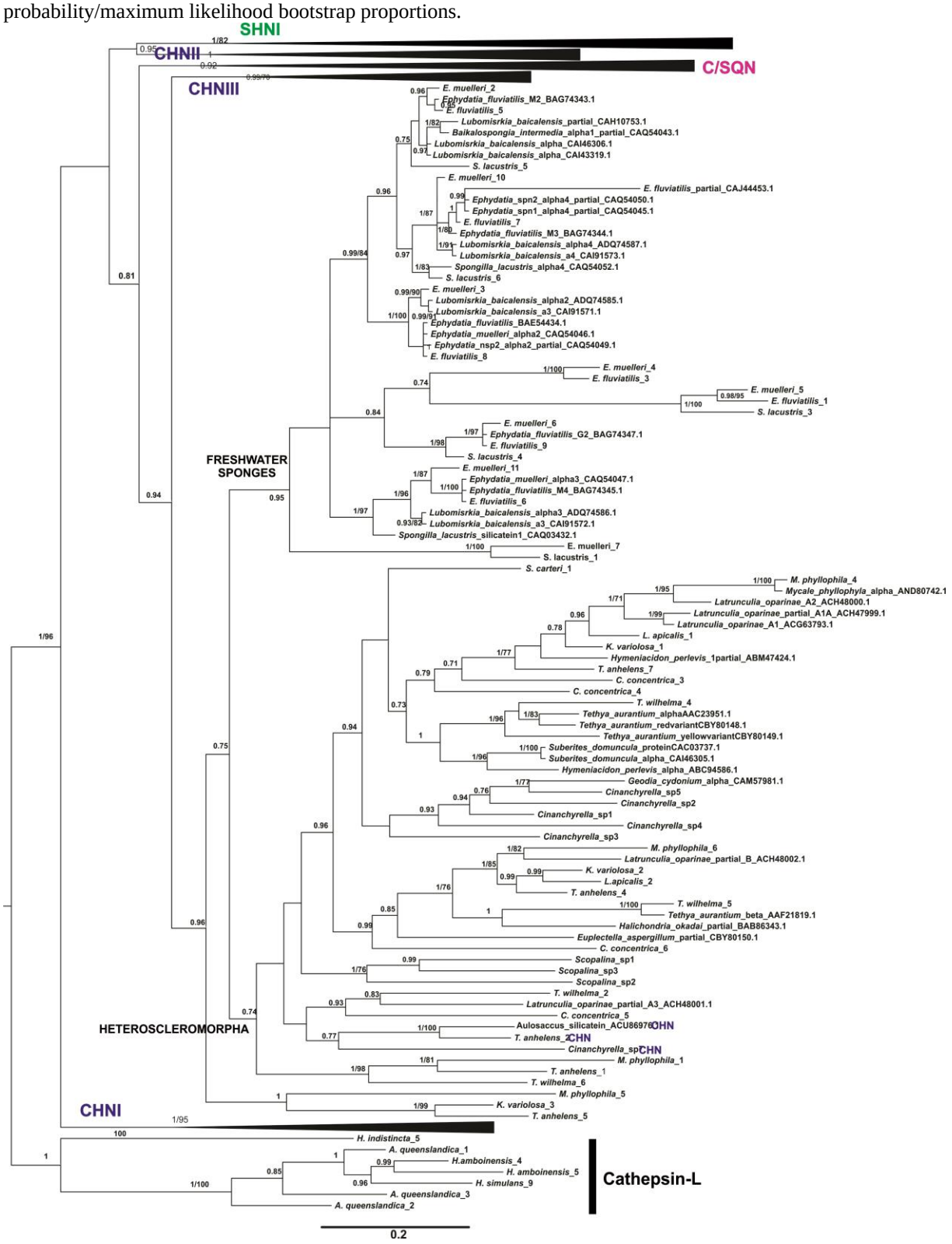

Appendix 7. Molecular phylogenetic tree from the second dataset (all shorts sequences removed) showing the relationships of sequences across six major clades (part 1: The SNHII clade is collapsed for clarity). The tree drawn is from Mr. Bayes which was congruent with the tree generated from PhyML. The trees presented are those reconstructed using Mr. Bayes which were congruent with those from PhyML Support on the branches represents Bayesian posterior probability/maximum likelihood bootstrap proportions.

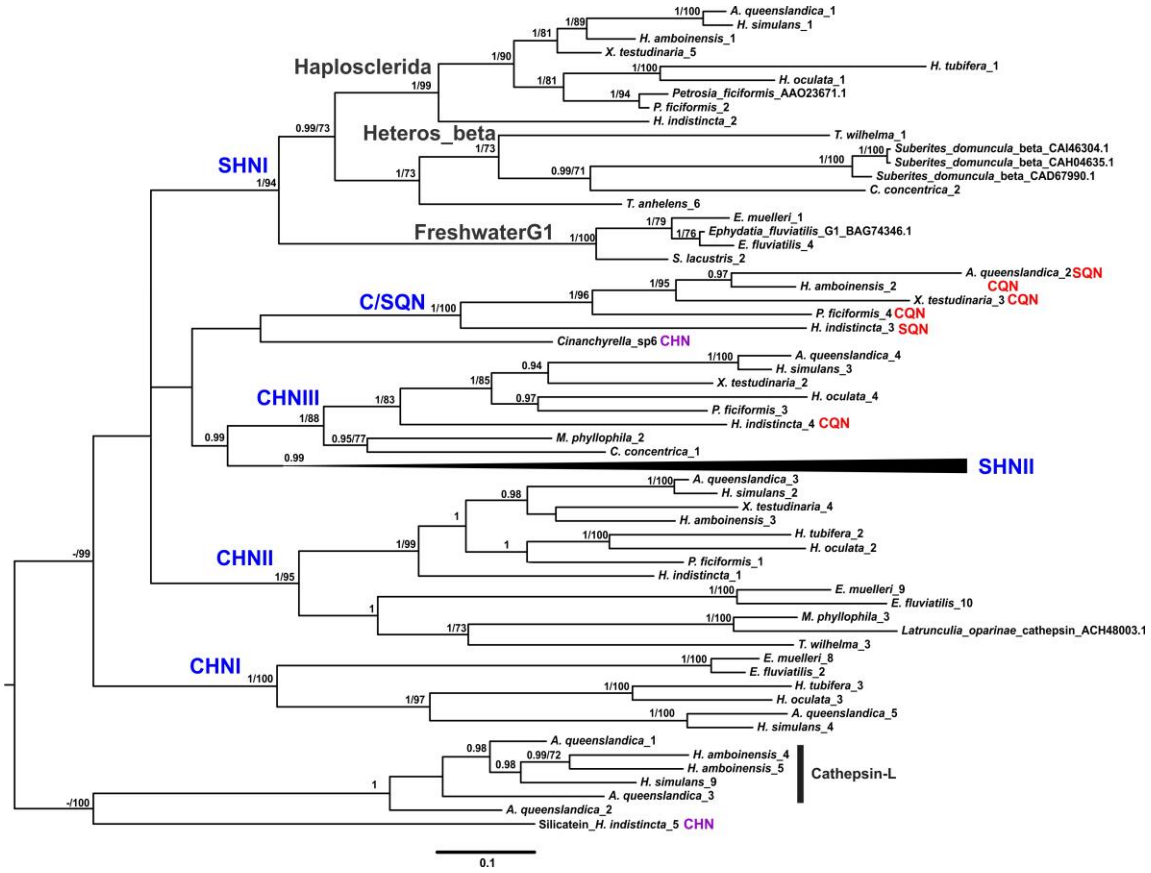

Appendix 8. Molecular phylogenetic tree from the second dataset (all shorts sequences removed) showing the relationships of sequences across six major clades (part 2: all clades apart from SHNII are collapsed for clarity). The tree drawn is from Mr. Bayes which was congruent with the tree generated from PhyML. The trees presented are those reconstructed using Mr. Bayes which were congruent with those from PhyML Support on the branches represents Bayesian posterior probability/maximum likelihood bootstrap proportions.

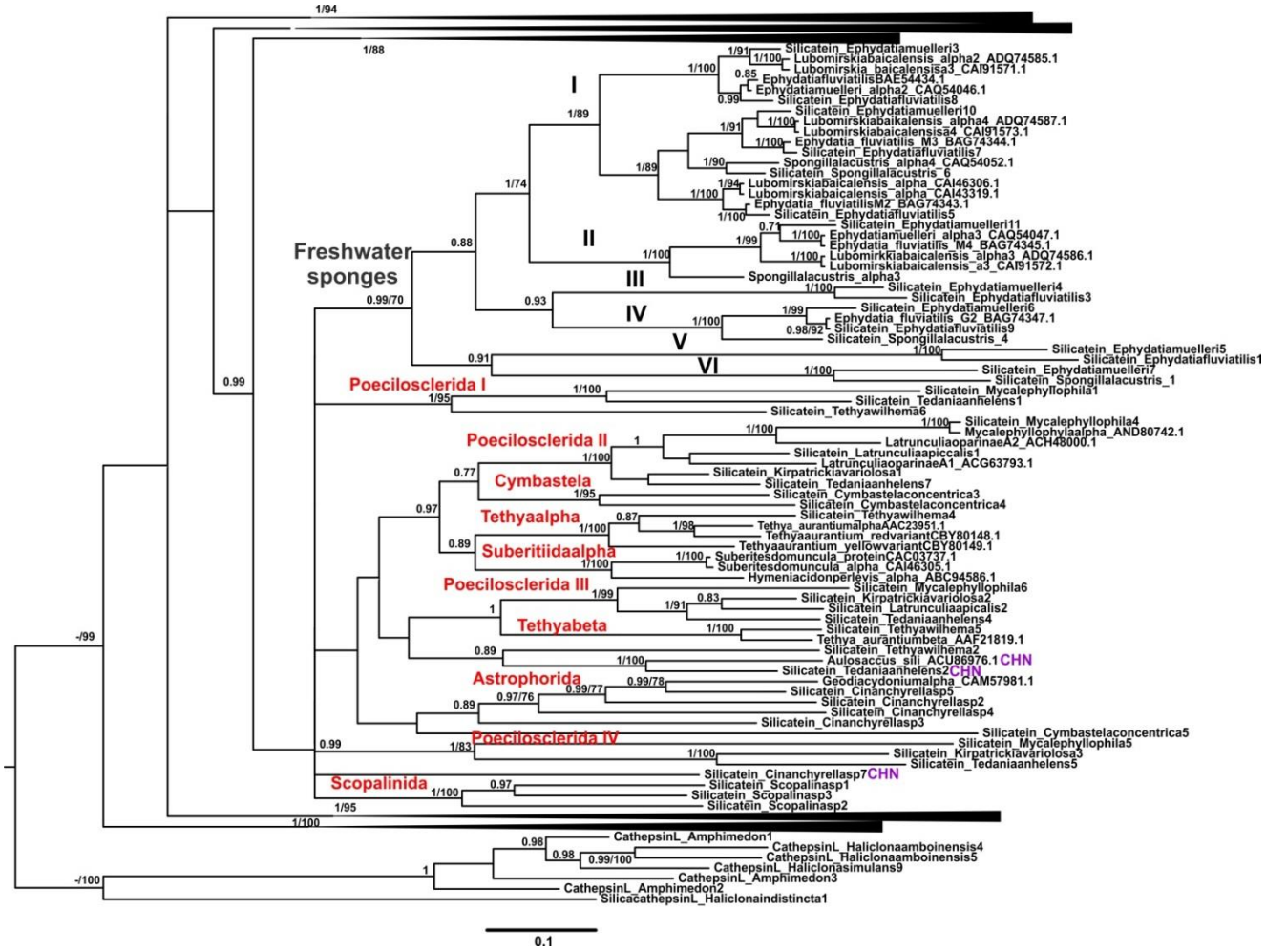

Appendix 9. Conserved amino acid motifs of all the silicatein genes. The star above indicates the amino acids forming the active site. The number below indicates the position in the alignment.

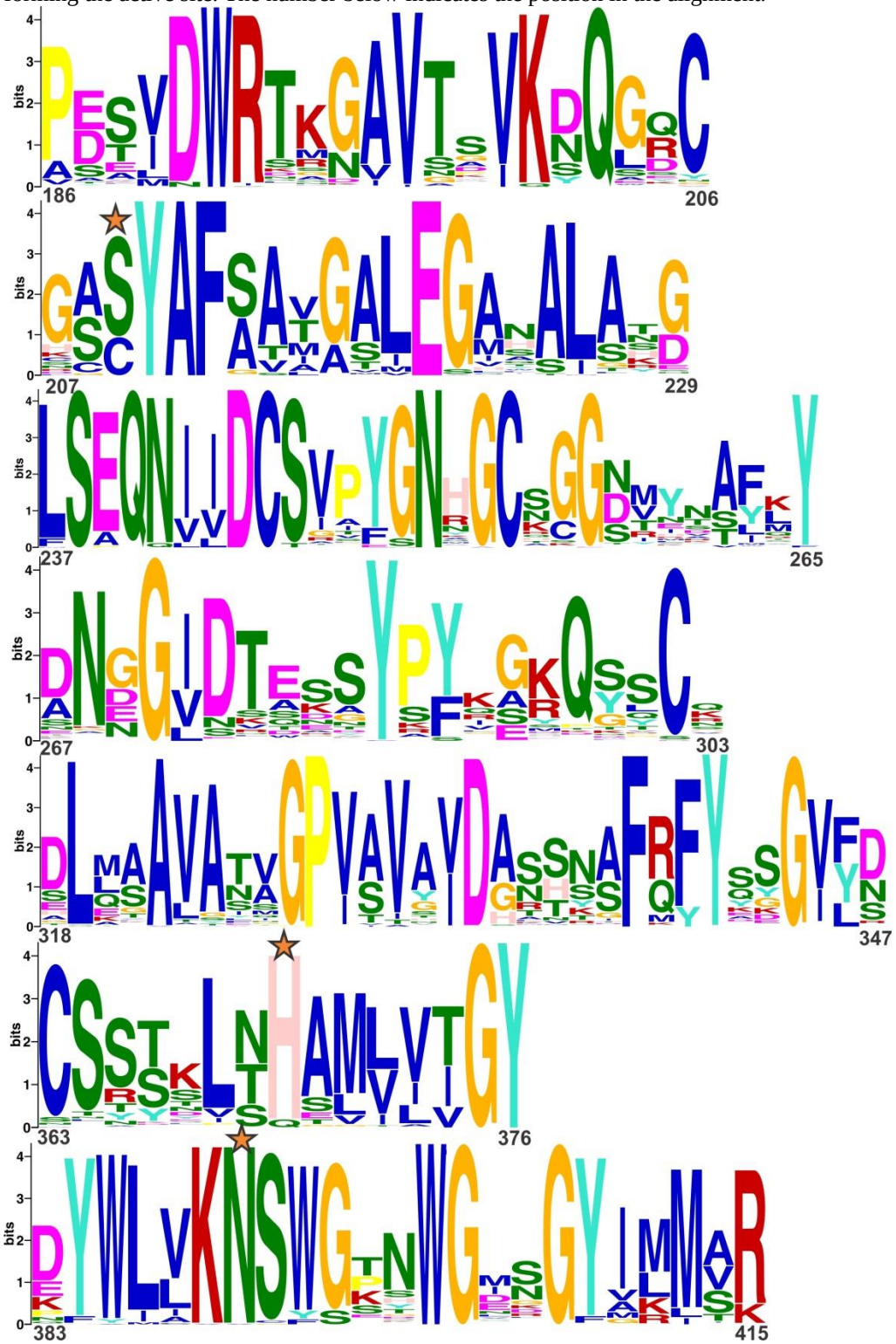

Appendix 10. Conserved amino acid motifs of all the silicatein genes of cladeSHNI. The star above indicates the amino acids forming the active site. The number below indicates the position in the alignment.

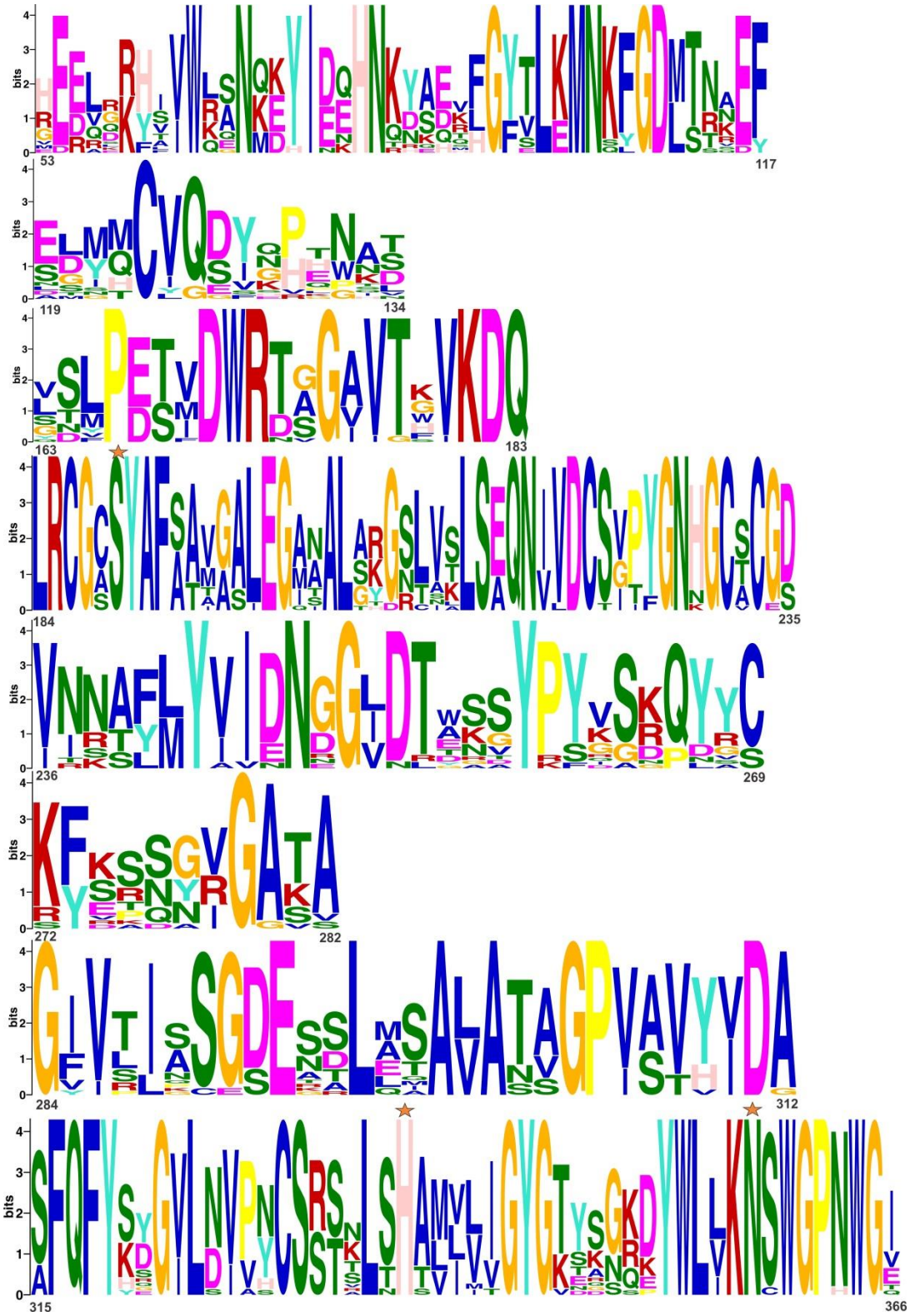

Appendix 11. Conserved amino acid motifs of all the silicateins of clade SHNII. The star above indicates the amino acids forming the active site. The number below indicates the position in the alignment.

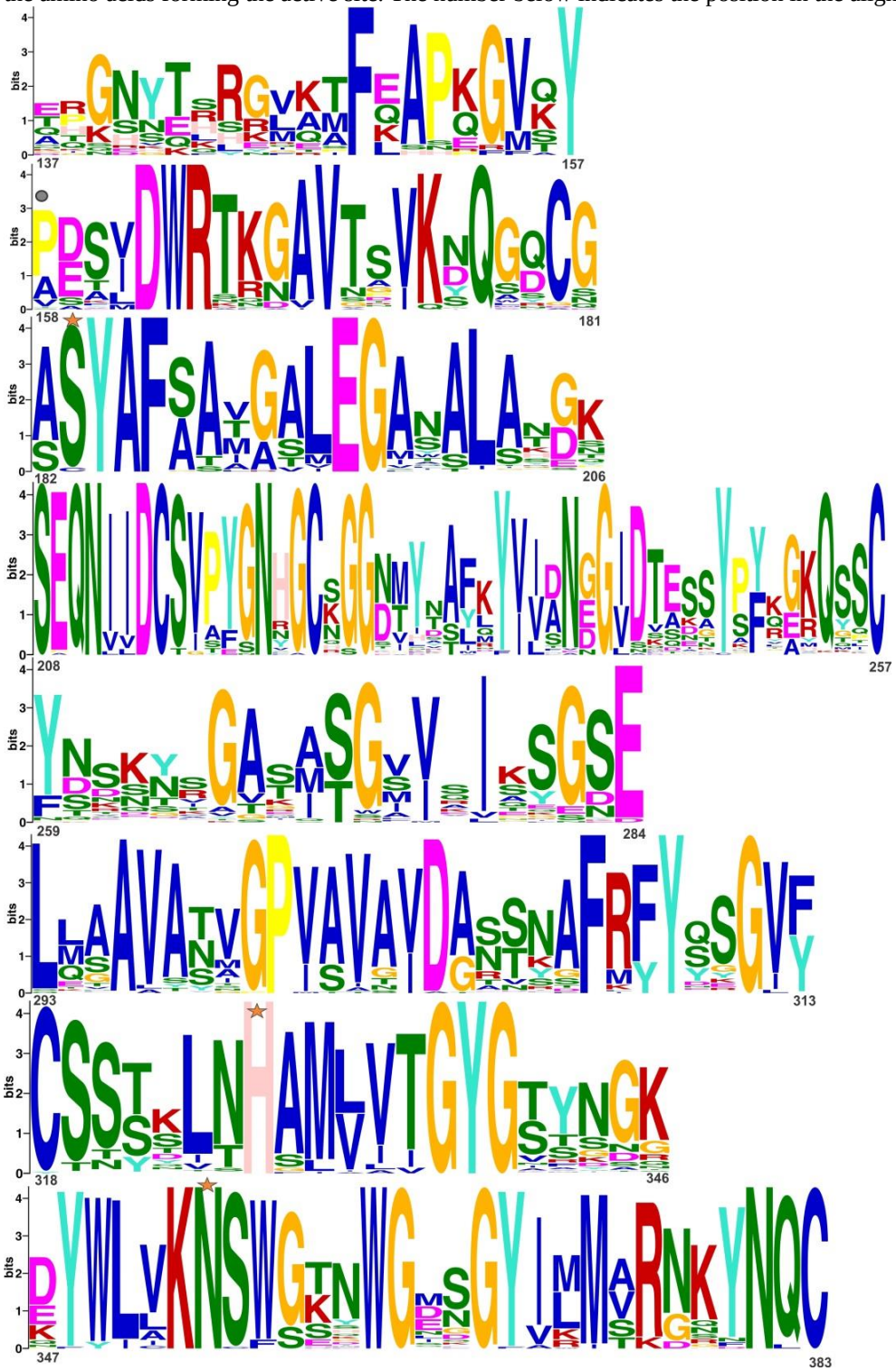

Appendix 12. Conserved amino acid motifs of all the silicateins of clade CHNI. The star above indicates the amino acids forming the active site. The number below indicates the position in the alignment.

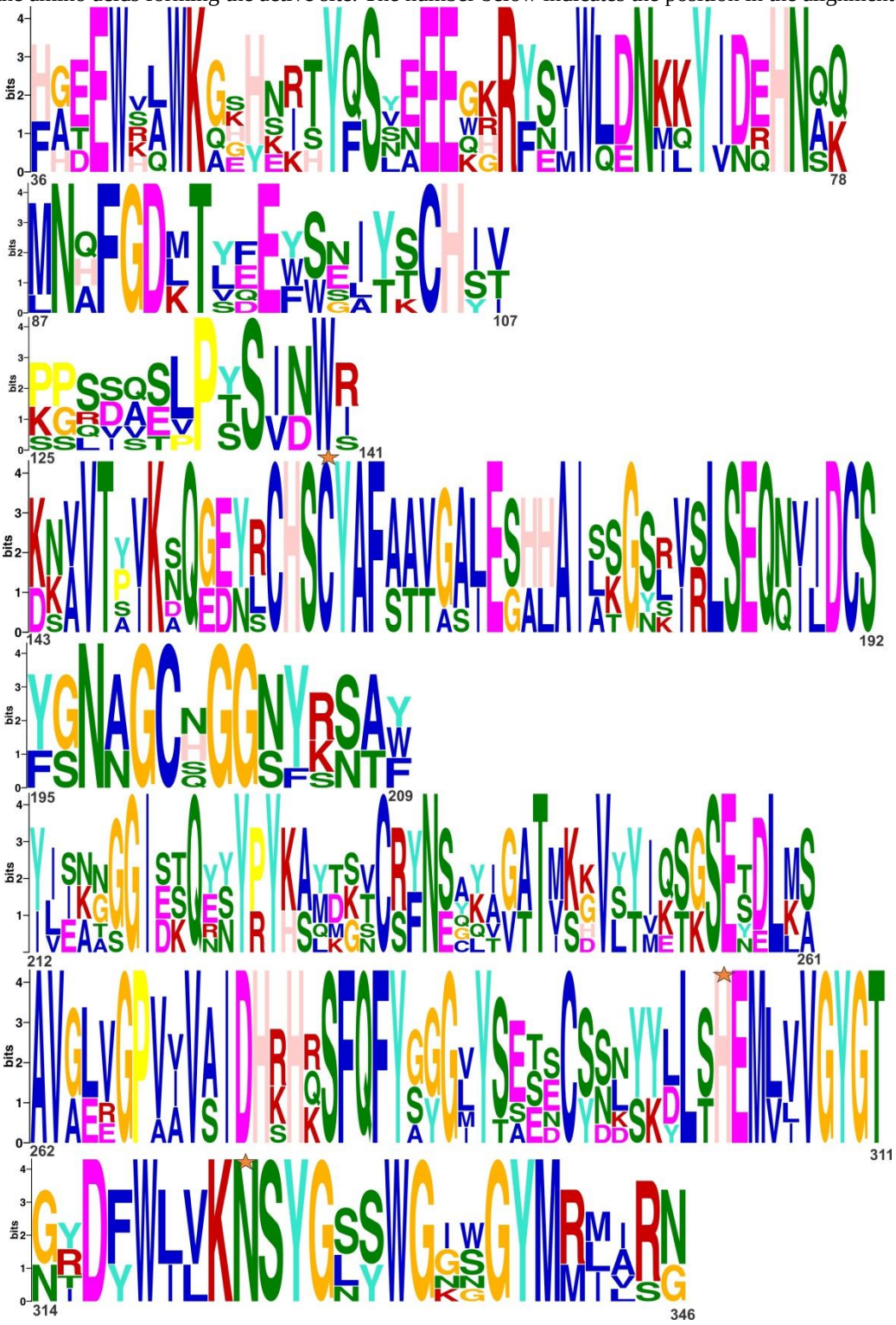

Appendix 13. Conserved amino acid motifs of all the silicateins of clade CHNII. The star above indicates the amino acids forming the active site. The number below indicates the position in the alignment.

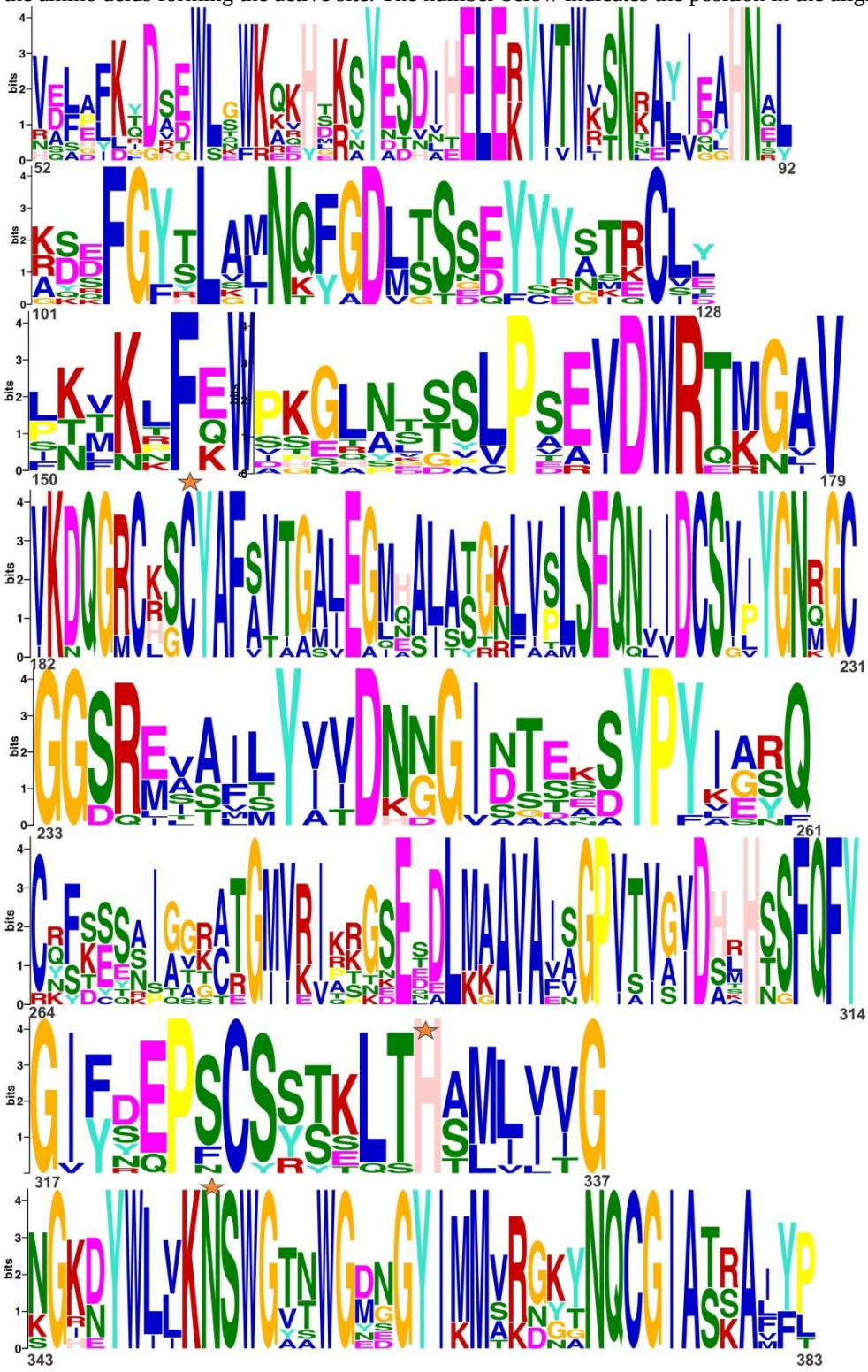

Appendix 14.Conserved amino acid motifs of all the silicateins of clade CHNIII. The star above indicates the amino acids forming the active site. The number below indicates the position in the alignment.

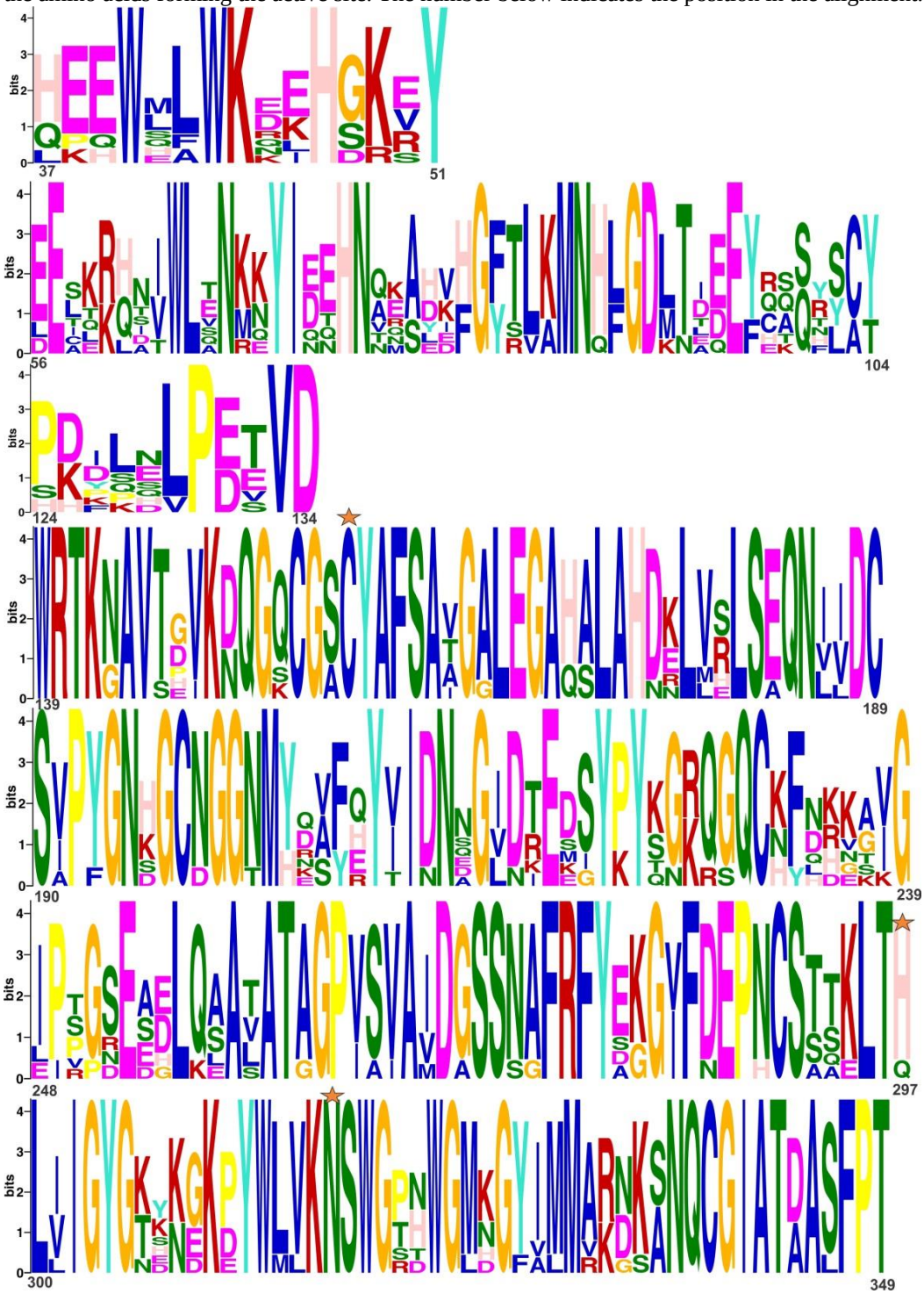

Appendix 15. Conserved amino acid motifs of all the silicateins of the C/SQN clade. The star above indicates the three amino acids forming the active site. The number below indicates the position in the alignment.

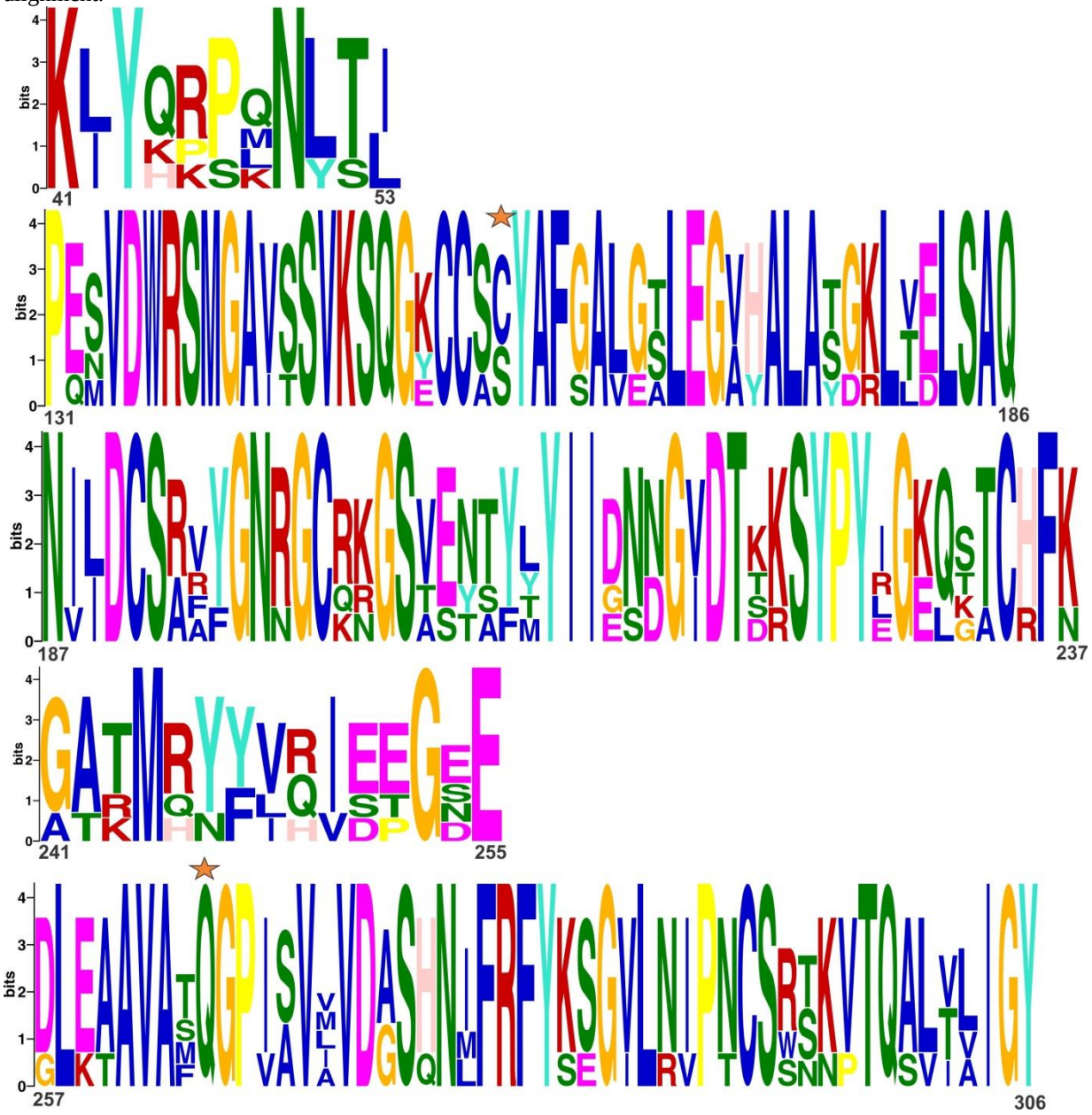

Appendix 16. Silicatein sequence of *Haliclona_indistincta5*. This sequence was located between the overall silicatein clade and cathepsins L clade.

>MKFNVVLLVALAAAAAVTGFQHTEEWEAWKKEHGRVYESDEIEHRRHAIWEKKMKFIEEHNA
NADETGFTVEMNKFGDMENDEITQFYMGYIPDDESDDSDDSSDNSTMTPDELEDEFELLRRLPST
VDWRRRGVVTPVKDQGRCGSCYAFGATGALEGQYARRTRRLVSFSEQQIVDCSGSYGNRGCHG
GRPAWSFEYLEHIRGIQSERTYPYRSRKQRCMYRRRQAVTGCKSYRHVTRGNEYALMRAVARIG
PIAVTIDASNTGFAHYKRGVYDEPRCNKRLSKLTHVVLVVGYGTHYGKRYWLVKNSWGRNWG
MNGYIMMSRFKNNQCGIATKAVYPRVRILRSSG

Appendix 17. Readings from the Bioanalyzer of the RNA extracted from the samples investigated for the Real Time PCR experiment; FSL= Free Swimming Larvae.

Sample	RNA concentration (ng/µL)	RIN
FSL1	113	7.0
FSL2	150	7.5
FSL3	220	7.5
Presettled/Settled1	235	7.5
Presettled/Settled2	320	8
Presettled/Settled3	430	8
Adult1	896	10
Adult2	1235	9.6
Adult3	1578	9.7
Adult4	950	9.3

Appendix 18. DNA sequences of the housekeeping genes tested for the Real Time PCR experiment. These genes were identified (blasted manually) in the transcriptome of *H. indistincta*.

>18SrNA

ATGATCCTTCCGCAGGTTCACCTACGGAAACCTTGTTACGACTTTTACTTCCTCTAGAGAGCTTATT
TAGAGCAACTTCTCCCCATCCAACGCGGCCCGTGAAGACCGCGCCGGCAGAGATCCAGAGATCTCA
ATAAGCCATCCAATCGGTAGTAGCGACGGGCGGTGTGTACAAAGGGCAGGGACGTAATCAACGCG
AGCTGGTGACTCGCGCTTACTAGGAATTCCTCGTTCAAGATCAATAATTGCAACCATCTATCCCCAG
CACGACGGAGGCTGCCAAGATTACCCGCACCTTTCGGCGAAGGACACGCTCGCTGGCTCCGTCAGT
GTAGCGCGCGTGCGGCCCAGGACATCTAAGGGCATCACAGACCTGTTATTGCCTCAAACTTCCTCT
GGCTCGAGCCAACTGTCCCTCTAAGAAGCTGCACGACAACCGTTCGGGAACGGCGCAGCTAGTTAG
CAGGTTAAGGTCTCGTTCGTTAACGGAATTAACCAGACAAGTCACCCCACCAACTAAGAACGGCCA
TGCACCACCACCCATAGAATCAAGAAAGAGCTCTCGATCTGTCAATCCTTCCCATGTCCGGACCTG
GTGAGTTGCCCCGTGTTGGGTCAAATTAAGCCGCAGGCTCCACTCCTGGTGGTGCCCTTCCGTCAAT
TCCTTTAAGTTTCAGCCTTGCGACCATACTCCCCCCGGAACCCAAAGGCTCTGATTTCTCTCAAGGT
GCCGACGGAGGCGATTGCGACCTCCGCCGATCCCTAGCCGGCATAGTTTATGGTTGGGACTACGAC
GGTATCTGATCGTCTTCGAACCCCCAACTTTCGTTCTTGATTAATGAAAACATCCTTGGCAAATGCT
TTCGCAGTTGTTCGTCTTCCATAAATCCAAGAATTTCACCTCTGACAATTGAATACGAATGCCCCCA
ACTGTCCCTCTTAACCATGACCTCGGTCCCGAAAACCAACAAAATAGGACCCAAGCCCTATTCCAT
TATTCCATGCTAATGTATCCAAGCACCGGCCTGCTTTGAACACTCTAATTTTTTCAAAGTAAACGTC
CCGAATCCCCTGCCCGCTCCAGTTAAGGGCAGCCAGGGCCTCCGAGAGGAAGAGCCACCGAGCAG
TGCGTGTCTCTCGACAGACCGCCCGGTCGGCTCCGAAATCCAACTACGAGCTTTTTAACTGCAACA
ACTTTAATATACGCTATTGGAGCTGGAATTACCGCGGCTGCTGGCACCAGACTTGCCCTCCAATTGT
TCCTCGTTAAGGGGTTTGGATTGTACTCATTCCAATTGCCGGCCTACTCAAGAGGCCGGCATTGTTA
TTTATTGTCACTACCTCCCCGAGTCGGGATTGGGTAATTTGCGCGCCTGCTGCCTTCCTTGGATGTG
GTAGCCGTTTCTCAGGCTCCCTCTCCGGAATCGAACCCTAATTCTCCGTTACCCGTTGCGACCATGG
TAGGCCAATACCCTACCATCGAAAGTTGATAGGGCAGAAACTTGAATGAATCATCGCCGGCACGA
AGGCCGTGCGATTCGAGCAGTTATCATGAATCACCATCTTCCCGAGACCGAAGCCTCGGCATTGGT
TTTGGATCTAATAAATACATCCCTTCCGTAAAGTCGGGACCTTCTGCATGTATTAGCTCTAGAATTA
CCACGGTTATCCATGTAATGGGGCACCATCAAATAAACTATAACTGATTTAATGAGCCATTCGCAG
TTTCACGGTGCAGATGCGTTCATACTTGCACATGCATGGCTTAGTCTTTGAGACAAGCATATGACTA
CTGGCAGGAC

>ETIF3 (Eukaryotic Translation Initiation Factor 3 subunit 3)

ATGGCGGAAGCAACCGTAGCTGACCCTGCGCCTGCCGCTCCGTTAAGGTTCGTGTTTCCACACATT
CATGATAACCCGTCCGGGTGGGGGCCCTGTGAGGTGCCTGAGCAGTTCAGAGACACGCCGTATCAG
CCTTTCTGCAAGGACGACCGACTGGGAAAAGTAGCTGACTGGACGGGGAATCTATACCAAGACAA
GAGGACCGTTAACAAGTATGGTAACGTGTATGGAGCTGGCGGTCAGAGTCAGACCTATGTCTACCG
CCATGAGCAAGACGAATCTACCTTCCAGCTGGTGGACACGTCACGGCCTCAGCGACCAATGTATCG
GCGTAGACCAATGCAAAGATATCATCGTCGTGACCGAGATCGCAAGGACGGAAAGAAAGGCGGCC
GGCAACCATTTCAGAAGAATAAACCTCAAGAGAGGCGTTCCAAGCACAGGAAATTCTTCCGTTCCT
ATCACTATGACAACCCTCCCTCTTTGAAGCCCCGCCTACCCTCTGTTGACATCAAGGCATCATGGAA
GGTCATGAGAGAGGTCACCTTTCCGGAACTAGCGAAATTGAACTTTGCACCAGAAAAACCTCACAA
CCTTTATCTGTGTGGTGCTGTTGGCTACTATGATAGTCGCAAGGAAAAATCTGTGTCTGTCAAGTTT
CCTCAGAAACTGGCAAAATTCGATCGAGTCTTTCATACTGTGTCTACTTCAAACGATCCCATCTTTC
GAAAATTAGCTAGGAGTCCAGAATGCAGCGATTGTAAAGTATTTGCTACTGACGCCATTTTGGCTA
CTCTTATGACAATGACACGCTCGAAATACTCGTGGGACATTGTAGTACATCGTGTTGGTGATTATGT
GTTCTTCGATAAAAGAGACGATTCACGGTTTGACTACCTCACTGTCAGTGAGACAGCCAAGCAACC
TCCTCAAGATGAAACAGGCATCAACTCCCCTCAGAGCCTTGCCGTAGAGGCGACCTACATCAATCA
GAACTTCTCACAGCAGATGCTCATGTATGGGCGGTTTCATCGTCTAAAGCACCCTAACCCTTTCATT
GAGGATGACTCTGAAGAAATCGCTTCTGTCGCTTATCGTTATCGCAAGTTCTATCTCAAGGATGGC
GTGGGGATGGTAGTGAGGTGTAAGTACGATGCTGTGATGCCTCCTGCTGATCCAAAGGGAGAGCCT
GACGTCTTTGTCAACATCAGATCACTCAATGAATGGGACCCAAAGCATTCTGGTGGTAACCATGTT
GATTGGAGGAAAAACCTTGATCGTCAGAGAGGAGCAGTGTTTGCTACTGAGCTCAAGAACAACAG
CTGTAAGATAGCCAAGTGGGTGCTGGCAGCCATGTTAGGTGGATCGTCCATCTTCAAGTGTGGCTT

CATTTCAAGGCAGTACAGTAAGGATTCCTCGAAACATGAGATACTGGGTATTCGTCAAGAGAGACC
AGAGCAGTTTGCACAGCAGCTCAACCTTGATGTCGGCAATGCCTGGGGCATCCTGCACGCCATTAT
AGACTATTGTAGAGAACTAGACTTGGGCAAGTATCTGATATTGAAGGACGCTAATAATCCGGTTGT
TCGGATATATTCAGTCTCGGAGGAGGAGTTTGAATCAGAGGAGAGTGGCAGTGAATCGGATGGAT
CTGCTGATGAGAAAGGATCAGAATGA

>HGPRT (Hypoxanthine-guanine phosphoribosyltransferase)

ATGGGCGTGGGTGGATGATGACGTAAGAGCTCCTGGCCTGCGAACGCGTGGTTCATCACCAGCTCT
CCCTAGCAAGATGTCCAAGCACAAGAAGACGTCAACTATTGTGATACCGGATAACTACACGGGAT
ACCGCCTGGAGGATTTCTGTATCCCGCCACATTACTATGATGATCTGAAATGTGTAATGCTACCTAA
AGGTCTCATAATGGACAGGGTGGAGCGACTAGCTCAGGATATCTGCCATGATCTGAGTGGGCCTCT
AGTAGCTCTGTGTGTGCTCAAGGGCGGCTACCAGTTCTTCACTGATCTACTGGACTACATCAAGAC
ACACAATGCTACTTCAGAGCGATCTTTCCGAATGCAAGTTGACTTTATCAGACTAAAGAGCTATGT
GGATGATCAATCAACTGGTACAGTACAAGTGATTGGAGGAGACAATCTATCATCACTTACAGGAA
AGAATGTCCTGATTGTAGAGGATATTATAGATACTGGAGGCACGATGACCAAGCTGCTCAAGGTAC
TAGAAGAGTACAAGCCGGCTAATGTCAGAGTGGCCAGTCTTCTAGTAAAGAGGACTCCAAAGAGT
GTCGGCTATAGACCAGATTACATCGGTTTTGAGATTCCTAATGAATTCGTAGTGGGCTATGCTCTGG
ATTACAATGAGTTTTTCCGTGACCTTAATCATGTGTGTATTATCAATGACTATGGCAAGGAGCACTA
CTCAGCTAGCTCACCAGTACCGAACAACTCTCACTAA

>B-Tubulin

ATGCGTGAAATCGTTCATCTTCAAGCTGGCCAATGCGGCAACCAGATCGGAGCCAAGTTCTGGGAG
GTCATCTCTGACGAGCATGGAATTGACCCGACAGGTACCTATCATGGTGACTCCGACTTGCAGCTG
GAGCGCATCAACGTCTATTACAACGAGGCTACAGGTGGCAAATACGTGCCTCGTGCCGTCCTGGTC
GACTTGGAGCCTGGAACCATGGACTCAGTCCGTTCCGGACCCTTCGGACAAATCTTTAGGCCAGAC
AACTTCGTATTCGGTCAAAGTGGAGCTGGTAACAACTGGGCTAAGGGTCACTACACAGAGGGTGCC
GAGCTTGTAGACTCAGTACTTGATGTGGTTCGTAAGGAGGCTGAGAGTTGTGACTGTCTGCAAGGT
TTCCAGCTGACACATTCTCTTGGTGGAGGCACCGGGTCTGGCATGGGCACACTTCTCATTTCTAAGA
TTCGTGAGGAGTATCCTGACAGGATCATGAACACCTTTAGTGTTGTACCATCACCCAAAGTATCCG
ATACTGTTGTCGAACCCTACAATGCCACCCTGTCTGTCCATCAACTGGTTGAAAACACAGATGAAA
CCTTCTGCATCGACAATGAAGCCCTGTACGATATCTGCTTCCGTACTCTGAAGCTTACCACCCCAAC
ATATGGAGATCTTAACCACCTTGTCTCAGCCACCATGAGCGGAGTCACCACTTGCCTGCGATTTCCT
GGCCAGCTCAATGCTGATTTGCGTAAGCTAGCTGTCAACATGGTTCCATTCCCTCGTCTTCACTTCT
TCATGCCTGGGTTTGCTCCTCTTACCAGCCGTGGATCCCAGCAGTACCGTGCCCTCACCGTCCCCGA
GCTCACCCAGCAAATGTTTGATGCCAAGAACATGATGGCTGCCTGTGATCCACGTCATGGCCGTTA
TCTTACTGTTGCTGCCATGTTCCGTGGACGCATGTCAATGAAGGAAGTCGACGAGCAAATGCTTAA
CGTGCAAAACAAGAACAGCTCCTACTTCGTTGAATGGATCCCAAACAATGTCAAGACTGCTGTCTG
TGACATTCCTCCTCGTGGTCTCAAGATGTCTGCCACCTTCATTGGCAACAGCACTGCCATCCAAGAG
CTCTTCAAGCGAATCAGCGAGCAATTCACTGCTATGTTCCGTCGTAAGGCTTTCCTTCATTGGTATA
CTGGCGAGGGTATGGACGAGATGGAGTTCACTGAGGCTGAATCCAACATGAATGATCTTGTATCTG
AATACCAGCAATATCAGGATGCCACTGCTGAGGATGAGGGAGACTTTGATGAAGATGAAGAGGGA
GAGGAAGAAGCTGCCTAA

Appendix 19. Primer sequences of the housekeeping genes tested for the Real Time PCR Analysis. Brackets include the length of the primer/ Melting temperature / %GC content.

Gene	5'-Forward Primer-3' (length/Tm/%GC)	5'-Reverse Primer-3' (length/Tm/%GC)
18s RNA	ATGGAAGACGAACAACTGCG (20bp/58.85°C/50%)	GATCCCTAGCCGGCATAGTT (20bp/59.02°C/55%)
ETIF3	GCCGGCAACCATTTCAGAAG (20 bp/60.11°C/55%)	CGCTAGTTCCGGAAAGGTGA (20 bp/59.75°C/55%)
B-Tubulin	CACCACTTGCCTGCGATTTC (20 bp/60.11°C/55%)	GGATCCACGGCTGGTAAGAG (20 bp/59.8.11°C/60%)
HGPRT	CCATGATCTGAGTGGGCCTC (20 bp/ 59.89°C/ 60%)	CTTGCATTCGGAAAGATCGCT (21 BP/ 59.33°C/ 47.62%)

Appendix 20. Ct values of the four housekeeping genes investigated from the Real Time PCR experiment. FSL= Free Swimming Larvae; SD= Standard deviation.

Samples	ETIF3	18S	B-tubulin	HGPRT
FSL1	26.85625	28.84443	26.70547	24.92834
	26.69811	28.91159	26.66729	24.63433
	27.02578	28.55076	26.86472	24.86091
FSL2	25.13939	30.90856	27.43087	24.76209
	24.96365	31.53133	27.14682	24.88732
	25.2012	30.74112	27.39853	24.98731
FSL3	25.55274	30.65431	26.95424	24.71523
	25.49264	31.03541	26.84681	24.93271
	25.92118	31.28531	26.69136	24.87412
Presettled/settled1	32.75891	30.92472	27.54914	25.06724
	32.8035	31.17259	27.68041	24.90375
	33.64942	30.90288	27.96221	24.81043
Presettled/settled2	31.20317	30.73403	27.99057	25.13793
	31.19761	30.54051	28.25812	24.94817
	30.98761	30.97168	28.10975	24.77301
Presettled/settled3	30.92395	30.5413	27.86053	25.01985
	31.14563	30.27134	27.80125	24.96518
	30.92457	30.19344	28.00814	24.8953
Adult1	27.65633	29.69983	27.05723	25.13957
	27.82092	29.91251	27.45114	24.91043
	27.8615	29.80164	27.2336	24.86481
Adult2	27.87695	29.95517	27.78045	25.10047
	27.98762	30.6585	27.96424	25.13583
	28.16543	30.26398	27.91473	24.88916
Adult3	27.98001	29.97425	28.49436	25.08764
	28.00183	29.54671	28.35742	24.78678
	28.33671	29.67473	28.27872	24.53461
Adult4	29.00348	30.14617	27.96012	24.90413
	28.99135	30.30285	27.86465	25.07844
	28.80249	30.12573	28.04613	25.14567
Mean	28.564331	30.29257933	27.61096733	24.922692
Min	24.96365	28.55076	26.66729	24.53461
Max	33.64942	31.53133	28.49436	25.14567
SD	2.444106525	0.724730669	0.541411009	0.152931824

Appendix 21. Box and whisker plot of the four housekeeping genes investigated. Threshold cycle (Ct) variation in the four gene transcripts among samples is plotted. Boxes indicate the 25/75 percentiles, the line inside each square indicates the median and the whiskers indicate the minimum and maximum values.HGPRT was the most stable gene and therefore was chosen as the reference for the real timePCR experiment

.

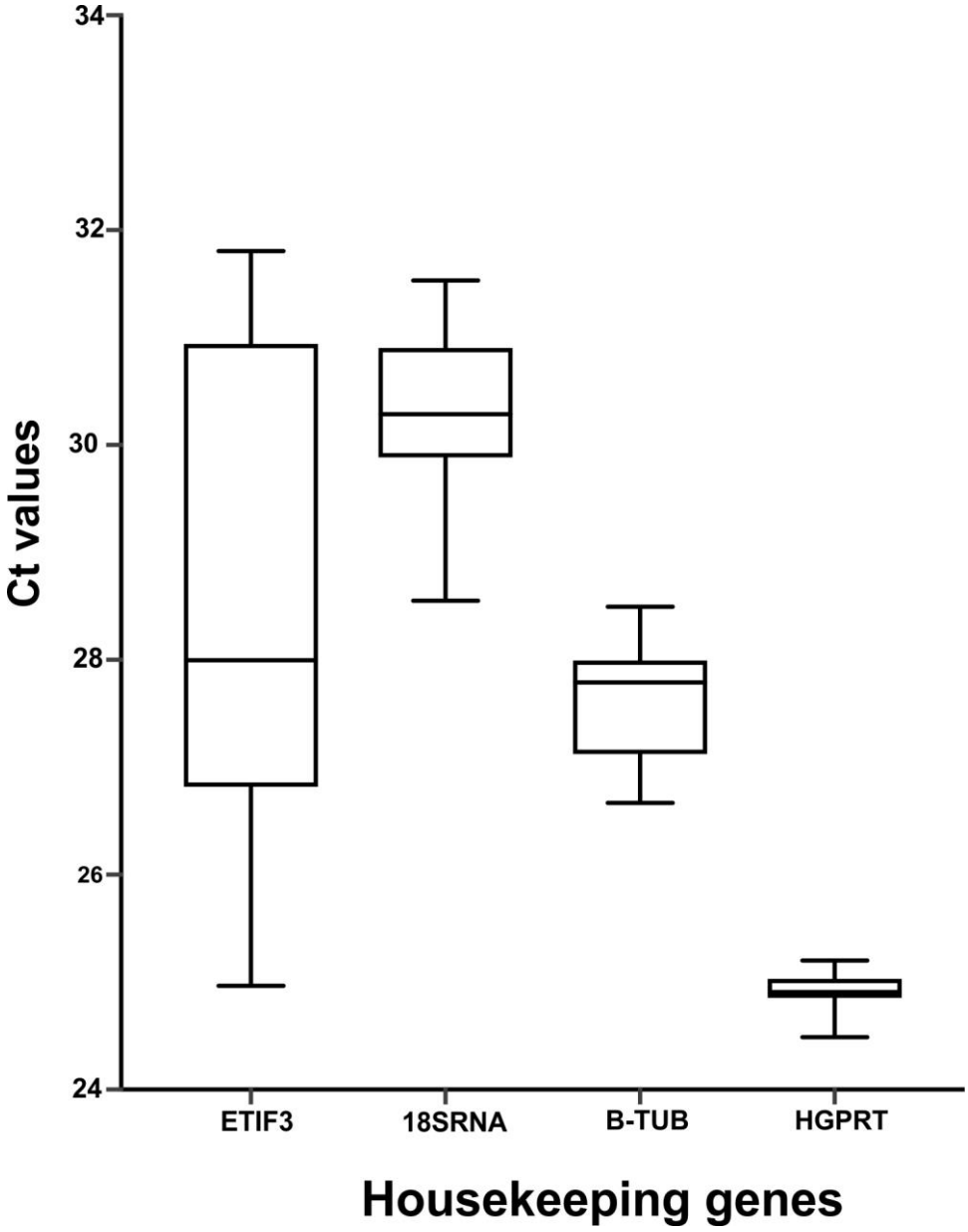

Appendix 22. Tukey's multicomparison tests to determine the significant differences of the 105 interactions between the relative expression levels of the five silicatein genes and the three life stages; $p < 0.05$. ns= 0.1234; * = 0.0332; **= 0.0021; ***= 0.0002; **** = <0.0001.

Tukey's multiple comparisons test	Mean Diff.	95.00% CI of diff.	Significant?	Summary	P Value
Larvae:CHNII vs. Larvae:SHNI	0	-1.524 to 1.524	No	ns	>0.9999
Larvae:CQN vs. Larvae:SHNI	0	-1.524 to 1.524	No	ns	>0.9999
Larvae:SQN vs. Larvae:SHNI	0	-1.524 to 1.524	No	ns	>0.9999
Larvae:CHNI vs. Larvae:SHNI	0	-1.524 to 1.524	No	ns	>0.9999
Presettled/Settled:SHNI vs. Larvae:SHNI	1.13	-0.3946 to 2.654	No	ns	0.3343
Presettled/Settled:CHNII vs. Larvae:SHNI	1.398	-0.1260 to 2.923	No	ns	0.0985
Presettled/Settled:CQN vs. Larvae:SHNI	0.9387	-0.5858 to 2.463	No	ns	0.6181
Presettled/Settled:SQN vs. Larvae:SHNI	**1.746**	**0.2215 to 3.270**	**Yes**	*****	**0.0137**
Presettled/Settled:CHNI vs. Larvae:SHNI	1.117	-0.4078 to 2.641	No	ns	0.3515
Adults:SHNI vs. Larvae:SHNI	-0.3438	-1.868 to 1.181	No	ns	>0.9999
Adults:CHNII vs. Larvae:SHNI	1.177	-0.3472 to 2.702	No	ns	0.2768
Adults:CQN vs. Larvae:SHNI	1.092	-0.4327 to 2.616	No	ns	0.3853
Adults:SQN vs. Larvae:SHNI	**1.742**	**0.2175 to 3.266**	**Yes**	*****	**0.014**
Adults:CHNI vs. Larvae:SHNI	**3.233**	**1.709 to 4.758**	**Yes**	********	**<0.0001**
Larvae:CQN vs. Larvae:CHNII	0	-1.524 to 1.524	No	ns	>0.9999
Larvae:SQN vs. Larvae:CHNII	0	-1.524 to 1.524	No	ns	>0.9999
Larvae:CHNI vs. Larvae:CHNII	0	-1.524 to 1.524	No	ns	>0.9999
Presettled/Settled:SHNI vs. Larvae:CHNII	1.13	-0.3946 to 2.654	No	ns	0.3343
Presettled/Settled:CHNII vs. Larvae:CHNII	1.398	-0.1260 to 2.923	No	ns	0.0985
Presettled/Settled:CQN vs. Larvae:CHNII	0.9387	-0.5858 to 2.463	No	ns	0.6181
Presettled/Settled:SQN vs. Larvae:CHNII	**1.746**	**0.2215 to 3.270**	**Yes**	*****	**0.0137**
Presettled/Settled:CHNI vs. Larvae:CHNII	1.117	-0.4078 to 2.641	No	ns	0.3515
Adults:SHNI vs. Larvae:CHNII	-0.3438	-1.868 to 1.181	No	ns	>0.9999
Adults:CHNII vs. Larvae:CHNII	1.177	-0.3472 to 2.702	No	ns	0.2768
Adults:CQN vs. Larvae:CHNII	1.092	-0.4327 to 2.616	No	ns	0.3853
Adults:SQN vs. Larvae:CHNII	**1.742**	**0.2175 to 3.266**	**Yes**	*****	**0.014**
Adults:CHNI vs. Larvae:CHNII	**3.233**	**1.709 to 4.758**	**Yes**	********	**<0.0001**
Larvae:SQN vs. Larvae:CQN	0	-1.524 to 1.524	No	ns	>0.9999
Larvae:CHNI vs. Larvae:CQN	0	-1.524 to 1.524	No	ns	>0.9999
Presettled/Settled:SHNI vs. Larvae:CQN	1.13	-0.3946 to 2.654	No	ns	0.3343
Presettled/Settled:CHNII vs. Larvae:CQN	1.398	-0.1260 to 2.923	No	ns	0.0985
Presettled/Settled:CQN vs. Larvae:CQN	0.9387	-0.5858 to 2.463	No	ns	0.6181
Presettled/Settled:SQN vs. Larvae:CQN	**1.746**	**0.2215 to 3.270**	**Yes**	*****	**0.0137**
Presettled/Settled:CHNI vs. Larvae:CQN	1.117	-0.4078 to 2.641	No	ns	0.3515
Adults:SHNI vs. Larvae:CQN	-0.3438	-1.868 to 1.181	No	ns	>0.9999
Adults:CHNII vs. Larvae:CQN	1.177	-0.3472 to 2.702	No	ns	0.2768
Adults:CQN vs. Larvae:CQN	1.092	-0.4327 to 2.616	No	ns	0.3853

Adults:SQN vs. Larvae:CQN	**1.742**	**0.2175 to 3.266**	**Yes**	*****	**0.014**
Adults:CHNI vs. Larvae:CQN	**3.233**	**1.709 to 4.758**	**Yes**	********	**<0.0001**
Larvae:CHNI vs. Larvae:SQN	0	-1.524 to 1.524	No	ns	>0.9999
Presettled/Settled:SHNI vs. Larvae:SQN	1.13	-0.3946 to 2.654	No	ns	0.3343
Presettled/Settled:CHNII vs. Larvae:SQN	1.398	-0.1260 to 2.923	No	ns	0.0985
Presettled/Settled:CQN vs. Larvae:SQN	0.9387	-0.5858 to 2.463	No	ns	0.6181
Presettled/Settled:SQN vs. Larvae:SQN	**1.746**	**0.2215 to 3.270**	**Yes**	*****	**0.0137**
Presettled/Settled:CHNI vs. Larvae:SQN	1.117	-0.4078 to 2.641	No	ns	0.3515
Adults:SHNI vs. Larvae:SQN	-0.3438	-1.868 to 1.181	No	ns	>0.9999
Adults:CHNII vs. Larvae:SQN	1.177	-0.3472 to 2.702	No	ns	0.2768
Adults:CQN vs. Larvae:SQN	1.092	-0.4327 to 2.616	No	ns	0.3853
Adults:SQN vs. Larvae:SQN	**1.742**	**0.2175 to 3.266**	**Yes**	*****	**0.014**
Adults:CHNI vs. Larvae:SQN	**3.233**	**1.709 to 4.758**	**Yes**	********	**<0.0001**
Presettled/Settled:SHNI vs. Larvae:CHNI	1.13	-0.3946 to 2.654	No	ns	0.3343
Presettled/Settled:CHNII vs. Larvae:CHNI	1.398	-0.1260 to 2.923	No	ns	0.0985
Presettled/Settled:CQN vs. Larvae:CHNI	0.9387	-0.5858 to 2.463	No	ns	0.6181
Presettled/Settled:SQN vs. Larvae:CHNI	**1.746**	**0.2215 to 3.270**	**Yes**	*****	**0.0137**
Presettled/Settled:CHNI vs. Larvae:CHNI	1.117	-0.4078 to 2.641	No	ns	0.3515
Adults:SHNI vs. Larvae:CHNI	-0.3438	-1.868 to 1.181	No	ns	>0.9999
Adults:CHNII vs. Larvae:CHNI	1.177	-0.3472 to 2.702	No	ns	0.2768
Adults:CQN vs. Larvae:CHNI	1.092	-0.4327 to 2.616	No	ns	0.3853
Adults:SQN vs. Larvae:CHNI	**1.742**	**0.2175 to 3.266**	**Yes**	*****	**0.014**
Adults:CHNI vs. Larvae:CHNI	**3.233**	**1.709 to 4.758**	**Yes**	********	**<0.0001**
Presettled/Settled:CHNII vs. Presettled/Settled:SHNI	0.2686	-1.256 to 1.793	No	ns	>0.9999
Presettled/Settled:CQN vs. Presettled/Settled:SHNI	-0.1911	-1.716 to 1.333	No	ns	>0.9999
Presettled/Settled:SQN vs. Presettled/Settled:SHNI	0.6161	-0.9083 to 2.141	No	ns	0.9684
Presettled/Settled:CHNI vs. Presettled/Settled:SHNI	-0.01316	-1.538 to 1.511	No	ns	>0.9999
Adults:SHNI vs. Presettled/Settled:SHNI	-1.474	-2.998 to 0.05088	No	ns	0.0662
Adults:CHNII vs. Presettled/Settled:SHNI	0.04739	-1.477 to 1.572	No	ns	>0.9999
Adults:CQN vs. Presettled/Settled:SHNI	-0.03811	-1.563 to 1.486	No	ns	>0.9999
Adults:SQN vs. Presettled/Settled:SHNI	0.6122	-0.9122 to 2.137	No	ns	0.97
Adults:CHNI vs. Presettled/Settled:SHNI	**2.103**	**0.5789 to 3.628**	**Yes**	******	**0.0014**
Presettled/Settled:CQN vs. Presettled/Settled:CHNII	-0.4597	-1.984 to 1.065	No	ns	0.9978
Presettled/Settled:SQN vs. Presettled/Settled:CHNII	0.3475	-1.177 to 1.872	No	ns	0.9999
Presettled/Settled:CHNI vs. Presettled/Settled:CHNII	-0.2818	-1.806 to 1.243	No	ns	>0.9999
Adults:SHNI vs. Presettled/Settled:CHNII	**-1.742**	**-3.267 to -0.2177**	**Yes**	*****	**0.014**
Adults:CHNII vs. Presettled/Settled:CHNII	-0.2212	-1.746 to 1.303	No	ns	>0.9999

Adults:CQN vs. Presettled/Settled:CHNII	-0.3067	-1.831 to 1.218	No	ns	>0.9999
Adults:SQN vs. Presettled/Settled:CHNII	0.3436	-1.181 to 1.868	No	ns	>0.9999
Adults:CHNI vs. Presettled/Settled:CHNII	**1.835**	**0.3103 to 3.359**	**Yes**	******	**0.0079**
Presettled/Settled:SQN vs. Presettled/Settled:CQN	0.8072	-0.7172 to 2.332	No	ns	0.8094
Presettled/Settled:CHNI vs. Presettled/Settled:CQN	0.1779	-1.346 to 1.702	No	ns	>0.9999
Adults:SHNI vs. Presettled/Settled:CQN	-1.282	-2.807 to 0.2420	No	ns	0.1742
Adults:CHNII vs. Presettled/Settled:CQN	0.2385	-1.286 to 1.763	No	ns	>0.9999
Adults:CQN vs. Presettled/Settled:CQN	0.153	-1.371 to 1.677	No	ns	>0.9999
Adults:SQN vs. Presettled/Settled:CQN	0.8033	-0.7211 to 2.328	No	ns	0.8143
Adults:CHNI vs. Presettled/Settled:CQN	**2.294**	**0.7700 to 3.819**	**Yes**	*******	**0.0004**
Presettled/Settled:CHNI vs. Presettled/Settled:SQN	-0.6293	-2.154 to 0.8951	No	ns	0.9628
Adults:SHNI vs. Presettled/Settled:SQN	**-2.09**	**-3.614 to -0.5652**	**Yes**	******	**0.0016**
Adults:CHNII vs. Presettled/Settled:SQN	-0.5687	-2.093 to 0.9557	No	ns	0.9837
Adults:CQN vs. Presettled/Settled:SQN	-0.6542	-2.179 to 0.8702	No	ns	0.9501
Adults:SQN vs. Presettled/Settled:SQN	-0.003933	-1.528 to 1.520	No	ns	>0.9999
Adults:CHNI vs. Presettled/Settled:SQN	1.487	-0.03720 to 3.012	No	ns	0.0614
Adults:SHNI vs. Presettled/Settled:CHNI	-1.46	-2.985 to 0.06405	No	ns	0.071
Adults:CHNII vs. Presettled/Settled:CHNI	0.06056	-1.464 to 1.585	No	ns	>0.9999
Adults:CQN vs. Presettled/Settled:CHNI	-0.02494	-1.549 to 1.499	No	ns	>0.9999
Adults:SQN vs. Presettled/Settled:CHNI	0.6253	-0.8991 to 2.150	No	ns	0.9645
Adults:CHNI vs. Presettled/Settled:CHNI	**2.116**	**0.5921 to 3.641**	**Yes**	******	**0.0013**
Adults:CHNII vs. Adults:SHNI	1.521	-0.003489 to 3.045	No	ns	0.051
Adults:CQN vs. Adults:SHNI	1.435	-0.08899 to 2.960	No	ns	0.0811
Adults:SQN vs. Adults:SHNI	**2.086**	**0.5613 to 3.610**	**Yes**	******	**0.0016**
Adults:CHNI vs. Adults:SHNI	**3.577**	**2.052 to 5.101**	**Yes**	********	**<0.0001**
Adults:CQN vs. Adults:CHNII	-0.0855	-1.610 to 1.439	No	ns	>0.9999
Adults:SQN vs. Adults:CHNII	0.5648	-0.9596 to 2.089	No	ns	0.9846
Adults:CHNI vs. Adults:CHNII	2.056	0.5315 to 3.580	Yes	**	0.0019
Adults:SQN vs. Adults:CQN	0.6503	-0.8741 to 2.175	No	ns	0.9523
Adults:CHNI vs. Adults:CQN	**2.141**	**0.6170 to 3.666**	**Yes**	******	**0.0011**
Adults:CHNI vs. Adults:SQN	1.491	-0.03327 to 3.016	No	ns	0.0601

Appendix 23. SDS-PAGE analysis of the production of the silicatein (SHN type) from *H. indstimcta* in *E. coli* . Lanes; T0: whole cell lysate of *E. coli* expressing silicatein at induction, T1-T4 whole cells lysate of *E. coli* expressing silicatein at hourly intervals from the induction. Black arrow indicates the protein band corresponding to the silicatein in the lanes T1-T4 (22 kDA).

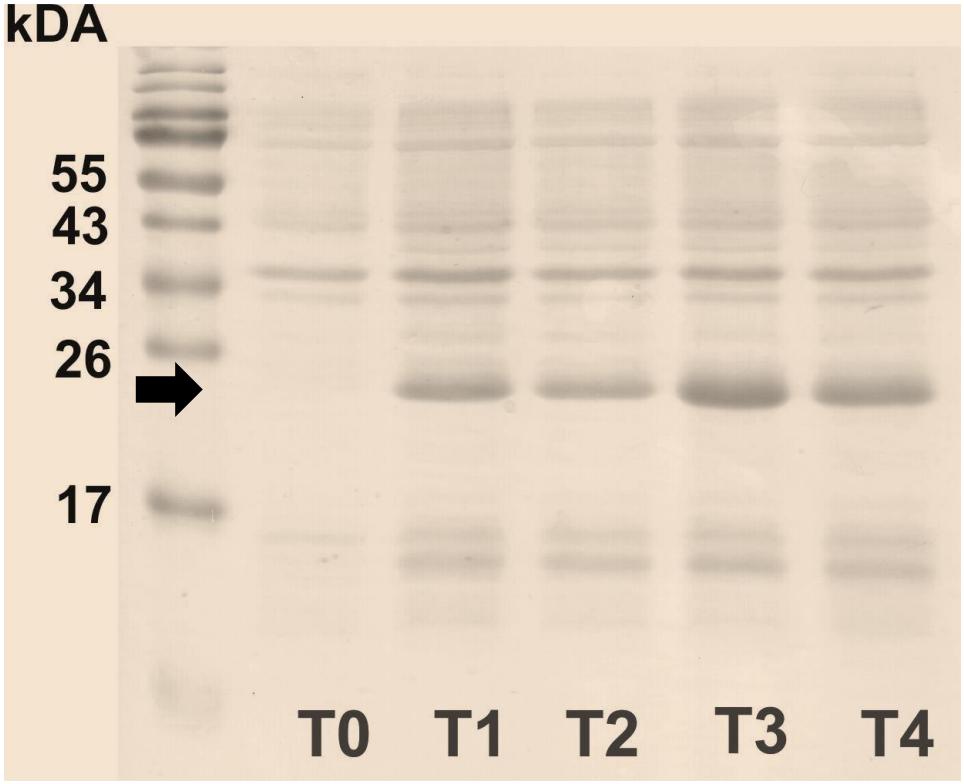

Publications

Molecular Phylogenetics and Evolution xxx (xxxx) xxx–xxx

Contents lists available at ScienceDirect

Molecular Phylogenetics and Evolution

journal homepage: www.elsevier.com/locate/ympev

Evolution of the main skeleton-forming genes in sponges (phylum Porifera) with special focus on the marine Haplosclerida (class Demospongiae)

Jose Maria Aguilar-Camacho, Liam Doonan, Grace P. McCormack*

Zoology, School of Natural Sciences and Ryan Institute, National University of Ireland Galway, University Rd., Galway, Ireland

ARTICLE INFO

Keywords:
Porifera
Haplosclerida
Skeleton
Spicules
Silicateins
Evolution

ABSTRACT

The skeletons of sponges (Phylum Porifera) are comprised of collagen, often embedded with small siliceous structures (spicules) arranged in various forms to provide strength and flexibility. The main proteins responsible for the formation of the spicules in demosponges are the silicateins, which are related to the cathepsins L of other animals. While the silicatein active site, necessary for the formation of biosilica crystals, is characterized by the amino acids SHN, different variants of the silicatein genes have been found, some that retain SHN at the active site and some that don't. As part of an effort to further understand skeleton formation in marine sponges of the order Haplosclerida, a search for all silicatein variants were made in Irish species representing the main clades of this large sponge group. For this task, transcriptomes were sequenced and *de novo* assembled from *Haliclona oculata*, *H. simulans* and *H. indistincta*. Silicatein genes were identified from these and all available genomes and transcriptomes from Porifera. These were analysed along with all complete silicateins from GenBank. Silicateins were only found in species belonging to the class Demospongiae but excluding Keratosa and Verongimorpha and there was significant duplication and diversity of these genes. Silicateins showing SHN at the active site were polyphyletic. Indeed silicatein sequences were divided into six major clades (CHNI, CHNII, CHNIII, SHNI, SHNII and C/SQN). In those clades where haplosclerids were well represented the silicatein phylogeny reflected previous ribosomal and mitochondrial topologies. The most basal silicatein clade (CHNI) contained sequences only from marine haplosclerids and freshwater sponges while one silicatein from *H. indistincta* was more related to cathepsins L (outgroup) than to the overall silicatein clade indicating the presence of an old silicatein or an intermediary form. This data could suggest that marine haplosclerids were one of the first groups of extant demosponges to acquire silicatein genes. Furthermore, we suggest that the paucity of spicule types in this group may be due to their single copy of SHNI variants, and the lack of a silintaphin gene.

1. Introduction

Sponges are simple filter-feeding animals with a body containing relatively few cell types supported by a skeleton of collagen and spongin fibres, and, if present, calcareous or siliceous spicules (Hooper and van Soest, 2002; Wörheide et al., 2012). Based on molecular phylogenetic studies, the phylum Porifera is divided into four main classes: Hexactinellida, Demospongiae, Homoscleromorpha and Calcarea, (Morrow and Cárdenas, 2015). For the first three classes the spicules are siliceous while for Calcarea they are calcium-based (Sperling et al., 2010). In the class Homoscleromorpha, species belonging to the family Oscarellidae Lendenfeld, 1887) lack spicules (Gazave et al., 2012) as do the demosponge members of the subclasses Keratosa and Verongimorpha (excluding members of the family Chondrillidae) (Erpenbeck et al., 2012). The current classification of Demospongiae is based on spicule shape and size when present, and the arrangement of the skeleton (Hooper and van Soest, 2002; Morrow and Cárdenas, 2015). Members of the order Haplosclerida have a simple skeleton made of needle-like oxeas and strongyle megascleres (large spicules), and microscleres if present are limited to sigmas, toxas and microxeas (van Soest, 2017). Freshwater sponges only have oxeas as megascleres but they possess a high diversity of microscleres and gemmuloscleres (Morrow and Cárdenas, 2015). In contrast, species belonging to the remaining demosponge orders have a wide diversity of megascleres and microscleres (Morrow and Cárdenas, 2015; Botting et al., 2015).

Molecular studies, based on mitochondrial and some nuclear genes, divide the class Demospongiae into four main clades: G1: Keratosa; G2: Verongimorpha; G3: Haploscleromorpha (marine haplosclerids) and G4: Heteroscleromorpha (Lavrov et al., 2008; Sperling et al., 2010; Hill et al., 2013; Ma and Yang, 2016). Conversely, some studies using

* Corresponding author.
E-mail address: grace.mccormack@nuigalway.ie (G.P. McCormack).

https://doi.org/10.1016/j.ympev.2018.11.015
Received 27 July 2018; Received in revised form 26 October 2018; Accepted 19 November 2018

ribosomal data (18S rRNA and 28S rRNA) prefer to include Haploscleromorpha within Heteroscleromorpha (Thacker et al., 2013; Morrow et al., 2013; Morrow and Cárdenas, 2015) until more data is available. Relationships within the Haploscleromorpha are also largely unresolved due to large discrepancies between molecular data and the existing classification based on morphology (e.g. McCormack et al., 2002; Redmond et al., 2011). Some species are morphologically similar, even being placed within the same subgenus grouping via morphology (De Weerdt, 2002) e.g. *H. oculata* and *H. simulans* but belonging to two different clades via molecular data (Redmond et al., 2011). Therefore a major question remains regarding the relative importance of environmental versus genetic factors in shaping the skeleton in marine haplosclerids and other sponges. Here we set out to investigate the evolutionary patterns of the genes responsible for skeleton formation to investigate if they will provide any further insight into the evolution of morphologies in sponges and particularly the Haplosclerida.

The primary genes responsible for spicule formation in Demospongiae are silicateins, DNA sequences of which have been generated from a number of species to date (Cha et al., 1999; Pozzolini et al., 2004; Kaluzhnaya et al., 2007; Veremeichik et al., 2011). Silicateins are unique to sponges, are monophyletic and were shown to have evolved from cathepsins L, a family of proteases with varied functions in collagen degradation and ecdysis amongst others, though their role in sponges is still poorly known (Riesgo et al., 2015 and references therein). Fractal monomers of silicatein proteins form an axial filament, which is a proteinaceous core found inside the spicule (Shimizu et al., 1998; Murr and Morse, 2005; Wang et al., 2014) while silicatein also acts as an enzyme that condenses silica to form the spicule around the protein core (Wang et al., 2014). Silicatein proteins have two main components: an inhibitor, and a peptidase containing the active site (Brutchey and Morse, 2008). The aminoacid composition of silicatein is similar to that of cathepsins L but instead of a cysteine (C), the silicateins have a serine (S) that in conjunction with a histidine (H) and asparagine (N) forms the active site (SHN) responsible for silica condensation (Cha et al., 1999; Zhou et al., 1999; Fairhead et al., 2008; Schröder et al., 2012). A particular motif following the serine in the silicateins (-YAF) is also different from the cathepsins L (-WAF).

Silicateins are currently grouped into three different clades, i.e. beta silicateins, alpha and gamma silicateins and silicateins from freshwater sponges (Kaluzhnaya et al., 2007: Mohri et al., 2008; Veremeichik et al., 2011). The number of silicatein variants that are found in the axial filament can vary across species (e.g. alpha, beta and gamma silicatein variants are all present in *Tethya californiana,* but in *Suberites domuncula* just alpha and beta variants are present) (Cha et al., 1999; Brutchey and Morse, 2008). Another protein named silintaphin has been reported in the axial filament interacting with the silicatein-alpha in biosilica synthesis from *S. domuncula* (Schloßmacher et al., 2011).

Kozhemyako et al. (2010) sequenced a putative silicatein from *Latrunculia oparinae* that had a cysteine instead of a serine at the active site (characteristic of cathepsins-L), but contained the YAF motif instead of WAF (characteristic of silicateins). Riesgo et al. (2015) found another two of these unusual silicateins in the transcriptome of the haplosclerid *Petrosia ficiformis* and one silicatein variant also having a glutamine (Q) instead of a histidine (H) in the active site (CQN). Gauthier (2015) found one SHN, one SQN and four CHN variants in the genome of yet another haplosclerid, *A. queenslandica*. The phylogenetic position of all these sequences was determined to be within the overall silicatein clade but distinct from the three SHN silicatein variants of other demosponges, (Kozhemyako et al., 2010; Gauthier, 2015; Riesgo et al., 2015). Currently, it is unknown if the silicateins with CHN and C/SQN amino acid configurations function in spicule formation because the active site does not have all three amino acids thought to be necessary for silica condensation (SHN) (Shimizu et al., 1998; Zhou et al., 1999; Fairhead et al., 2008). It is also unknown how common these silicatein variants are in marine haplosclerid and other demosponge species. As a precursor to functional studies we sought to explore the types and phylogenetic relationships of the silicatein genes present in three Irish *Haliclona* species, which were chosen to represent three major haplosclerid clades (Redmond et al., 2011). With the affordable development of genomic technologies, several sponge genomes and transcriptomes from the four classes are now available for comparison (reviewed in Aguilar-Camacho and McCormack, 2017) and here we identify and investigate the evolution of all the silicatein variants and silintaphins in Porifera with particular focus on the evolution of these genes in marine haplosclerids.

2. Materials and methods

2.1. Generation of transcriptome data

RNA was extracted from specimens that are representatives of the three main molecular clades from the order Haplosclerida: A) *H. oculata* (two specimens), B) *H. simulans* (two specimens) and C) *H. indistincta* (three specimens). Small pieces were dissected under a microscope to remove associated material. The pieces were flash – frozen with LN2 and stored at −80 °C. RNA was extracted from the frozen specimens following the TriReagent protocol (Riesgo et al., 2014) and its quality and quantity was checked using a 2100 Bioanalyzer RNA Eukaryotic Chip before being sent to an external Illumina platform (MACROGEN, INC) to construct libraries using the TruSeq Stranded mRNA sample prep Kit V2. The HiSeq2000 platform (Illumina, USA) was used for pair end sequencing and three small libraries of *H. indistincta* (10 Mb), two of *H. oculata* (120 Mb) and two of *H. simulans* (120 Mb) were constructed and sequenced. Transcriptome data is openly available in Mendeley (doi:https://doi.org//10.17632/xx7hgd3dg2.1).

The quality of the reads was checked using the FASTQC software (Gordon and Hannon, 2010). FAST –X Clipper software was employed to trim sequence reads with low quality score (below 30) leaving only sequences > 70 bp. For each of the paired sequences *de novo* assemblies were carried out using the Trinity software to construct the contigs for each species (Haas et al., 2013). Contig assemblies were carried out using an ICHEC account (Irish Center of High End Computing) and the NUIG Bioinformatics server (School of Mathematics, Statistics and Applied Mathematics).

2.2. Gene identification

A reference fasta file (proteins) with all the silicateins and cathepsins-L from the genome of the sponge *A. queenslandica* was constructed (Srivastava et al., 2010, Fernandez-Valverde et al., 2015). The three assembled transcriptomes generated were blasted (blastx) manually against this database. Resulting hits were translated using the best Open Reading Frame and complete silicatein and cathepsins L sequences were used for further phylogenetic analysis. The same process was carried out for the available assembled genomes and transcriptomes from the COMPAGEN dataset (Hemmrich and Bosch, 2008): *Oscarella carmella* (Nichols et al., 2012), *Xestospongia testudinaria* (Ryu et al., 2016), *Stylissa carteri* (Ryu et al., 2016), *Sycon cilliatum* (Fortunato et al., 2014), *Leucoselonia complicata* (Fortunato et al., 2014), *Ephydatia muelleri* (Peña et al., 2016), *Haliclona tubifera* and *H. amboinensis* (Guzman and Conaco, 2016); the genome of *Tethya wilhelma* (Francis et al., 2017), as well as, the assembled transcriptomes from *Aphrocallistes vastus, P. ficiformis, Ircina fasciculata, Chondrilla caribensis* and *Corticium candelabrum, Pseudospongorites suberitoides, Spongilla lacustris* (Riesgo et al., 2014 Harvard Dataverse Network, doi:https://doi.org//10.7910/DVN/24737); *Latrunculia apicalis*, *Kirkpatrickia variolosa*, *Hyalonema populiferum*, *Rosella fibulata* and *Sympagella nux* (Whelan et al., 2015, doi:https://doi.org//10.6084/m9.figshare.1334306), *Halisarca dujardini* (Borisenko et al., 2016 http://www.ebi.ac.uk/ena/data/view/HADA01000001-HADA01138992), *E. fluviatilis* (Alié et al., 2015), *Mycale phyllophyla* (Qiu et al., 2015), *Cymbastela concentrica*, *Tedania anhelens* and *Scopalina* sp. (Díez-Vives et al., 2017 http://datadryad.org/

resource/doi:10.5061/dryad.7717q) and the unpublished assembled transcriptome of *Cinanchyrella* sp. (Joe Lopez). DNA sequences of complete silicateins from Genbank were also downloaded and included for phylogenetic analysis (Supplementary Table 1). In addition, the silintaphin gene from *S. domuncu*la was blasted (blastx) manually against the transcriptomes and genomes used in this study and the glassin gene from *Euplectella* sp. was blasted (blastx) against the four hexactinellid transcriptomes. Silintaphin and glassin data have been deposited in Mendeley (doi:https://doi.org//10.17632/xx7hgd3dg2.1).

2.3. Phylogenetic analysis of silicatein genes

Amino acid sequences were aligned with the SEAVIEW software (Gouy et al., 2010). The initial alignment contained 421 aminoacid sequences (149 silicateins and 272 cathepsins L). Due to the very high number of cathepsins L in the alignment, from initial trees and the existing knowledge of the origin of silicateins (Shimizu et al., 1998; Riesgo et al., 2015), we selected a monophyletic group of six cathepsins L sequences from haplosclerids as outgroup sequences to the silicatein clade. A conservative alignment strategy was employed where all the positions that were spuriously aligned were excluded (by deleting questionable sites and saving the 'reduced' alignment each time). We analyzed three nested datasets to explore the impact of taxon removal/addition to relationships within the phylogeny; the first contained all the sequences (155) with fewest characters (179) due to alignment difficulties and short sequences. The second dataset excluded the significantly shorter sequences (21) and therefore additional characters (313) from 133 sequences were obtained. Based on phylogenetic trees reconstructed from the second dataset, sequences were pruned that generated very long branches. In addition a new outgroup sequence was selected that was closer to the main ingroup and thus the cathepsins L sequences were also removed (18) (Supplementary Table 2). The resulting alignment contained 320 characters from 116 sequences and the alignments have also been deposited in Mendeley (doi:https://doi.org//10.17632/xx7hgd3dg2.1). ProtTest 2.4 Software (Abascal et al., 2005) was employed to find the best evolutionary model for each dataset and WAG was the best fitting evolutionary substitution model for all the three datasets analyzed. Five random starting trees using SPR and NNI were executed in PhyML 3.0 (Guindon et al., 2010) for each dataset and the tree with the best likelihood value was selected (4 rate classes). Bootstrap analysis using 1000 replicates was also performed. Bayesian Inference was estimated using Mr Bayes 3.2.1 (Ronquist and Huelsenbeck, 2003), two runs of over 3,000,000 were carried out with sampling every 100 generations. The appropriate burnin value was determined by examining the standard deviation of split frequencies (< 0.01). A 50% majority rule consensus tree was constructed from all generations sampled after the burnin. The branch supports from Mr. Bayes are shown as posterior probabilities (PP) and those from ML are in bootstrap proportions (BP) in the trees and text.

3. Results

3.1. Transcriptome data from Irish species

Summary statistics of the raw reads and the assembled transcriptomes from the three *Haliclona* species are presented in Supplementary Tables 3 and 4. A total of 48,520 contigs (N50 = 1596) were assembled for *H. indistincta*, 76, 641 contigs (N50 = 1286) for *H. simulans* and 94, 360 contigs (N50 = 1357) for *H. oculata*. The distribution of contig size was similar for the three transcriptomes assembled (Supplementary Table 5).

Four silicatein variants were present in *H. oculata* (type species of the genus and representative here of clade A). These included one of the SHN type and three different variants with the CHN motif at the active site. The same silicatein variants were recovered from *H. simulans* (representative here of clade B) while five silicateins were present in *H. indistincta* (representative of clade C). Variants from this latter species included one of the SHN type, but just two CHN types, one of which was much closer to cathepsins-L sequences than other silicateins. In addition, one silicatein of the CQN type and one of the SQN type were also recovered. No silintaphin homologs were found in the three transcriptomes from the Irish species.

3.2. Presence/absence of silicateins, silintaphins and glassin in other available data

Silicatein sequences were not present in any of the transcriptomes or genomes of hexactinellid, calcareous or homoscleromorph sponges. Furthermore, silicateins were not found in three transcriptomes from Demospongiae: *I. fasciculata, C. caribensis,* and *H. dujardini* (the first species belongs to the subclass Keratosa and the remaining two to Verongimorpha). Silicateins of the SHN type were found in all the remaining genomes and transcriptomes including haplosclerid sponges. However, few clear patterns emerged for the distribution of silicatein variants across taxonomic ranks and no silicatein variant was present in all sponges investigated.

All haplosclerids contained one sequence variant of the SHN type while the number present in freshwater sponges and heteroscleromorphas ranged from two in *L. apicalis* to nine in *E. muelleri*. Silicatein variants containing CHN at the active site were found in all haplosclerid species examined and in some but not all of the genomes and transcriptomes from freshwater sponges and heteroscleromorpha (i.e. *E. muelleri and E. fluviatilis, and S. carteri, T. wilhelma, M. phyllophyla, C. concentrica, T. anhelens* and *Cynanchyrella* sp.). In total, three different silicateins of this type were found in three haplosclerid species (*H. oculata, H.simulans* and *A. queenslandica*) while all other sponges showed the presence of only one or two CHN variants. One silicatein variant with the C/SQN in the active site was found exclusively in five haplosclerid genomes and transcriptomes (*H. indistincta, H. amboinensis, P. ficiformis, A. queenslandica* and *X. testudinaria*) while *H. indistincta* possessed two of these variants. The distribution of the diverse silicatein types across the phylum is summarized in Table 1.

Silintaphins were not found in the transcriptomes and genomes from marine haplosclerids but one homolog of this gene was present in the genomes and transcriptomes from all other Heteroscleromorpha including freshwater sponges. In addition, glassin was found in three out of the four hexactinellid transcriptomes (not found *H. populiferum*).

3.3. Phylogenetic relationships of silicateins

The majority of silicatein sequences were monophyletic (Fig. 1a and b). Trees drawn from the first and second datasets suggest that one "silicatein" from *H. indistincta* (*Haliclona_indistincta*5) was more closely related to the cathepsins L sequences rather to the remaining silicatein sequences (Supplementary Figs. 1 and 2). Six well-supported clades (SHNI, SHNII, CHNI, CHNII, CHNIII and C/SQN) were recovered in all trees and while removal of sequences did not significantly alter relationships between clades, bootstrap support was low via ML for some internal branches (Fig. 1, Supplementary Figs. 1 and 2). One clade of sequences with a CHN motif (CHNI) was a sister clade to all remaining silicateins while sequences of the SHN type evolved twice. Support of the monophyly of most clades is strong from ML and BI analyses (Fig. 1, Supplementary Figs. 1 and 2).

The most basal silicatein clade (CHNI) contained sequences from marine haplosclerids and freshwater sponges but none from the other heteroscleromorpha examined (Supplementary Fig. 1a and 2a). Fig. 2 indicates that only two groups of haplosclerids contained silicateins of this type, i.e. haplosclerid clades A and B (with *H. indistincta* and other haplosclerids missing the CHNI variant). The CHNII clade contained sequences from the full range of haplosclerid species from which data was available. Relationships between the haplosclerid sequences were what might be expected from other molecular data (i.e. clade A and B

Table 1
Number of the complete silicateins of the three types found in poriferan genomes and transcriptomes. + incomplete silicateins not included in analysis.

Species	SHN	CHN	C/SQN
HAPLOSCLERIDA			
Haliclona oculata	1	3	0
H. simulans	1	3	0
H. indistincta	1	2	2
Amphimedon queenslandica	1	3	1
Xestospongia testudinaria	1	2	1
H. tubifera	1	2	0
H. amboinensis	1	1	1
Petrosia ficiformis	1	2	1
HETEROSCLEROMORPHA			
Ephydatia muelleri	9	2	0
E. fluviatilis	7	2	0
Spongilla lacustris	6	0	0
Stylissa carteri +	2	1	0
Tehthya wilhelma	5	1	0
Latrunculia apicalis	2	0	0
Kirkpatrickia variolosa	3	0	0
Mycale phyllophyla	4	2	0
Cymbastela concentrica	5	1	0
Tedania anhelens	5	2	0
Scopalina sp	3	0	0
Cinanchyrella sp	5	2	0
Ircina fasciculata	0	0	0
Chondrilla caribensis	0	0	0
Halisarca dujardini	0	0	0
HOMOSCLEROMORPHA			
Oscarella carmella	0	0	0
Corticium candelabrum	0	0	0
HEXACTINELLIDA			
Aphrocallistes vastus	0	0	0
Hyalonema populiferum	0	0	0
Rosella fibulata	0	0	0
Sympagella nux	0	0	0
CALCAREA			
Sycon cilliatum	0	0	0
Leucoselonia complicata	0	0	0

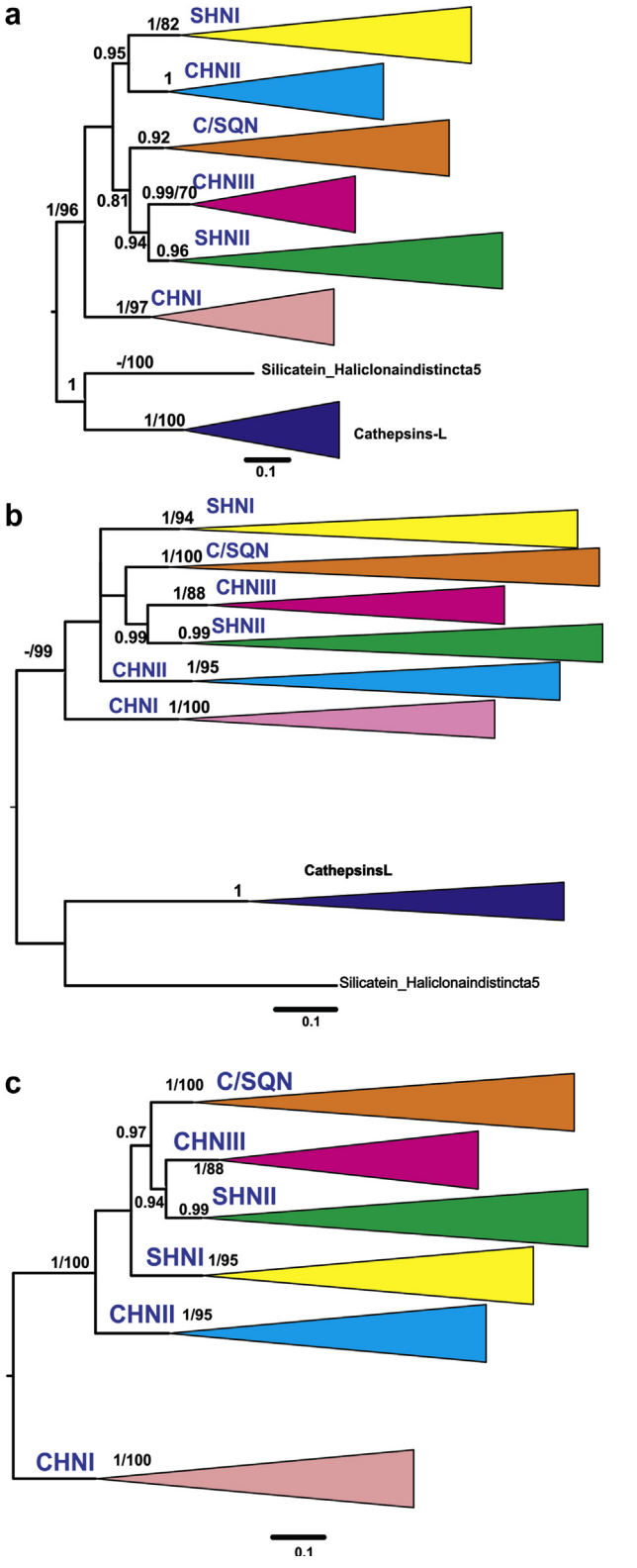

(caption on next page)

representatives as sister groups, and *H. indistincta* (clade C) sister taxon to clade of A + B). The data from fresh water sponges formed a sister clade to two representatives from the remaining heteroscleromorpha, i.e. *T.wilhelma*3 and *Latrunculia_oparinae*. The haplosclerida were also well represented in the CHNIII clade (present in six out of eight species included). No freshwater sponges were found that contained this variant and only two other demosponges were found to contain it, i.e. *Mycale* and *Cymbastela* (Fig. 2). The sequence of *Haliclonaindistincta*4, which fell into this clade, contained a Q (Glutamine) instead of a Histidine (H) (CQN type) at the active site.

The C/SQN clade only contained sequences from marine haplosclerids but this variant was not Supplementary Fig. 1b and 2b) universally present in this group. The sequences from *A. queenslandica*2 and *H. indistincta*3 had an SQN configuration, while the sequences from *H. amboinesis*2, *X.testudinaria*3 and *P. ficiformis*3 had a CQN configuration at the active site.

The SHNI clade, which can be defined as a silicatein beta clade due to the presence of the *Suberites* beta sequence contained sequences from freshwater sponges that formed a sister clade to a larger clade containing the Haplosclerida and the remaining Heteroscleromorpha. As with the CHN clades, relationships amongst the marine haplosclerid sequences followed an expected phylogenetic pattern, i.e. reflecting ribosomal and mitochondrial data (Fig. 2). The SHNII clade contained sequences that were characteristic of silicatein alpha and gamma, from Heteroscleromorpha including freshwater sponges but did not contain any sequences from haplosclerids (Fig. 3). Those from freshwater sponges were monophyletic and divided into six subclades. However multiple duplications of this gene is evident on Fig. 3 (and Supplementary Fig. 1b and 2b) with various copies of the gene forming small clades, e.g. sequences from Poecilosclerida were polyphyletic across four subclades, while the relationships between other sequences are unresolved, e.g. *Cinanchyrella*sp3, *Cinanchyrella*sp6, *Cinanchyrella*sp7, *Cymbastelaconcentrica*5. Three silicateins from the transcriptome from *Scopalina* sp formed a monophyletic subclade.

Fig. 1. Molecular phylogenetic trees reconstructed using silicatein data, a = all data, b = minus short sequences, c = minus cathepsins L (outgroup) sequences and those that generated very long branches. In the first and second datasets, cathepsins L were used as outgroup to root the tree while in the third dataset the CHNI clade was used as outgroup. For better clarity of the general relationships intraclade branches were collapsed and the six recovered clades labeled (CHNI, CHNII, CHIII, SHNI, SHNII, C/SQN). The best Log likelihood (ML) for the first tree was: − 19268.0428.; for the second tree: − 36357.3599 and for the third tree: − 34405.3319. The trees presented are those reconstructed using Mr. Bayes, which were congruent with those from PhyML. Support on the branches represent Bayesian posterior probability/maximum likelihood bootstrap proportions.

Sequences from *Tedaniaanhelens*2 and the hexactinellid *Aulosaccus* sp contained a CHN configuration at the active site but were found to cluster in the general SHNII clade rather than one of the CHN clades.

4. Discussion

Our study demonstrates a higher diversity of silicatein genes of the three types (CHN, SHN, C/SQN) in the transcriptomes and genomes of selected species belonging to the class Demospongiae than was previously recognized. Our results indicate a frequent duplication of the silicatein genes, which makes inferring their evolutionary relationships complex. We find the previous classification of silicatein genes into three main groups: beta, alpha/gamma and freshwater sponges (Mohri et al., 2008; Kozhemyako et al., 2010) to be too simple and instead show that the silicatein variants clustered into six major clades. Furthermore, the pattern of the phylogenetic trees generated indicates that CHN silicateins were the first to appear and are the more prevalent silicatein types in haplosclerid sponges.

CHN silicateins; While silicateins of the SHN type are reported to be necessary for silica condensation and thus spicule formation (Shimizu et al., 1998; Cha et al., 1999; Fairhead et al., 2008; Wang et al., 2014), we show that silicateins with CHN at the active site are common, have also diversified in demosponges bearing silica spicules and therefore are likely to have a role in forming spicules. Although, this needs further corroboration, a number of studies indicate a role for these silicatein types in spicule formation. For instance, silicatein transcripts of the CHN type were identified in the sclerocytes of juvenile *A. queenslandica* using whole mount in situ hybridization (Gauthier, 2015). Likewise, a recombinant silicatein of the CHN type from *L. oparinae* (named as a cathepsins by the authors, but clustered in clade CHNII) was able to precipitate hexahedral or octagonal silica nanoparticles in a medium with THEOS (Kamenev et al., 2015) and this variant was reported by Shkryl et al. (2016) as the second-most highly expressed gene among five silicateins using RT-qPCR. In addition, silicateins of the CHN type were the most highly expressed genes in *H. indistincta* adult specimens,

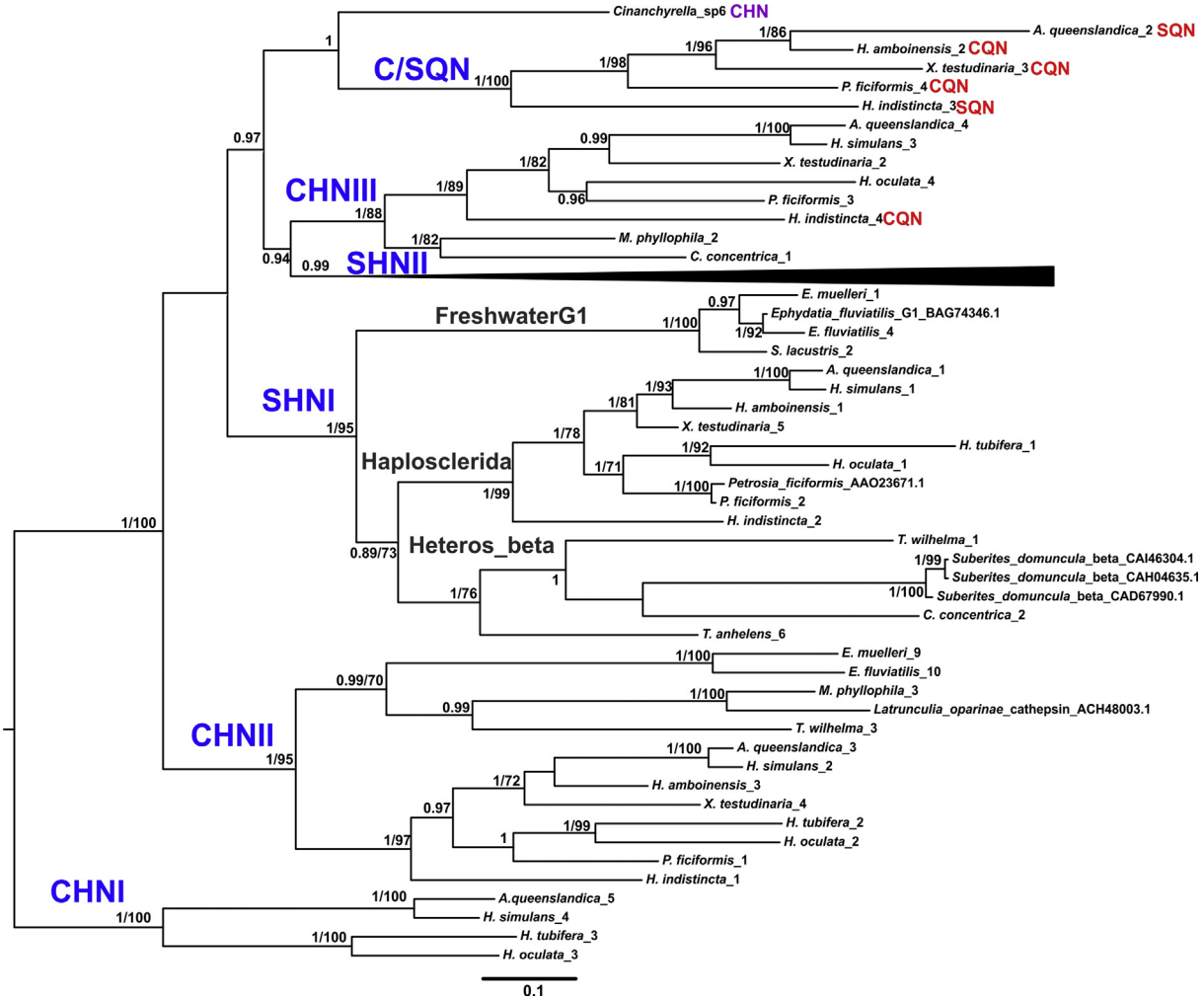

Fig. 2. Molecular phylogenetic tree from the final dataset showing relationships between sequences belonging to the CHN, CSQN and SHNI clades. Sequences from SHNII clade were collapsed for clarity. Silicatein variants SHNI and CHN are common in Haplosclerida but not as common in other demosponges investigated. The tree presented was reconstructed using Mr. Bayes, and was congruent with that from PhyML. Support on the branches represent Bayesian posterior probability/maximum likelihood bootstrap proportions.

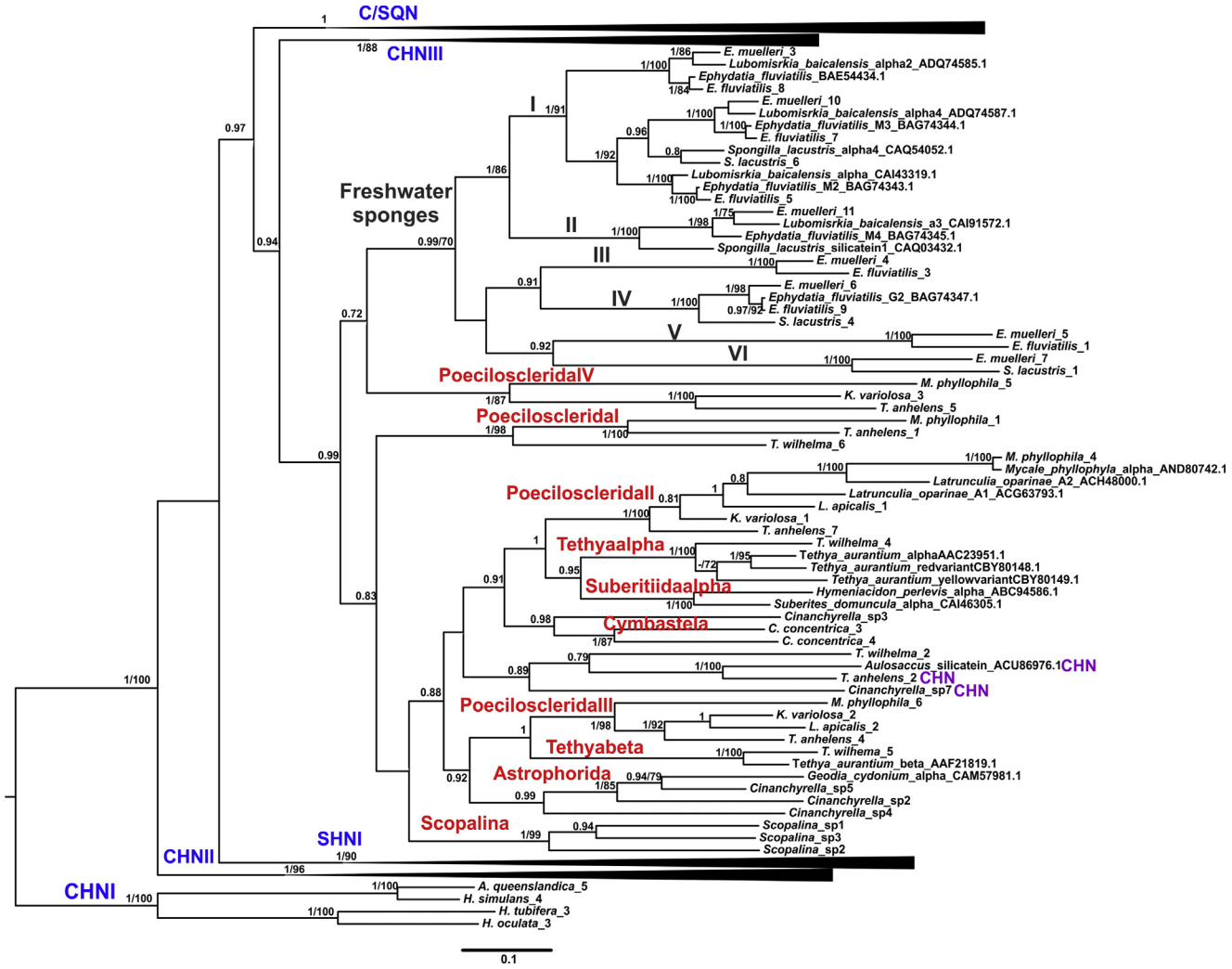

Fig. 3. Molecular phylogenetic tree from the final dataset showing the relationships between sequences of the SHII clade, other clades are collapsed for clarity. SHNII variants while absent in Haplosclerida have diversified in other Heteroslceromorpha. The tree presented was reconstructed using Mr. Bayes, and congruent with that from PhyML. Support on the branches represent Bayesian posterior probability/maximum likelihood bootstrap proportions.

and in the larval stage that produces spicules (Unpublished data). Therefore it is highly likely that silicatein variants with CHN at the active site can also condense silica and play a primary role in spicule formation in haplosclerid sponges.

Haplosclerid evolution: Given the arrangement of the silicatein variants on the phylogenies here it appears that CHN variants are the ancestral silicatein types and are commonly used silicateins in haplosclerids. Furthermore, *H. indistincta* contains perhaps an early silicatein form or a cathepsin/silicatein intermediate (*H. indistincta* belongs to clade C, a sister clade to the rest of the haplosclerids (Redmond et al., 2013)). When viewed together this data may suggest that the haplosclerid lineage was one of the first to acquire silicatein genes to form spicules when compared to Heteroscleromorpha and that some clade C species have retained older versions of silicatein copies.

The megascleres in haplosclerid species are confined to simple needle-like spicules similar to those found in some crown-group demosponge families, e.g. Hazelidae Walcott, 1920 (Li et al., 1998; Botting, 2003; Botting et al., 2013, 2015, 2017; Yang et al., 2017). We suggest that the simplicity of spicule morphology in marine haplosclerids could be due to the presence of only a single SHNI variant and the absence of the silintaphin gene. Different SHNII variants are differentially expressed in distinct spicule types in *E. fluviatilis* (Mohri et al., 2008) and silicatein alpha (missing in Haplosclerida) has been reported to have a role in the external shaping of spicules in *S. domuncula* (Müller et al., 2005). This data, especially when viewed in addition to the presence of multiple CHN copies in haplosclerids but not in other heterocleromorphs, provides support for a distinct Haploscleromorpha (Redmond et al., 2013) rather than haplosclerids being part of the Heteroscleromorpha.

The gene trees here reconstructed from orthologues of silicatein variants offer further support to existing molecular phylogenies of relationships within the Haplosclerida. While *H. simulans* sequences are consistently separated from those from *H. oculata* (both previously placed within the same subgenus) indicating a good deal of time since the species/clade separated, regrettably no taxon-specific variants of CHN or SHN were found nor indeed particular motifs in the silicatein variants, that would clearly explain taxonomic differences. It is likely that differences in expression of the variants, and/or epigenetic effects are responsible for the coincidental similarity in skeletal architecture. Much more work needs to be carried out now on functional and structural aspects of the silicatein variants, including different forms of CHN as well as C/SQN to further understand skeleton-formation in Haplosclerida, which in turn will assist in understanding more about the evolution of these enigmatic sponges.

Other sponges: No silicateins or silintaphins were found in the transcriptomes of the demosponges: *I. fasciculata, H. dujardini and C. caribensis*. The first species belongs to the subclass Keratosa in which the skeleton is formed of anastomosed spongin fibres lacking spicules

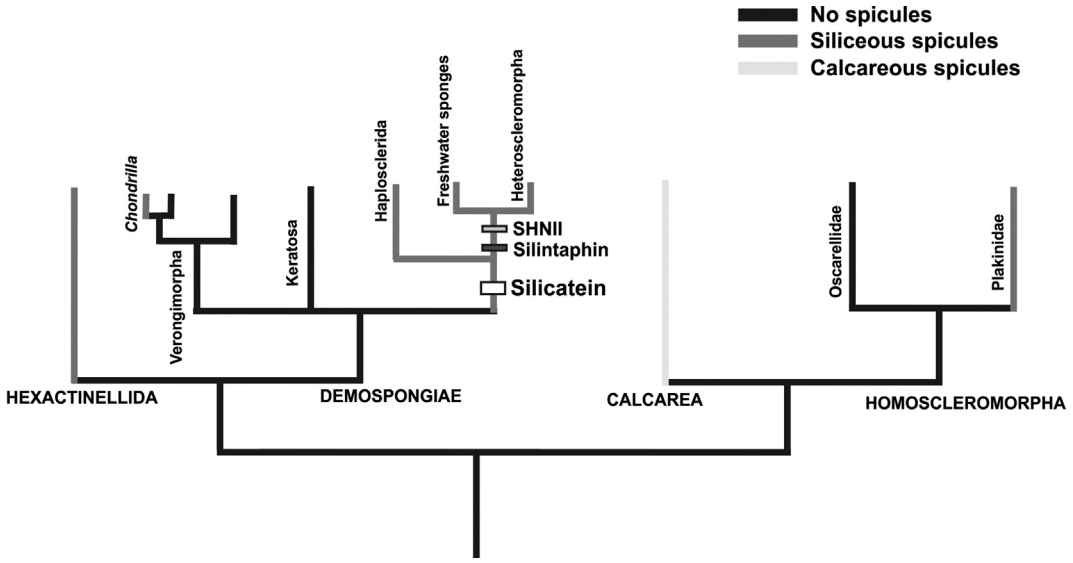

Fig. 4. A proposed cladogram (following Feuda et al. (2017)) showing a summary of our findings regarding the likely the acquisition of silicatein and silintaphin genes and the presence/absence of siliceous and calcareous spicules in the four sponge classes. While silicateins (SHNI type) first appear in Haplosclerida and some Heteroscleromorpha-proper, those of the SHNII type and silintaphins are absent in Haplosclerida. Silicateins-proper are not responsible for spicule formation in the demosponge *Chondrilla* (subclass Verongimorpha) or in Hexactinellid or Calcareous sponges with spicules. This cladogram also suggests that the last common ancestor of the Porifera had no spicules.

(Erpenbeck et al., 2012). The remaining two species belong to the subclass Verongimorpha: *H. dujardini* lacks spicules and the body is formed of fibrillar collagen while the body of *C. caribensis* is formed of nodular collagen but it does have silica microscleres (Redmond et al., 2013). These subclasses either form a monophyletic clade which is a sister to the remaining demosponges or Verongimorpha is a sister clade to Keratosa + other demosponges (Lavrov et al., 2008; Sperling et al., 2010; Hill et al., 2013; Redmond et al., 2013; Thacker et al., 2013). Given that silicateins were not identified here from these subclasses it is possible that the last common ancestor of Demospongiae had no spicules and silicatein genes were acquired exclusively in demosponges that contain spicules formed by these proteins. Fossil data, biomarkers and molecular clock analyses support this hypothesis by indicating that demosponges existed through the terminal of the Neoproterozoic era prior to the earliest biomineralizing fossil sponge record (Love et al., 2009; Sperling et al., 2010; Erwin et al., 2011; Antcliffe 2013; Yin et al., 2015; Gold et al., 2016; Chang et al., 2017; Botting and Muir, 2018). In this scenario, an as yet unknown protein is responsible for forming the oxyspherasters in species belonging to the family Chondrillidae (Fig. 4).

The picture becomes more complicated however, given that Kozhemyako et al. (2010) and Riesgo et al. (2015) reported the presence of 'silicateins' in the keratose and spicule-free species *Acanthodendrilla* sp and *Spongia lamella* respectively. The silicatein sequences of both species are incomplete (that from *S. lamellae* comprising of just a few amino acids) and were not included in our analysis. However, a phylogenetic tree reconstructed via neighbor-joining, which included the short sequence from *Acanthodendrilla* sp. showed it clustered in the SHNII clade. Given that the subclass Keratosa is more distantly related to the main heteroscleromorpha, than haplosclerids or freshwater sponges, we might expect that their silicateins would be distinct. Finding this short sequence clustering well inside the SHNII clade raises questions as to whether the silicateins reported from *Acanthodendrilla* sp. originate from another sponge species co-located with the specimen at the moment of collection or laboratory contamination. Given that the sequences are so short however and not having any further information on the specimens we cannot be sure. Therefore, confirming the presence/absence of silicateins in more spicule-less species would be very informative.

Silicateins were not found in the four transcriptomes from hexactinellids and two genomes from calcareous sponges which is not surprising given that calcareous sponges have spicules made of calcium carbonate and various carbonic anhydrases are the main proteins responsible for this process, while glassin is the main protein for the siliceous skeletal system in the hexactinellid *Euplectella* sp. (Voigt et al., 2014, 2017; Shimizu et al., 2015). Silicateins were previously reported however, in three hexactinellid species using molecular cloning approaches (Müller et al., 2008; Veremeichik et al., 2011). The sequence of *Crateromorpha meyeri* was incomplete and not included in our analysis while the sequences of *Aulosaccus* sp. and *Euplectella aspergillum* were included (clustered in the SHNII clade). We could assume that hexactinellid sequences should be distantly related to demosponge silicateins given the evolutionary distances and the divergence already noted amongst silicateins in the phylogenetic trees seen here. There are a number of possibilities for this result including that these short sequences might also represent contamination (a notorious issue for sponges), the gene fragments could represent cathepsin-like genes rather than silicateins and/or their position could be artifacts of the analyses due to their short length. Of course, silicateins could also be present in the genomes but not expressed (and so absent from the transcriptomes we examined), and perhaps even in a degenerated form, either case making it highly unlikely that they are responsible for skeleton formation in these sponges. The recently sequenced genome of *Oopsacas minuta,* is reported to also lack classic silicatein sequences (SYAF) but does contain many cathepsins and a single silicatein/cathepsin with a CYAF amino acid pattern (Jean-Michel Claverie, personal communication). No silicateins were found in the two transcriptomes from homoscleromorpha (*Oscarella carmela* and *Corticium candelabrum*) and currently, the protein responsible for spicule formation in members of this group that do have siliceous spicules is unknown (Maldonado and Riesgo, 2007; Riesgo et al., 2015). From our data it seems likely that the molecular mechanisms for spicule formation have evolved multiple times in sponges and perhaps the last common ancestor of Porifera had no spicules (Fig. 4).

Acknowledgements

This research did not receive any specific grant from funding agencies in the public, commercial, or not-for-profit sectors. JMAC is

funded by a Hardiman Scholarship (National University of Ireland Galway (NUIG) and the transcriptomes were sequenced thanks to the Thomas Crawford Award Scheme to JMAC funded by NUIG. Ana Riesgo, Sandie Degnan, Selene Fernandez-Valverde, Joe Lopez, Alexander Alie, Noriko Funayama and Warren Francis shared their assembled transcriptomes from some selected species. Sean D. McCarthy helped in the RNA extraction. Zixia Huang, Simon Chong, Cathal Seoighe and Tim Downing assisted in the bioinformatics analysis. We would also like to thank the two reviewers that helped us significantly improve the manuscript.

Appendix A. Supplementary material

Supplementary data to this article can be found online at https://doi.org/10.1016/j.ympev.2018.11.015.

References

Abascal, F., Zardoya, R., Posada, D., 2005. ProtTest: selection of best-fit models of protein evolution. Bioinformatics 21 (9), 2104–2105.

Aguilar-Camacho, J.M., McCormack, G.P., 2017. Molecular responses of sponges to climate change. In: Climate Change, Ocean Acidification and Sponges. Springer, Cham, pp. 79–104.

Alié, A., Hayashi, T., Sugimura, I., Manuel, M., Sugano, W., Mano, A., Sato, N., Agata, K., Funayama, N., 2015. The ancestral gene repertoire of animal stem cells. Proc. Natl. Acad. Sci. U.S.A. 112 (51), E7093–E7100.

Antcliffe, J.B., 2013. Questioning the evidence of organic compounds called sponge biomarkers. Palaeontology 56 (5), 917–925.

Borisenko, I., Adamski, M., Ereskovsky, A., Adamska, M., 2016. Surprisingly rich repertoire of Wnt genes in the demosponge Halisarca dujardini. BMC Evol. Biol. 16 (1), 123.

Botting, J.P., 2003. *Cyathophycus* and the origin of demosponges. Lethaia 36 (4), 335–343.

Botting, J.P., Cárdenas, P., Peel, J.S., 2015. A crown-group demosponge from the early Cambrian Sirius Passet Biota. North Greenland. Palaeontology 58 (1), 35–43.

Botting, J.P., Muir, L.A., 2018. Early sponge evolution: a review and phylogenetic framework. Palaeoworld 27 (1), 1–29.

Botting, J.P., Muir, L.A., Lin, J.P., 2013. Relationships of the Cambrian protomonaxonida (Porifera). Palaeontol. Electronica 16 (2), 1–23.

Botting, J.P., Zhang, Y., Muir, L.A., 2017. Discovery of missing link between demosponges and hexactinellids confirms palaeontological model of sponge evolution. Sci. Rep. 7 (1), 5286.

Brutchey, R.L., Morse, D.E., 2008. Silicatein and the translation of its molecular mechanism of biosilicification into low temperature nanomaterial synthesis. Chem. Revs. 108 (11), 4915–4934.

Cha, J.N., Shimizu, K., Zhou, Y., Christiansen, S.C., Chmelka, B.F., Stucky, G.D., Morse, D.E., 1999. Silicatein filaments and subunits from a marine sponge direct the polymerization of silica and silicones in vitro. Proc. Natl. Acad. Sci. U.S.A. 96 (2), 361–365.

Chang, S., Feng, Q., Clausen, S., Zhang, L., 2017. Sponge spicules from the lower Cambrian in the Yanjiahe Formation, South China: the earliest biomineralizing sponge record. Palaeogeogr.y Palaeoclim. Palaeoecol. 474, 36–44.

De Weerdt, W.H., 2002. Family Chalinidae Gray, 1867. In: Systema Porifera. Springer, Boston, MA, pp. 852–873.

Díez-Vives, C., Moitinho-Silva, L., Nielsen, S., Reynolds, D., Thomas, T., 2017. Expression of eukaryotic-like protein in the microbiome of sponges. Mol. Ecol. 26 (5), 1432–1451.

Erpenbeck, D., Sutcliffe, P., Cook, S.D.C., Dietzel, A., Maldonado, M., van Soest, R.W., Hooper, J.N.A., Wörheide, G., 2012. Horny sponges and their affairs: on the phylogenetic relationships of keratose sponges. Mol. Phylogenet. Evol. 63 (3), 809–816.

Erwin, D.H., Laflamme, M., Tweedt, S.M., Sperling, E.A., Pisani, D., Peterson, K.J., 2011. The Cambrian conundrum: early divergence and later ecological success in the early history of animals. Science 334 (6059), 1091–1097.

Fairhead, M., Johnson, K.A., Kowatz, T., McMahon, S.A., Carter, L.G., Oke, M., Liu, H., Naismith, J.H., van der Walle, C.F., 2008. Crystal structure and silica condensing activities of silicatein α–cathepsin L chimeras. Chem. Commun. 15, 1765–1767.

Fernandez-Valverde, S.L., Calcino, A.D., Degnan, B.M., 2015. Deep developmental transcriptome sequencing uncovers numerous new genes and enhances gene annotation in the sponge *Amphimedon queenslandica*. BMC Genom. 16 (1), 387.

Fortunato, S.A., Adamski, M., Ramos, O.M., Leininger, S., Liu, J., Ferrier, D.E., Adamska, M., 2014. Calcisponges have a ParaHox gene and dynamic expression of dispersed NK homeobox genes. Nature 514 (7524), 620.

Francis, W.R., Eitel, M., Vargas, S., Adamski, M., Haddock, S.H., Krebs, S., Blum, H., Erpenbeck, D., Wörheide, G., 2017. The genome of the contractile demosponge Tethya wilhelma and the evolution of metazoan neural signalling pathways. bioRxiv. https://doi.org/10.1101/120998.

Feuda, R., Dohrmann, M., Pett, W., Philippe, H., Rota-Stabelli, O., Lartillot, N., Wörheide, G., Pisani, D., 2017. Improved modeling of compositional heterogeneity supports sponges as sister to all other animals. Curr. Biol. 27 (24), 3864–3870.

Gauthier, A., 2005. Analysis of Silicatein Gene Expression and Spicule Formation in the Demosponge *Amphimedon queenslandica* (MS thesis). The University of Queensland, pp. 84.

Gazave, E., Lapébie, P., Ereskovsky, A.V., Vacelet, J., Renard, E., Cárdenas, P., Borchiellini, C., 2012. No longer Demospongiae: Homoscleromorpha formal nomination as a fourth class of Porifera. Hydrobiologia 687 (1), 3–10.

Gold, D.A., Grabenstatter, J., de Mendoza, A., Riesgo, A., Ruiz-Trillo, I., Summons, R.E., 2016. Sterol and genomic analyses validate the sponge biomarker hypothesis. Proc. Natl. Acad. Sci. U.S.A. 113 (10), 2684–2689.

Gordon, A., Hannon, G.J., 2010. Fastx-toolkit. FASTQ/A short-reads preprocessing tools (unpublished) http://hannonlab.cshl.edu/fastx_toolkit, 5.

Gouy, M., Guindon, S., Gascuel, O., 2010. SeaView version 4: a multiplatform graphical user interface for sequence alignment and phylogenetic tree building. Mol. Biol. Evol. 27 (2), 221–224.

Guindon, S., Dufayard, J.F., Lefort, V., Anisimova, M., Hordijk, W., Gascuel, O., 2010. New algorithms and methods to estimate maximum-likelihood phylogenies: assessing the performance of PhyML 3.0. Syst. Biol. 59 (3), 307–321.

Guzman, C., Conaco, C., 2016. Comparative transcriptome analysis reveals insights into the streamlined genomes of haplosclerid demosponges. Sci. Rep. 6, 18774.

Haas, B.J., Papanicolaou, A., Yassour, M., Grabherr, M., Blood, P.D., Bowden, J., MacManes, M.D., 2013. De novo transcript sequence reconstruction from RNA-seq using the Trinity platform for reference generation and analysis. Nat. Prot. 8 (8), 1494–1512.

Hemmrich, G., Bosch, T.C., 2008. Compagen, a comparative genomics platform for early branching metazoan animals, reveals early origins of genes regulating stem-cell differentiation. Bioessays 30 (10), 1010–1018.

Hill, M.S., Hill, A.L., Lopez, J., Perterson, K.J., Pomponi, S., Diaz, M.C., Thacker, R.W., Adamska, M., Boury-Esnault, N., Cárdenas, P., Chaves-Fonnegra, A., Danka, E., De Laine, B., Formica, D., Hajdu, E., Lobo-Hajdu, G., Klontz, S., Morrow, C.C., Patel, J., Picton, B., Pisani, D., Pohlmann, D., Redmond, N.E., Reed, J., Richie, S., Riesgo, A., Rubin, E., Russell, Z., Rützler, K., Sperling, E.A., di Stefano, M., Tarver, J.D., Collins, A.G., 2013. Reconstruction of family level phylogenetic relationships within Demospongiae (Porifera) using nuclear encoded housekeeping genes. Public Library of Science. PLOS One 8 (1), e50437.

Hooper, J.N., Van Soest, R.W.M., 2002. Systema Porifera. A Guide to the Classification of Sponges. Springer, Boston, MA.

Kaluzhnaya, O.V., Belikova, A.S., Podolskaya, E.P., Krasko, A.G., Müller, W.E.G., Belikov, S.I., 2007. Identification of silicateins in freshwater sponge *Lubomirskia baicalensis*. Mol. Biol. 41 (4), 554–561.

Kalyuzhnaya, O.V., Krasko, A.G., Grebenyuk, V.A., Itskovich, V.B., Semiturkina, N.A., Solovarov, I.S., Müller, W.E.G., Belikov, S.I., 2011. Freshwater sponge silicateins: comparison of gene sequences and exon-intron structure. Mol. Biol. 45 (4), 617–626.

Kamenev, D.G., Shkryl, Y.N., Veremeichik, G.N., Golotin, V.A., Naryshkina, N.N., Timofeeva, Y.O., Kovalchuk, S.N., Semiletova, I.V., Bulgakov, V.P., 2015. Silicon Crystals Formation Using Silicatein-Like Cathepsin of Marine Sponge *Latrunculia oparinae*. J. Nanosci. Nanotechnol. 15 (12), 10046–10049.

Kozhemyako, V.B., Veremeichik, G.N., Shkryl, Y.N., Kovalchuk, S.N., Krasokhin, V.B., Rasskazov, V.A., Zhuravlev, Y.N., Bulgakov, V.P., Kulchin, Y.N., 2010. Silicatein genes in spicule-forming and nonspicule-forming Pacific demosponges. Mar. Biotechnol. 12 (4), 403–409.

Lendenfeld, R.V., 1887. On the systematic position and classification of sponges. Proc. Zool. Soc. Lond. 1886, 558–662.

Lavrov, D.V., Wang, X., Kelly, M., 2008. Reconstructing ordinal relationships in the Demospongiae using mitochondrial genomic data. Mol. Phylogenet. Evol. 49 (1), 111–124.

Li, C.W., Chen, J.Y., Hua, T.E., 1998. Precambrian sponges with cellular structures. Science 279 (5352), 879–882.

Love, G.D., Grosjean, E., Stalvies, C., Fike, D.A., Grotzinger, J.P., Bradley, A.S., Kelly, A.E., Bhatia, M., Meredith, W., Snape, C.E., Bowring, S.A., Condon, D.J., Summons, R.E., 2009. Fossil steroids record the appearance of Demospongiae during the Cryogenian period. Nature 457 (7230), 718–721.

Ma, J.Y., Yang, Q., 2016. Early divergence dates of demosponges based on mitogenomics and evaluated fossil calibrations. Palaeoworld 25 (2), 292–302.

Maldonado, M., Riesgo, A., 2007. Intra-epithelial spicules in a homosclerophorid sponge. Cell Tissue Res. 328 (3), 639–650.

Mohri, K., Nakatsukasa, M., Masuda, Y., Agata, K., Funayama, N., 2008. Toward understanding the morphogenesis of siliceous spicules in freshwater sponge: Differential mRNA expression of spicule-type-specific silicatein genes in *Ephydatia fluviatilis*. Dev. Dyn. 237 (10), 3024–3039.

McCormack, G.P., Erpenbeck, D., Van Soest, R.W.M., 2002. Major discrepancy between phylogenetic hypotheses based on molecular and morphological criteria within the Order Haplosclerida (Phylum Porifera: Class Demospongiae). J. Zool. Syst. Evol. Res. 40 (4), 237–240.

Morrow, C.C., Redmond, N.E., Picton, B.E., Thacker, R.W., Collins, A.G., Maggs, C.A., Sigwart, J.D., Allcock, A.L., 2013. Molecular phylogenies support homoplasy of multiple morphological characters used in the taxonomy of Heteroscleromorpha (Porifera: Demospongiae). Integr. Comp. Biol. 53 (3), 428–446.

Morrow, C., Cárdenas, P., 2015. Proposal for a revised classification of the Demospongiae (Porifera). Front. Zool. 12 (1), 7.

Müller, W.E., Rothenberger, M., Boreiko, A., Tremel, W., Reiber, A., Schröder, H.C., 2005. Formation of siliceous spicules in the marine demosponge *Suberites domuncula*. Cell Tissue Res. 321 (2), 285–297.

Müller, W.E., Wang, X., Kropf, K., Boreiko, A., Schloßmacher, U., Brandt, D., Schröder, H.C., Wiens, M., 2008. Silicatein expression in the hexactinellid Crateromorpha meyeri: the lead marker gene restricted to siliceous sponges. Cell Tissue Res. 333 (2), 339–351.

Murr, M.M., Morse, D.E., 2005. Fractal intermediates in the self-assembly of silicatein

filaments. Proc. Natl. Acad. Sci. U.S.A. 102 (33), 11657–11662.
Nichols, S.A., Roberts, B.W., Richter, D.J., Fairclough, S.R., King, N., 2012. Origin of metazoan cadherin diversity and the antiquity of the classical cadherin/β-catenin complex. Proc. Natl. Acad. Sci. U.S.A. 109 (32), 13046–13051.
Peña, J.F., Alié, A., Richter, D.J., Wang, L., Funayama, N., Nichols, S.A., 2016. Conserved expression of vertebrate microvillar gene homologs in choanocytes of freshwater sponges. EvoDevo 7 (1), 13.
Pozzolini, M., Sturla, L., Cerrano, C., Bavestrello, G., Camardella, L., Parodi, A.M., Raheli, F., Benatti, U., Müller, W.E.G., Giovine, M., 2004. Molecular cloning of silicatein gene from marine sponge Petrosia ficiformis (Porifera, Demospongiae) and development of primmorphs as a model for biosilicification studies. Mar. Biotechnol. 6 (6), 594–603.
Qiu, F., Ding, S., Ou, H., Wang, D., Chen, J., Miyamoto, M.M., 2015. Transcriptome Changes during the Life Cycle of the Red Sponge, *Mycale phyllophila* (Porifera, Demospongiae, Poecilosclerida). Genes 6 (4), 1023–1052.
Redmond, N.E., Morrow, C.C., Thacker, R.W., Diaz, M.C., Boury-Esnault, N., Cárdenas, P., Hajdu, E., Lôbo-Hajdu, G., Picton, B.E., Pomponi, S.A., Kayal, E., Collins, A.G., 2013. Phylogeny and systematics of Demospongiae in light of new small-subunit ribosomal DNA (18S) sequences. Integr. Comp. Biol. 53, 388–415.
Redmond, N.E., Raleigh, J., van Soest, R.W., Kelly, M., Travers, S.A., Bradshaw, B., Vartia, S., Stephens, K., McCormack, G.P., 2011. Phylogenetic relationships of the marine Haplosclerida (Phylum Porifera) employing ribosomal (28S rRNA) and mitochondrial (cox1, nad1) gene sequence data. PLoS One 6 (9), e24344.
Riesgo, A., Farrar, N., Windsor, P.J., Giribet, G., Leys, S.P., 2014. The analysis of eight transcriptomes from all poriferan classes reveals surprising genetic complexity in sponges. Mol. Biol., Evol, msu057.
Riesgo, A., Maldonado, M., López-Legentil, S., Giribet, G., 2015. A proposal for the evolution of cathepsin and silicatein in sponges. J. Mol. Evol. 80 (5–6), 278–291.
Ronquist, F., Huelsenbeck, J.P., 2003. MrBayes 3: Bayesian phylogenetic inference under mixed models. Bioinformatics 19 (12), 1572–1574.
Ryu, T., Seridi, L., Moitinho-Silva, L., Oates, M., Liew, Y.J., Mavromatis, C., Wang, X., Haywood, A., Lafi, F.F., Kupresanin, M., Sougrat, R., Alzahrani, M.A., Giles, E., Ghosheh, Y., Shunter, C., Baumgarten, S., Berumen, M.L., Gao, X., Aranda, M., Foret, S., Gough, J., Voolstra, C.R., Henstchel, U., Ravasi, T., 2016. Hologenome analysis of two marine sponges with different microbiomes. BMC Genom. 17 (1), 158.
Schloßmacher, U., Wiens, M., Schröder, H.C., Wang, X., Jochum, K.P., Müller, W.E., 2011. Silintaphin1–interaction with silicatein during structure-guiding biosilica formation. FEBS J. 278 (7), 1145–1155.
Schröder, H.C., Wiens, M., Schloßmacher, U., Brandt, D., Müller, W.E., 2012. Silicatein-mediated polycondensation of orthosilicic acid: modeling of a catalytic mechanism involving ring formation. Silicon 4 (1), 33–38.
Shimizu, K., Amano, T., Bari, M.R., Weaver, J.C., Arima, J., Mori, N., 2015. Glassin, a histidine-rich protein from the siliceous skeletal system of the marine sponge *Euplectella*, directs silica polycondensation. Proc. Natl. Acad. Sci. U.S.A. 112 (37), 11449–11454.
Shimizu, K., Cha, J., Stucky, G.D., Morse, D.E., 1998. Silicatein α: cathepsin L-like protein in sponge biosilica. Proc. Natl. Acad. Sci. U.S.A. 95 (11), 6234–6238.
Shkryl, Y.N., Bulgakov, V.P., Veremeichik, G.N., Kovalchuk, S.N., Kozhemyako, V.B., Kamenev, D.G., Semiletova, I.V., Timofeeva, Y.O., Scchipunov, Y.A., Kulchin, Y.N., 2016. Bioinspired enzymatic synthesis of silica nanocrystals provided by recombinant silicatein from the marine sponge *Latrunculia oparinae*. Bioprocess Biosyst. Eng. 39 (1), 53–58.
Soest, R.W., 2017. *Flagellia*, a new subgenus of *Haliclona* (Porifera Haplosclerida). Eur. J. Taxon. 351.
Sperling, E.A., Robinson, J.M., Pisani, D., Peterson, K.J., 2010. Where's the glass? Biomarkers, molecular clocks, and microRNAs suggest a 200–Myr missing Precambrian fossil record of siliceous sponge spicules. Geobiology 8 (1), 24–36.
Srivastava, M., Simakov, O., Chapman, J., Fahey, B., Gauthier, M.E., Mitros, T., Richards, G.S., Conaco, C., Dacre, M., Hellsten, U., Larroux, C., Putnam, N.H., Stanke, M., Adamska, M., Darling, A., Degnan, S.M., Oakley, T.H., Plachetzki, D.C., Zhai, Y., Adamski, M., Calcino, A., Cummins, S.F., Goodstein, D.M., Harris, C., Jackson, D.J., Leys, S.P., Shu, S., Woodcroft, B.J., Vervoort, M., Kosik, K.S., Manning, G., Degnan, B.M., Rokhsar, D.S., 2010. The *Amphimedon queenslandica* genome and the evolution of animal complexity. Nature 466 (7307), 720–726.
Thacker, R.W., Hill, A.L., Hill, M.S., Redmond, N.E., Collins, A.G., Morrow, C.C., Spicer, L., Carmack, C., Zappe, M.E., Pohlmann, D., Hall, C., Diaz, M.C., Bangalore, P.V., 2013. Nearly complete 28S rRNA gene sequences confirm new hypotheses of sponge evolution. Integr. Comp. Biol. 53 (3), 373–387.
Veremeichik, G.N., Shkryl, Y.N., Bulgakov, V.P., Shedko, S.V., Kozhemyako, V.B., Kovalchuk, S.N., Krasokhin, V.B., Zhuralev, Y.N., Kulchin, Y.N., 2011. Occurrence of a silicatein gene in glass sponges (Hexactinellida: Porifera). Mar. Biotechnol. 13 (4), 810–819.
Voigt, O., Adamska, M., Adamski, M., Kittelmann, A., Wencker, L., Wörheide, G., 2017. Spicule formation in calcareous sponges: coordinated expression of biomineralization genes and spicule-type specific genes. Sci. Rep. 7, 45658.
Voigt, O., Adamski, M., Sluzek, K., Adamska, M., 2014. Calcareous sponge genomes reveal complex evolution of α-carbonic anhydrases and two key biomineralization enzymes. BMC Evol. Biol. 14, 230.
Wang, X., Schröder, H.C., Müller, W.E., 2014. Enzyme-based biosilica and biocalcite: biomaterials for the future in regenerative medicine. Trends Biotechnol. 32 (9), 441–447.
Whelan, N.V., Kocot, K.M., Moroz, L.L., Halanych, K.M., 2015. Error, signal, and the placement of Ctenophora sister to all other animals. Proc. Natl. Acad. Sci. U.S.A. 112 (18), 5773–5778.
Wörheide, G., Dohrmann, M., Erpenbeck, D., Larroux, C., Maldonado, M., Voigt, O., Borchiellini, C., Lavrov, D.V., 2012. Deep phylogeny and evolution of sponges (phylum porifera). Adv. Mar. Biol. 61, 1–78.
Yang, X.L., Zhao, Y.L., Babcock, L.E., Peng, J., 2017. Siliceous spicules in a vauxiid sponge (Demospongia) from the Kaili Biota (Cambrian Stage 5), Guizhou, South China. Sci. Rep. 7, 42945.
Yin, Z., Zhu, M., Davidson, E.H., Bottjer, D.J., Zhao, F., Tafforeau, P., 2015. Sponge grade body fossil with cellular resolution dating 60 Myr before the Cambrian. Proc. Natl. Acad. Sci. U.S.A. 112 (12), E1453–E1460.
Zhou, Y., Shimizu, K., Cha, J.N., Stucky, G.D., Morse, D.E., 1999. Efficient catalysis of polysiloxane synthesis by silicatein α requires specific hydroxy and imidazole functionalities. Angew. Chem. 38 (6), 779–782.

Chapter 4
Molecular Responses of Sponges to Climate Change

Jose Maria Aguilar-Camacho and Grace P. McCormack

Abstract We live in a time of concern regarding predicted environmental damage due to climate change, i.e. sea temperature increase and a reduction in ocean pH. Such changes will have severe consequences for at least some marine organisms. Developments in molecular and genomic techniques allow for genome-wide comparisons of genes and proteins that may be impacted by such changes with knock-on consequences for cell and organism function. Understanding of impacts at the molecular level is important to understand how organisms will respond to changes and to develop conservation strategies accordingly. Despite sponges having a very simple body plan, they possess gene diversity and genome complexity that mirrors other metazoa. The cellular stress response and adaptation of sponges to increased temperature and low pH are varied and diverse with many genes implicated and their expression patterns complex. Survival thresholds differ between species in their tolerance to temperature increase and lowering of ocean pH. The expression patterns of a variety of genes have been investigated particularly with regard to change in temperature but in few sponge species. Likewise genome and transcriptome data exists for few species, and even fewer studies focus on applying these approaches to stress response. Despite the requirement for more studies in this area, existing data suggests that some sponge species will be severely impacted if climate change predictions hold, while other species will adapt and thrive.

Keywords Sponges • Climate change • Gene expression • Genomics • Epigenetics

J.M. Aguilar-Camacho • G.P. McCormack (✉)
Zoology, School of Natural Sciences and Ryan Institute, National University of Ireland Galway, University Rd., Galway, Ireland
e-mail: grace.mccormack@nuigalway.ie

J.L. Carballo, J.J. Bell (eds.), *Climate Change, Ocean Acidification and Sponges*,
DOI 10.1007/978-3-319-59008-0_4

4.1 Introduction

Sponges (phylum Porifera) are important elements of bottom communities globally, both in marine and freshwater habitats (Bell 2008). They form a large portion of the biomass on coral reefs in sensitive habitats, in deep-sea environments, and also are common members of intertidal and subtidal communities. Essentially nonmotile as adults, these animals are filter feeders drawing in significant volumes of surrounding water from which to select organic material and dissolved nutrients, e.g. a 1 kg sponge can reportedly filter 24,000 L of seawater per day (Vogel 1977). Instead of the digestive, osmoregulatory and excretory organs that are found in most other animal phyla, sponges have evolved a unique aquiferous system through which they obtain food, release waste and obtain oxygen. Inside the majority of sponges is a maze of canals and small chambers connected by the mesohyl (a matrix of cells, collagen, spicule skeleton and where present symbionts/associated microorganisms). The canals are lined with choanocytes, which, via the beating of their flagella, draw in water through pores on the sponge surface (called ostia). This water travels through incurrent canals to the chambers and out via larger excurrent canals and oscula (Bergquist 1978; Leys and Hill 2012). As such almost the entire internal sponge body is also exposed to the external aqueous environment (Fig. 4.1a, b). This factor in addition to the fact that sponges do not move very much makes them potentially very vulnerable to any changes in their immediate environment.

Patterns of gene expression when integrated with organismal functional performance under normal and stressed situations can inform conservation strategies as

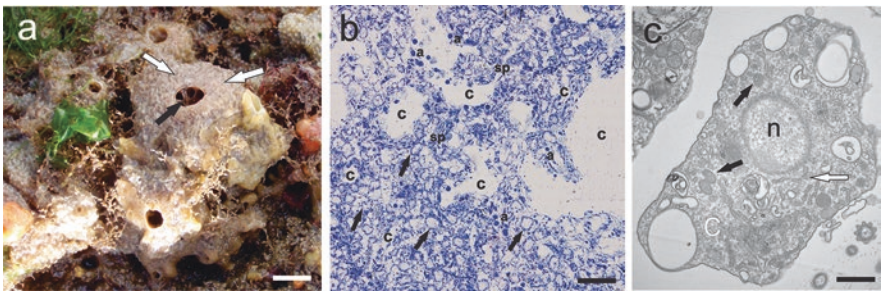

Fig. 4.1 (**a**) Photograph of a living specimen of *Haliclona indistincta* growing over flat boulders (*arrows* showing the incurrent (*white*) and excurrent (*black*) canals and obvious oscula). Water from the aqueous environment circulates deep within this sponge which has many such canals throughout. (**b**) A semi-thin section of *H. viscosa* using transmission electron microscopy (TEM) and stained with toluidine blue showing the canals penetrating to the centre of the sponge and very close to the cells: canals (c) choanocyte chambers (*black arrows*), spicules (sp) and amoebocytes (a). (**c**) A TEM micrograph of an amoebocyte from *H. simulans* showing the nucleus (n) which contains the sponge genome and where transcription occurs (mRNA being made from DNA); rough endoplasmic reticulum with ribosomes along it (*white arrow*), which is the site of translation (protein being made from mRNA); cytoplasm (c) where proteins are further modified; and mitochondria with their own small genomes involved in energy production primarily (*black arrow*). Scale (*a*) 5 mm, (*b*) 400 μm (*c*) 500 nm

part of the emerging field of conservation physiology (Evans and Hofmann 2012; Cooke et al. 2013). Nearly all cells will respond to environmental stress by inducing certain proteins that function in preventing and repairing damage in the cellular stress response, while others try to maintain homeostasis in the face of a change in an environmental variable (Kültz 2005). Many of the genes that are involved in the response to environmental stress are shared between distantly related organisms (e.g. heat-shock proteins), meaning that a universal set of biomarkers may be used to explore reactions across a wide set of organisms in a particular environment even though the levels of expression and the thresholds at which they are induced may differ (Evans and Hofmann 2012). Furthermore, the same set of genes can be induced as a result of different stressors and so can be used to explore an organisms' response to different physiological challenges (Kültz 2005). In most eukaryotes, including sponges, environmental stress induces expression of a number of genes most notably the acute-phase genes and heat-shock proteins. The former is reportedly triggered by lower-level stressors and is mediated by signalling molecules towards cell-specific responses, while the heat-shock response involves a range of genes (Hsp 70, Hsp 90, Hsp 50–60 and Hsp 20–30) to varying levels of environmental stress in efforts to maintain homeostasis (Koziol et al. 1997). This family of proteins is involved in protein folding/unfolding, minimizing the aggregation of non-native proteins and in targeting non-native proteins for removal (Feder and Hofmann 1999; López-Legentil et al. 2008). Hsps are useful as bioindicators because an increase in their gene expression is evident in response to stress, and as elucidated below, their expression changes in response to different kinds of stress. Apoptosis (programmed cell death) is also implicated in the stress response often followed by the death of the sponge (Wiens et al. 2000). Proteins involved in the cell death pathway include stress-activated protein kinases, caspases, BCl2 and tumour necrosis factor (Wiens et al. 2003; Pozzolini et al. 2016).

Despite their relatively simple body plan, sponges contain much of the genetic machinery present in higher animals and have a diversity of cell types that carry out various functions required for survival, growth and reproduction (Bergquist 1978; Riesgo et al. 2014a). Sponges have varying life spans, and while some species show 'boom-and-bust' patterns of rapid growth followed by a large degree of die off, others appear to be very long-lived (McCormack GP, Personal Observation; Wulff 2006). Therefore, sponges need mechanisms to adapt and survive environmental stress, and their responses to challenges introduced due to climate change such as increase in temperature and ocean acidification may vary depending on life history strategy and stage. What the molecular mechanisms are, how patterns of gene expression vary according to environmental challenge and how well sponges can adapt to environmental changes associated with climate change and ocean acidification are only now being investigated. Given that researchers have developed ways to maintain some species in aquaria and have also developed unique primmorph cultures from dissociated sponges means that sponges have become useful experimental animals (Custodio et al. 1998; Schippers et al. 2012; Fang et al. 2013). For many years before genomes and transcriptomes were available, genes could be isolated by cloning, and their activity studied using western and northern blots and

gel electrophoresis (see Glossary). More recently, quantitative polymerase chain reaction (qPCR) and genome and transcriptome techniques are available, and the fields of epigenetics and epigenomics are being developed. These methods are extremely valuable for studying acclimatory mechanisms, and how they have been applied to members of the Porifera are discussed in more detail below.

4.2 Gene Expression in Sponges

Isolating specific genes and investigating how they are expressed (switched on/off, producing high/low amounts of mRNA/protein) across organisms and tissues have been important for determining the evolutionary origin, function and importance of proteins. Most sponge genes are found in the genome of the sponge located in the cell nucleus with additional genes (involved in energy production primarily) located in the mitochondria (Fig. 4.1c). When cells are active (e.g. sclerocytes), the DNA of particular genes in the genome (e.g. silicateins) is transcribed to mRNA (i.e. expressed). The mRNA moves out of the nucleus to the ribosomes in the cytoplasm where the information they contain is translated into proteins (Fig. 4.2). Sponges have fewer cell types than other animals, but differentiated cells will produce different mRNAs and at differing amounts, e.g. sclerocytes would be expected to have some genes active that are different to those expressed by spherulous cells. A certain number of genes, e.g. housekeeping genes, which are those involved in basic cellular metabolism, are active/expressed in all cells. There are many studies published from the 1990s onwards describing the cloning and genetic characterization of genes from marine and freshwater sponges that had been previously found in other metazoa (e.g. polyubiquitin, integrin and receptor tyrosine kinase in *Geodia cydonium*, Pfeifer et al. 1993, Wimmer et al. 1999; longevity gene SDLAGL in *Suberites domuncula*, Schröder et al. 2000a).

To investigate patterns of expression of particular genes, first it involves obtaining cDNA of the targeted gene from extracted RNA using a specific commercial kit or via RT-PCR (see Glossary). Western or northern blots are then used to determine

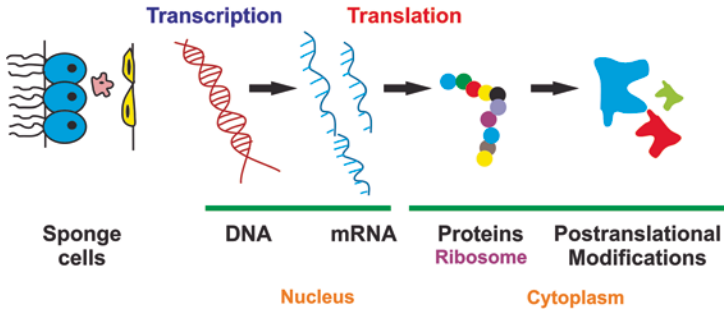

Fig. 4.2 A schematic representation of gene expression in sponges

to what degree a particular gene is active (e.g. Pfeifer et al. 1993). Another approach involves in situ hybridization where probes are applied directly to the tissue of the species to determine where the gene is expressed and at what level of expression (e.g. Adell et al. 2003). This approach can be applied to whole-mounted embryos or larvae, for example, or to complete specimens of small organisms or sections of larger ones (e.g. Larroux et al. 2006). Tissue is normally mounted on a microscope slide and stained with fluorescently labelled probes. More recently quantitative real-time PCR (see Glossary) is being applied to detect the copy number of specific mRNAs as a way to detect differential levels of expression (e.g. López-Legentil et al. 2008). High numbers of a particular mRNA would indicate that the gene in question is highly expressed and cause high levels of fluorescence, while lower fluorescence would indicate a lower number of copies of mRNA, which in turn indicates a lower level of expression. Thus animals under different environmental conditions can be compared to investigate how expression levels of particular genes change under different conditions. Finally, the entire set of expressed genes (the transcriptome) can be sequenced from sponges held under different environmental regimes, e.g. temperature, and compared to explore how gene expression varies (e.g. Guzman and Conaco 2016).

Many such studies have focused on expression patterns of developmental genes, e.g. EmH-3, a homeobox-containing gene in *Ephydatia muelleri* (Richelle-Maurer and Van de Vyver 1999), embryological body formation axis genes (Wnt and TG-Fβ) and hedgehog proteins at different life stages of *Amphimedon queenslandica* (Adamska et al. 2007a, b). Many other genes have been investigated in this latter sponge, e.g. sensory proteins such as delta and notch and postsynaptic scaffold genes (Sakarya et al. 2007; Richards et al. 2008), immunity genes such as toll like, interleukin receptor and NF-κB (Gauthier and Degnan 2008; Gauthier et al. 2010) and regulatory transcription factors related to embryo development (Homeobox genes) such as ANTP, *Pax*, POU, LIM-HD, Sox, NR, Fox, T-Box, Mef2 and Ets (Larroux et al. 2006). Recent studies also include differential expression in sponges with and without symbiont partners to help determine genes associated with the symbiotic state (e.g. Steindler et al. 2007; Riesgo et al. 2014b). Such studies are relevant to understanding climate change effects on sponges given the presence of photosynthetic symbionts in many sponge species which can vary in their response to changes in temperature in some situations offering potential benefit to the sponge (Bell et al. 2013). Furthermore, a large literature is accumulating on the genes associated with collagen and skeleton formation in sponges (e.g. Pozzolini et al. 2004; Voigt et al. 2014; Germer et al. 2015). The pressure of climate change on calcium-based organisms on coral reefs may increase the competitiveness of siliceous-based organisms (Bell et al. 2013; Vicente et al. 2015). However, there is likely to be some impact of increased temperature and reduced pH on metabolic pathways and biomineralization of all species; thus studies of biomineralization genes are also of interest here. Sponges need to sense their environment to cope with stress; therefore expression patterns of sensory and signalling proteins are also potentially very important in assessing sponge responses to changing environments.

Sponges are exposed to different kinds of environmental challenges such as changes in temperature, salinity, pH, organic matter and other pollutants (Wulff 2006; Webster et al. 2013; Vicente et al. 2015). Most published works on sponges have focused on expression of common genes related to stress response including the expression of the heat-shock protein, Hsp70. This protein is a large multigene protein that is found in several compartments of the cell and whose main function is to fold the peptides newly produced by the ribosomes (Mayer and Bukau 2005). An increase in activity of Hsp70 is detected when the cells response to disturbance is to fold more proteins that are required for the relevant response (Pratt and Toft 2003). Hsp70 has been reported to be a very good biomarker for environmental stress as the approaches used to study it require very little tissue and are therefore non-destructive (Koziol et al. 1996; Krasko et al. 1997; López-Legentil et al. 2008). This protein forms a complex with DNAJ-like proteins, which also respond to environmental stress and which may thus also be used as a biomarker and together are indicative of the presence of a heat-stress protection mechanism in sponges.

4.2.1 Response to Temperature

Given the predicted rise in seawater temperatures described in many studies (e.g. Bell et al. 2013), identifying indicators of thermal stress in coastal organisms is important as is developing an understanding of how well or poorly marine sponges will cope with rising temperatures. To this end there is a need to identify genes that have altered expression under thermal stress and investigate what the impacts of such changes in expression are. One of the first genes to be shown to be involved in adaptation to temperature stress in sponges was Hsp70 described above. Koziol et al. (1997) found that there was an 18- and 3-fold increase in the expression of Hsp70 and DNAJ-like protein, respectively, in *G. cydonium* when the temperature was raised by 7 °C. These authors showed DNAJ-like expression but not Hsp70 expression in untreated animals. A time-dependent increase in hsp70 expression was noted by Efremova et al. (2002) for Baikalian sponges exposed to temperature increases 10–16 °C above ambient, while increases in temperatures of a few degrees also resulted in increased expression of Hsp70 in *Xestospongia muta* (López-Legentil et al. 2008), while individuals maintained at lower temperatures showed no change in Hsp70 expression. This latter study also suggested that not all individuals respond in the same way to temperature increase given that there was variability in the expression levels between individuals undergoing the same treatment. These authors suggest that an increase in chaperone protein activity can assist the sponge in coping with minor stress, while larger degrees of stress may cause the metabolic defence system to collapse (López-Legentil et al. 2008).

This pattern was clearly shown by Pantile and Webster (2011) who investigated changes in expression of six genes in response to an increase in temperature of 4 and 5 °C above ambient (27 °C) in *Rhopaloeides odorabile.* Their work confirms that the molecular mechanisms to adapt to some thermal stress are evident (such as up to 4 °C above ambient), but there is a limit to the temperature at which the protective

functions of the heat-shock system can outweigh the damage caused. At 31 °C five proteins were significantly downregulated in comparison to the controls (held at ambient temperature). While the sponges survived the experiment and expression levels for genes involved in signalling (CaM) and removal of degraded proteins (UbC) recovered 24 h after temperature levels returned to normal, genes involved in cytoskeleton formation (arp2/3), oxidation (ferritin) and molecular chaperone (Hsp90) did not recover. The reduction of expression in these genes in response to an increase in temperature of 4 °C suggests that the sponge shuts down/reduces some cellular activity and perhaps indicates some permanent or longer-term physiological damage (Pantile and Webster 2011). Whether or not all of the genes would have eventually recovered to normal expression at ambient temperature remains to be seen but if so would indicate some adaptability of this species to recover from significant heat stress.

In the above study, a further increase in temperature of 1 °C (to 32 °C) resulted in all sponge clones showing signs of necrosis and subsequent death after 3 days (Pantile and Webster 2011). At this temperature, expression levels of the signal transducer gene, CaM, dropped significantly after a single day. While the patterns of expression of Arp2/3, ferritin and Hsp90 also showed a significant drop in expression after 1 day, expression of these genes increased again by day 3. Hsp40 and UbC all showed significant increase in expression by day 3. According to Pantile and Webster (2011), the perhaps surprising increase in expression of some of these genes by day 3 indicates further induction of the heat-shock system, activation and upregulation of systems to neutralize reactive oxygen species and to degrade damaged and unfolded proteins. But at 32 °C the physiological damage must be too great for the protective systems to overcome and the sponges all died. In Bolinao, Philippines, seawater temperature varies from 25 to 32 °C, and the shallow water sponge *Haliclona tubifera* is exposed to regular widely fluctuating temperatures. According to Guzman and Conaco (2016) who applied a comparative transcriptomics approach, thermal stress at 34 °C resulted in much greater changes in gene expression than sponges held at 32 °C, the latter temperature within the natural temperature range, if the extreme. In this latter sponge, genes that were downregulated were those involved in housekeeping or first line of defence, while stress-induced genes were upregulated.

As mentioned by Webster et al. (2013), seawater temperatures at the Great Barrier Reef have occasionally already exceeded 30 °C. If water temperatures increase by a further 1.8–4 °C (IPCC 2007), this would bring temperatures to a point at which adult *R. odorabile* could not physiologically adapt, an eventuality that may hold for many more sponges. Indeed *X. muta* is indicated to have a stricter thermal limit than *R. odorabile* with individuals suffering mortality after being held in tanks 2 °C above the control temperature of 28 °C (López-Legentil et al. 2008). In the study of Guzman and Conaco (2016), experiments were carried out over 12 h on sponge pieces, and it was not reported whether any of the sponge pieces survived afterwards.

Further work by Webster et al. (2013) investigated differences in stress response between adults and larvae of the same species, *R. odorabile.* Such work is of fundamental importance given the different environments utilized by different life history

stages of sponges and thus potentially different impacts of temperature increase on each stage. Both life history stages are obviously of importance in the continued survival of a species, so it is important to assess mechanisms of survival/adaptability in both. Using RT-qPCR (see Glossary) to measure differential gene expression, a whole suite of genes were investigated including those involved in cytoskeleton/skeleton arrangement, signal transduction, protein folding and heat shock, protein synthesis and degradation, oxidative stress and detoxification. Their research and others indicate that the sponge larvae of *R. odorabile* are more tolerant to thermal stress than the adults (Whalan et al. 2008; Webster et al. 2013) with the adult sponges displaying signs of necrosis after 3 days of exposure to 5 °C above ambient but larvae surviving temperatures up to 9 °C above ambient.

As the authors noted, larvae move from benthic to pelagic habitats experiencing a natural change of temperature. Thus larvae may have additional and different mechanisms in place to adapt to changing temperatures compared to adults, which remain on the benthos (Webster et al. 2013). In larvae, at 32 °C after 24 h, all of the genes showed some increase in their expression levels, but at 34–36 °C the heat shock (Hsp70, Hsp90) and the cell death pathway genes (Alg 2 1) were highly expressed. While larvae will survive temperature increases predicted (1–4 °C over the next 100 years), the fitness of the adult stage of some sponge species will clearly be negatively impacted (Webster et al. 2013). There is a need for information from more species and scenarios to fully understand the molecular and cellular mechanisms affected by temperature increases and subsequent likely impact on different habitats where sponges play a role. Higher temperatures will also cause a further impact to many sponges due to the relationship between them and their symbionts given that up to 40% of the biomass of some sponges may comprise of bacteria (Lesser et al. 2016). Cebrian et al. (2011) showed mortality in *Ircinia* in the Mediterranean in response to the higher temperatures evident in 2008 and 2009 due to mortality of their cyanobacterial symbionts. Differential responses of the sponge holobiont at adult and larval stages have also been described (Webster et al. 2008, 2011) and will be discussed further in Chaps. 5, 6 and 9.

4.2.2 Changes in pH

Animals form inorganic skeletons through biomineralization, a process that involves a number of different chemical reactions (Marin et al. 1996). Marine sponges have a wide variety of skeletons made predominantly of biogenic silica, calcium carbonate, collagen fibres and/or chitin (Ehrlich et al. 2013; Wang et al. 2012), and both the mechanisms to generate the skeletons and the genes/proteins involved vary significantly. It is well accepted that increased acidification of our oceans due to higher atmospheric CO_2 will have a significant effect on organisms with calcium-based skeletons (e.g. O'Donnell et al. 2010). Less is known about the impact of ocean acidification on species with silica-based skeletons.

Most published studies on biomineralization in sponges to date have focused on the chemical composition and mechanical properties of the spicules (Sundar et al. 2003; Sethmann et al. 2006); the identification, expression and evolution of the genes responsible for biomineralization (Krasko et al. 2000; Mohri et al. 2008; Ehrlich et al. 2013; Riesgo et al. 2015); biotechnological applications of the proteins and skeleton as new sources of biomaterials (Shkryl et al. 2016; Gardères et al. 2016); and variability in skeletal arrangement and spicule morphology with silica concentration (Maldonado et al. 1999, 2012). In the context of climate change, there are very few studies on its potential effects on the sponge skeleton, and none of these have applied gene expression approaches. Yet gene expression analyses are very important to help understand the genetic response of targeted species in response to climate change variables that impact the biomineralization process (Kaniewska et al. 2012). As might be expected, sponges that produce high Mg calcite and/or aragonite will be most vulnerable to ocean acidification because of the dissolution of the carbonates (Smith et al. 2013). Furthermore, saturation levels of CO_2 are predicted to be higher in temperate shallow waters than in deeper habitats, indicating that shallow water sponges with calcareous skeletons are more susceptible than those living in deeper habitats. Vicente et al. (2015) investigated the effects of high pCO_2 and warmer temperatures in silica uptake and spicule length of *Mycale grandis* and found a decrease in silica uptake and spicule length under high pCO_2 conditions. While the cause behind the impact was not determined, it is possible that the lower pH denatured the proteins responsible for spicule production.

Several proteins have been identified in sponges that are responsible for skeleton construction, and their function may be negatively impacted as conditions move away from ambient. For siliceous sponges they include silicateins, silinthaphins, galectin, BMP, short-chain collagen and others (Cha et al. 1999; Wang et al. 2014; Nakayama et al. 2015). In contrast, skeleton formation in calcareous sponges is due to their possession of two (one intracellular and one extracellular) specific α-carbonic anhydrases (Müller et al. 2012; Voigt et al. 2014). Coralline sponges (sclerosponges), in addition to siliceous spicules, have a calcareous basal skeleton made of intracellular spherulites, and the protein responsible for the formation of these structures has been identified as astrosclerin (Jackson et al. 2007, 2011; Germer et al. 2015). Recent studies have demonstrated that even bacteria are responsible for the calcification of the sponge skeleton in certain species such as *Hemimycale* (Uriz et al. 2012). O'Donnell et al. (2010) and Stumpp et al. (2011) both showed a reduction in expression of genes involved in the biomineralization process in echinoderm larvae under pH stress. It is likely that skeleton formation would slow down as mechanisms for survival are activated, an effect that may also occur in sponges. However, in a range of experiments investigating bioerosion, with progressively lower pH and higher temperatures in clionaid sponges, individual sponges not only survived experiments up to eight weeks but also showed an increase in biomass indicating that these sponges can physiologically adapt to lower pH and maintain the biomineralization processes (Fang et al. 2013).

Reducing pH does induce the stress response in some sponges (e.g. *G. cydonium;* Koziol et al. 1997). This latter study showed an increase in Hsp70 expression via western blots in one of the first studies of cloning and expression of functional genes in sponges. However, variability clearly exists in the ability of different species to survive with decreasing pH. While clionaid sponges may benefit from reduced pH due to ocean acidification, Goodwin et al. (2014) showed that sponge cover and species composition reduced with lower pH treatments. Four species (*Phorbas tenacior*, *Petrosia ficiformis*, *Chondrilla nucula* and *Hemimycale columella*) were very vulnerable to reduced pH, only surviving in sites with normal pH, while *Crambe crambe* was able to survive at pH of 6.6 (Goodwin et al. 2014), and reduced pH had no discernible impact on spicule form in those that survived at lower pH concentrations. What metabolic processes are impacted by reduced pH or what mechanisms help some sponge species to survive in lower pH environments have yet to be determined, and more gene expression profile studies are needed in relation to the ability of sponges to adapt to ocean acidification specifically.

Gene expression profiling has been very informative for other animal species, and lessons could be learnt here on what might be expected from sponges. In addition to biomineralization genes being downregulated in response to pH, O'Donnell et al. (2010) and Stumpp et al. (2011) showed that genes involved in ion regulation and acid-balance pathways showed an increase in expression in echinoderm larvae. Wells et al. (2012) showed that pH was also implicated in regulating potassium channels in *A. queenslandica*, and it may be likely that cell signalling would increase in individuals under pH stress. Kaniewska et al. (2012) described major physiological impacts resulting from lower pH in the coral *Acropora millepora* resulting in metabolic suppression, oxidative stress, apoptosis and symbiont loss, while genes involved in membrane transport were upregulated. Moya et al. (2012) also showed a decrease in the expression of metabolic genes and secreted carbonic anhydrases as pH was lowered in early stages of *A. millepora* using transcriptomic approaches, while they found no differences in the expression of the ion transporter genes. Rocker et al. (2015), however, found no significant changes in 19 out of 20 metabolism and calcification genes in the same coral species under high pCO_2 and warmer temperatures using RT-qPCR. Such variation in results from the same species using different approaches and the lack of studies on sponges cries out for more work to be done and a consistency of approach across researchers to allow comparisons to be made and general patterns drawn. The recent development of a panel of reference genes for stress response using a qPCR approach for coral by Shimpi et al. (2016) may help to standardize approaches.

4.2.3 Other Impacts

In addition to environmental challenges as a result of climate change such as increased temperatures and lower pH, sponges must acclimate to other factors implicated in environmental change such as changes in salinity, exposure to sedimentation and pollutants [e.g. Evans and Hofmann (2012)]. López-Legentil et al. (2008)

suggested that an increase in salinity may cause temporary stress to *X. muta* but that after a period of time, the sponges appeared to adapt to the change and Hsp70 expression levels were seen to drop suggesting that the sponges had adjusted and recovered. Koziol et al. (1996) found no change in Hsp70 expression in *G. cydonium* under different ionic conditions, while Böhm et al. (2000) showed an increase in expression of the stress-activated protein kinase (SPAK) p38 in the tissue and cells of *S. domuncula* under different salinity concentrations using western blot assay. These studies again suggest variability amongst sponge species in adapting to environmental stress.

Sponges can be used as indicators of toxic metals because the metals accumulate in the tissues of some species with varied impacts from reduced survival, induction of gemmule formation to simple accumulation of the metal. Wagner et al. (1998) investigated the response of *S. domuncula* to cadmium using expression of a metazoan apoptosis marker (the MA-3 gene), which increased on the addition of the metal. Hsp70, GRP78, metallothionein expression and DNA damage also increased in this sponge in response to higher loads of zinc and cadmium (Müller et al. 1998; Schröder et al. 1999b, 2000b). While exposure to cadmium did not result in the death of the sponge, it accumulated in the tissue and induced apoptosis, which in turn lead to gemmule formation. *Halichondria panicea* was also shown to accumulate this metal, as well as copper, zinc and chromium (Olesen and Weeks 1994; Hansen et al. 1995). In comparison, Cebrian et al. (2006) found that copper accumulation did not occur in *Chondrosia reniformis* exposed to an environment with moderately high levels of copper pollution. In this case there was also no change in expression of heat-shock protein or sponge growth or shape. These authors however did detect a negative impact on sponge physiology leading to a lower survival rate. A lack of hsp70 induction in response to copper was also shown by Efremova et al. (2002) in sponges from Lake Baikal, while Hsp70 induction was seen for exposure to lead and zinc.

Some sponge species are able to accumulate other heavy metals and contaminants in their tissue such as plumb, aluminium, titanium, PHAs and PCBs as well as copper, cadmium and zinc (Cebrian et al. 2007; Gentric et al. 2016; Batista et al. 2013), and metallothionein is used as a common biomarker for accumulation of such heavy metals in sponges and other filter-feeding organisms (Berthet et al. 2005; Amiard et al. 2006; Aly et al. 2014). When polychlorinated biphenyls (PCB77, PCB118 and PCB153) accumulated in the tissue of *S. domuncula*, the heat-shock system was activated with Hsp73 consistently expressed at high levels in all samples tested, while Hsp75 was expressed at low levels (Schröder et al. 1999a). Two stress-activated protein kinases (PKAS), which are signalling molecules, were reported in *S. domuncula* in response to TBT (tributyltin) exposure by Fafanđel et al. (2003) who suggested that this indicates the presence of a mechanism that promotes apoptosis in sponges that are under oxidative stress. Châtel et al. (2011) described activation in ERK (extracellular signal-regulated kinase) and p38 (involved in cell differentiation and apoptosis) and increase in expression of cyclin D1 (involved in regulation of cell cycle) in the presence of TBT, hydrogen peroxide and water-accommodated fraction (WAF) of diesel oil in the same sponge species. An increase in apoptosis activity was determined based on the high levels of DNA fragmentation and caspase activity.

In these studies apoptosis seems to feature in the stress response quite significantly and is advocated by Wagner et al. (1998) as a biomarker for environmental stress in sponges. Apoptosis is a complicated process involved in cell death, which is necessary to prevent overgrowth of tissues as new cells are being generated and to get rid of unwanted cells. Sponge cells are thought to have unlimited proliferation capacity (Koziol et al. 1998). However, apoptosis can occur in response to physiological necessity to get rid of infected cells or those that are no longer necessary when the sponge undergoes metamorphosis and gemmule formation or has exhausted a need for a particular cell type (Wiens and Müller 2006). It can also be used to remove cells that have been damaged due to exposure to a damaging environmental variable (e.g. Wagner et al. 1998). The process is complicated, involves a whole range of mechanisms including signalling pathways that must be regulated and has been detected in sponges by DNA fragmentation assays, by caspase activity and by the expression of particular apoptosis-related genes (Wiens et al. 2000, 2003).

4.3 Genomics and Epigenetics

With the advent of affordable high-throughput whole genome and transcriptome sequencing, a new avenue opens up for investigations of comparative gene expression, e.g. in response to environmental change. Being able to identify genes with known functions in other metazoa as well as those specific to the Porifera, and being able to determine changes in expression of many thousands of genes simultaneously in response to particular sets of conditions, allows a picture to emerge of how sponges respond to their environment (Evans and Hofmann 2012). Given the many studies utilizing these approaches in recent years for sponges and other organisms, many standardized pipelines and analysis software now exist that can be applied to climate change investigations.

4.3.1 Genomics

There are still very few sponge genomes available (summarized in Table 4.1), but efforts of GIGA (Global Invertebrate Genome Alliance) will undoubtedly lead to additional sponge genomes and established protocols and expertise to facilitate their application to sponge adaptation (giga-cos.org). The first sponge genome sequenced was that of *A. queenslandica* with an initial assembly of 30,060 predicted protein-coding loci (Srivastava et al. 2010). This number increased to 40,122 after deep transcriptome sequencing of this species under different life stages (Fernandez-Valverde et al. 2015). The genome contains a large number of genes related to cell cycling and growth (i.e. p53, cyclin-dependent kinases, Myc), apoptosis (i.e. Bcl-2, caspases, APAF1, TNRF), cell-matrix adhesion (i.e. collagens, integrins, cadherins), developmental signalling and gene regulation pathways (i.e. Sox, Fkh, Wnt,

TG-Fβ), allorecognition and innate immunity (toll-like receptors, MDA-5-like RNA helicases, aggregation factors) and specialization of cell types (laminin-like domains, GPCRs, Dlgs) (Srivastava et al. 2010) in addition to universal genes involved in the stress response. The genome of the homoscleromorph *Oscarella carmela* (Nichols et al. 2012) and the genomes of the calcareous sponges *Sycon ciliatum* and *Leucosolenia complicata* have since also been released (Fortunato et al. 2012, 2014a, b) as have genomes from two additional demosponges, *Stylissa carteri* and *Xestospongia testudinaria*, from the Red Sea (Ryu et al. 2016). The availability of these genomes allows the identification of homologs of stress response genes across the entire phylum for further investigation.

4.3.2 Transcriptomics

Transcriptomes have been generated for a larger number of species also allowing investigations of differential gene expression in these species (Table 4.1), but almost all of the work to date in this field involves different life history stages rather than response to environmental change. Knowledge of the data that exists and optimization of the technology required however pave the way for planning valuable experiments in the area. Conaco et al. (2012), Pérez-Porro et al. (2013) and Qiu et al. (2015) studied differential gene expression of developmental genes from *A. queenslandica*, *Crella elegans* and *Mycale phyllophila*, respectively, under different life stages. Riesgo et al. (2014b) studied the differential gene expression of the bioeroding sponge *Cliona varians* in relationship with its *Symbiodinium* symbiont in three different experimental cases (normal, aposymbiotic and reinfected). Many transcriptomes have been sequenced to identify metazoan genes in sponges and to compare patterns of evolution across phyla (Riesgo et al. 2014a; Schenkelaars et al. 2015, 2016; Alié et al. 2015; Pozzolini et al. 2016), as well as to provide additional data for phylogenomic studies (Whelan et al. 2015) and biomineralization (Germer et al. 2015). Guzman and Conaco (2016a) sequenced the transcriptome of *Haliclona amboinensis* and *H. tubifera* from the coast of the Philippines identifying genes related to the stress response such as Hsp90, Hsp70, death effector domain, glutathione S-transferase, thioredoxin, caspase domains and death domains. These authors (Guzman and Conaco 2016) went on to generate transcriptome data from *H. tubifera* held at different temperatures and were able to analyse 1584 genes that showed differential expression across temperature treatments including an assessment of the functional groups impacted by temperature. The transcriptomes of three additional *Haliclona* species (*H. oculata*, *H. simulans* and *H. indistincta*) have been sequenced by the authors to investigate environmental plasticity of the skeleton in the Haplosclerida. Many EST (expressed sequence tags) libraries are also available for many sponges now and can be found in the public databases such as GenBank (www.ncbi.nlm.nih.gov/ncest).

Table 4.1 List of sponge genomes and transcriptomes available

Genomes			
Species	Class	Contigs (DNA) or proteins assembled	Reference
Amphimedon queenslandica	Demospongiae	40,122 proteins	Fernandez-Valverde et al. (2015)[a]
Oscarella carmela	Homoscleromorpha	67,767 contigs	Nichols et al. (2012)[a]
Xestospongia testudinaria	Demospongiae	22,327 proteins	Ryu et al. (2016)[a]
Stylissa carteri	Demospongiae	26,967 proteins	Ryu et al. (2016)[a]
Sycon ciliatum	Calcareous	50,731 proteins	Fortunato et al. (2014a, b)[a]
Leucosolenia complicata	Calcareous	92,106 proteins	Fortunato et al. (2014a, b)[a]
Transcriptomes			
Species	Class	Contigs (DNA) or proteins assembled	Reference
Ephydatia muelleri	Demospongiae	85,751 contigs 28,154 proteins	Peña et al (2016)[a]
Haliclona amboinensis	Demospongiae	44,693 contigs 20,280 proteins	Guzman and Conaco (2016a)[a]
Haliclona tubifera	Demospongiae	50,067 contigs 18,000 proteins	Guzman and Conaco (2016a)[a]
Oscarella sp.	Homoscleromorpha	172,354 contigs	Hemmrich and Bosch (2008)[a]
Aphrocallistes vastus	Hexactinellid	46,897 contigs 28,243 proteins	Riesgo et al. (2014a)
Spongilla lacustris	Demospongiae	70,220 contigs 15,025 proteins	Riesgo et al. (2014a)
Petrosia ficiformis	Demospongiae	49,507 contigs 20,152 proteins	Riesgo et al. (2014a)
Pseudospongosorites suberitoides	Demospongiae	20,925 contigs 11,536 proteins	Riesgo et al. (2014a)
Ircinia fasciculata	Demospongiae	34,868 contigs 16,898 proteins	Riesgo et al. (2014a)
Chondrilla nucula	Demospongiae	56,696 contigs 21,229 proteins	Riesgo et al. (2014a)
Sycon coactum	Calcareous	41,571 contigs 19,062 proteins	Riesgo et al. (2014a)
Corticium candelabrum	Homoscleromorpha	141,629 contigs 41,146 proteins	Riesgo et al. (2014a)
Cliona varians	Demospongiae	292,108 contigs	Riesgo et al. (2014b)
Mycale phyllophila	Demospongiae	76,640 contigs 12,142 proteins	Qiu et al. (2015)
Crella elegans	Demospongiae	203,078 contigs	Pérez-Porro et al. (2013)

(continued)

Table 4.1 (continued)

Transcriptomes			
Species	Class	Contigs (DNA) or proteins assembled	Reference
Latrunculia apicalis	Demospongiae	76,210 contigs	Whelan et al. (2015)
Kirkpatrickia variolosa	Demospongiae	100,231 contigs	Whelan et al. (2015)
Hyalonema populiferum	Hexactinellid	58,839 contigs	Whelan et al. (2015)
Rosella fibulata	Hexactinellid	40,103 contigs	Whelan et al. (2015)
Sympagella unix	Hexactinellid	85,237 contigs	Whelan et al. (2015)
Chondrosia reniformis	Demospongiae	19,678 contigs	Pozzolini et al. (2016)
Ephydatia fluviatilis	Demospongiae	17,149 proteins	Alié et al. (2015)
Xestospongia muta	Demospongiae	35,219 contigs	Fiore et al. (2015)
Cinachyrella sp.	Demospongiae	34,147 contigs	Smith et al. (2013)
Halisarca dujardini	Demospongiae	138,992 contigs	Borisenko et al. 2016)
Vaceletia sp.	Demospongiae	Unknown	Germer et al. (2015)
Oscarella carmela	Homoscleromorpha	Unknown	Schenkelaars et al. (2015, 2016)
Oopsacas minuta	Hexactinellid	Unknown	Schenkelaars et al. (2015, 2016)
Microciona prolifera	Demospongiae	Unknown	Gaiti et al. (2015)
Haliclona oculata	Demospongiae	Unpublished data	Unpublished data
Haliclona indistincta	Demospongiae	Unpublished data	Unpublished data
Haliclona simulans	Demospongiae	Unpublished data	Unpublished data

[a]The genomes and transcriptomes of these species are available in the COMPAGEN website (Hemmrich and Bosch 2008)

As comparative genomics/transcriptomics in Porifera is still in its infancy, these data have not yet been used to explore the range of genes whose expression is/might be affected by climate change and other stressful situations. However, establishing the gene families present and active in different species under normal life history stages and environments will pave the way for exploring how these patterns change under stress. Despite the costs of data generation reducing wholesale, the main obstacle to widespread use of such approaches is the bioinformatics expertise and hardware necessary to be able to handle and interpret the data.

4.3.3 Epigenetics

The response of organisms to environmental change can occur through both genetic and non-genetic processes. Adaptation often refers to Darwinian evolution where changes to a phenotype from one generation to the next are via natural selection,

and most often refers to changes in the DNA of an individual becoming fixed in the population if it confers an advantage. However acclimatization, which is a phenotypic response to variation in an environment, doesn't always involve a genetic change meaning that modification of gene expression does not necessarily involve changes in DNA structure or sequence (van Oppen et al. 2015). The term "epigenetics" can refer to a change in gene expression directly in response to environmental and/or development triggers or to the "transgenerational heritability" of mechanisms that get passed down through generations and affect the phenotype or fitness of the population (Mirouze and Paszkowski 2011; Verhoeven et al. 2016). Research and development in the area of transgenerational acclimatization has become popular because it is possible to select candidates through experimental manipulation, which are better able to survive various stresses (Boyko and Kovalchuk 2011; van Oppen et al. 2015). A glimpse at some epigenetic patterns in sponges was discussed by Webster et al. (2013) in relation to differences in physiological adaptations of larvae and adults and how this was reflected in their tolerance to temperature increases. Similar physiological flexibility may be found in sponges that occupy a broad ecological niche, perhaps leaving them more tolerant to climate change.

Changes in regulation/expression of a particular gene can be altered by enzymatic and RNA-based mechanisms (Gibney and Nolan 2010). Despite some preliminary work in both of these mechanisms existing for Porifera (e.g. Conaco et al. 2012; Levin et al. 2016; Riesgo et al. 2014b), applications of these approaches to investigate acclimatization of sponges to climate change or other stressors have not yet occurred, and so again lessons can be learnt from studies on other organisms. During methylation, DNA is modified by a methyl group being added to the fifth carbon of cytosine, which in turn can modify expression of the genes impacted (Angers et al. 2010; Deaton and Bird 2011). In the coral *A. millepora*, genes involved in basic biological functions (i.e. cellular and nucleic acid metabolism) tend to be strongly methylated, while genes responsible for functions that are dynamically regulated (i.e. development, cell signalling pathways) tend to be sparsely methylated (Dixon et al. 2014). DNA methylation patterns between coral colonies from native and transplanted locations highlighted 321 genes with differential gene expression that were all indicated to have low DNA methylation. These genes are more likely to display environmentally driven variation in expression and could be targets for further studies on coral acclimatization. Indeed it is possible that sponges will show the same DNA methylation patterns, and those with low methylation may suggest themselves as targets for further study on sponge adaptation to environmental change.

Normalized CpG content (CpG O/E) is a well-established evolutionary signal of DNA methylation with low values indicating strong methylation, while high values indicate weak methylation (Roberts and Gavery 2012; Dixon et al. 2014). CpG O/E content can be identified using transcriptomic and genomic data but is more precise with bisulfite genomic data (Grunau et al. 2001). Currently, several bisulfite genomes (see Glossary) have been sequenced from invertebrates and the CpG O/E content identified (Zemach et al. 2010) but none yet from sponges. Sarda et al. (2012) identified and compared the CpG O/E content of four invertebrate species: sea anemone (*Nematostella vectensis*), sea squirt (*Ciona intestinalis*), honeybee

(*Apis mellifera*) and silkworm (*Bombyx mori*) confirming the same pattern as above; highly methylated genes were more conserved than sparsely methylated or non-methylated genes and were often housekeeping genes. This implies that strong methylation leads to more stable gene expression, while weak methylation facilitates flexible expression in the coral genome and may therefore also indicate genes that may adapt more easily to climate change effects and those that will not. Dimond and Roberts (2016) confirmed this pattern regarding genes with low methylation, using transcriptome data from six coral species under different life stages, finding similar patterns of methylation across the species and to those above. Highly methylated genes, however, were more variable across species but generally corresponded to DNA metabolism and protein metabolism. More relevant to the focus of this chapter, Dixon et al. (2016) also evaluated CpG O/E content for 24,320 genes expressed in response to environmental stress for *A. millepora* and found that the most highly expressed genes under stressful conditions tended to have intermediate rather than high levels of methylation. Highly expressed genes were, on average, strongly methylated and were less likely to be differentially expressed across developmental stages and environmental regimes.

DNA in eukaryotes is packaged into a compact structure called chromatin that includes eight histone molecules (two each of H2A, H2B, H3 and H4) and a histone linker (H1) that binds to the DNA between the nucleosomes (Cedar and Bergman 2009). The histones have residues called "tails" protruding from the nucleosomes that are subjected to post-translational modification (PTM), i.e. modification to the protein (Henikoff and Shilatifard 2011; Huang et al. 2015). Several enzymes are responsible for histone PTM some of which are able to change the structure of the chromatin arrangement, which in turn can affect expression or repression of a particular gene (Grunstein 1997). Current knowledge on histone modifications in sponges have been focused on genome-wide mapping and expression patterns of the elements regulating this process (i.e. H3 PTM, distal enhancers, PCR2) at different life stages of *A. queenslandica* (Gaiti et al. 2017). Furthermore, the detection, expression and manipulation of the proteins involved in nucleosome remodeling and the deacetylase complex (NuRD) has been investigated in the freshwater sponge *E. muelleri* (Cramer et al. 2017). Given the dearth of studies in this area, it is likely to be sometime before sufficient understanding exists on chromatin biochemistry in sponges to allow its application for specific gene expression studies in the context of climate change.

RNA-based mechanisms involve a number of different types of RNA molecules that function in gene regulation. Long non-coding RNAs (lncRNA) are molecules >200 nucleotides in length that are non-conservative, evolving faster than sRNAs or functional genes (Mercer et al. 2009). In humans and plants, lncRNAs are implicated in RNA maturation and transcriptional gene silencing through regulation of the chromatin structure (Gupta et al. 2010). For example, lincRNA-p21 acts as a transcriptional repressor in the canonical p53 pathway in human cells triggering apoptosis as a stress cue (Huarte et al. 2010). In sponges studies on lncRNAs are currently limited to their identification and expression. Again, *A. queenslandica* life stages have been a focus of research in this regard with 2935 lncRNAs identified

and classified according to their genomic location (Gaiti et al. 2015). The authors suggest that the expression of lncRNAs varies throughout the life history stages of this sponge and correlated their expression with morphogenetic and developmental events. This pattern was confirmed by Bråte et al. (2015) in the calcareous sponge *S. ciliatum* also using a transcriptomic approach where certain transcripts were upregulated during specific life history stages. More work will need to be carried out to investigate if expression of these RNAs is altered during acclimatization and evaluate their utility as biomarkers of environmental stress.

MicroRNAs (miRNAs) are single-stranded RNA molecules greater than 22 nt, which bind to target mRNA suppressing the translation of the genes involved (Krol et al. 2010; Volinia et al. 2006). As above, studies of miRNAs in sponges have been focused on their identification and expression and largely during life history stages. Grimson et al. (2008) identified eight miRNAs in *A. queenslandica*, six of which were highly expressed in adult specimens and two were only expressed at the embryo stage. No similarity was found between these transcripts and miRNAs from other metazoa; however, homologs of the enzymes responsible for the biosynthesis of the miRNAs in humans were identified in this sponge (Grimson et al. 2008). miRNAs have subsequently been identified in a range of demosponges, homoscleromorphs and calcareous species though miRNA presence/absence and the similarity of miRNAs between species appear to be variable across sponges, raising questions about the extent of their independent evolution (Wheeler et al. 2009; Robinson et al. 2013; Sperling et al. 2010; Liew et al. 2016). Robinson (2015) investigated differential expression of miRNAs on disassociated cells, cell aggregations of varying densities, on different parts of the sponge, between juveniles and gemmules and between eight species overall. Results from these experiments revealed that miRNA expression is likely related to cell cycle and differentiation and survival mechanisms because low miRNA expression levels were found where the tissue was dissociated (cell aggregations or cell suspensions) or in stand-by conditions (gemmules). The decrease in the expression of the miRNAs witnessed may also be related to cellular inactivation and apoptotic tendency making miRNA expression a good candidate for studies related to stress response in sponges. However a lot of work needs to be done initially on the homology of these RNAs to enable comparison across taxa.

4.4 Conclusions

There is clear evidence that sponges possess mechanisms to respond and adapt to various stressors in the environment. Heat-shock proteins prove to be useful indicators of stress in sponges as would be expected, but many other genes are implicated in the stress response. Some genes are involved in maintaining homeostasis in the face of adverse environmental conditions, while others are involved in limiting damage. At the same time, there are a myriad of genes involved in specific functions whose expression is up- or downregulated as the sponge undergoes stressful time. In addition factors implicated in epigenetic mechanisms affecting gene expression

have also been identified in sponges. Currently, however, there are too few studies to enable us to unravel the complexity of responses. At the same time, it appears that sponge species vary in their capacity to survive increases in environmental challenges such as increase in temperature and decrease in pH with some sponges having very broad niche requirements and others having stricter thresholds for environmental factors. Only few sponge species have been targets of focused research in the area of climate change adaptability, *R. odorabile, X. muta, G. cydonium, S. domuncula* and *A. queenslandica* being the source of most of the current information with regard to gene expression and genomics approaches. More data is necessary utilising these techniques to develop the field of conservation physiology for Porifera but also for the complete range of habitats they inhabit.

Acknowledgements JMA-C is funded by a Hardiman Scholarship at the National University of Ireland, Galway. The authors would like to thank anonymous reviewers for suggesting improvements to the manuscript.

Glossary

Bisulfite Sequence Determination of the patterns of DNA methylation (CpG islands) of the genome of an organism using bisulfite treatment.

cDNA (complimentary DNA) cDNA is DNA that is produced from mRNA of cells or tissues and therefore consists of the genes that are being expressed at that time in a particular tissue or specimen.

EST Determination of short sequences of cDNA (mRNA) in a biological sample in a particular time. A portion of the genes expressed is available by this approach, but not entire genes or the entire transcriptome.

Genome Sequence Determination of the sequence of the entire DNA from a particular organism.

mRNA (messenger RNA) mRNA represents all of the genes that are active in a cell at a particular time and will vary between differentiated cells due to the different functions of the cell.

PCR (polymerase chain reaction) a method where a targeted portion of an organisms' DNA is copied in an eppendorf tube creating billions of copies that can then be used in downstream processes such as being sequenced.

qPCR/QRT-PCR (quantitative realtime PCR) A further development of the PCR technique where fluorescence is used to detect the amount of mRNA copies present in cells or tissues.

RT-PCR (reverse transcriptase PCR) a method where the mRNA of an organism is turned back into DNA as it is being copied. The method uses reverse transcriptase, an enzyme that 'reverse transcribes' RNA back to DNA.

Transcriptome Sequence Determination of the DNA sequence of the entire mRNA from a particular organism, i.e. a sequence from all genes that are active in the tissue at that time.

References

Adamska M, Degnan SM, Green KM et al (2007a) Wnt and TGF–β expression in the sponge *Amphimedon queenslandica* and the origin of metazoan embryonic patterning. PLoS One 2(10):e1031

Adamska M, Matus DQ, Adamski M et al (2007b) The evolutionary origin of hedgehog proteins. Curr Biol 17(19):R836–R837

Adell T, Nefkens I, Müller WEG (2003) Polarity factor 'Frizzled' in the demosponge *Suberites domuncula*: identification, expression and localization of the receptor in the epithelium/pinacoderm. FEBS Lett 554:363–368

Alié A, Hayashi T, Sugimura I et al (2015) The ancestral gene repertoire of animal stem cells. Proc Natl Acad Sci U S A 112(51):E7093–E7100

Aly W, Williams ID, Hudson MD (2014) Limitations of metallothioneins in common cockles (*Cerastoderma edule*) and sponges (*Haliclona oculata*) as biomarkers of metal contamination in a semi–enclosed coastal area. Sci Total Environ 473:391–397

Amiard JC, Amiard-Triquet C, Barka S et al (2006) Metallothioneins in aquatic invertebrates: their role in metal detoxification and their use as biomarkers. Aquat Toxicol 76(2):160–202

Angers B, Castonguay E, Massicotte R (2010) Environmentally induced phenotypes and DNA methylation: how to deal with unpredictable conditions until the next generation and after. Mol Ecol 19(7):1283–1295

Batista D, Tellini K, Nudi AH et al (2013) Marine sponges as bioindicators of oil and combustion derived PAH in coastal waters. Mar Environ Res 92:234–243

Bell JJ (2008) Functional roles of sponges. Estuar Coast Shelf Sci 79:342–352

Bell JJ, Davy SK, Jones T et al (2013) Could some coral reefs become sponge reefs as our climate changes? Glob Chang Biol 19(9):2613–2624

Bergquist PR (1978) Sponges. University of California Press, Berkeley

Berthet B, Mouneyrac C, Pérez T et al (2005) Metallothionein concentration in sponges (*Spongia officinalis*) as a biomarker of metal contamination. Comp Biochem Physiol C 141(3):306–313

Böhm M, Schröder HC, Müller IM et al (2000) The mitogen-activated protein kinase p38 pathway is conserved in metazoans: Cloning and activation of p38 of the SAPK2 subfamily from the sponge *Suberites domuncula*. Biol Cell 92(2):95–104

Boyko A, Kovalchuk I (2011) Genome instability and epigenetic modification—heritable responses to environmental stress? Curr Opin Plant Biol 14(3):260–266

Borisenko I, Adamski M, Ereskovsky A, Adamska M (2016) Surprisingly rich repertoire of Wnt genes in the demosponge Halisarca dujardini. BMC Evol Biol 16(1):123

Bråte J, Adamski M, Neumann RS et al (2015) Regulatory RNA at the root of animals: dynamic expression of developmental lincRNAs in the calcisponge *Sycon ciliatum*. Proc R Soc B Biol Sci 282:20151746

Cebrian E, Agell G, Martí R, Uriz MJ (2006) Response of the Mediterranean sponge *Chondrosia reniformis* Nardo to copper pollution. Environ Pollut 141(3):452–458

Cebrian E, Uriz MJ, Turon X (2007) Sponges as biomonitors of heavy metals in spatial and temporal surveys in northwestern Mediterranean: multispecies comparison. Environ Toxicol Chem 26(11):2430–2439

Cebrian M, Uriz MJ, Garrabou J et al (2011) Sponge mass mortalities in a warming Mediterranean sea: are cyanobacteria–harboring species worse off? PLoS One 6:E20211

Cedar H, Bergman Y (2009) Linking DNA methylation and histone modification: patterns and paradigms. Nat Rev Genet 10(5):295–304

Cha JN, Shimizu K, Zhou Y et al (1999) Silicatein filaments and subunits from a marine sponge direct the polymerization of silica and silicones in vitro. Proc Natl Acad Sci U S A 96(2):361–365

Châtel A, Talarmin H, Hamer B et al (2011) MAP kinase cell signaling pathway as biomarker of environmental pollution in the sponge *Suberites domuncula*. Ecotoxicology 20(8):1727–1740

Conaco C, Neveu P, Zhou H et al (2012) Transcriptome profiling of the demosponge *Amphimedon queenslandica* reveals genome–wide events that accompany major life cycle transitions. BMC Genomics 13(1):209

Cooke SJ, Sack L, Franklin CE et al (2013) What is conservation physiology? Perspectives on an increasingly integrated and essential science. Conserv Physiol 1:1–23

Cramer JM, Pohlmann D, Gomez F, Mark L, Kornegay B, Hall C, Siraliev-Perez E, Walavalkar NM, Jeannette Sperlazza M, Bilinovich S, Prokop JW, Hill AL, Williams DC Jr (2017) Methylation specific targeting of a chromatin remodeling complex from sponges to humans. Sci Rep 7:40674

Custodio MR, Prokic I, Steffen R et al (1998) Primmorphs generated from dissociated cells of the sponge *Suberites domuncula*: a model system for studies of cell proliferation and cell death. Mech Ageing Dev 105:45–59

Deaton AM, Bird A (2011) CpG islands and the regulation of transcription. Genes Dev 25(10):1010–1022

Dimond JL, Roberts SB (2016) Germline DNA methylation in reef corals: patterns and potential roles in response to environmental change. Mol Ecol 25(8):1895–1904

Dixon GB, Bay LK, Matz MV (2014) Bimodal signatures of germline methylation are linked with gene expression plasticity in the coral *Acropora millepora*. BMC Genomics 15(1):1109

Dixon G, Bay LK, Matz MV (2016) Evolutionary consequences of DNA methylation in a basal metazoan. Mol Biol Evol 33(9):2285–2293

Efremova SM, Margulis BA, Guzhova IV et al (2002) Heat shock protein Hsp70 expression and DNA damage in Baikalian sponges exposed to model pollutants and wastewater from Baikalsk pulp and paper plant. Aquat Toxicol 57(4):267–280

Ehrlich H, Kaluzhnaya OV, Tsurkan MV et al (2013) First report on chitinous holdfast in sponges (Porifera). Proc R Soc B Biol Sci 280(1762):20130339

Evans TG, Hofmann GE (2012) Defining the limits of physiological plasticity: how gene expression can assess and predict the consequences of ocean change. Philos Trans R Soc B 367(1596):1733–1745

Fafanđel M, Müller WE, Batel R (2003) Molecular response to TBT stress in marine sponge *Suberites domuncula*: proteolytical cleavage and phosphorylation of KRS_SD protein kinase. J Exp Mar Biol Ecol 297(2):239–252

Fang JKH, Mello-Athayde MA, CHL S et al (2013) Sponge biomass and bioerosion rates increase under ocean warming and acidification. Glob Chang Biol 19:3582–3591

Feder ME, Hofmann GE (1999) Heat–shock proteins, molecular chaperones and the stress response: evolutionary and ecological physiology. Annu Rev Physiol 61:243–282

Fernandez-Valverde SL, Calcino AD, Degnan BM (2015) Deep developmental transcriptome sequencing uncovers numerous new genes and enhances gene annotation in the sponge *Amphimedon queenslandica*. BMC Genomics 16(1):387

Fiore CL, Labrie M, Jarett JK, Lesser MP (2015) Transcriptional activity of the giant barrel sponge, Xestospongia muta Holobiont: molecular evidence for metabolic interchange. Front Microbiol 6:364

Fortunato S, Adamski M, Bergum B et al (2012) Genome–wide analysis of the sox family in the calcareous sponge *Sycon ciliatum*: multiple genes with unique expression patterns. EvoDevo 3:14

Fortunato SA, Adamski M, Ramos OM et al (2014a) Calcisponges have a ParaHox gene and dynamic expression of dispersed NK homeobox genes. Nature 514(7524):620–623

Fortunato SA, Leininger S, Adamska M (2014b) Evolution of the Pax–Six–Eya–Dach network: the calcisponge case study. EvoDevo 5:23

Gaiti F, Fernandez-Valverde SL, Nakanishi N et al (2015) Dynamic and widespread lncRNA expression in a sponge and the origin of animal complexity. Mol Biol Evol 32(9):2367–2382

Gaiti F, Jindrich K, Fernandez-Valverde SL, Roper KE, Degnan BM, Tanurdžić M (2017) Landscape of histone modifications in a sponge reveals the origin of animal cis-regulatory complexity. eLife 6

Gardères J, Elkhooly TA, Link T et al (2016) Self–assembly and photocatalytic activity of branched silicatein/silintaphin filaments decorated with silicatein–synthesized TiO_2 nanoparticles. Bioprocess Biosyst Eng 39(9):1477–1486

Gauthier M, Degnan BM (2008) The transcription factor NF–κB in the demosponge *Amphimedon queenslandica*: insights on the evolutionary origin of the Rel homology domain. Dev Genes Evol 218(1):23–32

Gauthier ME, Du Pasquier L, Degnan BM (2010) The genome of the sponge *Amphimedon queenslandica* provides new perspectives into the origin of Toll-like and interleukin 1 receptor pathways. Evol Dev 12(5):519–533

Gentric C, Rehel K, Dufour A et al (2016) Bioaccumulation of metallic trace elements and organic pollutants in marine sponges from the South Brittany Coast, France. J Environ Sci Health Part A 51(3):213–219

Germer J, Mann K, Wörheide G et al (2015) The skeleton forming proteome of an early branching metazoan: a molecular survey of the biomineralization components employed by the coralline sponge *Vaceletia* sp. PLoS One 10(11):e0140100

Gibney ER, Nolan CM (2010) Epigenetics and gene expression. Heredity 105(1):4–13

Goodwin C, Rodolfo-Metalpa R, Picton B et al (2014) Effects of ocean acidification on sponge communities. Mar Ecol 35(S1):41–49

Grimson A, Srivastava M, Fahey B et al (2008) Early origins and evolution of microRNAs and Piwi–interacting RNAs in animals. Nature 455(7217):1193–1197

Grunau C, Clark SJ, Rosenthal A (2001) Bisulfite genomic sequencing: systematic investigation of critical experimental parameters. Nucleic Acids Res 29(13):e65

Grunstein M (1997) Histone acetylation in chromatin structure and transcription. Nature 389(6649):349–352

Gupta RA, Shah N, Wang KC et al (2010) Long non–coding RNA HOTAIR reprograms chromatin state to promote cancer metastasis. Nature 464(7291):1071–1076

Guzman C, Conaco C (2016a) Comparative transcriptome analysis reveals insights into the streamlined genomes of haplosclerid demosponges. Sci Rep 6:18774

Guzman C, Conaco C (2016) Gene expression dynamics accompanying the sponge thermal stress response. PLoS One 11(10):e0165368

Hansen IV, Weeks JM, Depledge MH (1995) Accumulation of copper, zinc, cadmium and chromium by the marine sponge *Halichondria panicea* Pallas and the implications for biomonitoring. Mar Pollut Bull 31(1):133–138

Hemmrich G, Bosch TCG (2008) Compagen, a comparative genomics platform for early branching metazoan animals, reveals early origins of genes regulating stem-cell differentiation. BioEssays 30(10):1010–1018

Henikoff S, Shilatifard A (2011) Histone modification: cause or cog? Trends Genet 27(10):389–396

Huang H, Lin S, Garcia BA, Zhao Y (2015) Quantitative proteomic analysis of histone modifications. Chem Rev 115(6):2376–2418

Huarte M, Guttman M, Feldser D et al (2010) A large intergenic noncoding RNA induced by p53 mediates global gene repression in the p53 response. Cell 142(3):409–419

IPCC (2007) Summary for policymakers, Intergovernmental Panel on Climate Change fourth assessment report climate change 2007: synthesis report. Cambridge University Press

Jackson DJ, Macis L, Reitner J et al (2007) Sponge paleogenomics reveals an ancient role for carbonic anhydrase in skeletogenesis. Science 316(5833):1893–1895

Jackson DJ, Macis L, Reitner J et al (2011) A horizontal gene transfer supported the evolution of an early metazoan biomineralization strategy. BMC Evol Biol 11:238

Kaniewska P, Campbell PR, Kline DI et al (2012) Major cellular and physiological impacts of ocean acidification on a reef building coral. PLoS One 7(4):e34659

Koziol C, Wagner-Hülsmann C, Mikoc A et al (1996) Cloning of a heat–inducible biomarker, the cDNA encoding the 70 kDa heat shock protein, from the marine sponge *Geodia cydonium*: response to natural stressors. Mar Ecol Prog Ser 136(1):153–161

Koziol C, Batel R, Arinc E et al (1997) Expression of the potential biomarker heat shock protein 70 and its regulator, the metazoan DnaJ homolog, by temperature stress in the sponge *Geodia cydonium*. Mar Ecol Prog Ser 154:261–268

Koziol C, Borojevic R, Steffen R et al (1998) Sponges (Porifera) model systems to study the shift from immortal to senescent somatic cells: the telomerase activity in somatic cells. Mech Ageing Dev 100(2):107–120

Krasko A, Scheffer U, Koziol C et al (1997) Diagnosis of sublethal stress in the marine sponge *Geodia cydonium:* application of the 70 kDa heat–shock protein and a novel biomarker, the Rab GDP dissociation inhibitor, as probes. Aquat Toxicol 37(2):157–168

Krasko A, Lorenz B, Batel R et al (2000) Expression of silicatein and collagen genes in the marine sponge *Suberites domuncula* is controlled by silicate and myotrophin. Eur J Biochem 267(15):4878–4887

Krol J, Loedige I, Filipowicz W (2010) The widespread regulation of microRNA biogenesis, function and decay. Nat Rev Genet 11(9):597–610

Kültz D (2005) Molecular and evolutionary basis of the cellular stress response. Annu Rev Physiol 67:225–257

Larroux C, Fahey B, Liubicich D et al (2006) Developmental expression of transcription factor genes in a demosponge: insights into the origin of metazoan multicellularity. Evol Dev 8(2):150–173

Lesser MP, Fiore C, Slattery M et al (2016) Climate change stressors destabilize the microbiome of the Caribbean barrel sponge, *Xestospongia muta*. J Exp Mar Biol Ecol 475:11–18

Levin M, Anavy L, Cole AG et al (2016) The mid–developmental transition and the evolution of animal body plans. Nature 531:637–641

Leys SP, Hill A (2012) The physiology and molecular biology of sponge tissues. Adv Mar Biol 62:1–56

Liew YJ, Ryu T, Aranda M et al (2016) miRNA repertoires of demosponges *Stylissa carteri* and *Xestospongia testudinaria*. PLoS One 11(2):e0149080

López-Legentil S, Song B, Mcmurray SE et al (2008) Bleaching and stress in coral reef ecosystems: hsp70 expression by the giant barrel sponge *Xestospongia muta*. Mol Ecol 17(7):1840–1849

Maldonado M, Carmona MC, Uriz MJ et al (1999) Decline in mesozoic reef–building sponges explained by silicon limitation. Nature 401(6755):785–788

Maldonado M, Cao H, Cao X et al (2012) Experimental silicon demand by the sponge *Hymeniacidon perlevis* reveals chronic limitation in field populations. Hydrobiologia 687(1):251–257

Marin F, Smith M, Isa Y et al (1996) Skeletal matrices, muci, and the origin of invertebrate calcification. Proc Natl Acad Sci U S A 93(4):1554–1559

Mayer MP, Bukau B (2005) Hsp70 chaperones: cellular functions and molecular mechanism. Cell Mol Life Sci 62(6):670–684

Mercer TR, Dinger ME, Mattick JS (2009) Long non–coding RNAs: insights into functions. Nat Rev Genet 10(3):155–159

Mirouze M, Paszkowski J (2011) Epigenetic contribution to stress adaptation in plants. Curr Opin Plant Biol 14(3):267–274

Mohri K, Nakatsukasa M, Masuda Y et al (2008) Toward understanding the morphogenesis of siliceous spicules in freshwater sponge: differential mRNA expression of spicule type specific silicatein genes in *Ephydatia fluviatilis*. Dev Dyn 237(10):3024–3039

Moya A, Huisman L, Ball EE et al (2012) Whole transcriptome analysis of the coral *Acropora millepora* reveals complex responses to CO_2 driven acidification during the initiation of calcification. Mol Ecol 21(10):2440–2454

Müller WE, Batel R, Lacorn M et al (1998) Accumulation of cadmium and zinc in the marine sponge *Suberites domuncula* and its potential consequences on single–strand breaks and on expression of heat–shock protein: a natural field study. Mar Ecol Prog Ser 167:127–135

Müller WE, Wang X, Grebenjuk VA et al (2012) Common genetic denominators for Ca^{++}−based skeleton in metazoa: role of osteoclast–stimulating factor and of carbonic anhydrase in a calcareous sponge. PLoS One 7(4):e34617

Nakayama S, Arima K, Kawai K et al (2015) Dynamic transport and cementation of skeletal elements build up the pole–and–beam structured skeleton of sponges. Curr Biol 25(19):2549–2554

Nichols SA, Roberts BW, Richter DJ et al (2012) Origin of metazoan cadherin diversity and the antiquity of the classical cadherin/β–catenin complex. Proc Natl Acad Sci U S A 109(32):13046–13051

O'Donnell MJ, Todgham AE, Sewell MA et al (2010) Ocean acidification alters skeletogenesis and gene expression in larval sea urchins. Mar Ecol Prog Ser 398:157–171

Olesen TME, Weeks JM (1994) Accumulation of Cd by the marine sponge *Halichondria panicea* Pallas: effects upon filtration rate and its relevance for biomonitoring. Bull Environ Contam Toxicol 52(5):722–728

Pantile R, Webster N (2011) Strict thermal threshold identified by quantitative PCR in the sponge *Rhopaloeides odorabile*. Mar Ecol Prog Ser 431:97–105

Pérez-Porro AR, Navarro-Gómez D, Uriz MJ et al (2013) A NGS approach to the encrusting Mediterranean sponge *Crella elegans* (Porifera, Demospongiae, Poecilosclerida): transcriptome sequencing, characterization and overview of the gene expression along three life cycle stages. Mol Ecol Resour 13(3):494–509

Peña JF, Alié A, Richter DJ, Wang L, Funayama N, Nichols SA (2016) Conserved expression of vertebrate microvillar gene homologs in choanocytes of freshwater sponges. EvoDevo 7(1):13

Pfeifer K, Frank W, Schröder HC et al (1993) Cloning of the polyubiquitin cDNA from the marine sponge *Geodia cydonium* and its preferential expression during reaggregation of cells. J Cell Sci 106(2):545–553

Pozzolini M, Sturla L, Cerrano C et al (2004) Molecular cloning of silicatein gene from marine sponge *Petrosia ficiformis* (Porifera, Demospongiae) and development of primmorphs as a model for biosilicification studies. Mar Biotechnol 6(6):594–603

Pozzolini M, Scarfì S, Ghignone S et al (2016) Molecular characterization and expression analysis of the first Porifera tumor necrosis factor superfamily member and of its putative receptor in the marine sponge *Chondrosia reniformis*. Dev Comp Immunol 57:88–98

Pratt WB, Toft DO (2003) Regulation of signaling protein function and trafficking by the hsp90/hsp70–based chaperone machinery. Exp Biol Med 228(2):111–133

Qiu F, Ding S, Ou H et al (2015) Transcriptome changes during the life cycle of the red sponge, *Mycale phyllophila* (Porifera, Demospongiae, Poecilosclerida). Genes 6(4):1023–1052

Richards GS, Simionato E, Perron M et al (2008) Sponge genes provide new insight into the evolutionary origin of the neurogenic circuit. Curr Biol 18(15):1156–1161

Richelle-Maurer E, Van de Vyver G (1999) Temporal and spatial expression of EmH–3, a homeobox–containing gene isolated from the freshwater sponge *Ephydatia muelleri*. Mech Ageing Dev 109(3):203–219

Riesgo A, Farrar N, Windsor PJ et al (2014a) The analysis of eight transcriptomes from all poriferan classes reveals surprising genetic complexity in sponges. Mol Biol Evol 31:1102–1120

Riesgo A, Peterson K, Richardson C et al (2014b) Transcriptomic analysis of differential host gene expression upon uptake of symbionts: a case study with *Symbiodinium* and the major bioeroding sponge *Cliona varians*. BMC Genomics 15(1):376

Riesgo A, Maldonado M, López-Legentil S et al (2015) A proposal for the evolution of cathepsin and silicatein in sponges. J Mol Evol 80(5–6):278–291

Roberts SB, Gavery MR (2012) Is there a relationship between DNA methylation and phenotypic plasticity in invertebrates. Front Physiol 2:116

Robinson JM (2015) MicroRNA expression during demosponge dissociation, reaggregation, and differentiation and a evolutionarily conserved demosponge miRNA expression profile. Dev Genes Evol 225(6):341–351

Robinson JM, Sperling EA, Bergum B et al (2013) The identification of microRNAs in calcisponges: independent evolution of microRNAs in basal metazoans. J Exp Zool B Mol Dev Evol 320(2):84–93

Rocker MM, Noonan S, Humphrey C et al (2015) Expression of calcification and metabolism–related genes in response to elevated pCO_2 and temperature in the reef–building coral *Acropora millepora*. Mar Genomics 24:313–318

Ryu T, Seridi L, Moitinho-Silva L et al (2016) Hologenome analysis of two marine sponges with different microbiomes. BMC Genomics 17(1):158

Sakarya O, Armstrong KA, Adamska M et al (2007) A post–synaptic scaffold at the origin of the animal kingdom. PLoS One 2(6):e506
Sarda S, Zeng J, Hunt BG et al (2012) The evolution of invertebrate gene body methylation. Mol Biol Evol 29(8):1907–1916
Schenkelaars Q, Fierro-Constain L, Renard E et al (2015) Insights into Frizzled evolution and new perspectives. Evol Dev 17(2):160–169
Schenkelaars Q, Fierro-Constain L, Renard E et al (2016) Retracing the path of planar cell polarity. BMC Evol Biol 16:69
Schippers KJ, Sipkema D, Osinga R et al (2012) Cultivation of sponges, sponge cells and symbionts: achievements and future prospects. Adv Mar Biol 62:273–337
Schröder HC, Batel R, Lauenroth S et al (1999a) Induction of DNA damage and expression of heat shock protein HSP70 by polychlorinated biphenyls in the marine sponge *Suberites domuncula* Olivi. J Exp Mar Biol Ecol 233(2):285–300
Schröder HC, Hassanein HMA, Lauenroth S et al (1999b) Induction of DNA strand breaks and expression of HSP70 and GRP78 homolog by cadmium in the marine sponge *Suberites domuncula*. Arch Environ Contam Toxicol 36(1):47–55
Schröder HC, Kruse M, Batel R et al (2000a) Cloning and expression of the sponge longevity gene SDLAGL. Mech Dev 95(1):219–220
Schröder HC, Shostak K, Gamulin V et al (2000b) Purification, cDNA cloning and expression of a cadmium–inducible cysteine–rich metallothionein–like protein from the marine sponge *Suberites domuncula*. Mar Ecol Prog Ser 200:149–157
Sethmann I, Hinrichs R, Wörheide G et al (2006) Nano–cluster composite structure of calcitic sponge spicules—a case study of basic characteristics of biominerals. J Inorg Biochem 100(1):88–96
Shimpi GG, Vargas S, Wörheide G (2016) Evaluation and validation of reference genes for qPCR analysis to study climate change-induced stresses in *Sinularia* cf. *cruciata* (Octocorallia: Alcyonidae). J Exp Mar Biol 483:42–52
Shkryl YN, Bulgakov VP, Veremeichik GN et al (2016) Bioinspired enzymatic synthesis of silica nanocrystals provided by recombinant silicatein from the marine sponge *Latrunculia oparinae*. Bioprocess Biosyst Eng 39(1):53–58
Smith AM, Berman J, Key MM et al (2013) Not all sponges will thrive in a high–CO_2 ocean: review of the mineralogy of calcifying sponges. Palaeogeogr Palaeoclimatol Palaeoecol 392:463–472
Sperling EA, Robinson JM, Pisani D et al (2010) Where's the glass? Biomarkers, molecular clocks, and microRNAs suggest a 200–Myr missing Precambrian fossil record of siliceous sponge spicules. Geobiology 8(1):24–36
Srivastava M, Simakov O, Chapman J et al (2010) The *Amphimedon queenslandica* genome and the evolution of animal complexity. Nature 466(7307):720–726
Steindler L, Schuster S, Ilan M et al (2007) Differential gene expression in a marine sponge in relation to its symbiotic state. Mar Biotechnol 9(5):543–549
Stumpp M, Dupont S, Thorndyke MC et al (2011) CO_2 induced seawater acidification impacts sea urchin larval development II: gene expression patterns in pluteus larvae. Comp Biochem Physiol Part A 160(3):320–330
Sundar VC, Yablon AD, Grazul JL et al (2003) Fibre–optical features of a glass sponge. Nature 424(6951):899–900
Uriz MJ, Agell G, Blanquer A et al (2012) Endosymbiotic calcifying bacteria: a new cue to the origin of calcification in metazoa? Evolution 66(10):2993–2999
van Oppen MJ, Oliver JK, Putnam HM et al (2015) Building coral reef resilience through assisted evolution. Proc Natl Acad Sci U S A 112(8):2307–2313
Verhoeven KJ, vonHoldt BM, Sork VL (2016) Epigenetics in ecology and evolution: what we know and what we need to know. Mol Ecol 25(8):1631–1638
Vicente J, Silbiger NJ, Beckley BA et al (2015) Impact of high pCO_2 and warmer temperatures on the process of silica biomineralization in the sponge *Mycale grandis*. ICES J Mar Sci 73(3):704–714
Vogel S (1977) Current–induced flow through living sponges in nature. Proc Natl Acad Sci U S A 74(5):2069–2071
Voigt O, Adamski M, Sluzek K et al (2014) Calcareous sponge genomes reveal complex evolution of α–carbonic anhydrases and two key biomineralization enzymes. BMC Evol Biol 14(1):230

Volinia S, Calin GA, Liu CG et al (2006) A microRNA expression signature of human solid tumors defines cancer gene targets. Proc Natl Acad Sci U S A 103(7):2257–2261

Wagner C, Steffen R, Koziol C et al (1998) Apoptosis in marine sponges: a biomarker for environmental stress (cadmium and bacteria). Mar Biol 131(3):411–421

Wang X, Schloßmacher U, Wiens M et al (2012) Silicateins, silicatein interactors and cellular interplay in sponge skeletogenesis: formation of glass fiber–like spicules. FEBS J 279(10):1721–1736

Wang X, Schröder HC, Müller WE (2014) Enzyme–based biosilica and biocalcite: biomaterials for the future in regenerative medicine. Trends Biotechnol 32(9):441–447

Webster NS, Cobb RE, Negri AP (2008) Temperature thresholds for bacterial symbiosis with a sponge. ISME J 2(8):830–842

Webster NS, Botté ES, Soo RM et al (2011) The larval sponge holobiont exhibits high thermal tolerance. Environ Microbiol Rep 3(6):756–762

Webster N, Pantile R, Botte E et al (2013) A complex life cycle in a warming planet: gene expression in thermally stressed sponges. Mol Ecol 22(7):1854–1868

Wells GD, Tang QY, Heler R et al (2012) A unique alkaline pH–regulated and fatty acid–activated tandem pore domain potassium channel (K2P) from a marine sponge. J Exp Biol 215(14):2435–2444

Whalan S, Ettinger-Epstein P, de Nys R (2008) The effect of temperature on larval pre–settlement duration and metamorphosis for the sponge, *Rhopaloeides odorabile*. Coral Reefs 27(4):783–786

Wheeler BM, Heimberg AM, Moy VN et al (2009) The deep evolution of metazoan microRNAs. Evol Dev 11(1):50–68

Whelan NV, Kocot KM, Moroz LL et al (2015) Error, signal, and the placement of Ctenophora sister to all other animals. Proc Natl Acad Sci U S A 112(18):5773–5778

Wiens M, Müller WE (2006) Cell death in Porifera: molecular players in the game of apoptotic cell death in living fossils. Can J Zool 84(2):307–321

Wiens M, Krasko A, Müller CI et al (2000) Molecular evolution of apoptotic pathways: cloning of key domains from sponges (Bcl–2 homology domains and death domains) and their phylogenetic relationships. J Mol Evol 50(6):520–531

Wiens M, Krasko A, Perovic S et al (2003) Caspase–mediated apoptosis in sponges: cloning and function of the phylogenetic oldest apoptotic proteases from metazoa. Biochim Biophys Acta 1593(2):179–189

Wimmer W, Blumbach B, Diehl-Seifert B et al (1999) Increased expression of integrin and receptor tyrosine kinase genes during autograft fusion in the sponge *Geodia cydonium*. Cell Commun Adhes 7(2):111–124

Wulff JL (2006) Ecological interactions of marine sponges. Can J Zool 84(2):146–166

Zemach A, McDaniel IE, Silva P et al (2010) Genome–wide evolutionary analysis of eukaryotic DNA methylation. Science 328(5980):916